UBV PHOTOMETRY OF DQ CEPHEI

By

ROBERT LEROY JENKS

Bachelor of Arts
University of Omaha
Omaha, Nebraska
1959

Master of Science
Oklahoma State University
Stillwater, Oklahoma
1963

Submitted to the Faculty of the Graduate College of
the Oklahoma State University
in partial fulfillment of the requirements
for the degree of
DOCTOR OF PHILOSOPHY
May, 1966

UBV PHOTOMETRY OF DQ CEPHEI

Thesis Approved:

Leon W. Schroeder
Thesis Adviser

H. S. Mendenhall

Thomas S. Winter

H. E. Harrington

V. L. Pollak

J. H. Boggs
Dean of the Graduate School

ACKNOWLEDGMENTS

I would like to thank Dr. Leon W. Schroeder, my adviser, who suggested this topic for my thesis, provided me generously with his time and advice, and went to the effort of obtaining the observations upon which this paper is based.

I am also in debt to Dr. A. M. Heiser, of the Dyer Observatory, who suggested this star as an object of study, provided time at the observatory, supervised the observations, and provided advice about the reduction.

Dr. W. S. Fitch generously provided me with the results of his observations which were of great aid during the study.

Also, I am greatly appreciative to the National Aeronautics and Space Administration which provided a Traineeship that substantially reduced the amount of time required to complete this study.

Financial support for obtaining the observations was supplied by the Research Foundation of Oklahoma State University.

TABLE OF CONTENTS

TABLE OF CONTENTS (Continued)

LIST OF TABLES

LIST OF TABLES (Continued)

LIST OF FIGURES

LIST OF FIGURES (Continued)

LIST OF FIGURES (Continued)

LIST OF FIGURES (Continued)

Figure

CHAPTER I

INTRODUCTION

Merle F. Walker (1952) discovered the variability of the star DQ Cephei* in 1951. It has a period which he determined to be either 0.07546 or 0.07886 day. He observed the star in yellow and blue, classified it as F2 II, estimated the spectroscopic absolute visual magnitude as -2, and introduced the possibility that the star may be a "borderline" Cepheid.

In 1952 Walker (1953) again observed the star in order to uniquely determine the period. He noted that the star was bluest at maximum light and that the range in brightness varied from cycle to cycle. A phase shift between green and ultraviolet light curves was noted, the green light curve maximum being about 0.007 day later than that of the ultraviolet. The period 0.07546 day was eliminated and an improved period was obtained. The value, however, was still ambiguous, either 0.0788456, 0.0788653, or 0.0788850 day.

In 1954 and 1955 J. Sahade, O. Struve, O. C. Wilson, and V. Zebergs (1956) measured the radial velocity of DQ Cephei from spectrograms obtained at the Mt. Wilson and Palomar Observatories. They found a change in the radial velocity with the same period as that found photoelectrically by Walker. They found that the amplitude of the velocity

---

*This star is number 199908 in the Henry Draper catalogue.

curve is variable, and they calculated a beat period of 0.3751 day. This beat period corresponds to an interfering period of either 0.06516 or 0.09986 day. Their principal period is 0.0788650 day which is in good agreement with one of Walker's values. They found, by comparison with some light curves made by Walker at the same time, that the epoch of maximum brightness occurs about halfway on the descending branch of the velocity curve and minimum light about halfway on the ascending branch of the velocity curve. They estimated the spectral type to be approximately F1 IV-V, and they note that the star is undoubtedly a member of the group of variables of the AI Velorum type. It also resembles δ Scuti.

In 1958, W. S. Fitch (1959) observed DQ Cephei and noted that any overtone pulsation must have extremely small amplitude since he could represent his light curves by a mean sine curve in the fundamental period with a probably error of a single observation of from 0.004 to 0.007 magnitude. Because of the small amplitude of his residuals, he concluded that Sahade's reported period is probably one cycle per day too long. If this is true, the interfering period has a value of 0.061177 day. Fitch was searching for a relationship between P_1/P_0 and P_0(P_0 is the primary period and P_1 is the secondary period) and this value of P_1 was needed to fit his interpolation formula. Fitch and William Wehlau (1965) subjected Fitch's and Walker's data to further analysis. They found the primary period to be 0.07886455 day and they found a secondary component of small amplitude to be present with a period of 0.1241987 day. This component would cause a beat with a period of 0.2756 day. Neither of the secondary periods implied by the beat period found in the radial velocities by Sahade was found by Fitch and Wehlau.

In a study of the δ Scuti variables, D. H. McNamara and Gordon Augason (1962) calculated the absolute visual magnitude, M_V, of DQ Cephei as +1.8, the B-V color as +0.29 and the mass as 3.5 solar masses. They report a spectral type of F1 IV-V based on the P-V color reported by O. Eggen (1957) which corresponds to a B-V color of +0.31.

It was decided to observe DQ Cephei photoelectrically in the U, B, V system of colors in order that the observations would be directly comparable with those made on other stars. U, B, V color information is used in stellar evolution studies and in determinations of interstellar absorption, spectral classification, and effective temperatures of stars.

The light curves obtained from the observations are used to determine a refined primary period and photoelectric values of the B-V and U-B colors. Cycle to cycle variations in the amplitude of the light curves are investigated.

The star was observed photoelectrically in U, B, V on five nights in 1964 by A. M. Heiser, R. L. Jenks, and L. W. Schroeder with the 24-inch Seyfert Telescope at the Dyer Observatory. The observations cover six cycles, two of which are consecutive. The coordinates of DQ Cephei in 1964 were right ascension $20^h\ 56^m.8$, declination $+55^\circ.35$.

CHAPTER II

REDUCTION OF PHOTOELECTRIC DATA

The data which are produced during a photoelectric observation program consist of a series of deflections of a measuring device which is connected to a photomultiplier tube. In order for these data to be useful it is necessary to translate these deflections into quantities which can be compared with observations made by other observers.

Atmospheric Extinction

As light passes through an absorbing medium its intensity is decreased by

$$dI_\nu = -\kappa_\nu I_\nu \rho \, ds, \tag{2.1}$$

where I_ν is the intensity of light at frequency ν, ρ is the density of the medium, ds is the differential path length, and κ_ν is defined as the mass absorption coefficient. Dropping the subscript ν, if I_o and I are the intensities at some frequency outside, and at the bottom of the earth's atmosphere, respectively, then

$$\ln \frac{I}{I_o} = -\int_o^\infty \kappa \rho \, ds. \tag{2.2}$$

The limits of the integrand result from treating the atmosphere as being semi-infinite in extent. In accordance with convention, ln represents log to the base e. Let us define the optical depth of the atmosphere along a path which makes an angle Z with the vertical at the surface as

$$\tau_z = \int_0^\infty \kappa\rho\, ds, \qquad (2.3)$$

and, in particular, define the zenith optical depth (z=0) as

$$\tau_0 = \int_0^\infty \kappa\rho\, dh, \qquad (2.4)$$

where dh is along a radial direction and ds=dh sec Z.

Then, Equation (2.2) becomes

$$\ln \frac{I}{I_0} = -\tau_z. \qquad (2.5)$$

From the relationship between magnitude (m) and intensities, $I/I_0 = (\sqrt[5]{100})^{m_0-m}$, in conjunction with Equation (2.5), we obtain

$$m_0 - m = -2.5\tau_z \log e, \qquad (2.6)$$

where log means log to the base 10. Now, if we set $k = 2.5\tau_0 \log e$ and $X = \frac{\tau_z}{\tau_0}$, we obtain

$$m_0 = m - kX, \qquad (2.7)$$

where k is the extinction coefficient and X is the relative air mass. k is seen to be a measure of the light-loss expressed in magnitudes for a star at the zenith. Thus the magnitude of a star observed by a fictitious observer just outside the atmosphere is readily deduced from the observed magnitude, provided that both k and X are known.

Different expressions can be obtained for X depending on the model atmosphere employed. An empirical expression has been developed by

Hardie (1962) which is accurate to 1/10 per cent up to $X = 6.8$ and better than 1 per cent up to $X = 10$. His expression is

$$X = \sec Z - 0.0018167(\sec Z-1) - 0.002875(\sec Z-1)^2 - 0.0008083(\sec Z-1)^3. \qquad (2.8a)$$

Other expressions, based upon various models of the atmosphere, are developed in Appendix A.

The value of sec Z is readily determinable for any observation through the relation

$$\sec Z = (\sin \phi \sin \delta + \cos \phi \cos \delta \cos h)^{-1} \qquad (2.8b)$$

in which ϕ is the observer's latitude (for the Dyer Observatory 36°03'), while δ and h are the declination and hour angle of the star. While it is often convenient to use relation (2.8b) to compute sec Z as needed, there are other occasions when it is easier to use an extensive table giving sec Z for a wide range of declinations and hour angles. It is also possible to construct air-mass nomograms which permit rapid determinations of air mass. It should be noted that for a plane parallel atmosphere Equation (2.8a) would reduce to simply $X = \sec Z$.

Since we are able to measure the magnitude m and the zenith distance z, the law of extinction (2.7) will give us the magnitude m_o as seen just outside the atmosphere if we know the extinction coefficient. The classical method for the determination of k is to observe a suitable star at several zenith distances and to plot the observed magnitudes *versus* air mass. As Equation (2.7) indicates, the slope of the resulting curve is equal to k. A quicker method is one advocated by Hardie (1959).

According to this method, one establishes a series of standard stars for which m_o is known. Then, in order to determine the extinction at any time, it is necessary to measure m for several standard stars with different air masses and then plot $m_o - m$ *versus* **X**. The slope of the resulting curve yields k, the extinction coefficient, without it being necessary to wait for a star to move through a large zenith distance.

It should be noted that the discussion thus far in this section has dealt with light of a single color. It must be remembered that the atmosphere not only diminishes but also reddens the light passing through it. There are three primary factors which cause extinction: molecular absorption bands, haze, and scattering by molecules (Rayleigh scattering), which is approximately proportional to λ^{-4} (van de Hulst 1949).

When working in several colors, it is convenient to use a single magnitude and one or more color indices in a differential manner. That is, let $C = m_{\lambda_1} - m_{\lambda_2}$. Then

$$C_o = C - k_c \mathbf{X}, \tag{2.9}$$

where $k_c = k_{\lambda_1} - k_{\lambda_2}$ and C_o and C are color indices for a star as seen from just outside and within the atmosphere respectively. Since a color index is a measure of the different intensity of light at different wave lengths, it serves as a measure of temperature.

The extinction is therefore seen to be a function of color index. Let us set

$$k = k' + k'' C, \tag{2.10}$$

where C is the color index of the star, uncorrected for extinction, k' is the magnitude extinction coefficient for a star of zero color index, and $k' + k''$ is the extinction coefficient for a star of color index equal to one. Similarly we have

$$k_c = k_c' + k_c'' C, \tag{2.11}$$

where k_c' is the color extinction coefficient for a star of zero color index and $k_c' + k_c''$ is the color extinction coefficient for a star of color index equal to one. The primed coefficients are referred to as the "principal coefficients" and the double-primed coefficients are "second-order coefficients." This decomposition of the extinction into first and second-order terms is justified solely because any higher order terms are not measurable with present techniques.

It is found that the second order coefficient, k'', for the magnitude extinction is negligibly small in the red and yellow regions, and has a value of -0.02 to -0.04 in the blue when the color index has a scale and zero point close to the International or B-V system. It is relatively constant compared with the principal coefficient k'. Likewise, the second-order coefficient, k_c'', is small and not subject to much variation. Once these second order terms have been determined, they will need only occasional checks, for they do not appear subject to much variation. We will assume henceforth that the second-order terms are known.

Taking account of the second-order terms, Equations (2.7) and (2.9) become

$$\begin{aligned} m_o &= m - k'X - k''CX, \\ C_o &= C - k_c'X - k_c''CX, \\ &= C(1 - k_c''X) - k_c'X. \end{aligned} \tag{2.12}$$

Magnitude and Color Transformations

In medium-band width photometry such as the U, B, V system, the relative measures of both magnitude and color index are determined by the particular bands chosen. Each combination of optics, filters, and phototube will define its own set of magnitudes and colors, which will be the observer's "natural" system. It is necessary to be able to relate measurements made in one system to those in another. It can be shown (Hardie 1962) that under some fairly non-restrictive conditions it is possible to relate color indices for two natural systems by a linear equation of the form

$$C_2 = \mu C_1 + \zeta_c. \quad (2.13)$$

In order for a relation of this simple form to hold with sufficient accuracy it is necessary that the color systems be as nearly identical as possible as to band widths and effective wave lengths, that the major spectral discontinuities be avoided, and to be aware that stars of widely differing characteristics may require different relations. The magnitude transformation takes the form

$$m_2 = m_1 + \epsilon C_1 + \zeta_m. \quad (2.14)$$

The scale constants, ϵ and μ, and the "zero-point" constants, ζ_m and ζ_c, can be determined from a sufficient number of stars observed in both systems.

The U, B, V Photometric System

The three-color U, B, V photometric system of Johnson and Morgan (1953) is a widely used general purpose system based originally upon the Sb-Cs photosurface of the RCA 1P21 photomultiplier with glass absorption filters. The three colors are at effective wave lengths of about 3600, 4300, and 5500 angstroms. The color differences, (U-B) and (B-V), are made equal to zero for main sequence stars of spectral class A0.

In this system, Equations (2.12) become

$$\begin{aligned} v_o &= v - k_v X, \\ (b-v)_o &= (b-v) J_x - k'_{bv} X, \\ (u-b)_o &= (u-b) G_x - k'_{ub} X, \end{aligned} \tag{2.15}$$

where $J_x = (1-k''_{bv}X)$; $G_x = (1-k''_{ub}X)$ and k''_v is taken as equal to zero. v, $(b-v)$, and $(u-b)$ are the local magnitude and colors, uncorrected for extinction and in the natural system of colors. v_o, $(b-v)_o$, $(u-b)_o$ are the extra-atmosphere magnitude and colors, and the subscripts bv and ub refer to the B-V and U-B colors respectively. The transformations from the natural system to the standard U, B, V system are made by means of equations of the form:

$$\begin{aligned} V &= v_o + \epsilon(B-V) + \zeta_v, \\ B-V &= \mu(b-v)_o + \zeta_{bv}, \\ U-B &= \psi(u-b)_o + \zeta_{ub}, \end{aligned} \tag{2.16}$$

where V, B-V, and U-B are the standard U, B, V magnitude and colors. The coefficients μ and ψ are of the same type as the ones in Equation (2.13) and refer to the B-V and U-B colors respectively.

Equations (2.15) and (2.16) combine into the following working equations:

$$V = v - k_v X + \epsilon(B-V) + \zeta_v,$$
$$B-V = \mu(b-v)J_x - \mu k'_{bv} X + \zeta_{bv}, \qquad (2.17)$$
$$U-B = \psi(u-b)G_x - \psi k'_{ub} X + \zeta_{ub}.$$

Hardie (1962) describes a program of observations which enables one to find the values of ε, μ, ψ, J_x, and G_x for a particular observatory. The extinction coefficients can be determined by Hardie's short method. That is, where several high and low stars are observed, a plot of $[v + \epsilon(B-V)-V]$, $[\mu(b-v)J_x-(B-V)]$, and $[\psi(u-b)G_x-(U-B)]$ versus X will yield lines whose slopes are k_v, $\mu k'_{bv}$, and $\psi k'_{ub}$. By using standard stars frequently during the observing period the zero-point terms are found. With mean or interpolated zero-point values the desired magnitude and color indices can be obtained. It has been observed by Hardie that this method of taking the zero-point terms as unknown and determining them at the same time as the program star values compensates for some of the errors which might be present in the extinction coefficients.

Heliocentric Julian Day Correction

In the case of a short period variable star which may have a period of only an hour or two, it is necessary to predict the time that a fictional observer situated at the center of the sun would observe the measurement taken on the earth. Only by referring all measurements to this common point can allowance be made for the fact that the earth occupies different points in its orbit throughout the year. In the geocentric ecliptic system we have

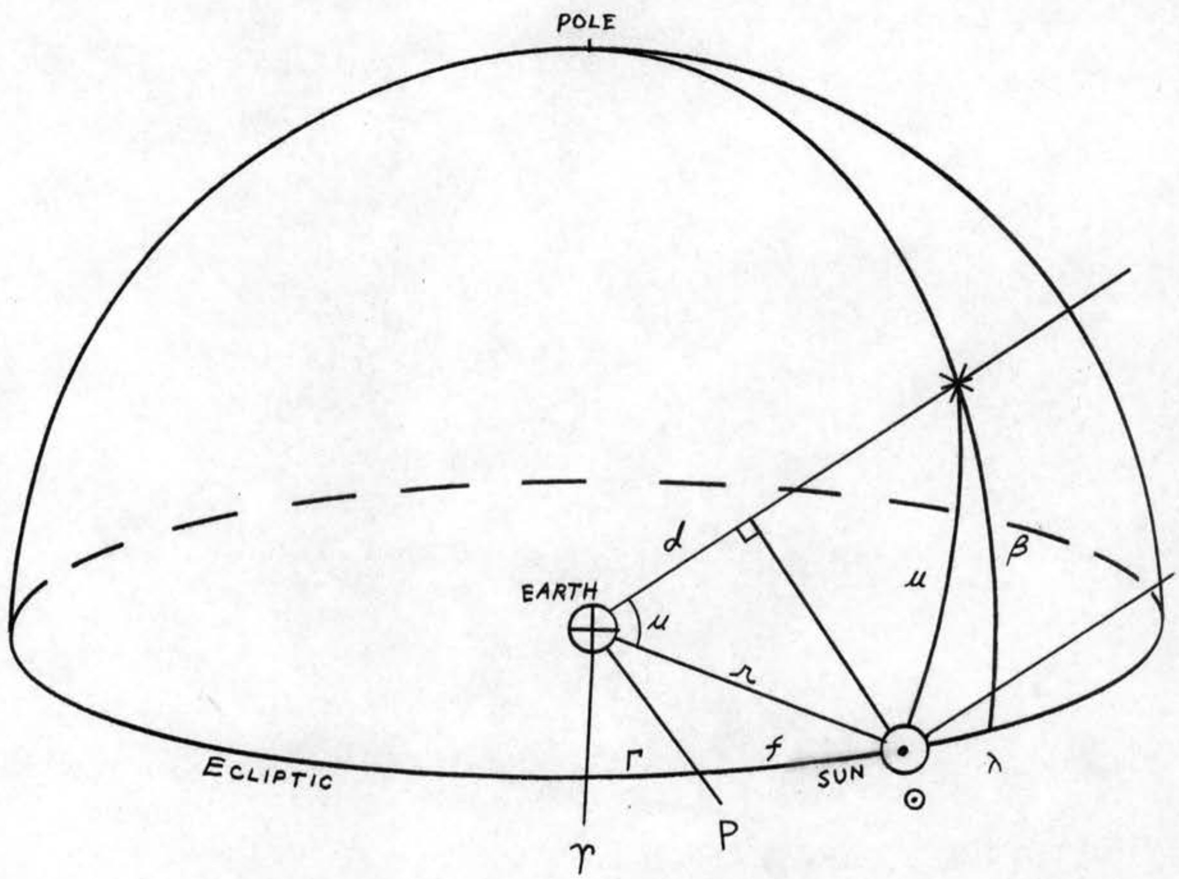

Figure 1. The Geocentric Ecliptic System

$$d = r\cos\mu = r\cos\beta\,\cos(\lambda - L),$$

where r is the distance from the earth to the sun, β is the latitude of the star, f is the true anomaly, λ is the longitude of the star, P is the perigee point, Γ is the longitude of perigee, and $\odot$ is the longitude of the sun. d is the distance the light travels to reach the earth after meeting the sun, and ♈ is the vernal equinox.

The time interval between observations, at the earth and at the sun, of a particular ray of light from a star, results in the correction

$$HJD = JD + \Delta t = JD - \frac{d}{c}. \tag{2.18}$$

HJD is the heliocentric Julian day and JD is the Julian date as observed on the earth at the same instant. c is the speed of light.

The distance, d, is given by

$$d = \pi \cos\mu = \pi \cos\beta \cos(\lambda - \odot), \tag{2.19}$$

$$d = \pi(\cos\beta \cos\lambda \cos\odot + \cos\beta \sin\lambda \sin\odot). \tag{2.20}$$

Transforming the star's coordinates from the ecliptic to the equatorial system by,

$$\cos\beta \cos\lambda = \cos\delta \cos\alpha,$$

$$\cos\beta \sin\lambda = \sin\epsilon \sin\delta + \cos\epsilon \cos\delta \sin\alpha,$$

where δ is the star's declination, α is its right ascension and ϵ is the obliquity of the ecliptic, we have

$$d = \pi[\cos\delta \cos\alpha \cos\odot + (\sin\epsilon \sin\delta + \cos\epsilon \cos\delta \sin\alpha)\sin\odot]. \tag{2.21}$$

Now converting the sun's coordinates to rectangular form by:

$$X = \frac{\pi}{a}\cos\odot,$$

$$Y = \frac{\pi}{a}\sin\odot \cos\epsilon,$$

$$d = \alpha[\cos\delta \cos\alpha X + (\tan\epsilon \sin\delta + \cos\delta \sin\alpha)Y], \tag{2.22}$$

or

$$\Delta t = -\frac{a}{c}[\cos\delta \cos\alpha X + (\tan\epsilon \sin\delta + \cos\delta \sin\alpha)Y]. \tag{2.23}$$

The coordinate X is directed along the line to the vernal equinox, Υ, and Y is at right angles to it in the plane of the ecliptic. With Allen's (1955) values for c and a,

$$c = 2.99791 \times 10^{10} \text{ cm - sec}^{-1},$$
$$a = 1.496 \times 10^{13} \text{ cm}, \tag{2.24}$$

$$\Delta t = -0.^{d}005770\left[\cos\delta \cos\alpha \mathbf{X} + (\tan\epsilon \sin\delta + \cos\delta \sin\alpha)\mathbf{Y}\right],$$
$$= A\mathbf{X} + B\mathbf{Y}. \tag{2.25}$$

For any given star the values of α, δ, and ϵ are known; hence, so are A and B. $\mathbf{X}$, and $\mathbf{Y}$ are tabulated in the <u>American Ephemeris and Nautical Almanac</u> for any given date.

CHAPTER III

DETAILED COMPUTATION OF THE REDUCTION

The data used in this study were obtained on the five nights of August 12-13, 16-17, 17-18, 27-28, and November 21-22, 1964. These dates will hereafter be specified by the morning date, e.g., August 13. The measurements were in the form of deflections on a strip chart recorder, and these were read off the charts as local magnitudes, u, b, and v by means of a transparent magnitude scale described by Hardie (1962) and supplied by the Dyer observatory. The Julian day was noted on the recordings from time to time during the observations. Figure 2 gives an illustration of the recordings. Data shown on the figure include amplifier gains, hour angles, Julian days, and color identifications. Star 5 is one of the comparison stars.

A mirror was attached to the photometer which enabled either the star being observed or the background sky radiation to be observed. The signal was fed from the 1P21 photometer to an amplifier which had been previously calibrated and was fitted with a gain switch in half-magnitude steps. Normally, two sets of observations of the program star were made between each set of observations of the comparison star. For the first three nights the order of observations was: comparison star-v-b-u-program star-v-b-u-v-b-u- comparison star-v-b-u. The last two nights, the sequence of observations for the program star was v-b-u-u-b-v so that the average time of observation of the two readings in each color was

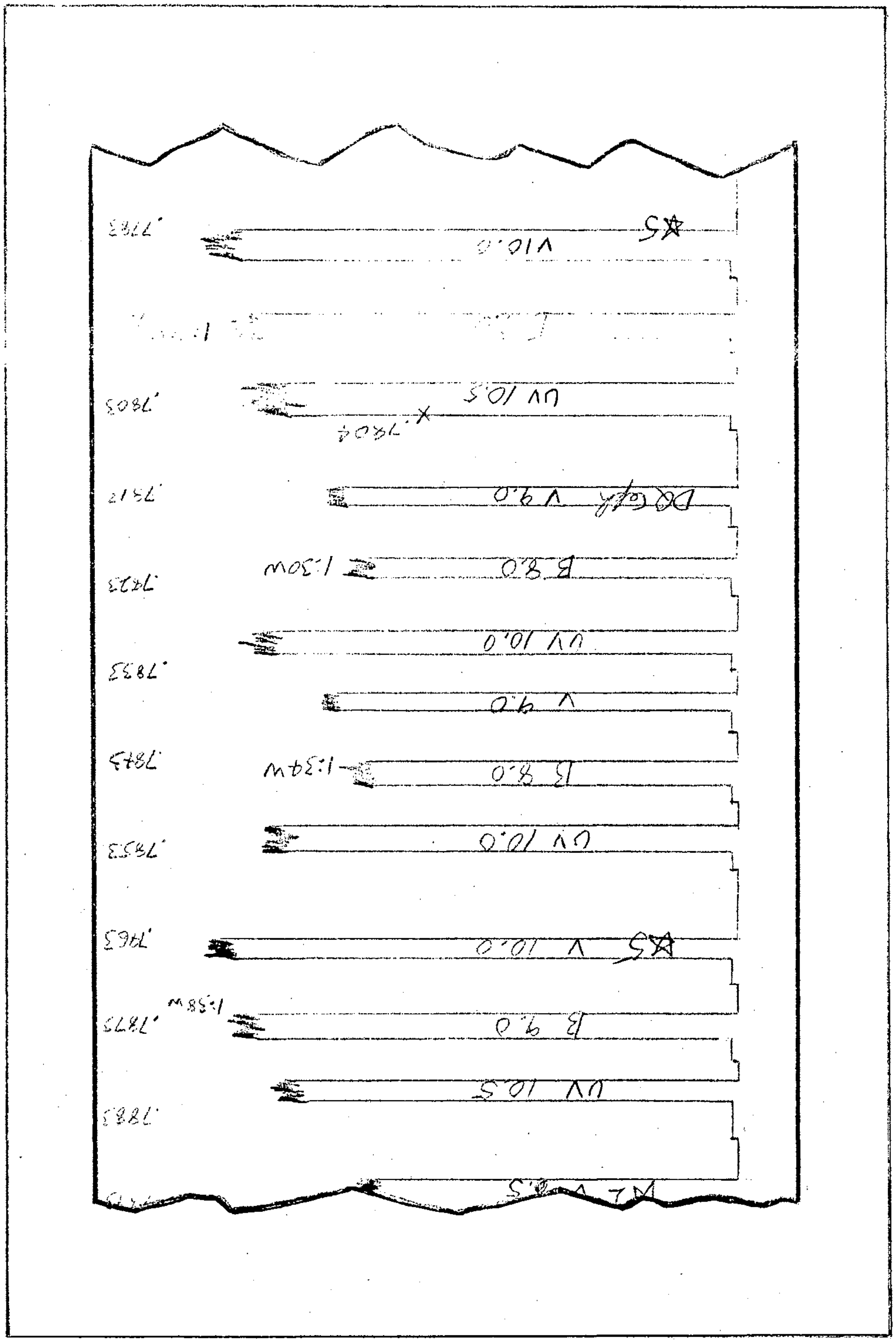

Figure 2. Sample Strip Chart Recording.

nearly equal. From time to time, a second comparison star, or control star, was observed in order to ensure that the first comparison star is not itself variable. The two comparison stars were selected to be close to the program star and of nearly the same color in order to make the differential reduction more accurate. From time to time, a radium source located in the photometer was observed in order to determine whether the amplifier gain had drifted. The photometer was located at the f/17 Cassegrain focus of the telescope whose aperture was limited to 21.5 inches (the result of insertion of a diaphragm over the mirror to avoid using the edges). A diaphragm within the photometer limited the field of view seen by the photocell to 22".2 (seconds of arc). The filters used for the colors were as follows: the V filter was an OG4-4mm (Schott), the B filter was a 5543 (Corning) plus a GG 13 (Schott), and the U filter was a UG 2 (Schott) plus "H" (a red leak suppressor). The photocell was maintained at a low temperature by refrigerating it with dry ice in order to reduce the dark current and stabilize the tube's response.

Preliminary Investigation

The unreduced magnitudes of the comparison star, HD 199938, were plotted for each night's observations to assess the quality of the night. These plots appear in Figures 3, 4, 5, 6 and 7. The graph for August 13 shows a steady decrease in brightness of the comparison star. This decrease is in accordance with the constantly increasing air mass through which the star was observed that night. At the beginning of the night's observations the star stood at hour angle $h = 0^h 44^m$ west and at the end of the night it was at $h = 3^h 24^m$ west.

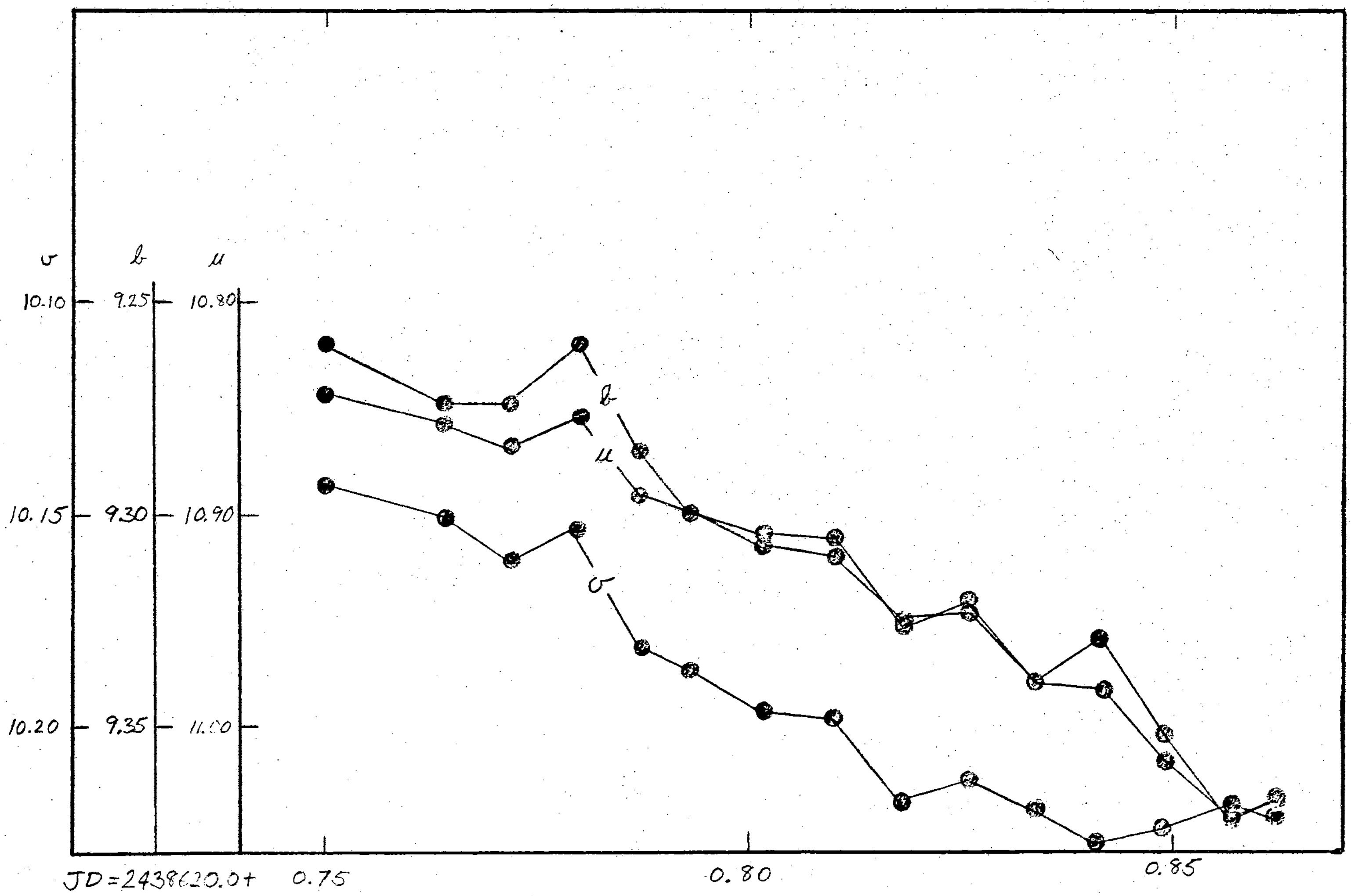

Figure 3. Preliminary Light Curves of HD199938 for August 13, 1964.

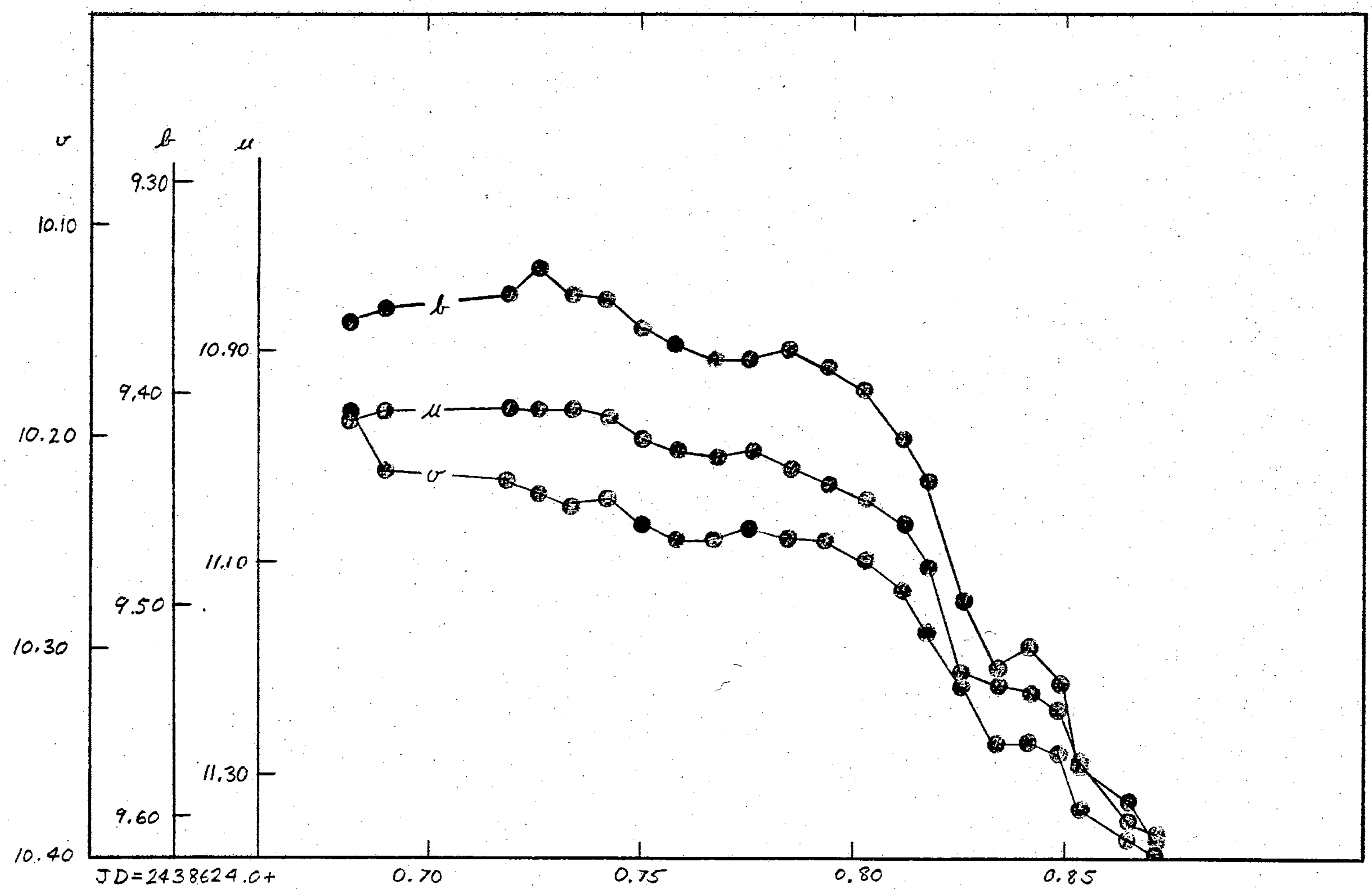

Figure 4. Preliminary Light Curves of HD199938 for August 17, 1964.

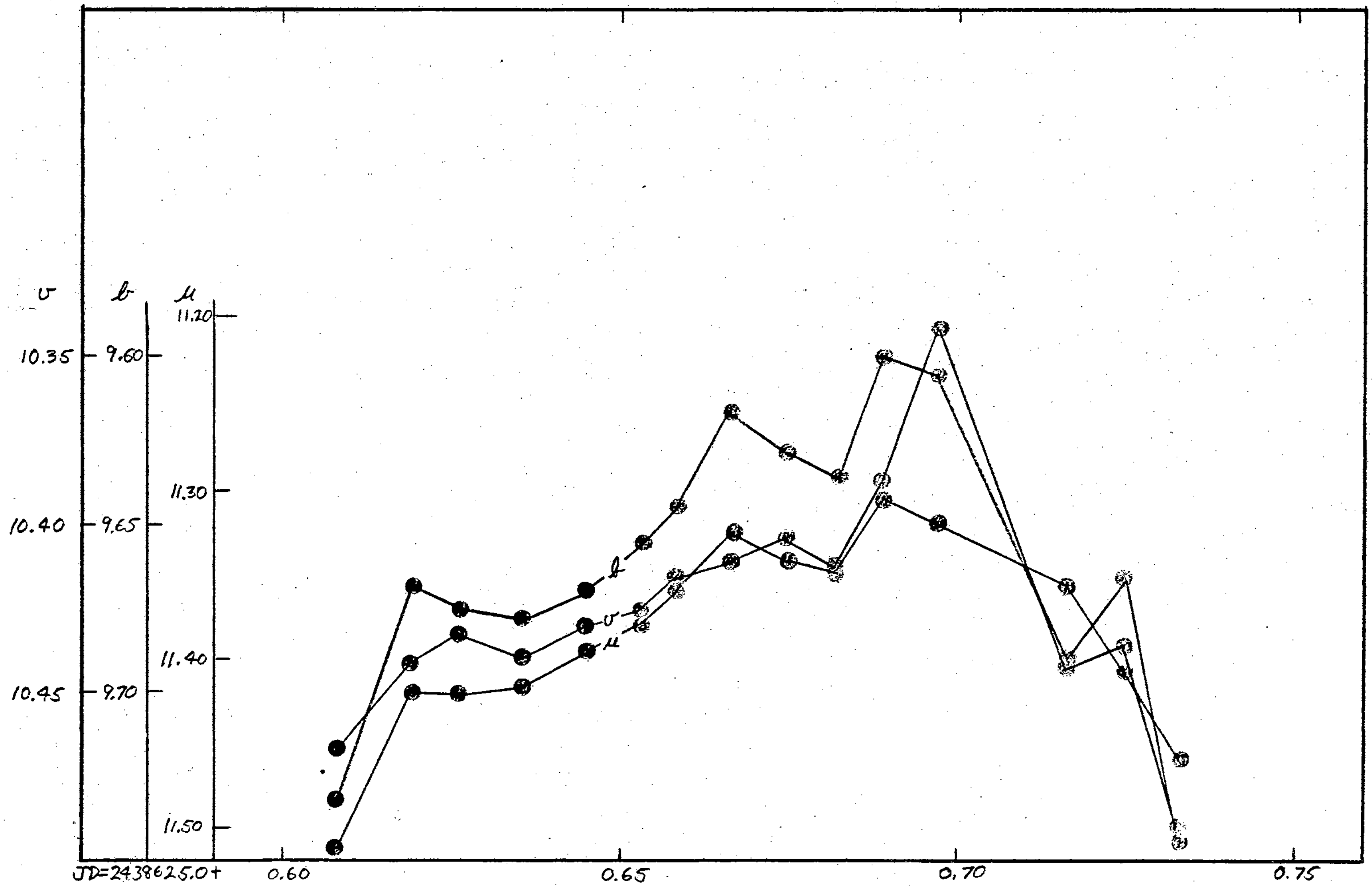

Figure 5. Preliminary Light Curves of HD199938 for August 18, 1964.

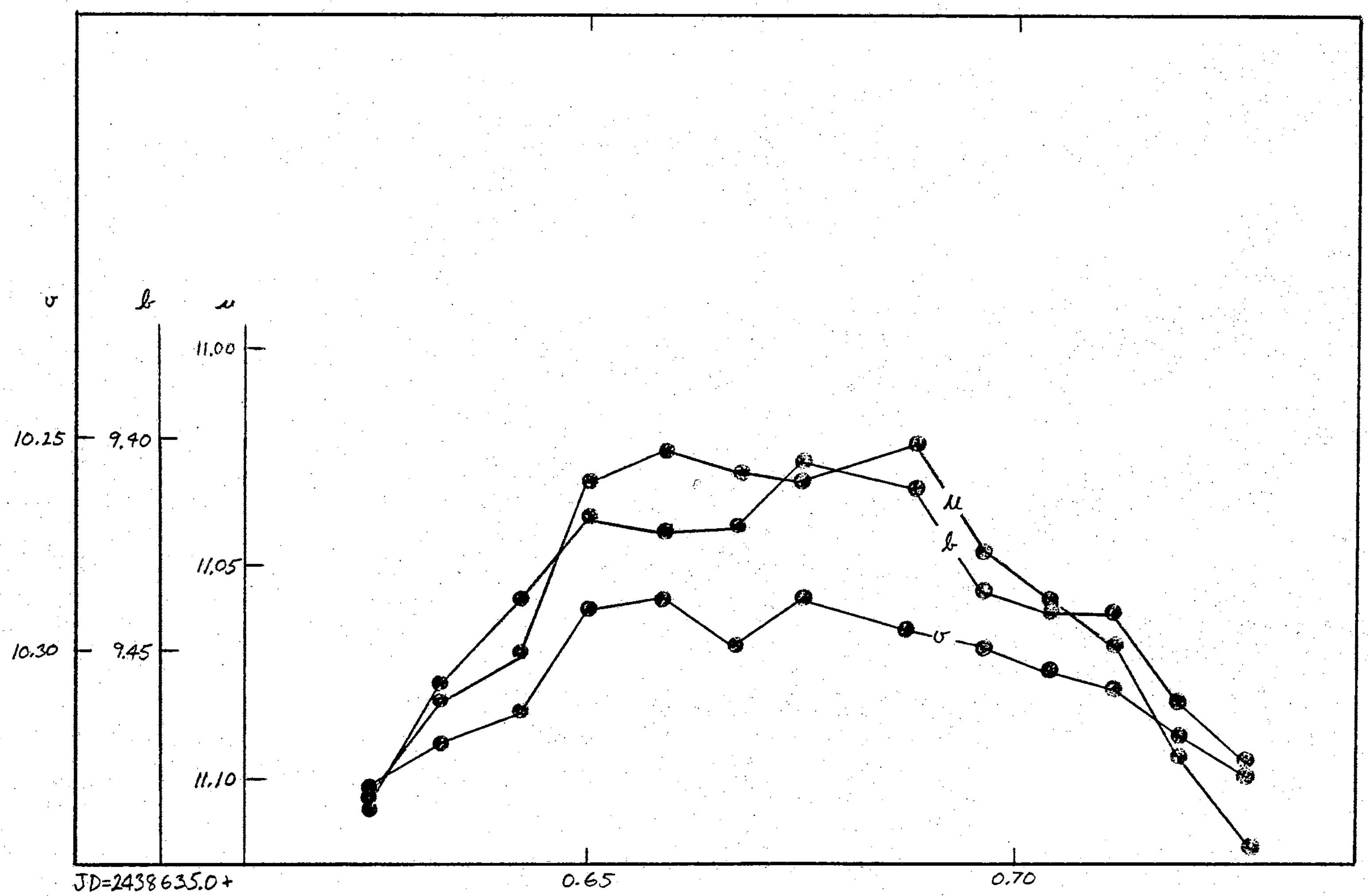

Figure 6. Preliminary Light Curves of HD199938 for August 28, 1964.

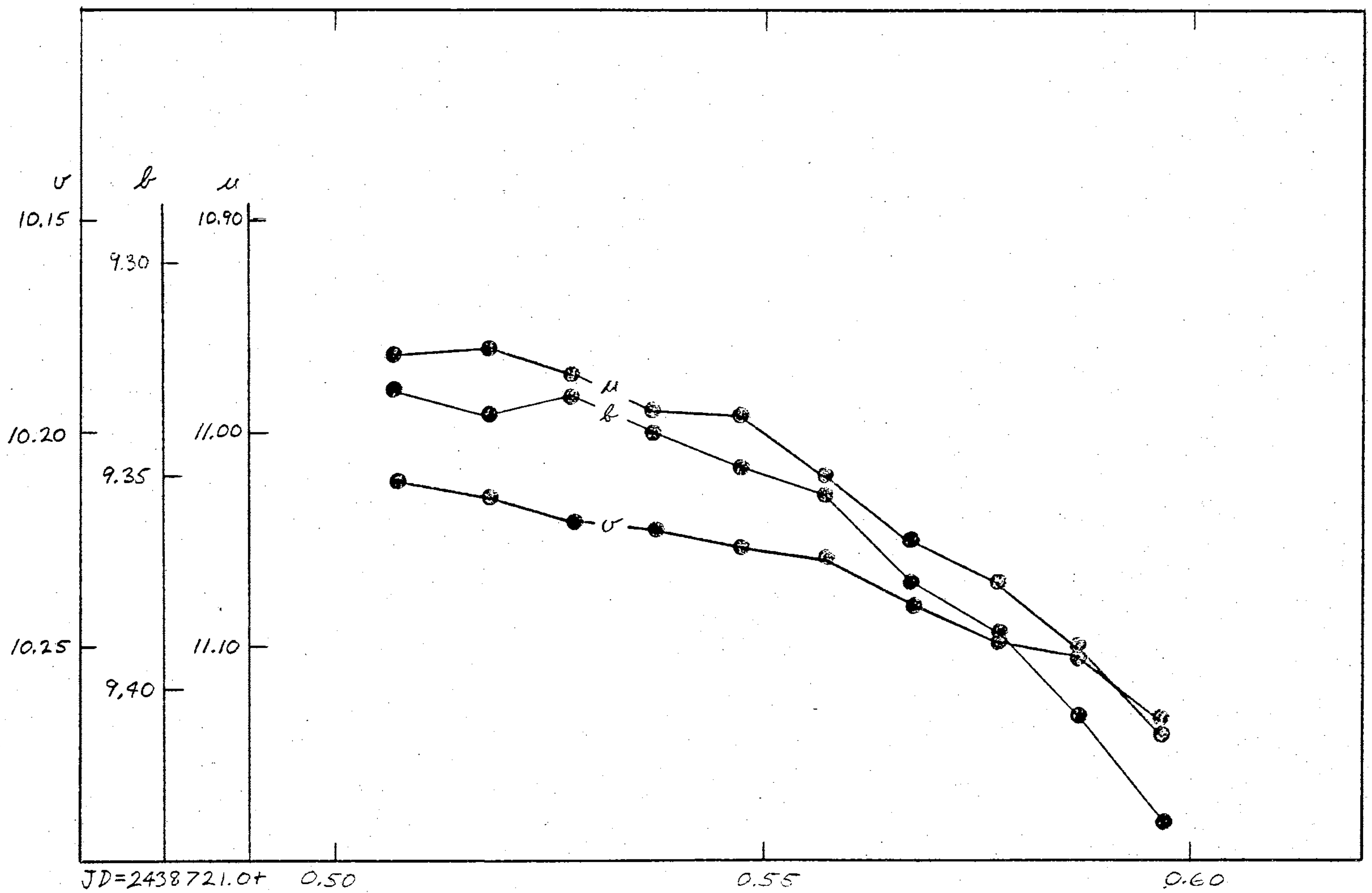

Figure 7. Preliminary Light Curves of HD199938 for November 22, 1964.

On August 17, the light curve again shows a decrease in the amount of light, after a short preliminary rise. This corresponds to decreasing hour angle for the first three observations and subsequently increasing hour angle and, hence, air mass. It should be noted that between about JD = 2438624.80 and .82 there is a knee in the curve, suggesting a change in extinction. An extinction change is also confirmed by the fact that the night ended with a fog layer extending 25 feet above the dome of the observatory! This fog layer made it impossible to obtain extinction star measurements; a fact that will complicate the reduction of the night.

On August 18, the light curves again follow the change in air mass quite closely, the peaks of the curves corresponding to the time of culmination. This night also ended with haze affecting the measurements.

The curve for August 28 is comparable to that of the 18th. Maximum light occurs at culmination and the extinction appears to be uniform through the night.

The air mass was constantly increasing on November 22, as is reflected by the light curve. From the curve it appears that the extinction for the night was reasonably constant.

Extinction (Excluding August 17, 1964)

Equations (2.17) are used to obtain the extinction and the short method described by Hardie is used. The values of the various parameters which are used in these equations have been carefully determined by the astronomers of the Dyer observatory by the methods of Hardie (1962), and are given in Table I. Tables II through V give the extinction data for the four nights when extinction star observations were taken, and

Figures 8 through 11 show the plotted points and the least squares line fitted to each set. The values of the coefficients of these lines, which are the extinctions and zero points, are given in Table VI.

TABLE I

COEFFICIENTS OF EXTINCTION EQUATIONS AT THE DYER OBSERVATORY IN 1964

coefficient	value
ϵ	-0.007
ψ	+0.976
μ	+1.035
G_x	+1.000
k_{bv}	-0.04

TABLE II

EXTINCTION DATA FOR AUGUST 13, 1964

Star	HR 8832	10 Lac	β Aql	ϵ Aqr	74 Aqr	ι Psc
V	5.57	4.88	3.71	3.77	5.81	4.13
B-V	+1.010	-0.203	+0.86	+0.01	-0.08	+0.51
U-B	+0.89	-1.04	+0.48	+0.04	-0.32	0.00
v	7.782	7.094	6.435	6.508	8.183	6.393
b	7.474	5.603	6.232	5.619	6.969	5.609
u	9.983	6.202	9.158	7.950	8.462	7.274
$v+\epsilon(B-V)-V$	2.205	2.215	2.719	2.738	2.374	2.260
$\mu J_x(b-v)-(B-V)$	-1.343	-1.407	-1.096	-1.047	-1.264	-1.361
$\psi G_x(u-b)-(U-B)$	1.559	1.625	2.376	2.235	1.777	1.625
X	1.098	1.086	3.045	3.178	1.746	1.223

(For magnitude and colors of listed stars, see Johnson and Morgan 1953).

TABLE III

EXTINCTION DATA FOR AUGUST 18, 1964

Star	κ Aql	β Aql	α Del	ϵ Aqr	10 Lac	HR 8832	10 Lac	HR 8832
V	4.96	3.71	3.77	3.77	4.88	5.57	4.88	5.57
B-V	-0.01	+0.86	-0.06	+0.01	-0.203	+1.010	-0.203	+1.010
U-B	-0.87	+0.48	-0.22	+0.04	-1.04	+0.89	-1.04	+0.89
v	7.539	6.225	6.295	6.562	7.568	8.275	7.333	8.060
b	6.625	6.023	5.214	5.668	6.411	8.209	5.978	7.859
u	7.731	8.364	6.879	7.733	7.374	11.160	6.686	10.544
$v+\epsilon(B-V)-V$	2.579	2.509	2.525	2.792	2.689	2.698	2.454	2.483
$\mu J_X(b-v)-(B-V)$	-0.994	-1.080	-1.116	-1.005	-1.069	-1.083	-1.260	-1.228
$\psi G_X(u-b)-(U-B)$	1.949	1.805	1.845	1.975	1.980	1.990	1.731	1.731
X	1.524	1.286	1.286	1.883	1.561	1.587	1.072	1.165

TABLE IV

EXTINCTION DATA FOR AUGUST 28, 1964

Star	κ Aql	β Aql	ϵ AQR	ι Psc	10 Lac	HR 8832	10 Lac	HR 8832
V	4.96	3.71	3.77	4.13	4.88	5.57	4.88	5.57
B-V	-0.01	+0.86	+0.01	+0.51	-0.203	+1.010	-0.203	+1.010
U-B	-0.87	+0.48	+0.04	0.00	-1.04	+0.89	-1.04	+0.89
v	7.382	6.083	6.297	7.052	7.302	8.020	7.172	7.893
b	6.290	5.732	5.209	6.642	5.931	7.783	5.710	7.590
u	7.207	7.928	7.079	8.890	6.637	10.485	6.303	10.132
$v+\epsilon(B-V)-V$	2.422	2.367	2.527	2.918	2.423	2.443	2.293	2.316
$\mu J_x(b-v)-(B-V)$	-1.183	-1.240	-1.208	-0.980	-1.290	-1.269	-1.371	-1.337
$\psi G_x(u-b)-(U-B)$	1.765	1.663	1.785	2.194	1.729	1.747	1.619	1.591
X	1.396	1.184	1.102	1.147	1.089	1.092	1.077	1.080

TABLE V

EXTINCTION DATA FOR NOVEMBER 22, 1964

Star	β Aql	ϵ Aqr	ι Psc	β Aql	ϵ Aqr	α Aql	74 Aqr	η Psc
V	3.71	3.77	4.13	3.71	3.77	3.77	5.81	3.62
B-V	+0.86	+0.01	+0.51	+0.86	+0.01	-0.06	-0.08	+0.97
U-B	+0.48	+0.04	0.00	+0.48	+0.04	-0.22	-0.32	+0.76
v	6.045	6.100	6.431	6.614	6.698	6.326	8.269	5.937
b	5.636	4.935	5.660	6.501	5.929	5.187	7.053	5.577
u	7.855	6.755	7.358	9.828	8.470	7.009	8.689	7.955
$v+\epsilon(B-V)-V$	2.329	2.330	2.297	2.898	2.928	2.556	2.458	2.310
$\mu J_x(b-v)-(B-V)$	-1.306	-1.291	-1.347	-0.994	-0.931	-1.342	-1.435	-1.359
$\psi G_x(u-b)-(U-B)$	1.686	1.736	1.657	2.767	2.440	1.998	1.917	1.561
X	1.360	1.559	1.216	3.724	3.934	2.176	1.912	1.072

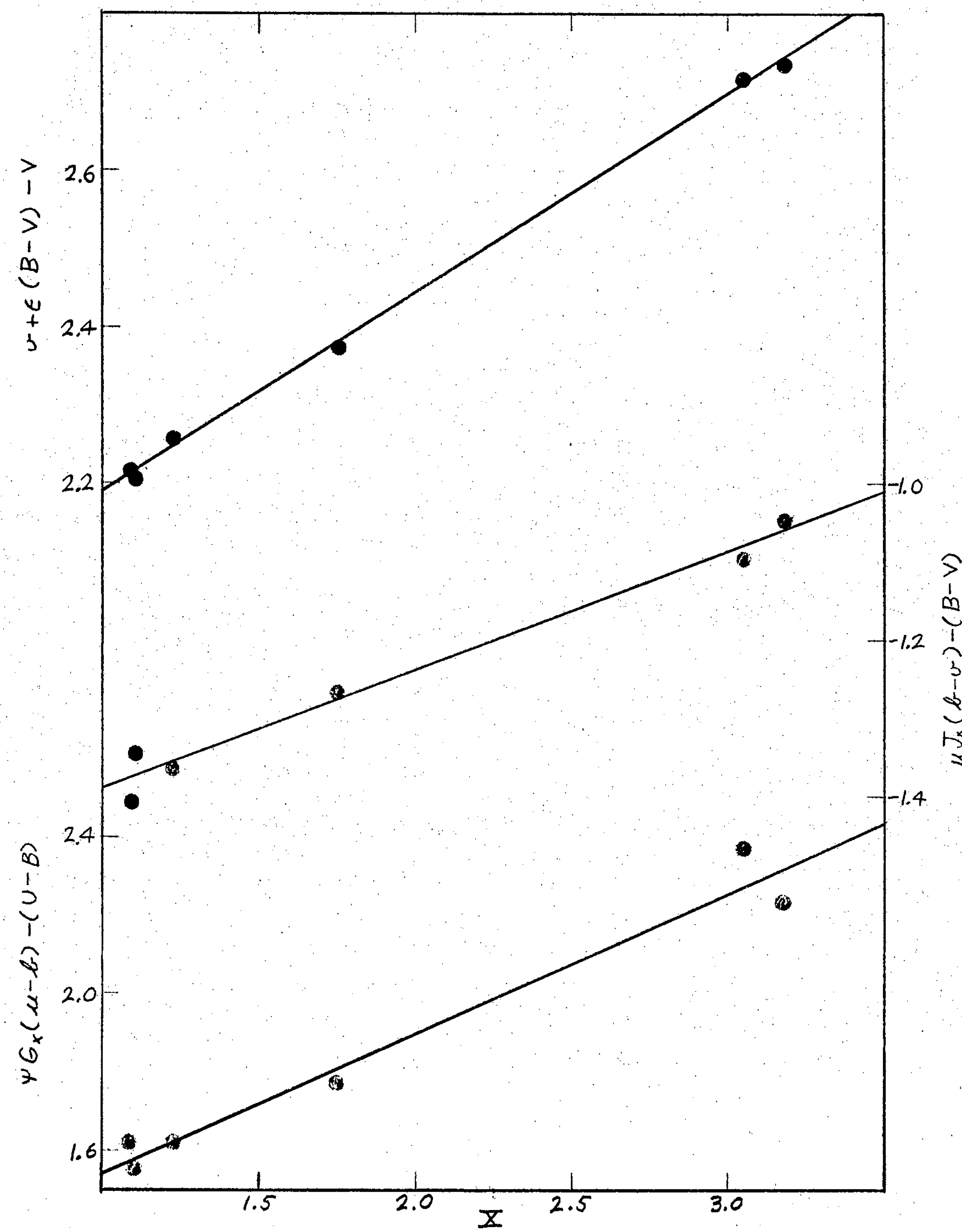

Figure 8. Extinction Regression Lines for August 13, 1964.

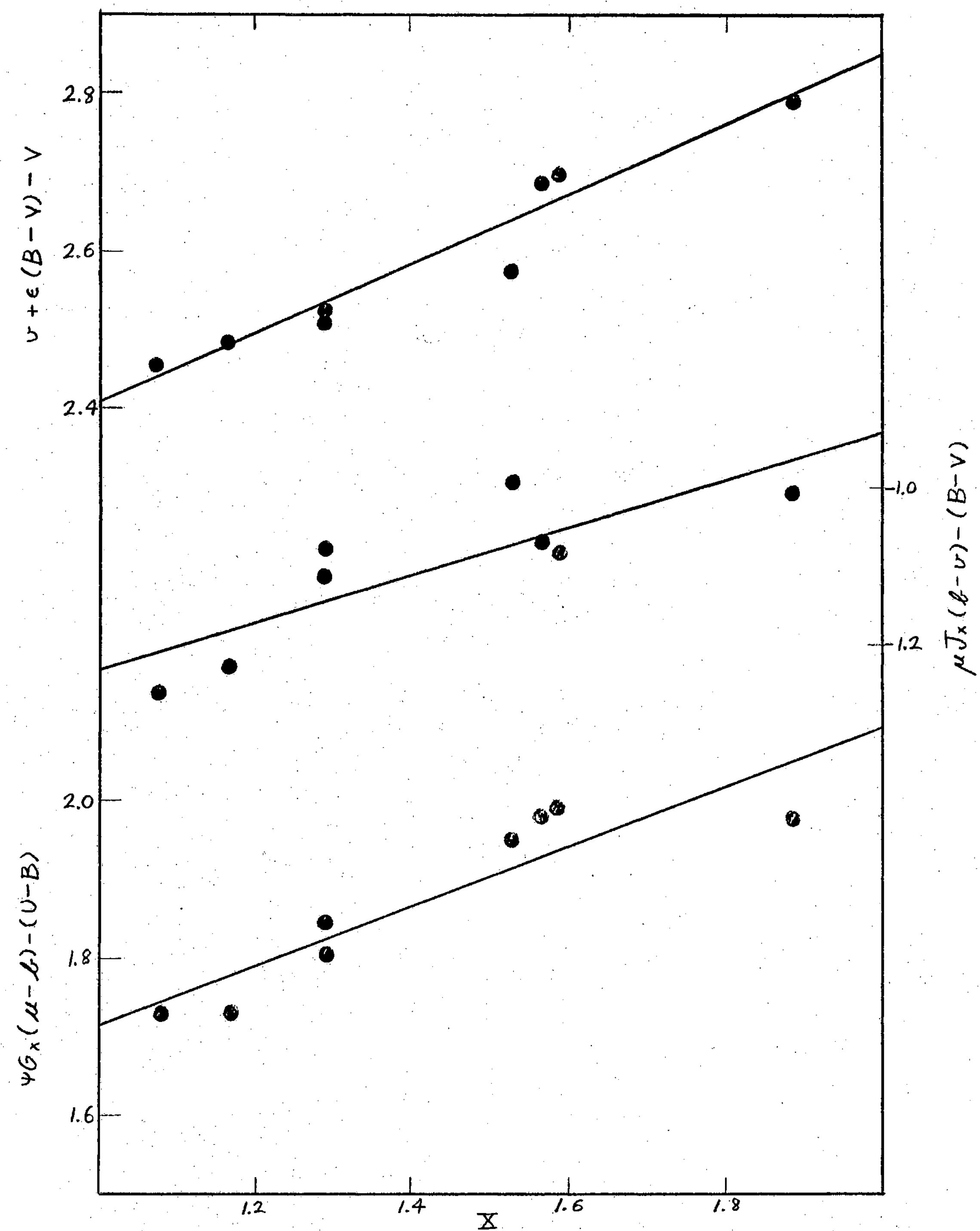

Figure 9. Extinction Regression Lines for August 18, 1964.

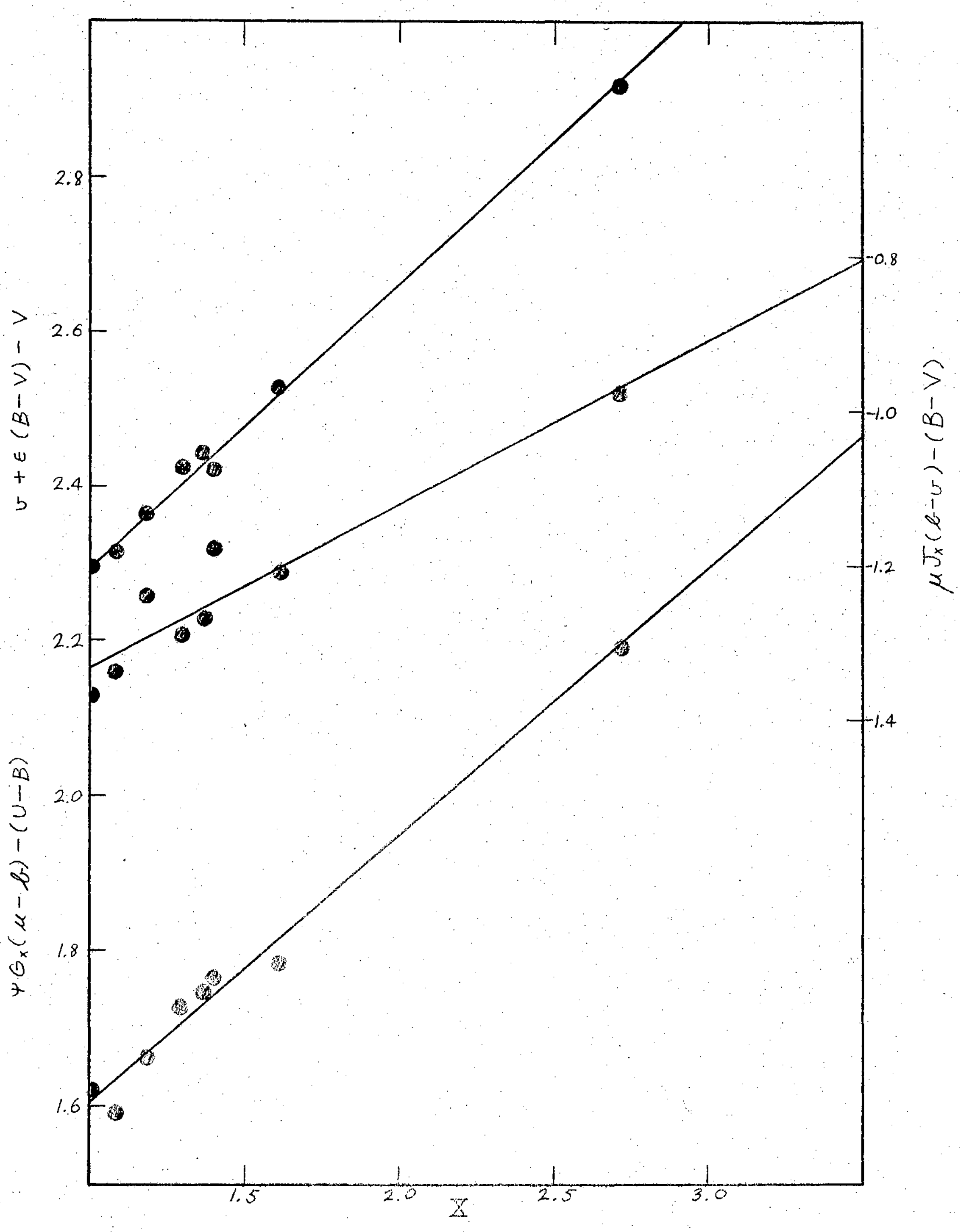

Figure 10. Extinction Regression Lines for August 28, 1964.

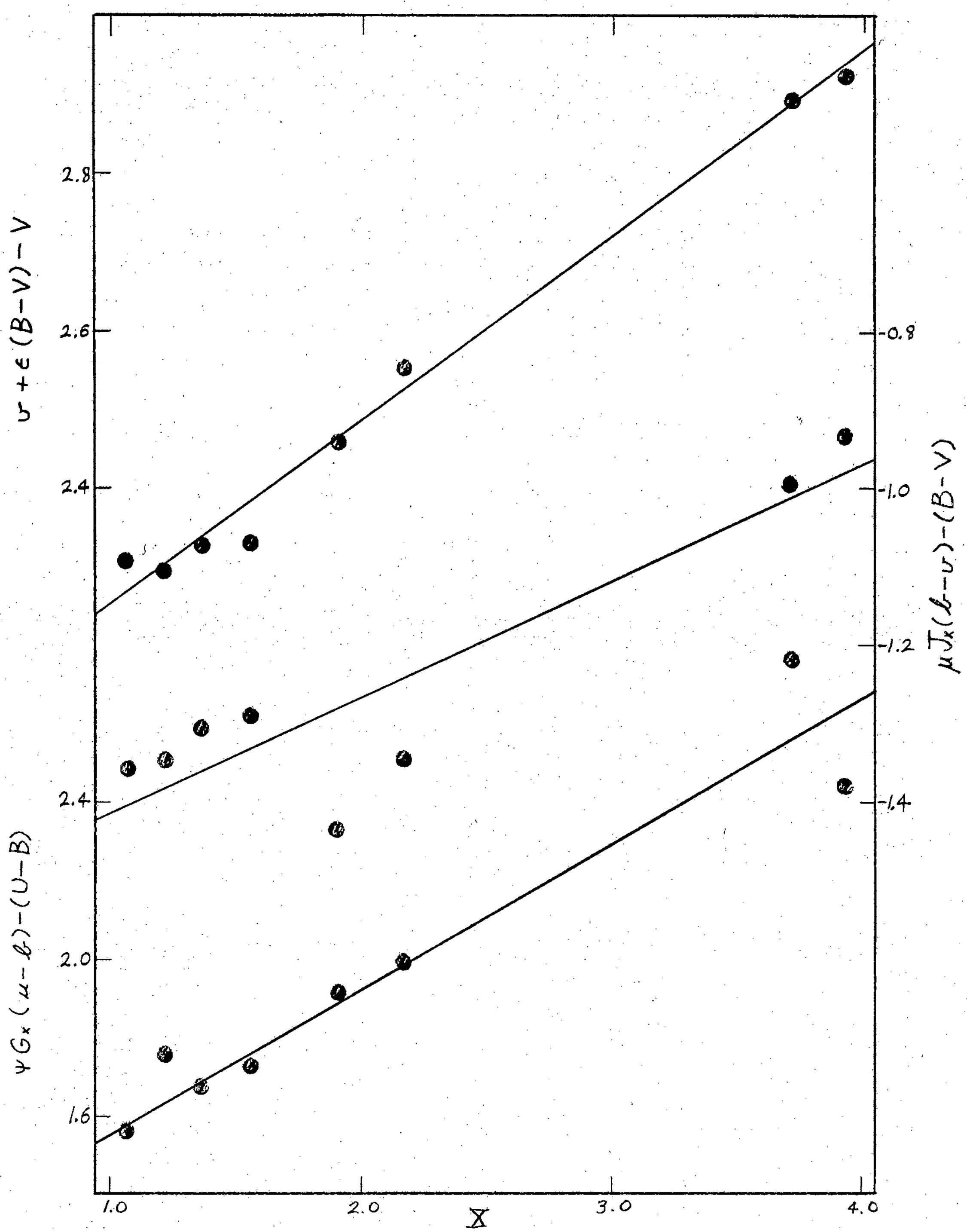

Figure 11. Extinction Regression Lines for November 22, 1964.

TABLE VI

EXTINCTION AND ZERO-POINT VALUES FOR AUGUST 13, 18, 28, AND NOVEMBER 22, 1964

	k_V	ζ_V	k'_{bv}	ζ_{bv}	k'_{ub}	ζ_{ub}
August 13	0.254	-1.936	0.151	1.540	0.354	-1.195
August 18	0.441	-1.964	0.303	1.534	0.381	-1.334
August 28	0.364	-1.933	0.211	1.542	0.344	-1.261
November 22	0.233	-2.019	0.148	1.564	0.367	-1.192

Comparison Star Evaluation

Using the values of the extinction listed in Table VI, Equations (2.17) are used to obtain values of V, B-V, U-B for the comparison star, HD199938, and a control star, HD199067, on each night when extinction coefficients are available. The reductions are given in Tables VII through X.

The magnitudes and colors obtained for the comparison and control stars are plotted together in Figures 12 through 15 for purposes of comparison. An examination of the figures shows that the magnitudes and colors of the two stars tend to vary together, indicating that the variability is due to changes in extinction rather than to intrinsic variability of the stars.

In order to arrive at "best" values for magnitude and color it was decided to take the values nearest the extinction measurement for each night. When extinction was taken at the beginning and end of a night, a weighted mean of the nearest values was taken (the weight was 2 for the value near the larger group of extinction stars and 1 for the value near the smaller). The results are given in Table XI.

TABLE VII

COMPARISON AND CONTROL STAR REDUCTION FOR AUGUST 13, 1964
HD199938

JD = 2438620+	v	b	u	V	B-V	U-B	X
0.7502	10.143	9.260	10.843	7.931	0.424	-0.030	1.073
0.7642	10.156	9.275	10.857	7.941	0.425	-0.035	1.084
0.7717	10.162	9.275	10.869	7.946	0.416	-0.025	1.092
0.7796	10.154	9.260	10.854	7.934	0.408	-0.029	1.100
0.7874	10.182	9.285	10.891	7.960	0.401	-0.022	1.112
0.7929	10.187	9.300	10.900	7.964	0.411	-0.029	1.119
0.8014	10.197	9.305	10.915	7.970	0.404	-0.026	1.134
0.8097	10.199	9.306	10.921	7.968	0.399	-0.026	1.150
0.8177	10.218	9.327	10.952	7.982	0.398	-0.022	1.166
0.8255	10.213	9.321	10.947	7.973	0.394	-0.028	1.186
0.8335	10.220	9.340	10.981	7.975	0.403	-0.020	1.206
0.8409	10.228	9.330	10.985	7.977	0.379	-0.014	1.227
0.8485	10.225	9.353	11.018	7.969	0.403	-0.012	1.248
0.8562	10.219	9.373	11.045	7.954	0.427	-0.015	1.276
0.8618	10.222	9.367	11.036	7.954	0.413	-0.024	1.294
			HD199067				
0.7544	8.954	7.753	9.457	6.745	0.081	0.089	1.072
0.7615	8.968	7.757	9.448	6.758	0.069	0.073	1.078
0.7902	8.992	7.766	9.488	6.772	0.045	0.091	1.115
0.8590	9.050	7.861	9.624	6.788	0.052	0.072	1.284

TABLE VIII

COMPARISON AND CONTROL STAR REDUCTION FOR AUGUST 18, 1964
HD199938

JD = 2438625+	v	b	u	V	B-V	U-B	X
0.6087	10.467	9.732	11.513	7.984	+0.384	-0.042	1.170
0.6182	10.442	9.669	11.420	7.967	+0.349	-0.063	1.149
0.6262	10.433	9.675	11.421	7.977	+0.360	-0.062	1.133
0.6356	10.440	9.678	11.416	7.980	+0.372	-0.064	1.118
0.6445	10.431	9.670	11.396	7.977	+0.377	-0.069	1.104
0.6526	10.426	9.656	11.381	7.976	+0.371	-0.068	1.095
0.6585	10.416	9.645	11.360	7.969	+0.372	-0.075	1.088
0.6661	10.412	9.617	11.326	7.969	+0.348	-0.078	1.081
0.6736	10.405	9.629	11.343	7.963	+0.370	-0.071	1.075
0.6816	10.413	9.637	11.348	7.974	+0.373	-0.072	1.070
0.6892	10.388	9.600	11.307	7.951	+0.361	-0.075	1.067
0.6968	10.392	9.606	11.319	7.958	+0.373	-0.068	1.065
0.7162	10.443	9.690	11.356	8.006	+0.400	-0.114	1.065
0.7246	10.436	9.667	11.409	7.998	+0.381	-0.041	1.067
0.7325	10.490	9.745	11.460	8.051	+0.406	-0.068	1.071

HD199067

JD = 2438625+	v	b	u	V	B-V	U-B	X
0.6056	9.279	8.230	10.102	6.803	+0.047	+0.050	1.161
0.6556	9.229	8.125	9.939	6.788	+0.015	+0.024	1.081
0.6998	9.213	8.109	9.905	6.783	+0.023	+0.016	1.057
0.7112	9.220	8.114	9.922	6.789	+0.021	+0.028	1.058

TABLE IX

COMPARISON AND CONTROL STAR REDUCTION FOR AUGUST 28, 1964

HD199938

JD = 2438635+	v	b	u	V	B-V	U-B	X
0.6245	10.297	9.451	11.068	7.962	+0.397	-0.060	1.095
0.6330	10.286	9.423	11.048	7.954	+0.381	-0.049	1.086
0.6413	10.280	9.403	11.012	7.952	+0.369	-0.061	1.075
0.6496	10.255	9.383	10.995	7.929	+0.376	-0.056	1.070
0.6583	10.255	9.390	10.995	7.930	+0.384	-0.063	1.068
0.6671	10.261	9.389	10.992	7.937	+0.377	-0.063	1.065
0.6747	10.251	9.373	11.000	7.927	+0.371	-0.039	1.064
0.6878	10.257	9.380	10.988	7.933	+0.372	-0.048	1.065
0.6961	10.269	9.402	11.012	7.944	+0.381	-0.057	1.067
0.7036	10.272	9.408	11.020	7.946	+0.385	-0.056	1.070
0.7112	10.272	9.408	11.040	7.944	+0.383	-0.038	1.075
0.7188	10.292	9.434	11.058	7.962	+0.387	-0.048	1.080
0.7267	10.297	9.441	11.083	7.965	+0.389	-0.032	1.088

HD199067

JD = 2438635+	v	b	u	V	B-V	U-B	X
0.6198	9.130	7.956	9.683	6.800	+0.044	+0.050	1.090
0.6777	9.069	7.855	9.578	6.751	+0.009	+0.057	1.057
0.6838	9.082	7.865	9.582	6.764	+0.006	+0.051	1.058
0.7294	9.113	7.927	9.656	6.784	+0.032	+0.053	1.088

TABLE X

COMPARISON AND CONTROL STAR REDUCTION FOR NOVEMBER 22, 1964
HD199938

JD = 2438721+	v	b	u	V	B-V	U-B	X
0.5075	10.212	9.330	10.963	7.932	+0.447	-0.005	1.108
0.5179	10.215	9.336	10.960	7.932	+0.449	-0.017	1.117
0.5277	10.221	9.331	10.972	7.933	+0.433	-0.008	1.138
0.5378	10.223	9.340	10.988	7.931	+0.437	-0.010	1.159
0.5474	10.227	9.348	10.991	7.930	+0.445	-0.022	1.181
0.5577	10.230	9.355	11.020	7.927	+0.437	-0.010	1.206
0.5681	10.241	9.375	11.050	7.930	+0.441	-0.011	1.238
0.5776	10.250	9.388	11.070	7.932	+0.438	-0.016	1.269
0.5871	10.253	9.406	11.101	7.927	+0.450	-0.016	1.302
0.5964	10.267	9.431	11.142	7.933	+0.455	-0.013	1.337
			HD199067				
0.5037	9.025	7.821	9.550	6.780	+0.102	+0.092	1.100
0.5999	9.102	7.939	9.761	6.765	+0.092	+0.084	1.366

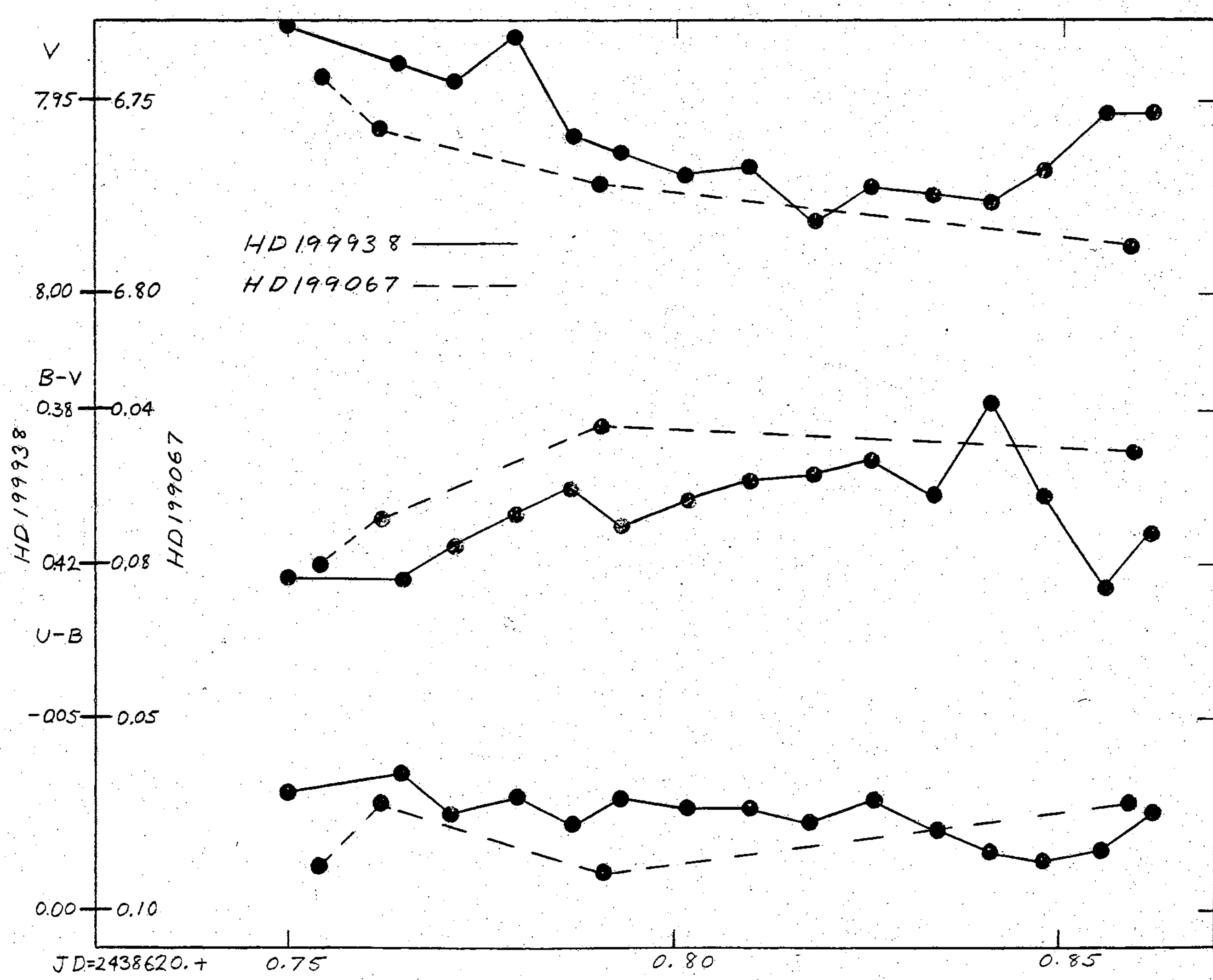

Figure 12. Light Curves of HD199938 and HD199067 for August 13, 1964.

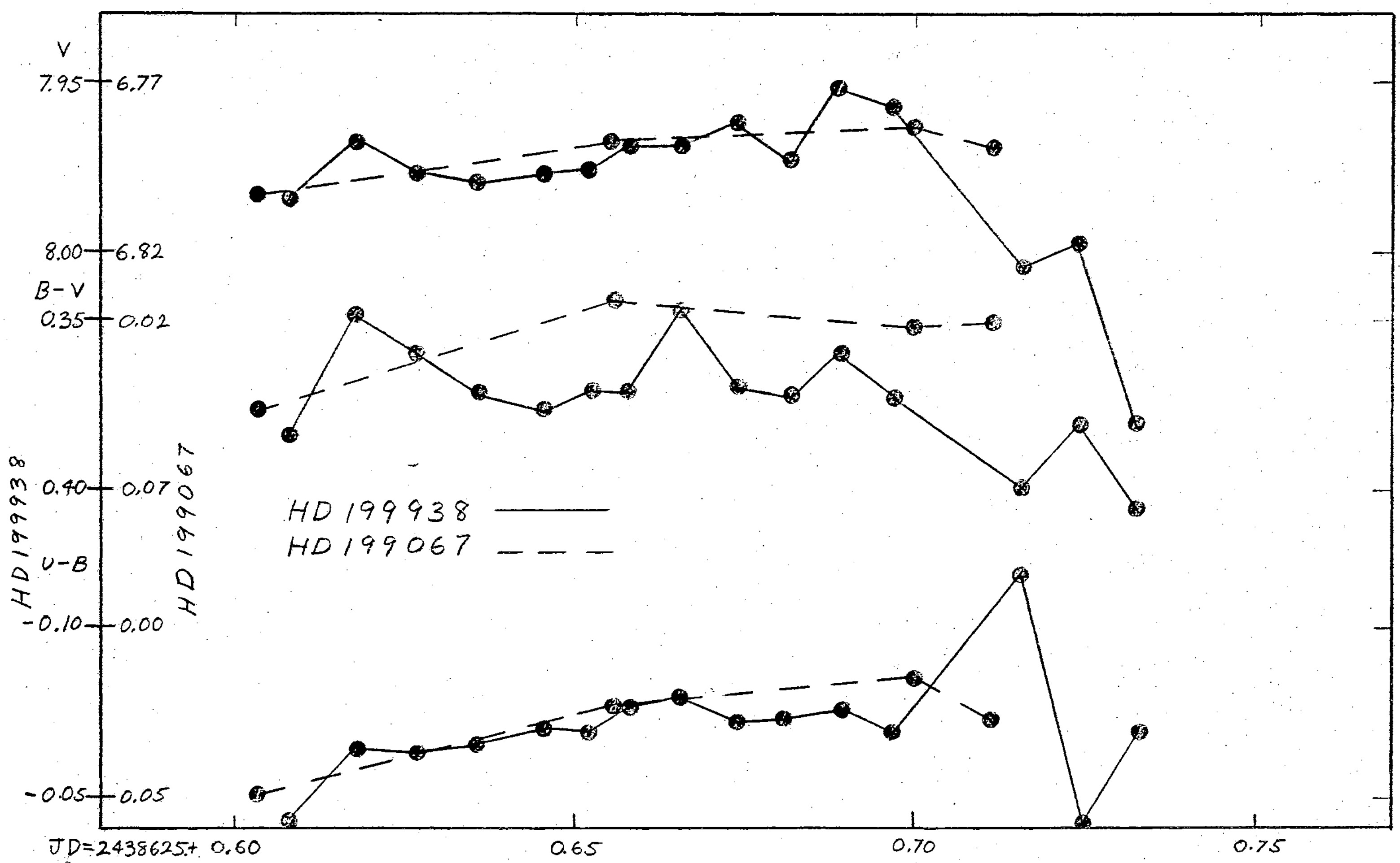

Figure 13. Light Curves of HD199938 and HD199067 for August 18, 1964.

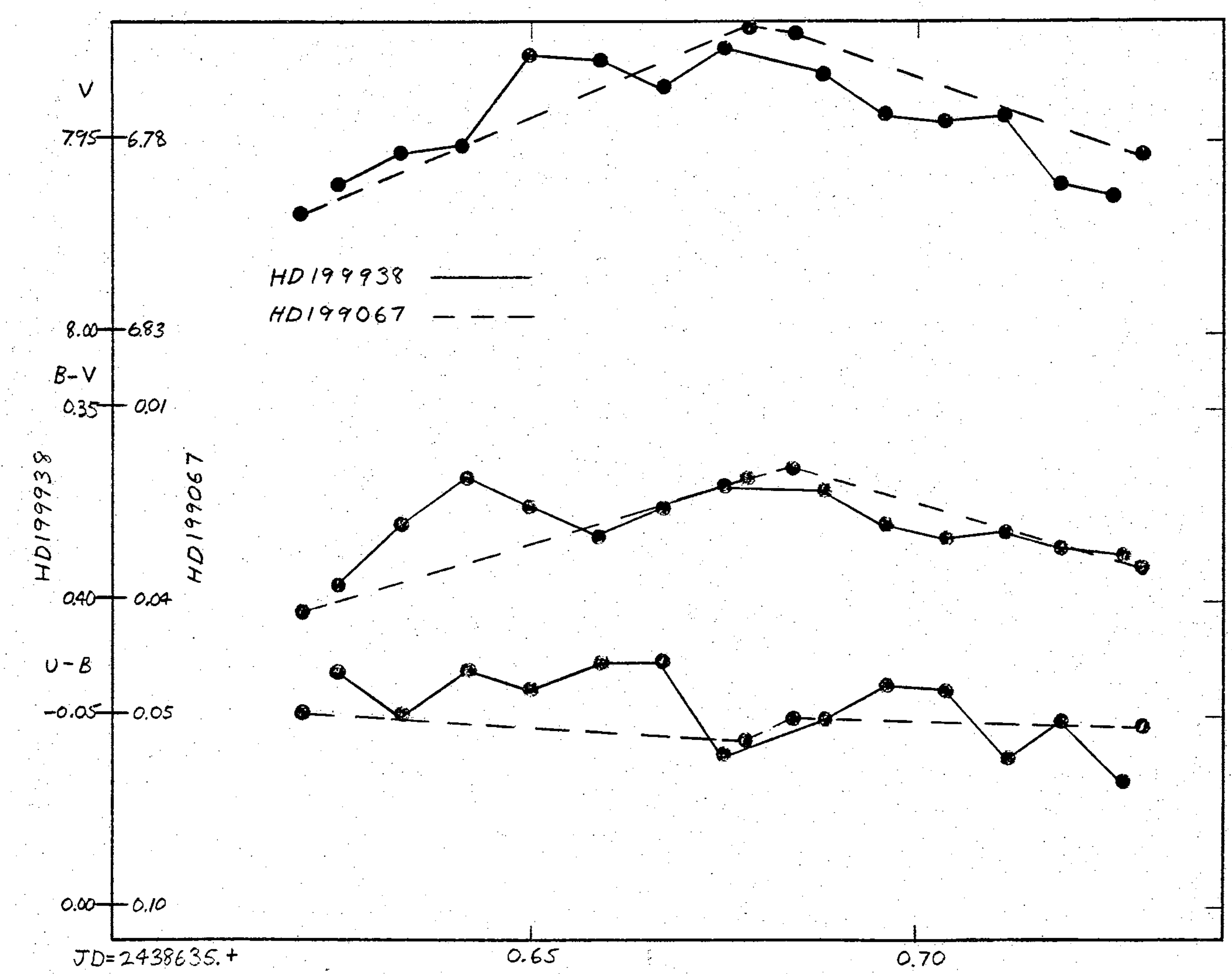

Figure 14. Light Curves of HD199938 and HD199067 for August 28, 1964.

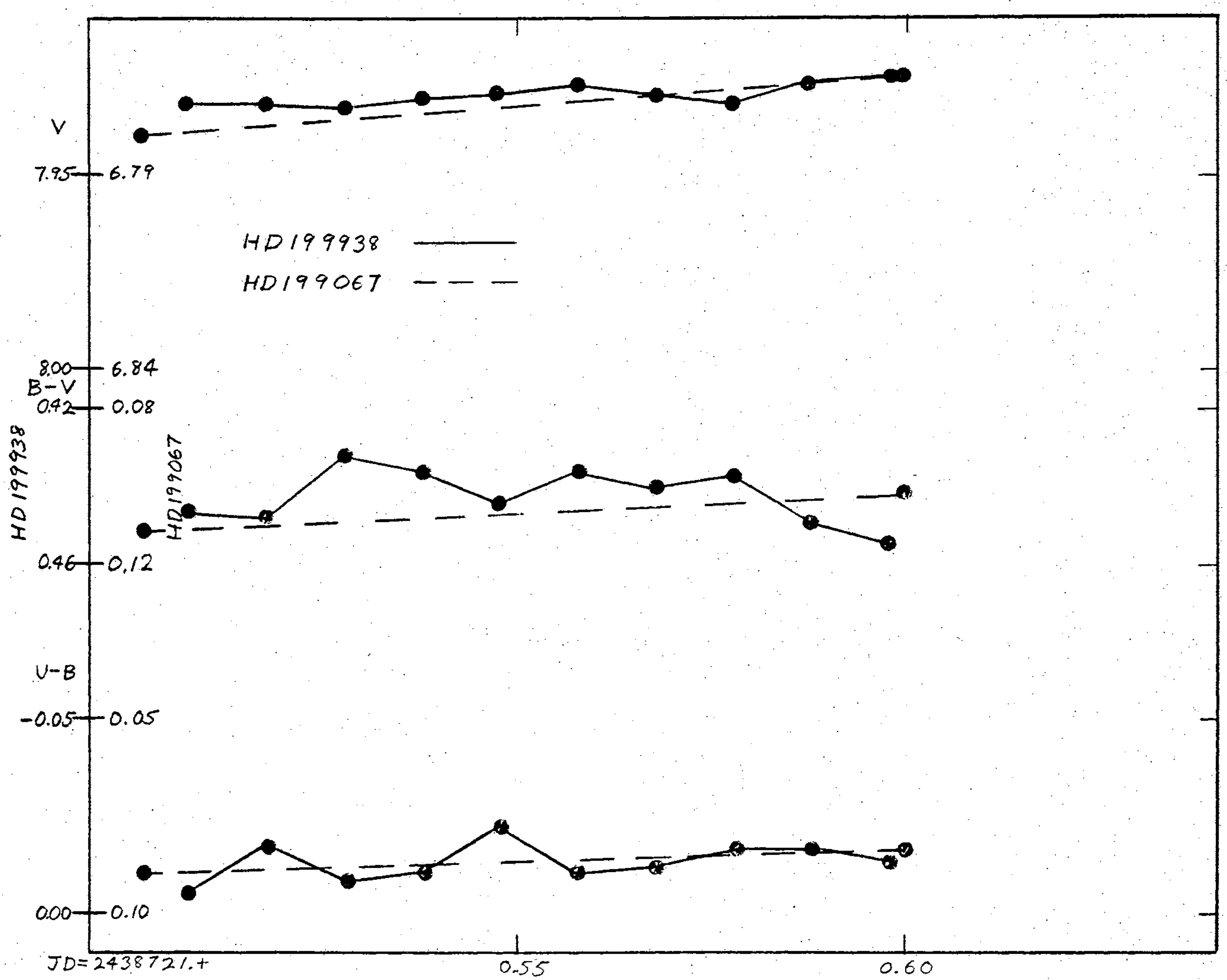

Figure 15. Light Curves of HD199938 and HD199067 for November 22, 1964.

TABLE XI

UBV CALIBRATION OF COMPARISON STARS

	V	B-V	U-B
HD199938	7.96 ± .010	0.41 ± .019	-0.03 ± .012
HD199067	6.79 ± .007	0.06 ± .010	0.06 ± .016

Extinction for August 17, 1964

On the basis of the preliminary light curve of HD199938 (Figure 4) there is evidence that the extinction changed considerably during the night. Therefore, the night was split into an early and a late half and separate extinctions determined for each half. With values of magnitudes and colors now available, the extinction can be found by using the comparison stars as extinction stars. Table XII gives the extinction data for August 17, 1964, and Figure 16 shows the points with regression lines fitted from observations 6 through 17 and from 18 through 28. The values of the extinction obtained are given in Table XIII.

TABLE XII

EXTINCTION DATA FOR AUGUST 17, 1964

OBS#	v	b	u	$v+\varepsilon(B-V)$ $-V$	$\mu J_x(b-v)$ $-(B-V)$	$\nu G_x(u-b)$ $-(U-B)$	X
1	7.109	5.774	6.410	2.230	-1.246	1.661	1.177
2	7.823	7.637	10.227	2.246	-1.212	1.638	1.263
3	9.007	7.860	9.561	2.217	-1.298	1.600	1.065
4	10.193	9.367	10.971	2.230	-1.302	1.596	1.071
5	10.217	9.361	10.959	2.254	-1.334	1.590	1.068

TABLE XII (Continued)

OBS#	v	b	u	v+ε(B-V) -V	μJ_x(b-v) -(B-V)	ψG_x(u-b) -(U-B)	X
6	9.045	7.838	9.544	2.255	-1.362	1.605	1.058
7	10.223	9.355	10.956	2.260	-1.346	1.593	1.065
8	10.228	9.342	10.958	2.265	-1.366	1.607	1.066
9	10.234	9.355	10.957	2.271	-1.359	1.594	1.070
10	10.231	9.356	10.970	2.268	-1.355	1.605	1.075
11	10.243	9.370	10.985	2.280	-1.353	1.606	1.081
12	10.250	9.379	10.998	2.287	-1.351	1.610	1.089
13	10.250	9.385	11.003	2.287	-1.344	1.609	1.099
14	10.245	9.385	10.996	2.282	-1.340	1.602	1.110
15	10.249	9.380	11.012	2.286	-1.350	1.623	1.122
16	10.255	9.390	11.028	2.292	-1.346	1.629	1.138
17	10.260	9.402	11.042	2.297	-1.339	1.631	1.157
18	10.274	9.421	11.069	2.311	-1.334	1.638	1.178
19	9.100	7.929	9.678	2.310	-1.330	1.647	1.190
20	10.293	9.443	11.103	2.330	-1.332	1.650	1.191
21	10.319	9.498	11.204	2.356	-1.301	1.695	1.211
22	10.346	9.531	11.218	2.383	-1.295	1.676	1.238
23	10.345	9.520	11.225	2.382	-1.307	1.694	1.260
24	10.351	9.537	11.240	2.388	-1.296	1.692	1.289
25	10.376	9.575	11.291	2.413	-1.283	1.705	1.318
26	10.391	9.602	11.326	2.428	-1.271	1.713	1.349
27	10.399	9.608	11.355	2.436	-1.274	1.735	1.377
28	9.239	8.126	9.973	2.449	-1.277	1.743	1.407

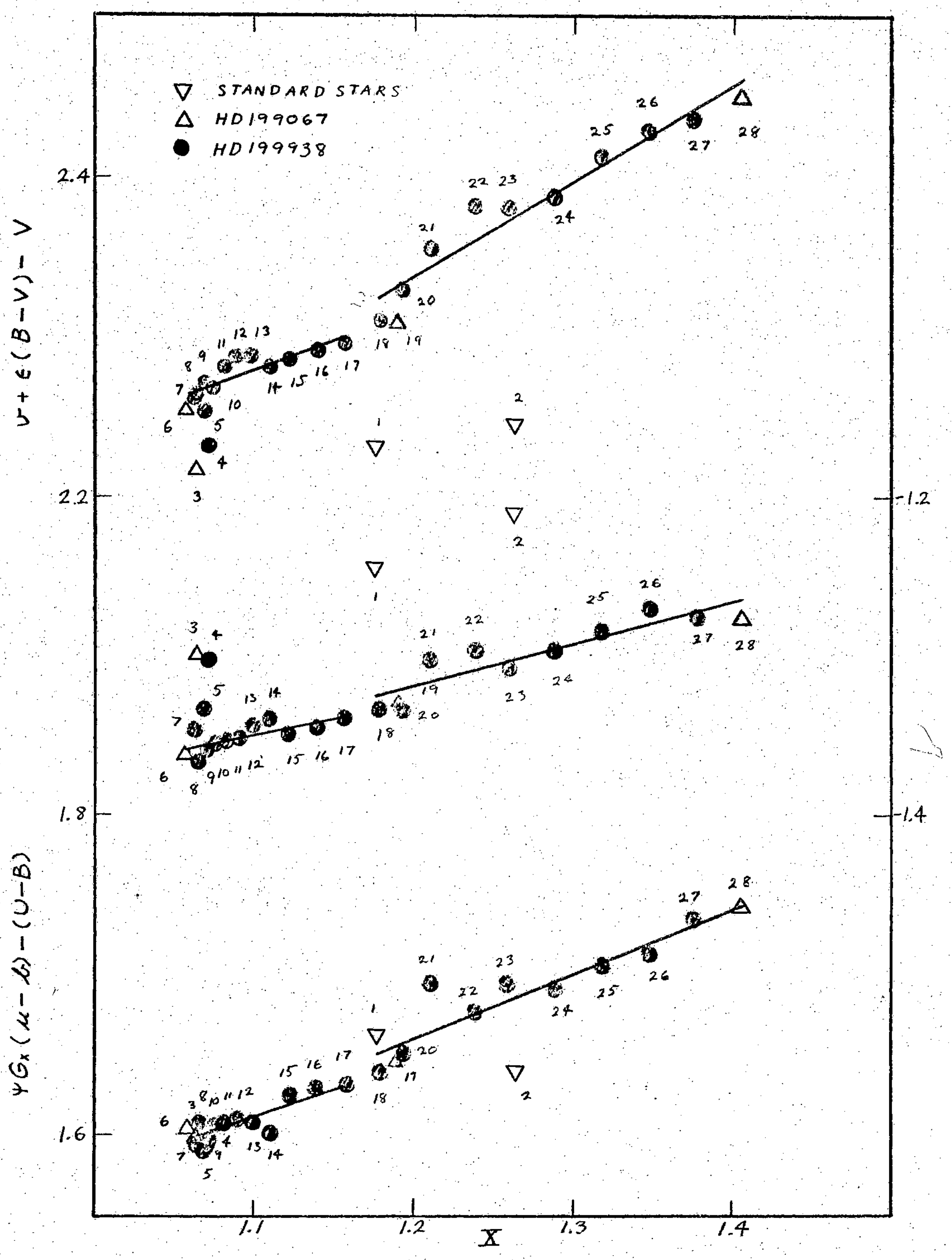

Figure 16. Extinction Regression Lines for August 17, 1964.

TABLE XIII

EARLY AND LATE EXTINCTION AND ZERO-POINT VALUES FOR AUGUST 17, 1964

	k_v	ζ_v	$\mu k'_{bv}$	ζ_{bv}	$\psi k'_{ub}$	ζ_{ub}
Early	0.376	-1.866	0.331	-1.248	0.196	1.565
Late	0.590	-1.630	0.403	-1.177	0.266	1.639

Computation of DQ Cephei Light Curves

The values of the zero-point terms at each observation of the comparison star are obtained by inserting the values given in Table XI in Equations (2.17). Interpolated values of the zero-point terms are then available for computation of the reduction for the variable star. The Julian Day was reduced to the center of the sun by the method outlined in the previous chapter. The correction terms are given in Table XIV. Table XV presents the raw and reduced data for DQ Cephei. The data marked doubtful either required an extrapolation of the zero-point term, or were obviously affected by haze. The light curves are given in Figures 17 through 46 where, as elsewhere, Δ = HD199938 minus DQ Cephei.

TABLE XIV

HELIOCENTRIC JULIAN DAY CORRECTION TERMS

Date			Δt(Days)
August	13.3	U.T.*	+0.0020
	17.3	U.T.	+0.0020
	18.2	U.T.	+0.0021
	28.2	U.T.	+0.0022
November	22.1	U.T.	+0.0023

*U.T. is Universal Time.

TABLE XV

DQ CEPHEI REDUCTION

V = 7.956 - ΔV
B = 8.366 - ΔB
U = 8.332 - ΔU
B-V = 0.410 - Δ(B-V)
U-B = -0.034 - Δ(U-B)

HJD = 2438600.+	v	b	u	ΔV	ΔB	ΔU	Δ(B-V)	Δ(U-B)
20.7461	9.390	8.480	10.228	+0.746*	+0.773*	+0.611*	+0.027*	-0.162*
20.7687	9.488	8.532	10.291	.668	.746	.575	.078	.171
20.7708	9.498	8.566	10.306	.660	.710	.562	.050	.148
20.7765	9.507	8.570	10.324	.650	.700	.543	.050	.157
20.7788	9.492	8.549	10.305	.663	.716	.556	.053	.160
20.7843	9.514	8.561	10.317	.648	.709	.554	.061	.155
20.7866	9.510	8.581	10.341	.659	.694	.537	.035	.157
20.7979	9.540	8.594	10.350	.649	.710	.560	.061	.150
20.8006	9.520	8.579	10.341	.672	.725	.571	.053	.154
20.8065	9.509	8.543	10.319	.686	.765	.604	.079	.161
20.8092	9.492	8.533	10.305	.704	.775	.619	.071	.156
20.8145	9.482	8.523	10.295	.722	.794	.644	.072	.150
20.8169	9.489	8.525	10.299	.721	.798	.649	.077	.149
20.8225	9.477	8.510	10.295	.737	.817	.660	.080	.157
20.8248	9.486	8.532	10.316	.727	.794	.638	.067	.156
20.8306	9.481	8.526	10.321	.733	.805	.645	.072	.160
20.8330	9.481	8.544	10.337	.735	.792	.637	.057	.155
20.8381	9.518	8.580	10.368	.703	.759	.620	.056	.139
20.8405	9.521	8.594	10.371	.702	.739	.615	.037	.124
20.8455	9.544	8.598	10.421	+0.682	+0.743	+0.582	+0.061	-0.161

TABLE XV (Continued)

HJD = 2438600.+	v	b	u	ΔV	ΔB	ΔU	Δ(B-V)	Δ(U-B)
20.8478	9.557	8.625	10.434	+0.668	+0.722	+0.577	+0.054	−0.145
20.8529	9.560	8.635	10.458	.661	.727	.574	.066	.153
20.8554	9.580	8.652	10.456	.639	.717	.584	.078	.133
24.6870	9.479	8.559	10.315	.720	.810	.658	.090	.152
24.6890	9.481	8.553	10.313	.725	.814	.657	.089	.157
24.6941	9.493	8.559	10.318	.722	.802	.644	.080	.158
24.6962	9.497	8.559	10.331	.718	.803	.632	.085	.171
24.7232	9.564	8.624	10.386	.658	.728	.575	.070	.153
24.7253	9.563	8.630	10.387	.661	.718	.574	.057	.144
24.7304	9.567	8.630	10.401	.661	.718	.562	.057	.156
24.7328	9.569	8.636	10.396	.660	.715	.564	.055	.151
24.7389	9.566	8.628	10.391	.665	.729	.575	.064	.154
24.7415	9.560	8.625	10.385	.669	.731	.584	.062	.147
24.7468	9.559	8.614	10.378	.673	.741	.594	.068	.147
24.7492	9.550	8.610	10.379	.686	.753	.601	.067	.152
24.7548	9.550	8.613	10.381	.693	.762	.612	.069	.150
24.7577	9.549	8.605	10.376	.696	.774	.624	.078	.150
24.7634	9.539	8.597	10.375	.708	.786	.630	.078	.156
24.7659	9.542	8.604	10.379	.705	.781	.627	.076	.154
24.7718	9.545	8.604	10.379	.700	.783	.626	.083	.157
24.7745	9.544	8.604	10.392	.701	.785	.613	.084	.172
24.7805	9.555	8.613	10.395	.689	.773	.612	.084	.161
24.7832	9.559	8.622	10.408	.687	.763	.605	.076	.158
24.7892	9.569	8.634	10.425	.680	.753	.599	.073	.154
24.7919	9.575	8.645	10.442	+0.676	+0.744	+0.586	+0.068	−0.158

TABLE XV (Continued)

HJD = 2438600.+	v	b	u	ΔV	ΔB	ΔU	Δ(B-V)	Δ(U-B)
24.7983	9.581	8.660	10.458	+0.674	+0.736	+0.580	+0.062	-0.156
24.8013	9.587	8.665	10.488	.669	.735	.556	.066	.179
24.8079	9.595	8.677	10.523*	.668	.733	.533*	.065	.200*
24.8108	9.602	8.682	10.490*	.665	.735	.575*	.070	.160*
24.8218	9.615	8.710	10.526*	.684	.753	.615*	.069	.138*
24.8243	9.621	8.707	10.575*	.688	.778	.604*	.090	.174*
24.8298	9.622	8.729	10.567*	.705	.785	.650*	.080	.135*
24.8325	9.622	8.740	10.580*	.711	.781	.636*	.070	.145*
24.8381	9.626	8.741	10.643*	.717	.788	.583*	.071	.205*
24.8404	9.636	8.720	10.591*	.708	.811	.643*	.103	.168*
24.8453	9.626	8.727	10.626*	.719	.803	.612*	.084	.191*
24.8476	9.633	8.735	10.631*	.713	.799	.610*	.086	.189*
24.8527	9.647	8.770	10.655*	.709	.782	.607*	.073	.175*
24.8550	9.654	8.774	10.679*	.708	.787	.615*	.079	.172*
24.8609	9.687	8.817	10.706*	.692	.770	.602*	.078	.168*
24.8635	9.696	8.831	10.745*	.688	.766	.577*	.078	.189*
24.8683	9.724	8.854	10.741*	.668	.754	.602*	.086	.152*
24.8703	9.720	8.867	10.766*	.675	.743	.587*	.068	.156*
25.6141	9.774	8.977	10.870	.681	.733	.613	.052	.120
25.6170	9.755	8.932	10.855	.694	.761	.602	.067	.159
25.6229	9.728	8.898	10.801	.708	.773	.622	.065	.151
25.6252	9.729	8.904	10.801	.705	.770	.623	.065	.147
25.6317	9.715	8.877	10.813	.718	.802	.612	.084	.190
25.6340	9.714	8.873	10.768	.720	.805	.653	.085	.152
25.6411	9.735	8.894	10.794	+0.699	+0.784	+0.620	+0.085	-0.164

TABLE XV (Continued)

HJD = 2438600.+	v	b	u	ΔV	ΔB	ΔU	Δ(B-V)	Δ(U-B)
25.6435	9.734	8.894	10.774	+0.698	+0.781	+0.634	+0.083	-0.147
25.6498	9.729	8.883	10.778	.697	.784	.616	.087	.168
25.6520	9.734	8.896	10.790	.691	.766	.601	.075	.165
25.6633	9.737	8.900	10.771	.674	.735	.580	.061	.155
25.6655	9.738	8.896	10.765	.672	.731	.576	.059	.155
25.6710	9.734	8.895	10.759	.672	.725	.574	.053	.151
25.6732	9.724	8.895	10.768	.682	.730	.571	.048	.159
25.6783	9.737	8.903	10.770	.668	.729	.577	.061	.152
25.6808	9.737	8.903	10.768	.670	.731	.581	.061	.150
25.6863	9.723	8.875	10.726	.679	.751	.611	.072	.140
25.6885	9.708	8.854	10.703	.687	.761	.622	.074	.139
25.6939	9.700	8.849	10.704	.687	.755	.611	.068	.144
25.6962	9.690	8.829	10.676	.697	.776	.641	.079	.135
25.7212	9.730	8.883	10.753	.707	.801	.626	.094	.175
25.7242	9.731	8.890	10.768	.704	.786	.629	.082	.157
25.7294	9.767	8.929	10.845	.685	.767	.587	.082	.180
25.7317	9.770	8.964	10.869	.697	.752	.575	.055	.177
25.7377	9.859*	9.019*	10.937*	.650*	.762*	.552*	.112*	.210*
25.7406	9.974*	9.117*	---	.554*	.694*	---	.140*	---
35.6296	9.593	8.668	10.452	.696	.772	.611	.076	.161
35.6323	9.582	8.653	10.456	.705	.781	.603	.076	.178
35.6379	9.572	8.636	10.409	.711	.784	.634	.073	.150
35.6408	9.560	8.627	10.402	.721	.786	.629	.065	.157
35.6463	9.550	8.608	10.374	.720	.791	.638	.071	.153
35.6489	9.545	8.602	10.380	+0.717	+0.790	+0.627	+0.073	-0.163

TABLE XV (Continued)

HJD = 2438600.+	v	b	u	ΔV	ΔB	ΔU	Δ(B-V)	Δ(U-B)
35.6546	9.548	8.606	10.380	+0.705	+0.782	+0.621	+0.077	-0.161
35.6572	9.557	8.601	10.380	.695	.790	.622	.095	.168
35.6637	9.558	8.612	10.389	.696	.780	.611	.084	.169
35.6663	9.568	8.621	10.392	.688	.771	.606	.083	.165
35.6719	9.579	8.637	10.412	.676	.748	.587	.072	.161
35.6743	9.584	8.642	10.415	.666	.735	.586	.069	.149
35.6929	9.590	8.664	10.435	.669	.725	.566	.056	.159
35.6954	9.596	8.663	10.430	.666	.733	.577	.067	.156
35.7009	9.603	8.674	10.439	.665	.732	.580	.067	.152
35.7032	9.592	8.661	10.435	.676	.746	.586	.070	.160
35.7085	9.579	8.643	10.423	.690	.767	.609	.077	.158
35.7108	9.577	8.648	10.418	.693	.761	.618	.068	.143
35.7160	9.568	8.637	10.413	.705	.777	.633	.072	.144
35.7183	9.571	8.623	10.411	.705	.799	.641	.094	.158
35.7238	9.569	8.625	10.426	.724	.818	.652	.094	.166
35.7262	9.567	8.633	10.418	.727	.811	.665	.084	.146
121.5140	9.545	8.600	10.371	.667	.737	.598	.070	.139
121.5169	9.541	8.588	10.370	.672	.751	.600	.079	.151
121.5236	9.519	8.563	10.342	.697	.776	.631	.079	.145
121.5266	9.512	8.566	10.352	.704	.768	.617	.064	.151
121.5336	9.520	8.560	10.352	.700	.778	.631	.078	.147
121.5366	9.513	8.555	10.356	.708	.785	.631	.077	.154
121.5434	9.519	8.568	10.375	.703	.777	.618	.074	.159
121.5464	9.521	8.572	10.372	.703	.776	.623	.073	.153
121.5532	9.537	8.595	10.419	+0.690	+0.758	+0.588	+0.068	-0.170

TABLE XV (Continued)

HJD = 2438600.+	v	b	u	ΔV	ΔB	ΔU	Δ(B-V)	Δ(U-B)
121.5564	9.548	8.606	10.420	+0.680	+0.750	+0.597	+0.070	-0.153
121.5643	9.566	8.631	10.459	.666	.734	.577	.068	.157
121.5672	9.564	8.629	10.456	.672	.743	.591	.071	.152
121.5736	9.568	8.641	10.481	.673	.740	.580	.067	.160
121.5766	9.569	8.651	10.478	.676	.735	.590	.059	.145
121.5833	9.572	8.642	10.488	.677	.756	.599	.079	.157
121.5862	9.571	8.651	10.498	.679	.752	.598	.073	.154
121.5926	9.568	8.651	10.500	.688	.767	.621	.079	.146
121.5955	9.561	8.645	10.499	+0.700	+0.784	+0.639	+0.084	-0.145

*Doubtful Data

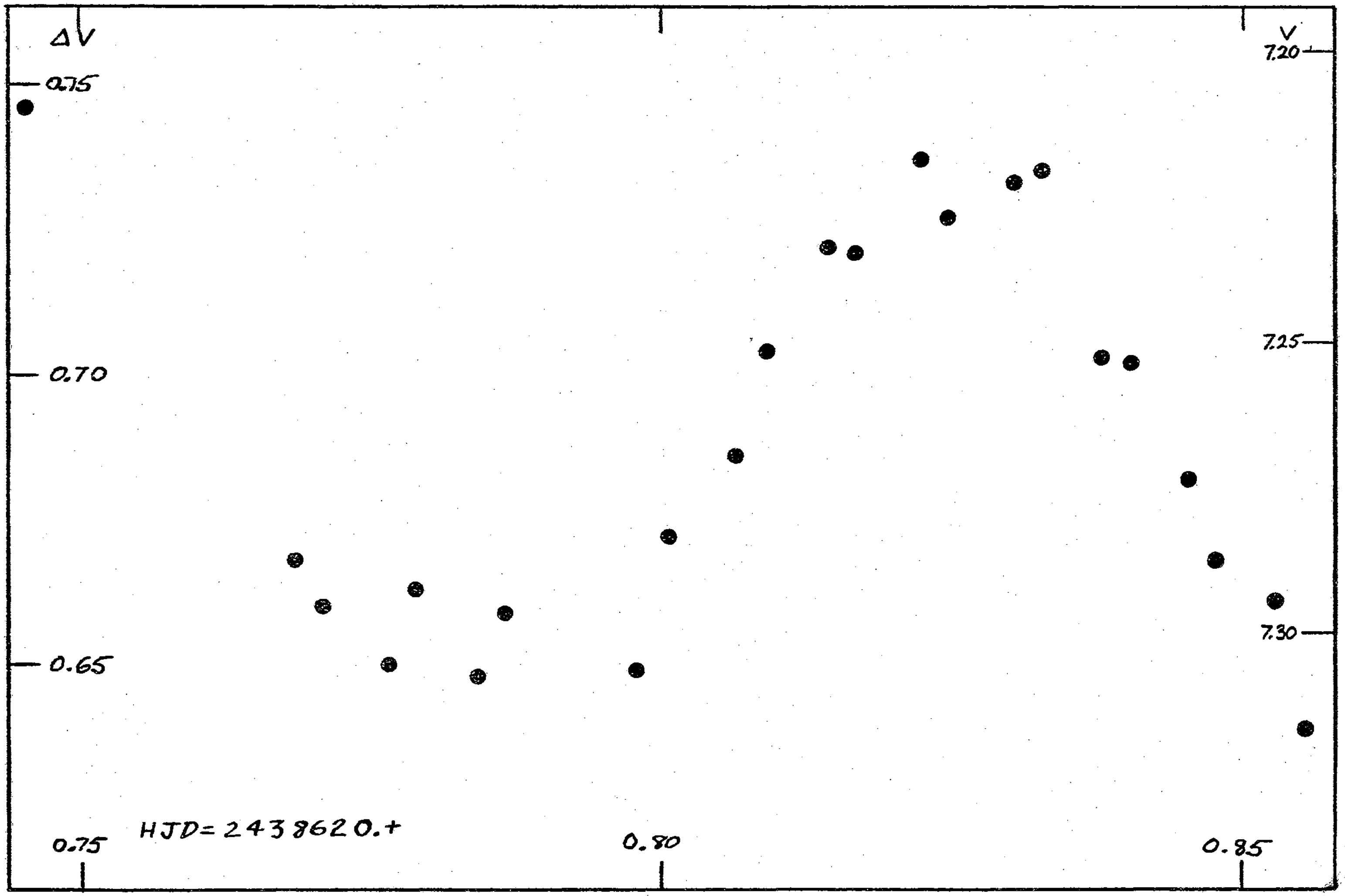

Figure 17. Light Curve in V of DQ Cephei for August 13, 1964.

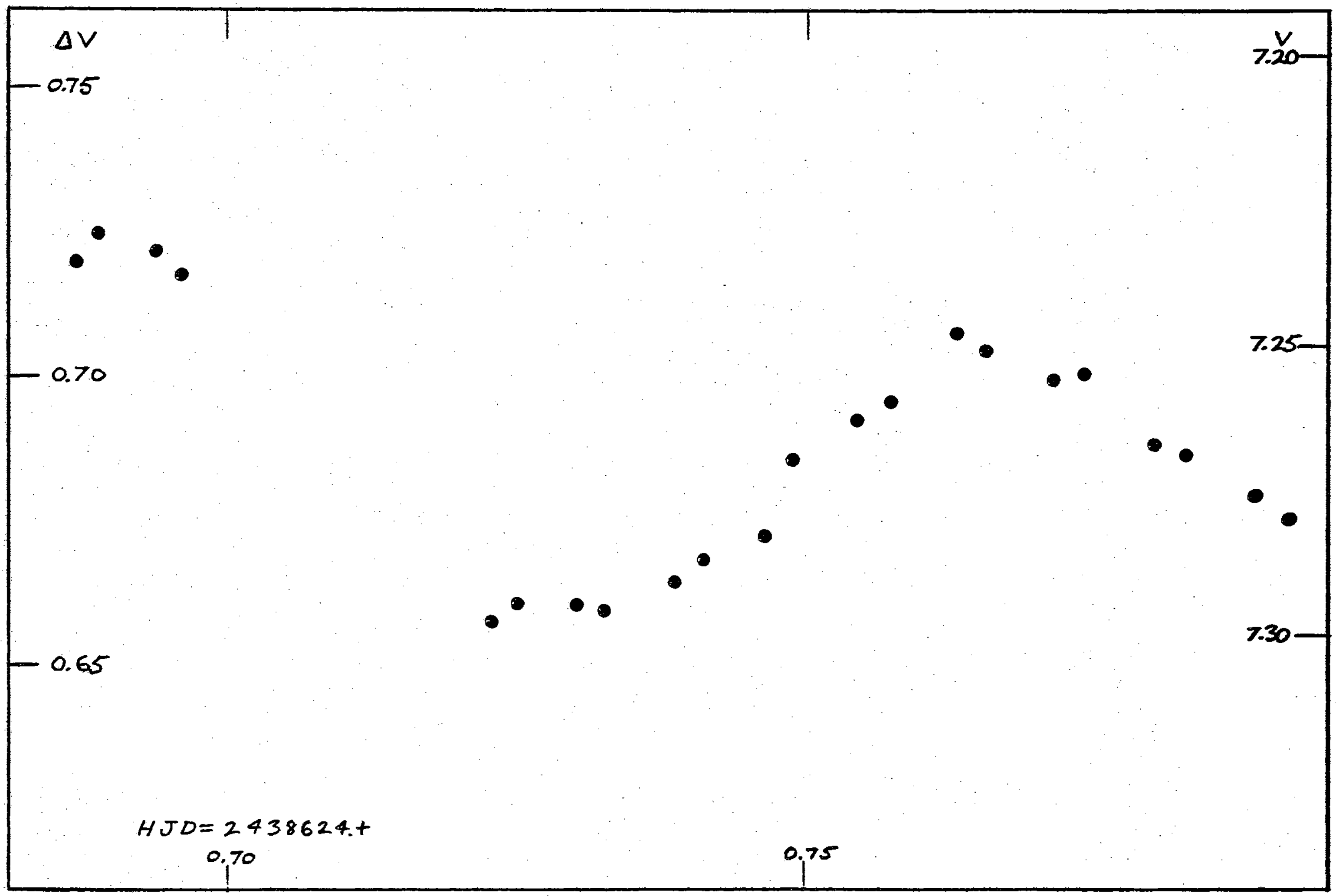

Figure 18. Light Curve in V of DQ Cephei for August 18, 1964 (Early).

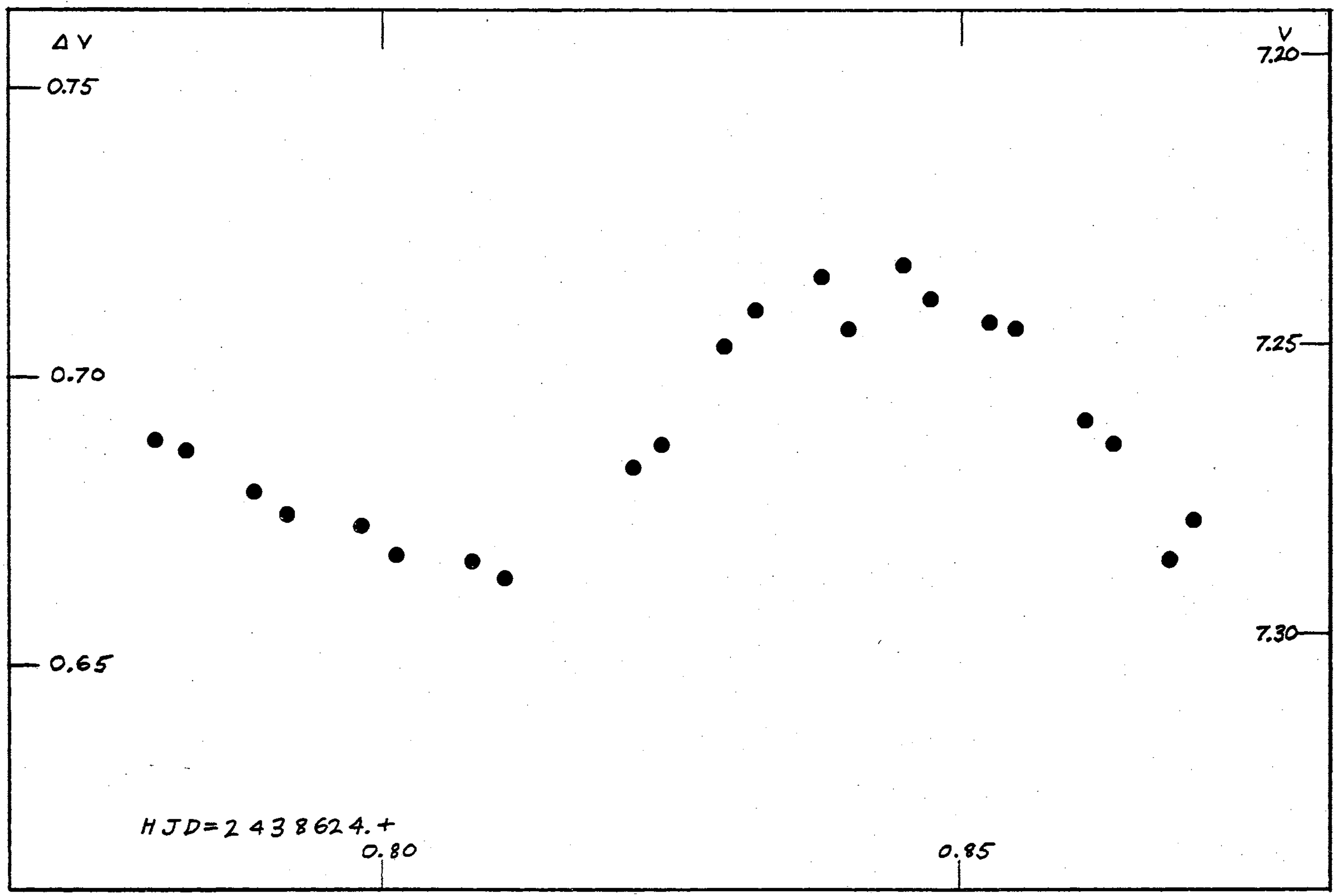

Figure 19. Light Curve in V of DQ Cephei for August 17, 1964 (Late).

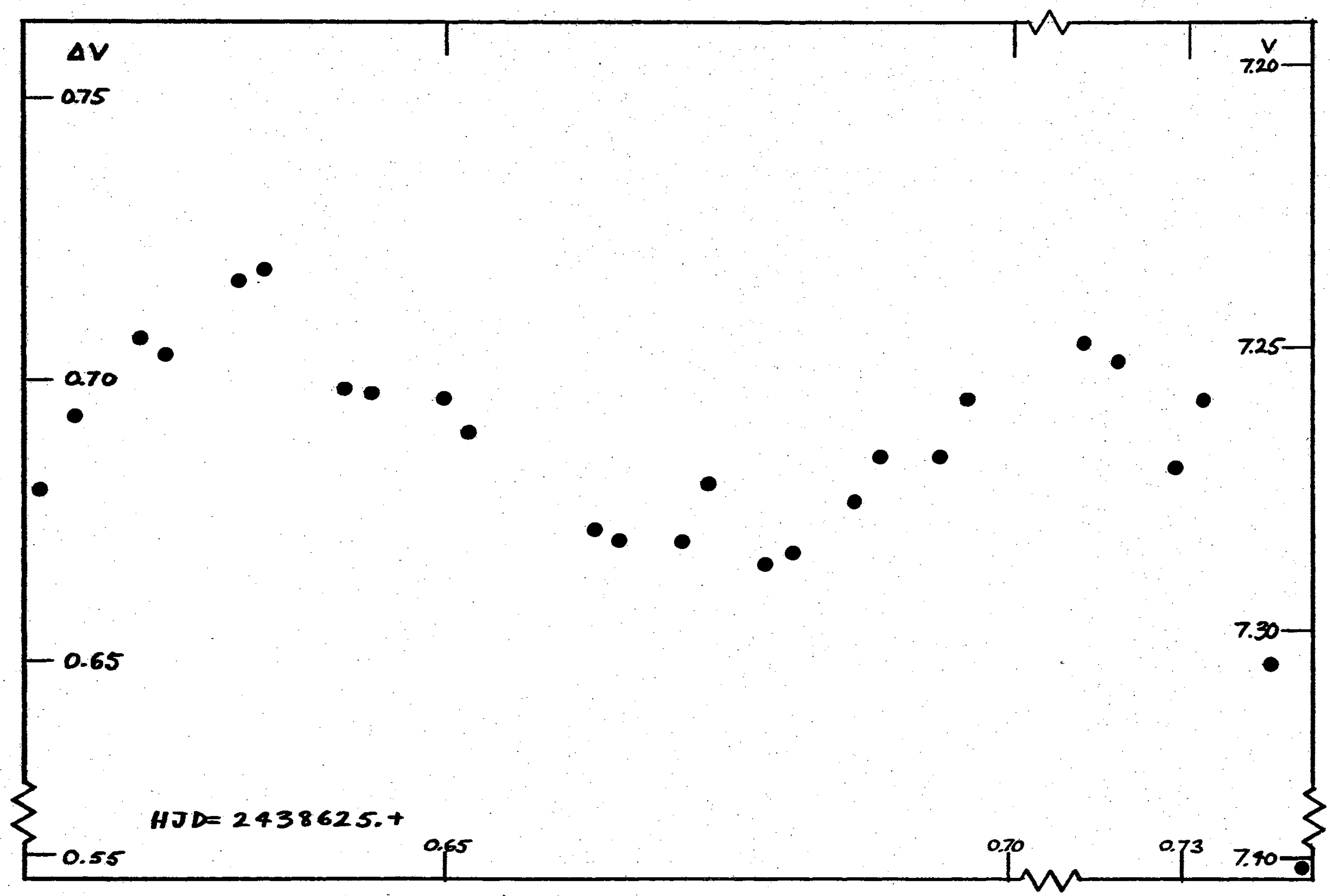

Figure 20. Light Curve in V of DQ Cephei for August 18, 1964.

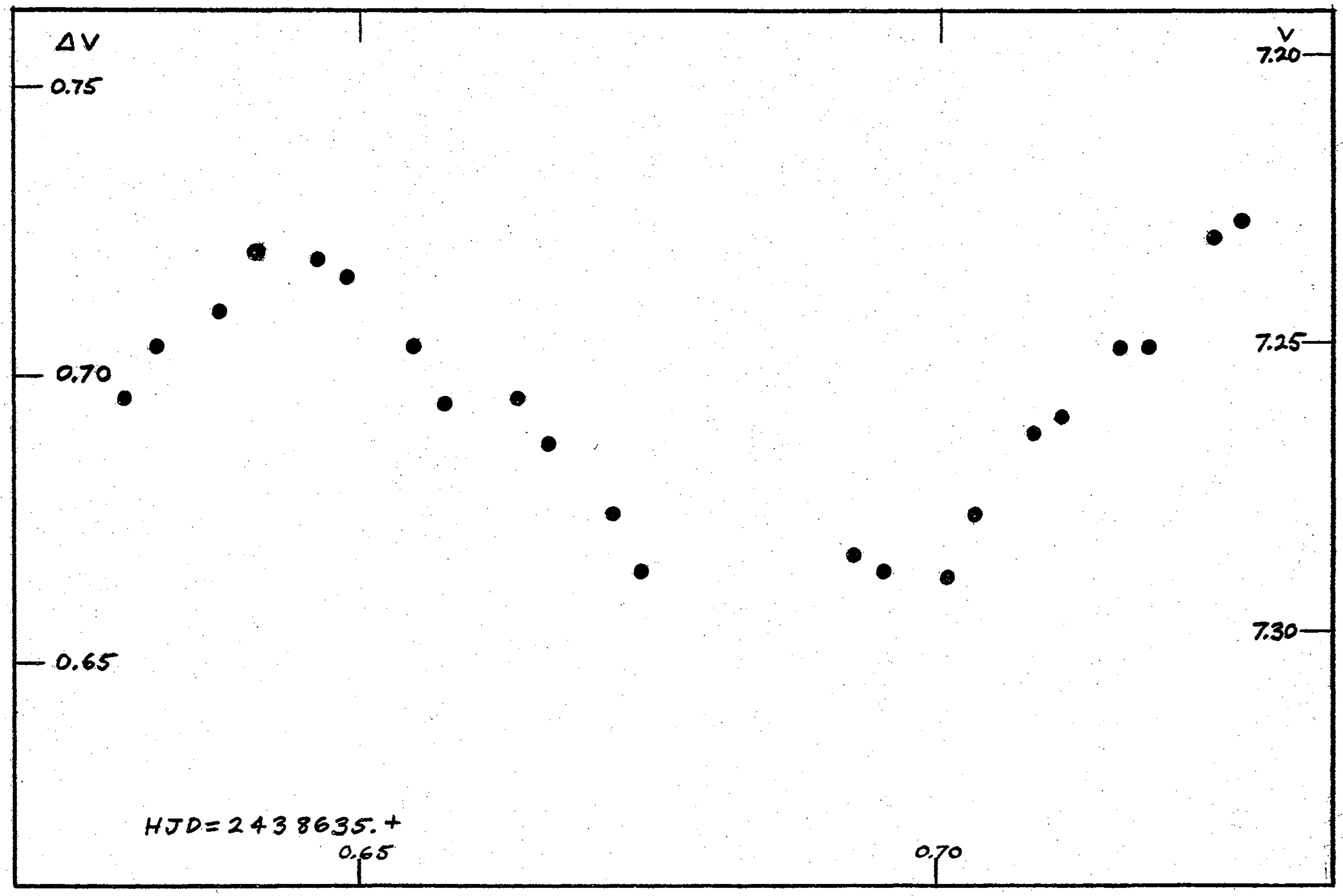

Figure 21. Light Curve in V of DQ Cephei for August 28, 1964.

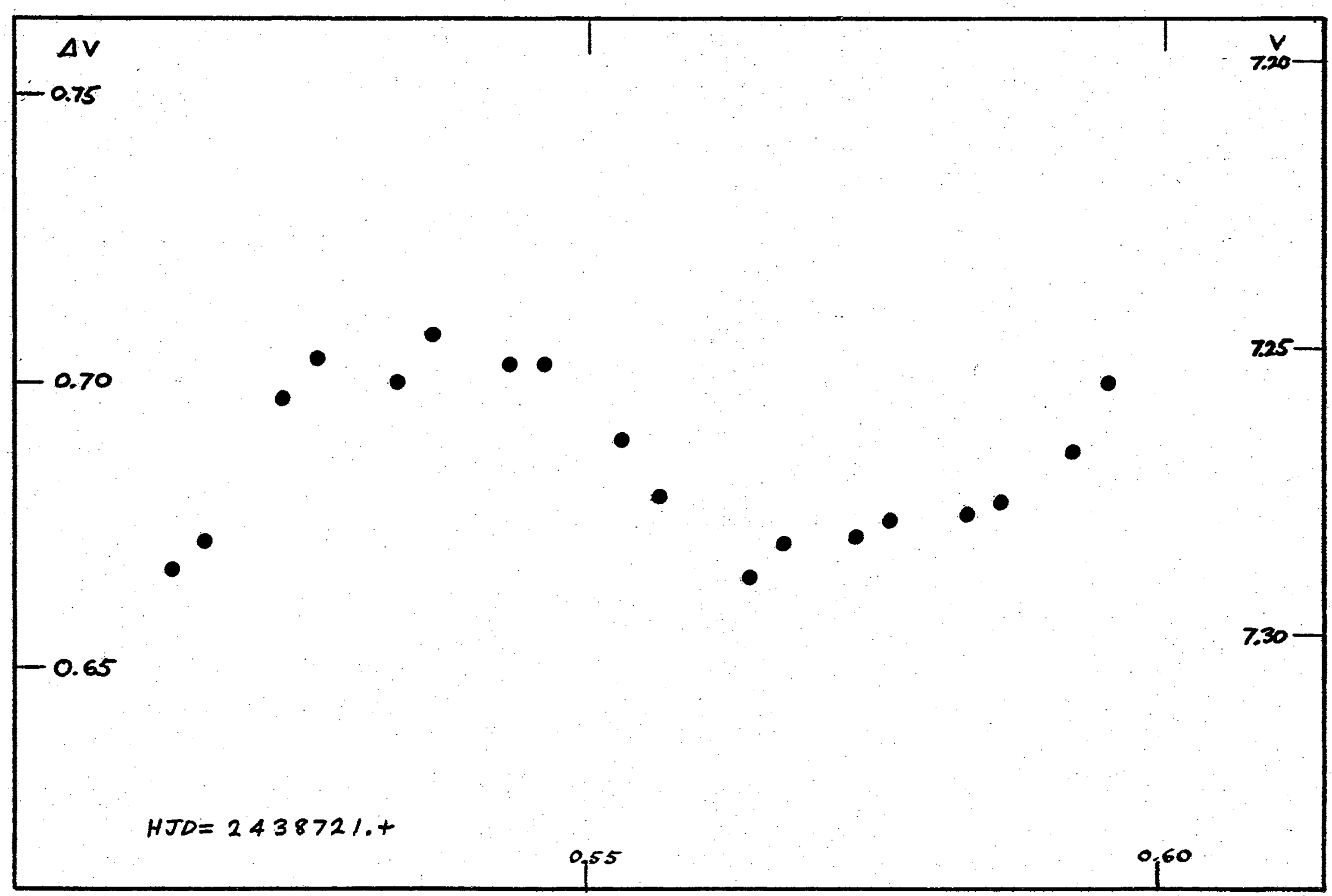

Figure 22. Light Curve in V of DQ Cephei for November 22, 1964.

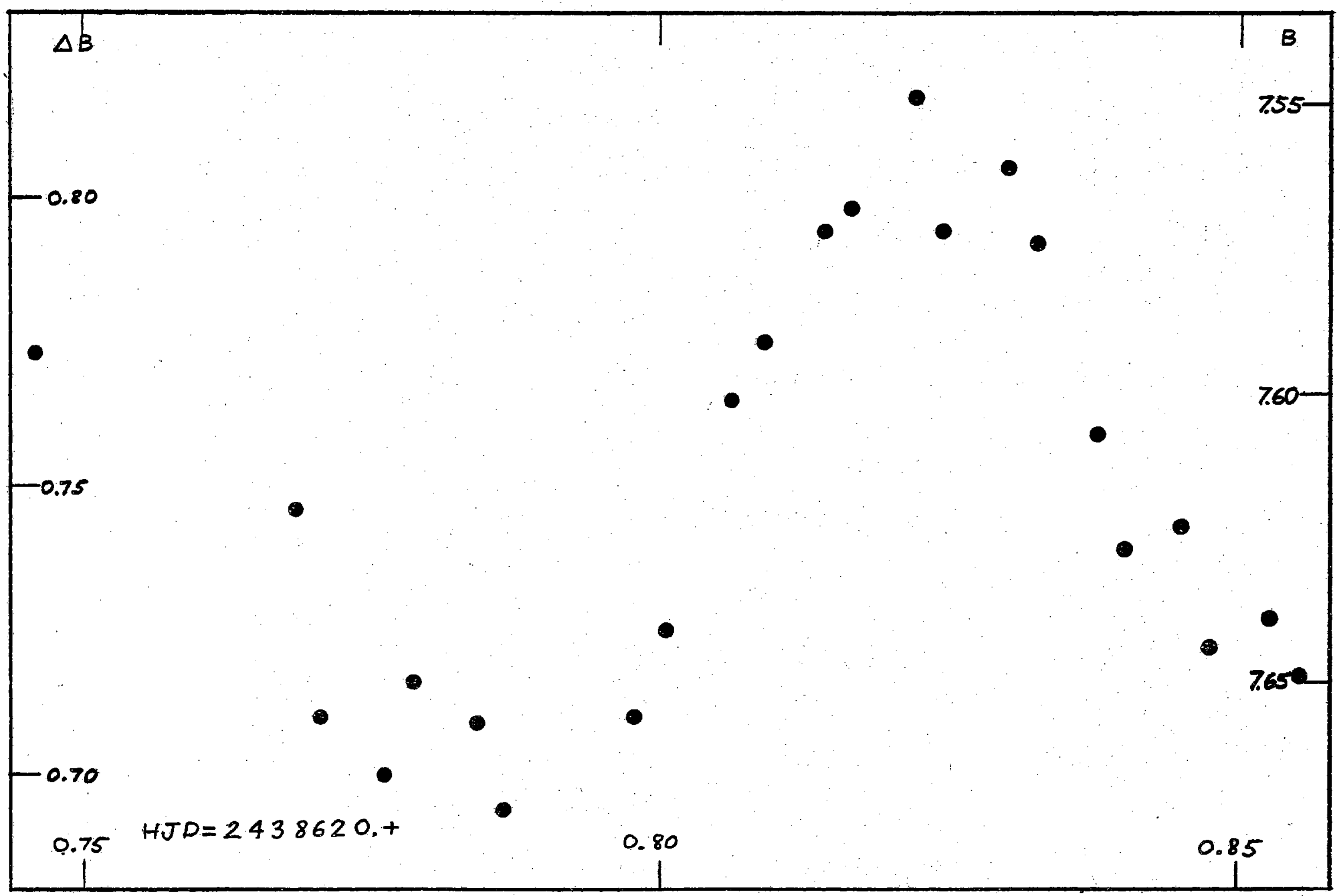

Figure 23. Light Curve in B of DQ Cephei for August 13, 1964.

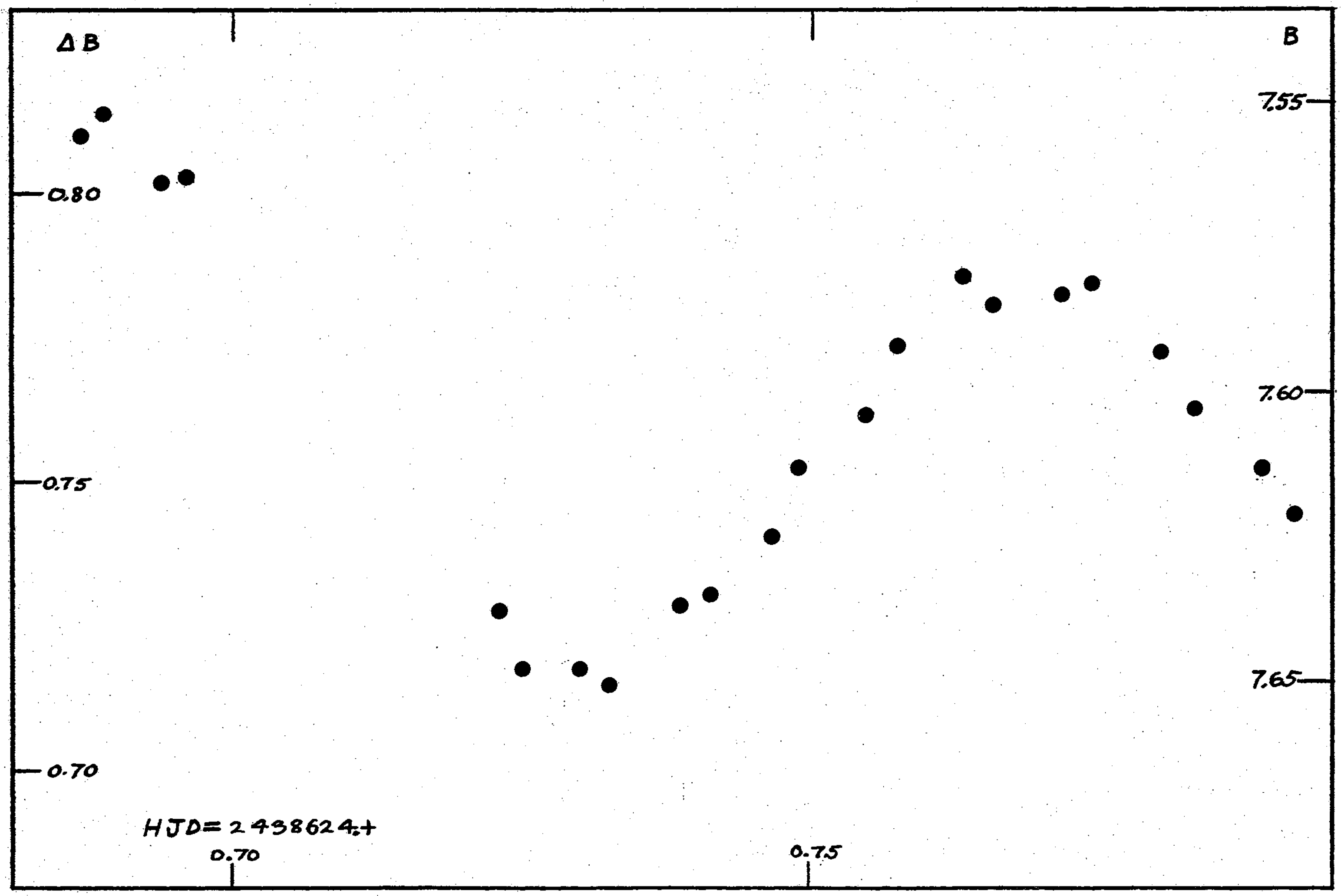

Figure 24. Light Curve in B of DQ Cephei for August 17, 1964 (Early).

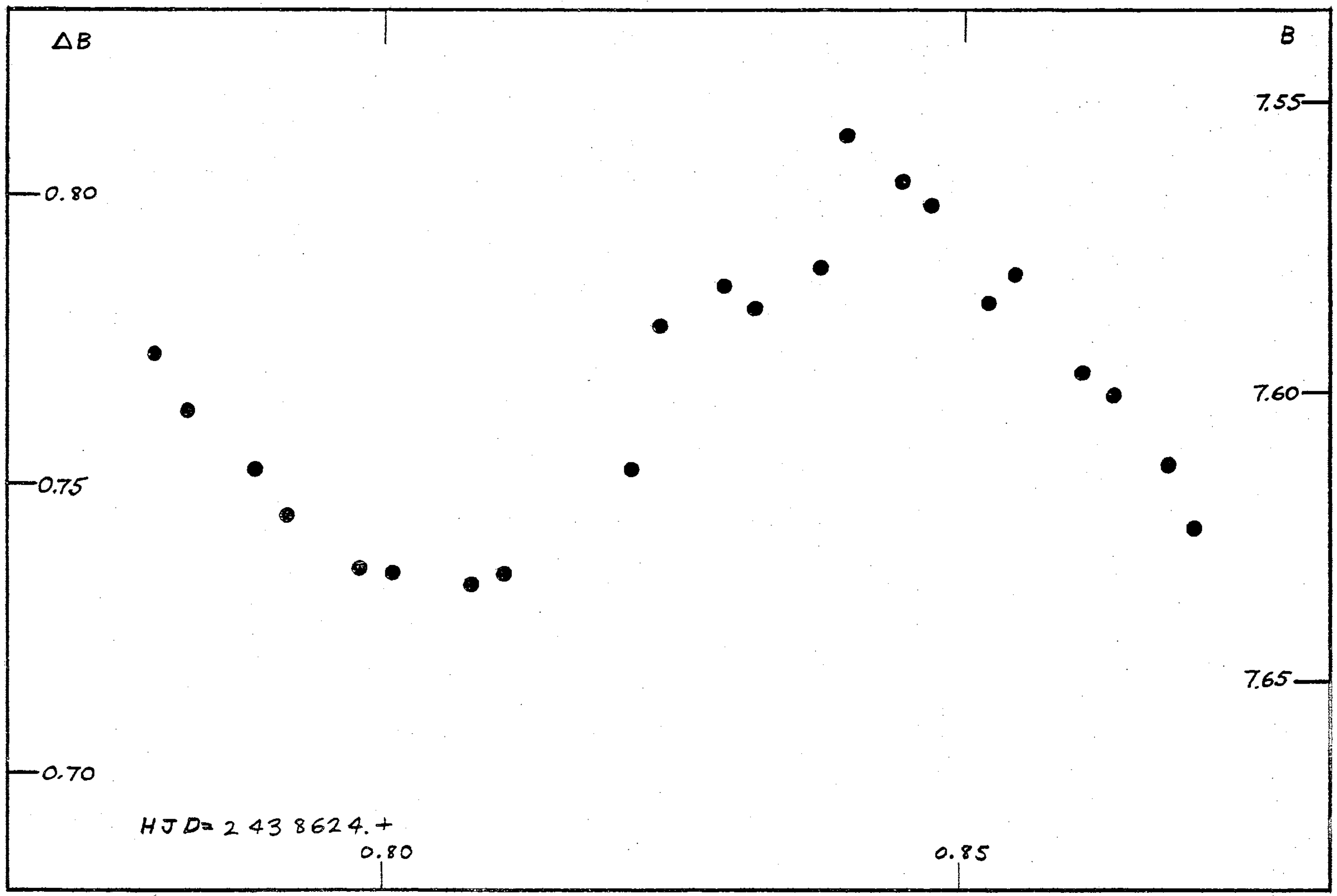

Figure 25. Light Curve in B of DQ Cephei for August 17, 1964 (Late).

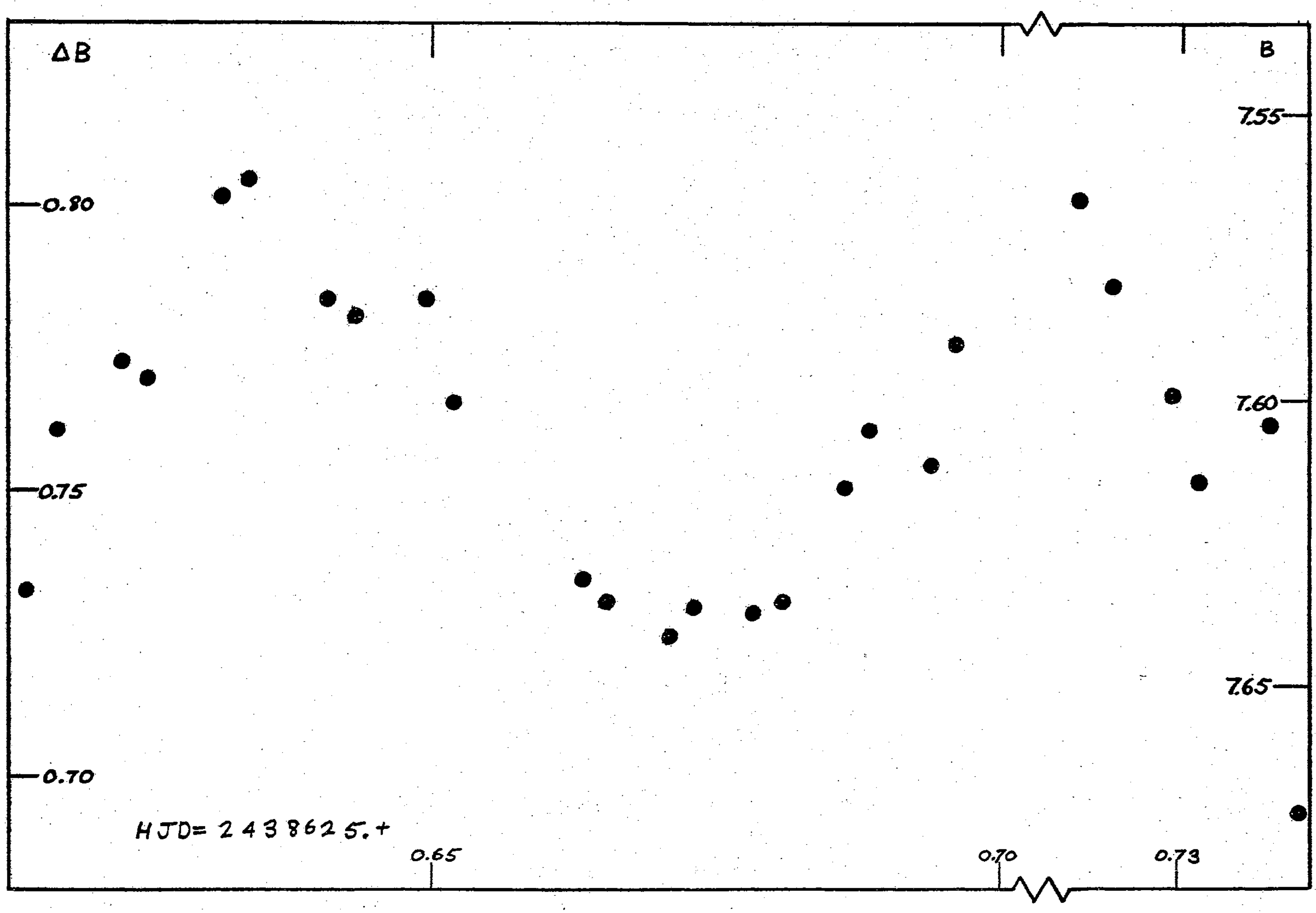

Figure 26. Light Curve in B of DQ Cephei for August 18, 1964.

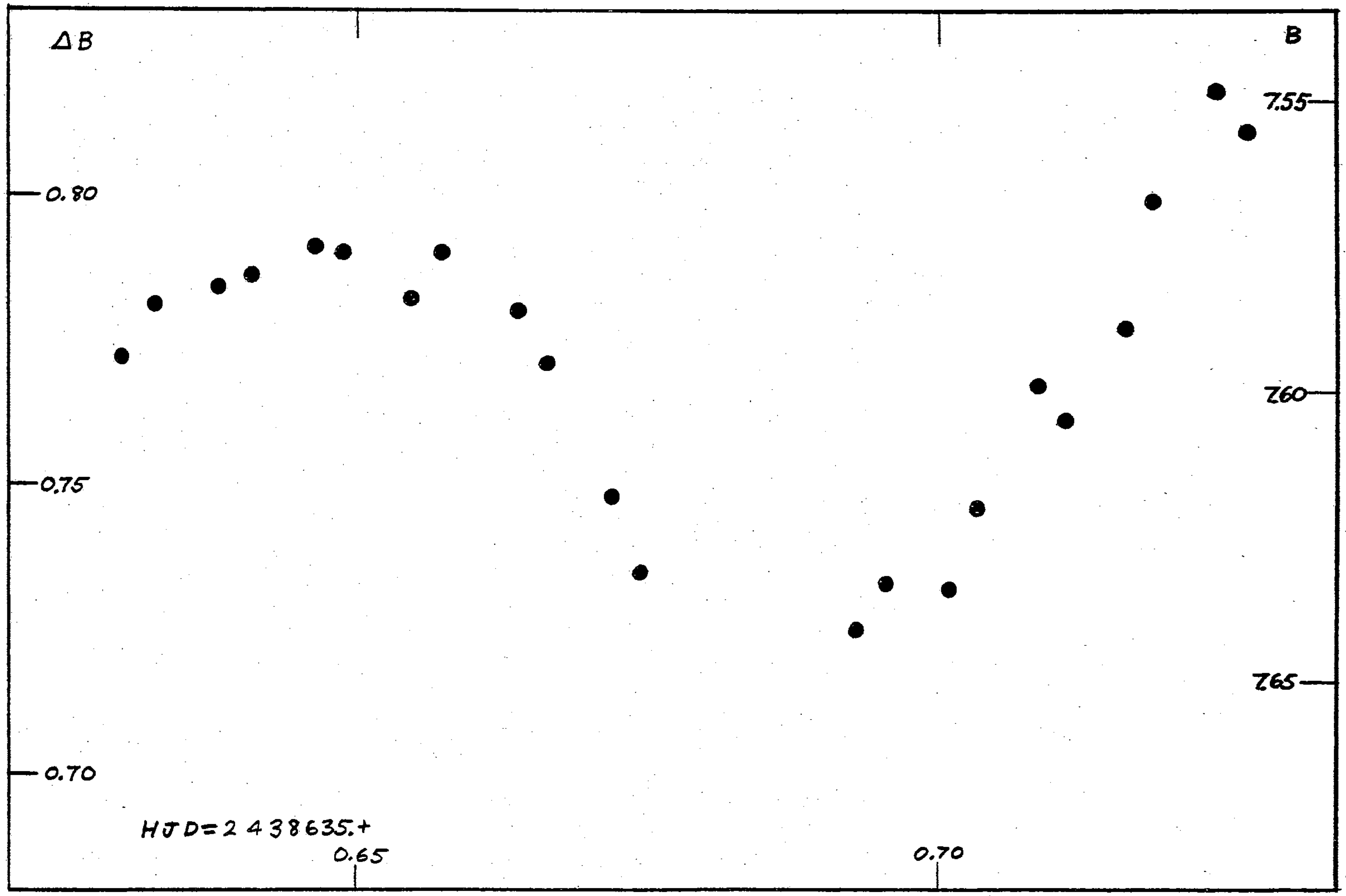

Figure 27. Light Curve in B of DQ Cephei for August 28, 1964.

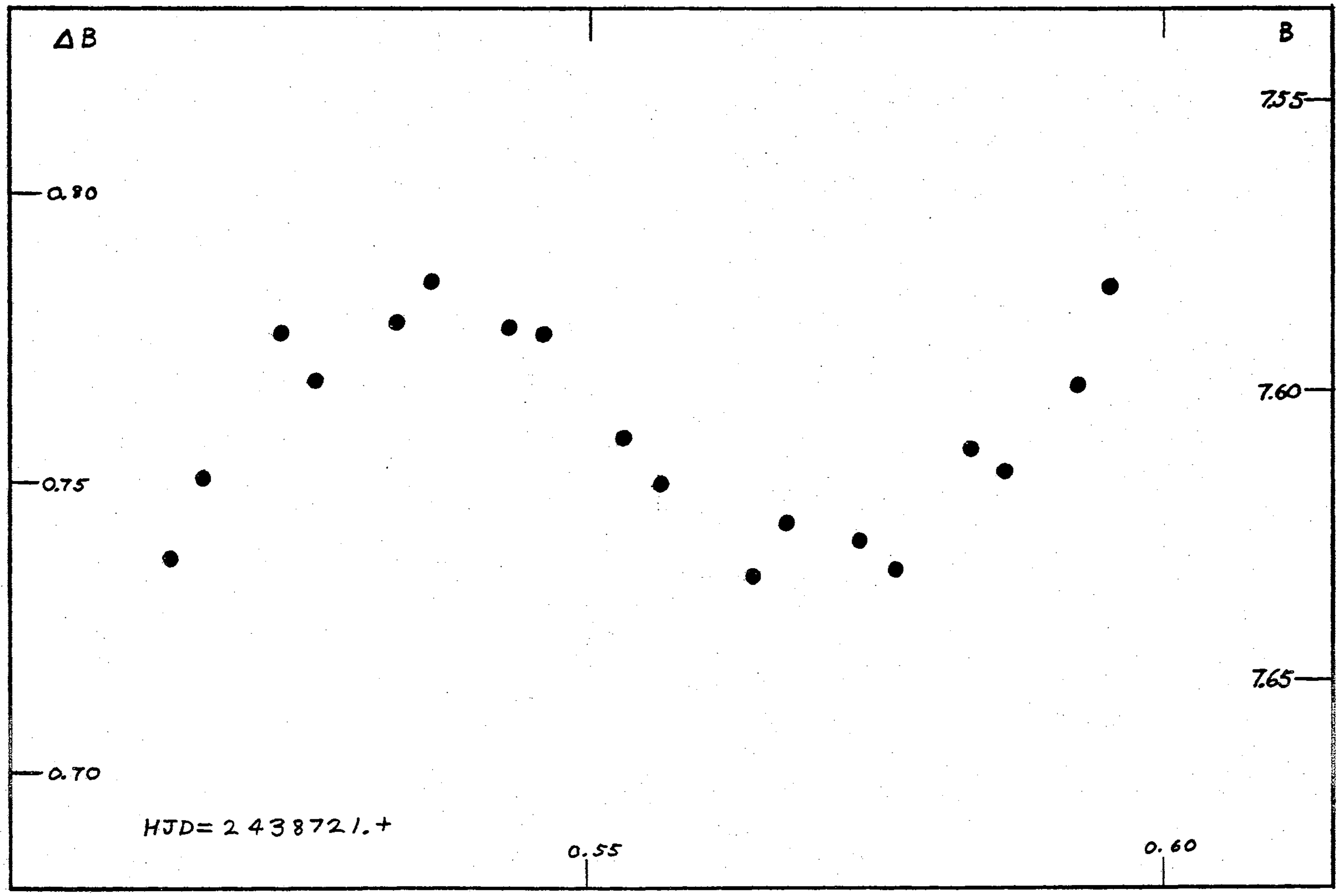

Figure 28. Light Curve in B of DQ Cephei for November 22, 1964.

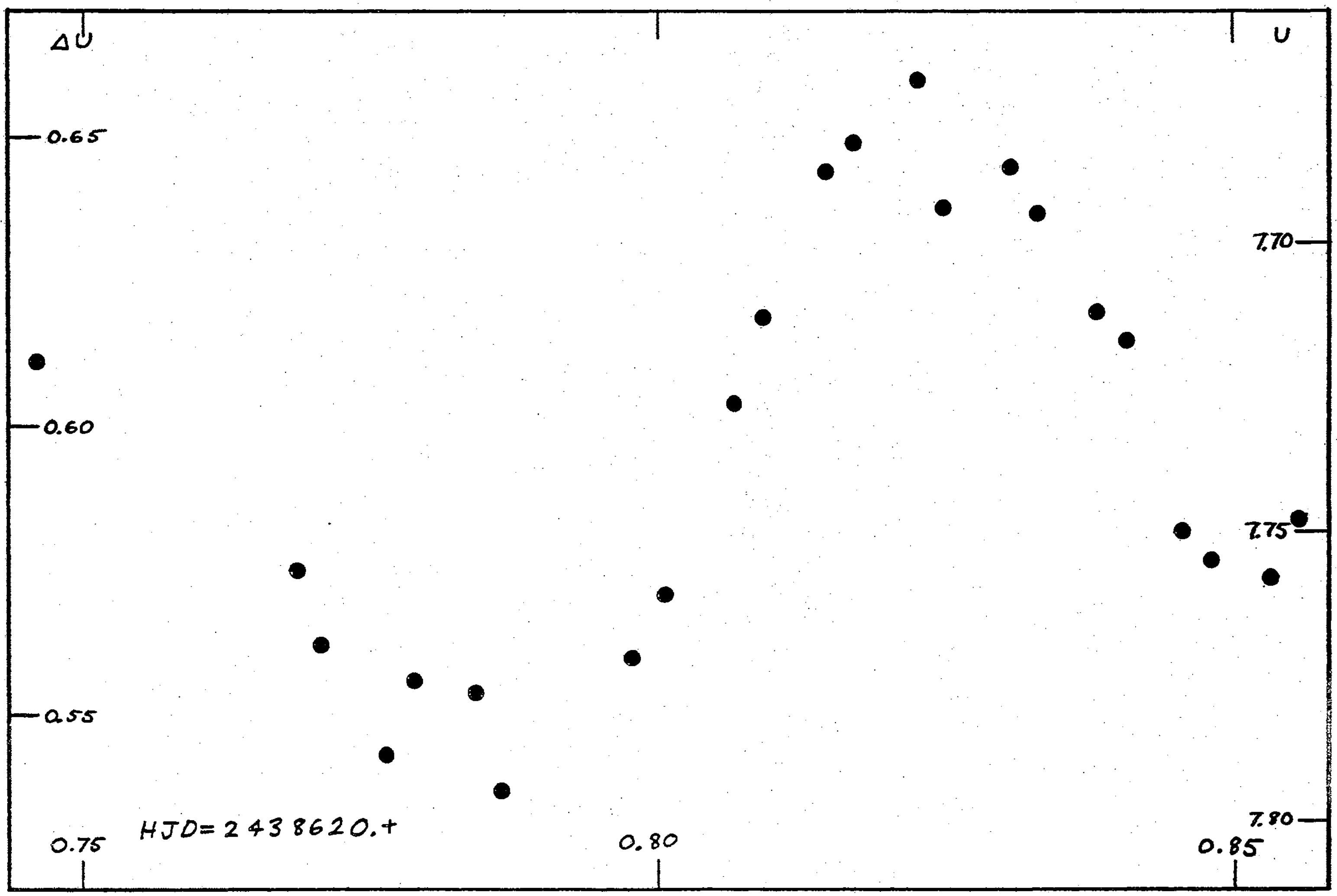

Figure 29. Light Curve in U of DQ Cephei for August 13, 1964.

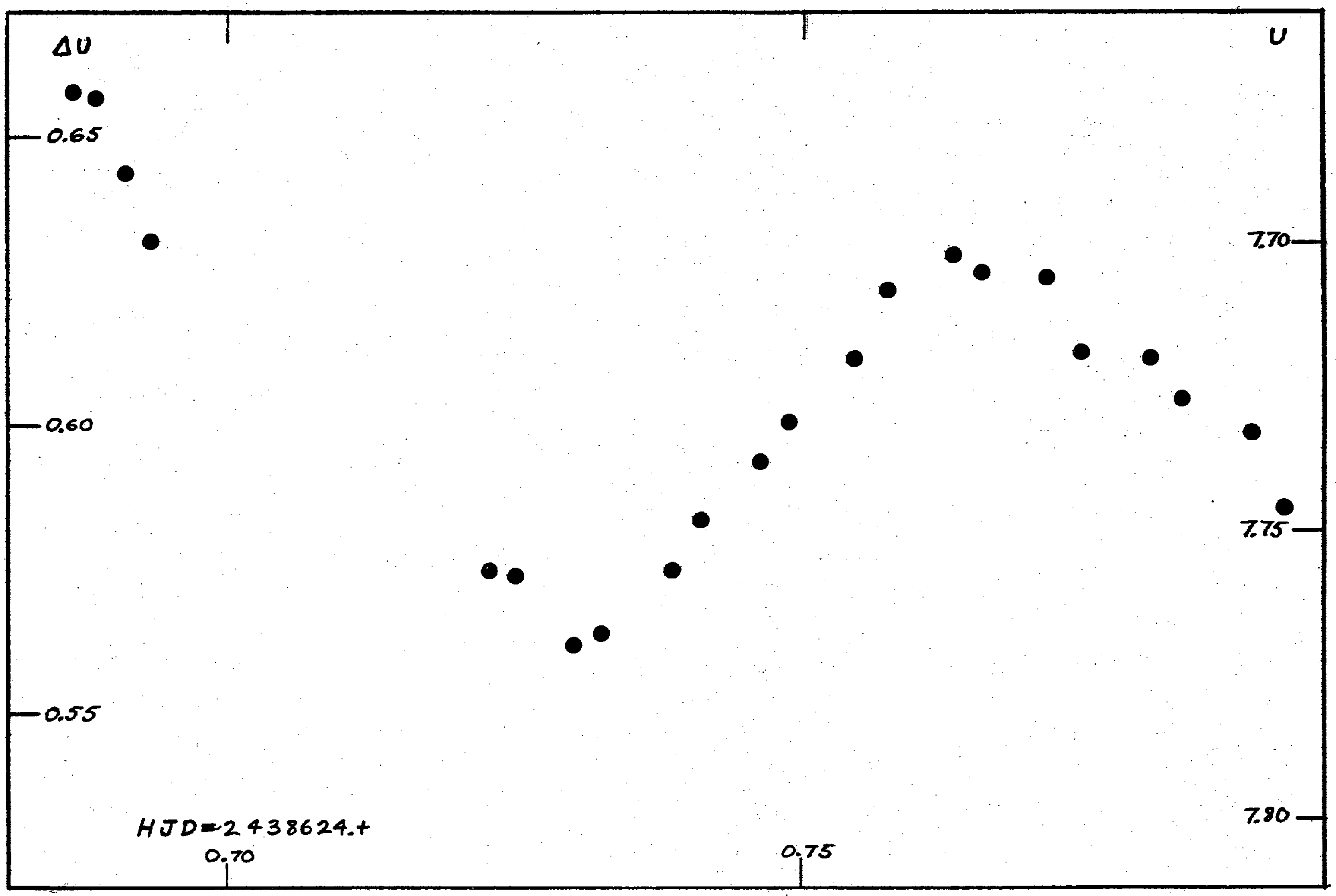

Figure 30. Light Curve in U of DQ Cephei for August 17, 1964 (Early).

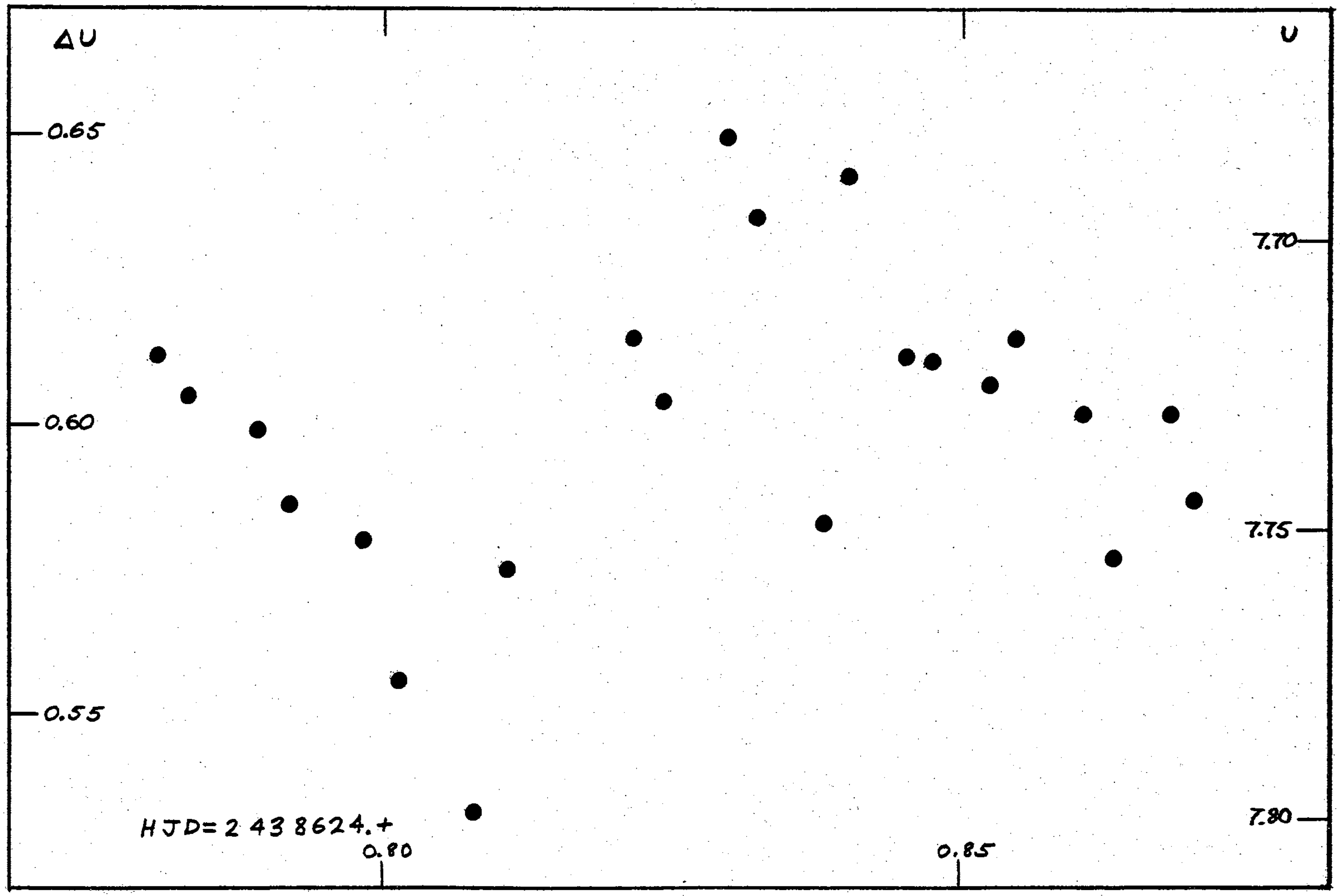

Figure 31. Light Curve in U of DQ Cephei for August 17, 1964 (Late).

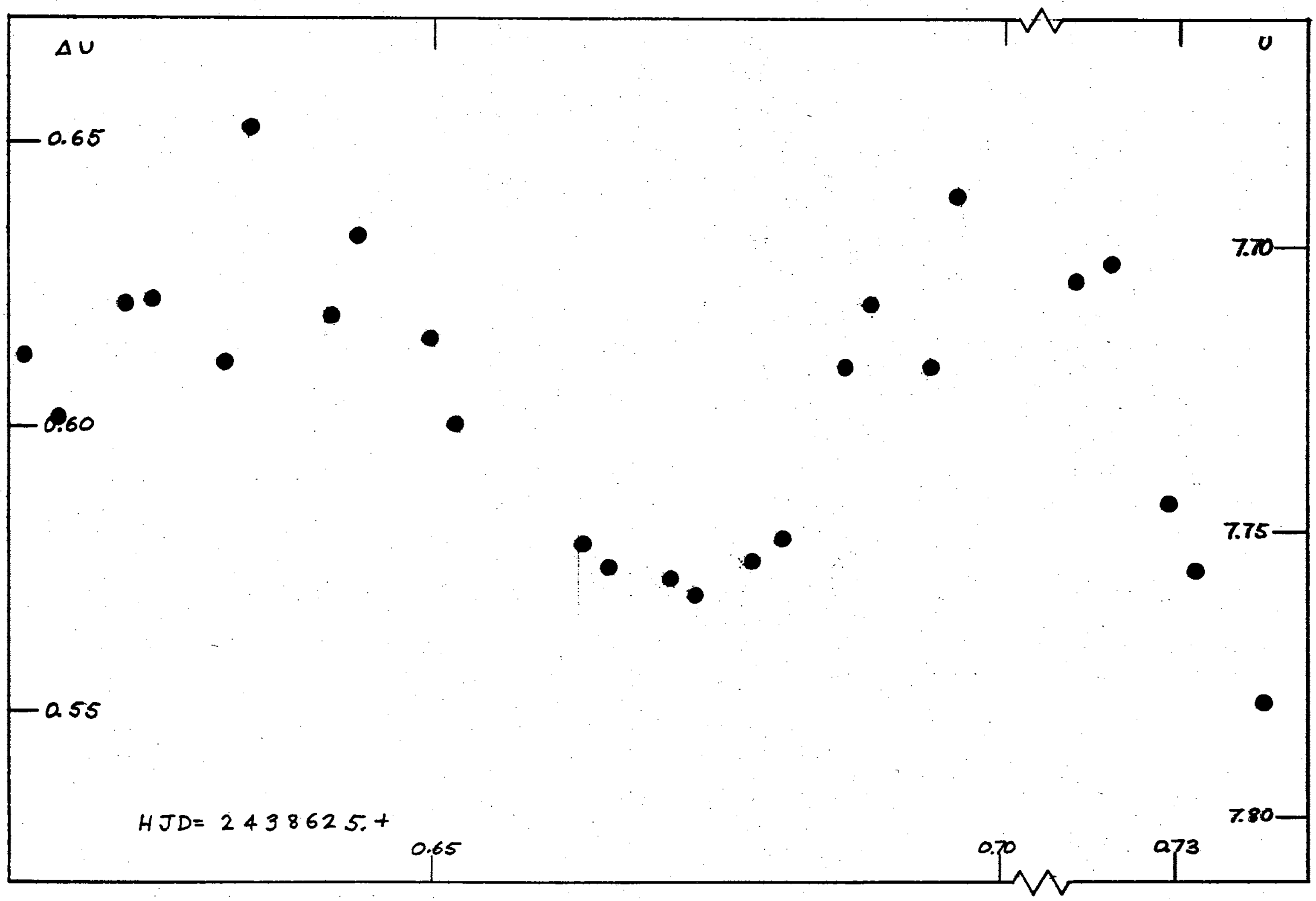

Figure 32. Light Curve in U of DQ Cephei for August 18, 1964.

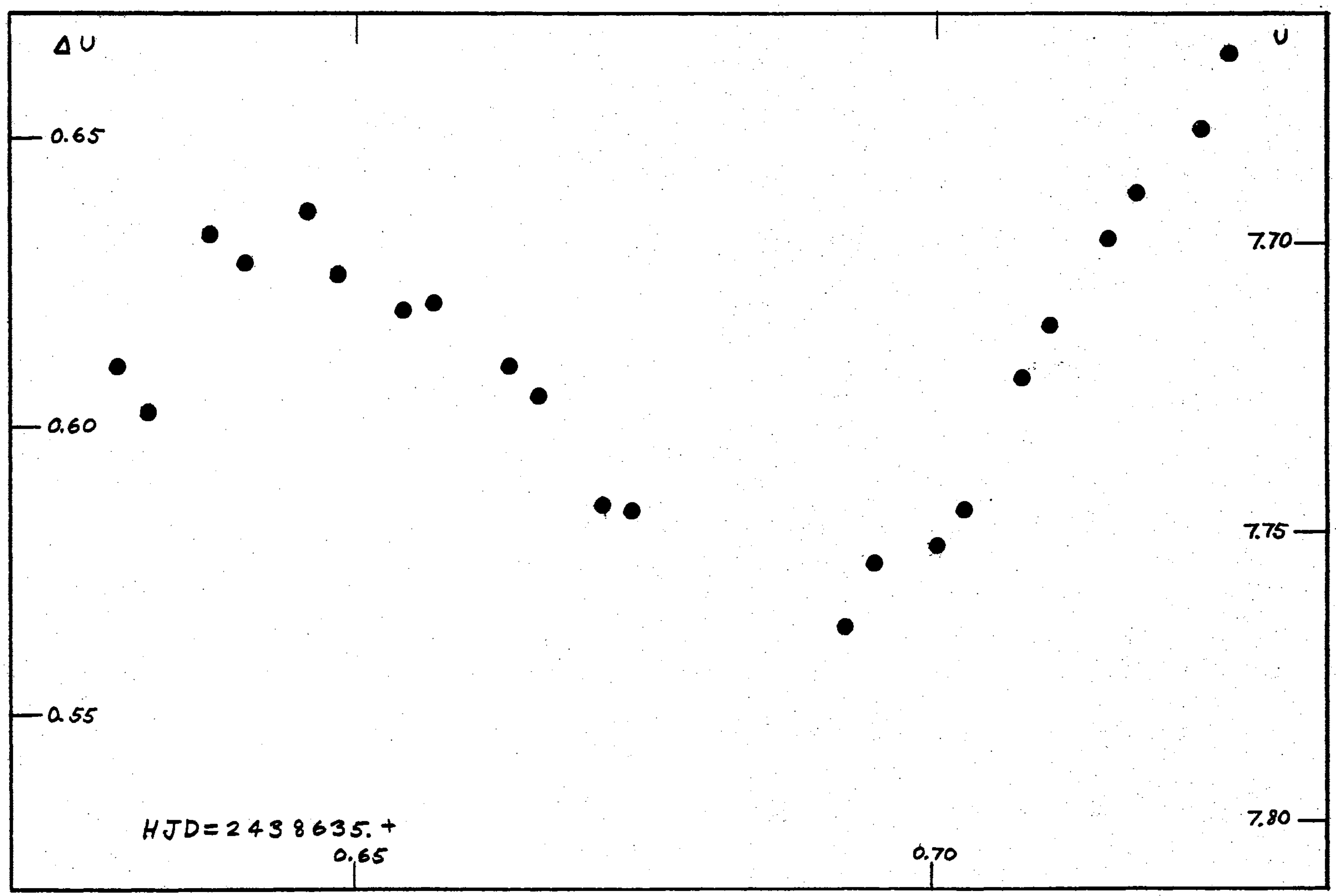

Figure 33. Light Curve in U of DQ Cephei for August 28, 1964.

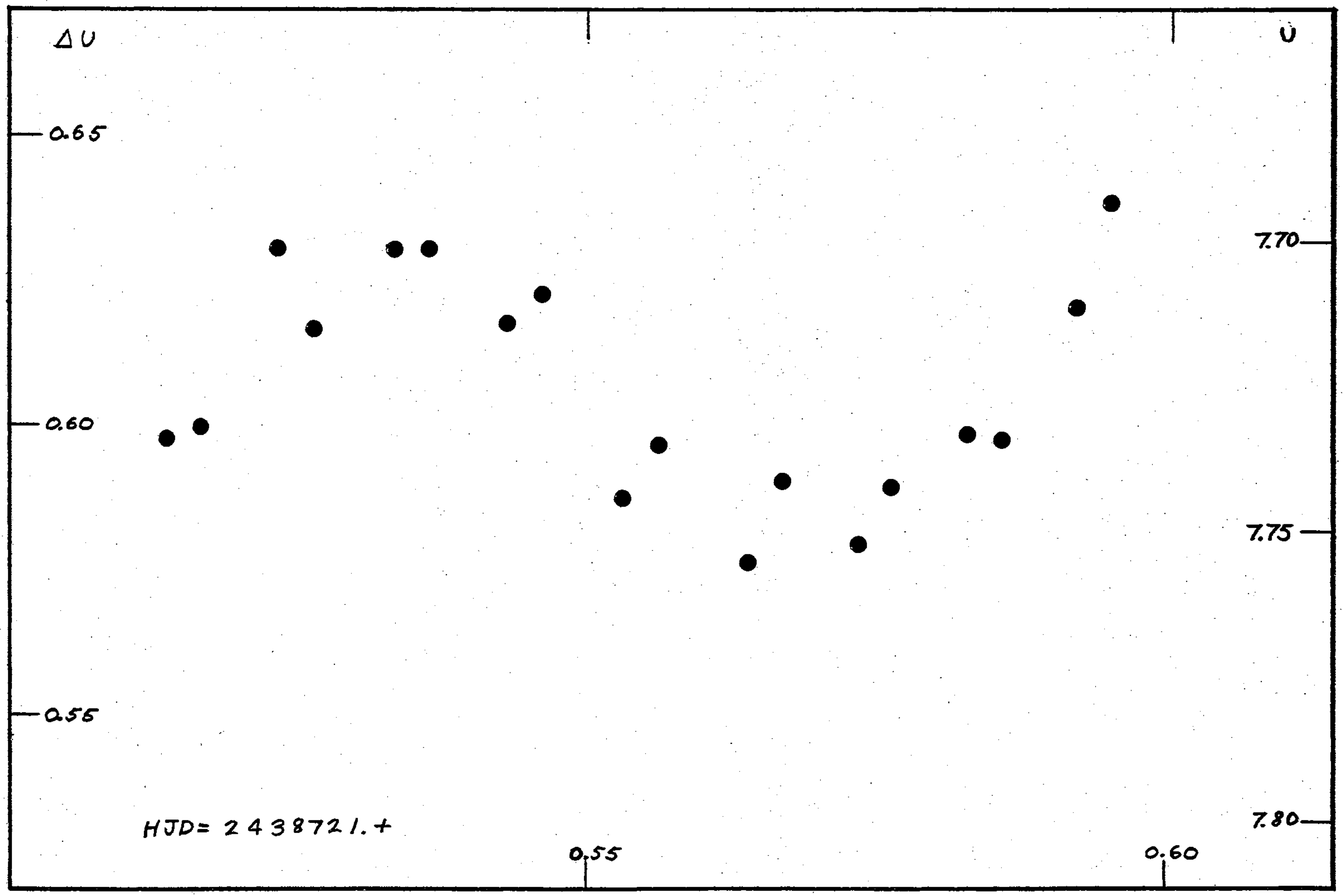

Figure 34. Light Curve in U of DQ Cephei for November 22, 1964.

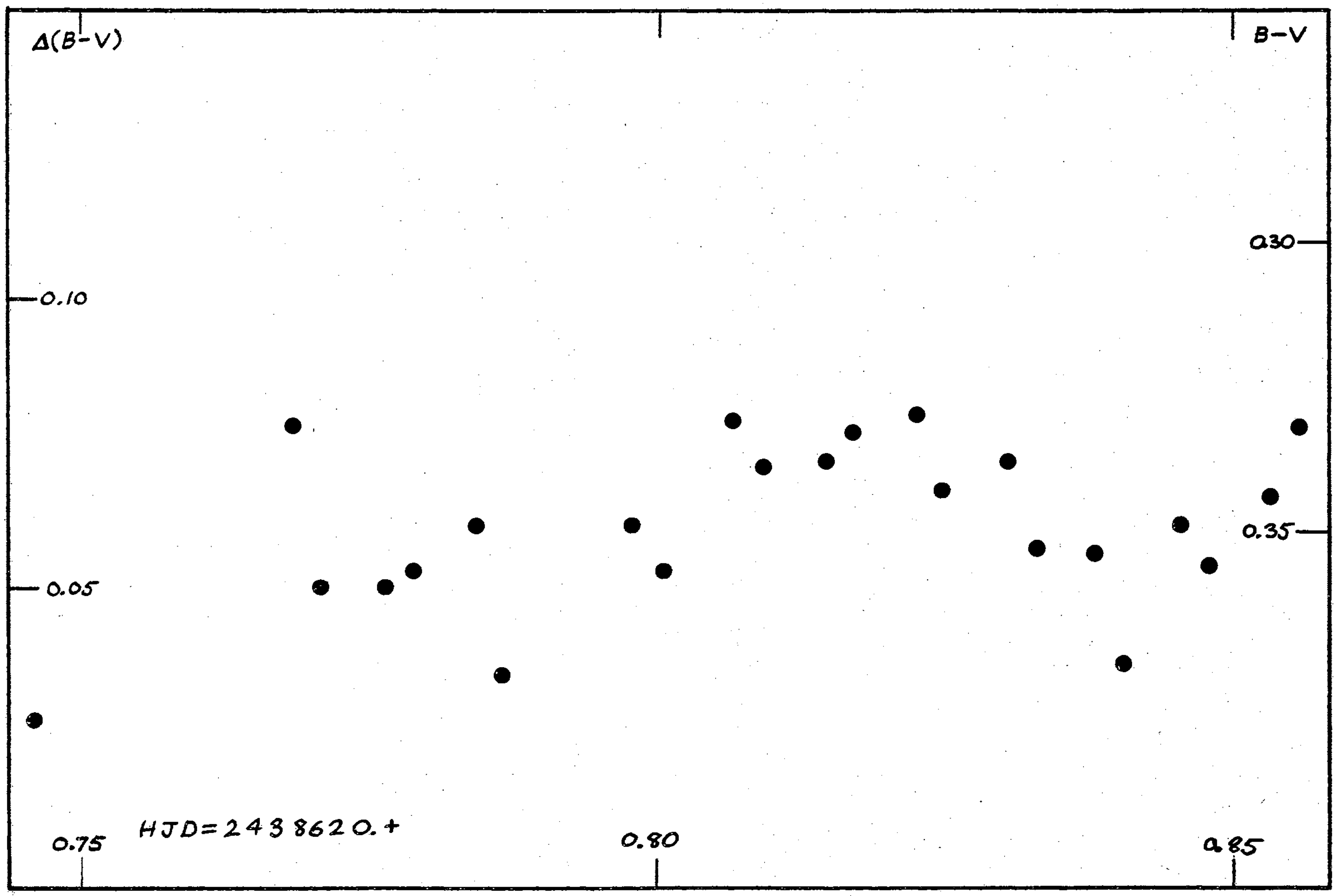

Figure 35. Light Curve in B-V of DQ Cephei for August 13, 1964.

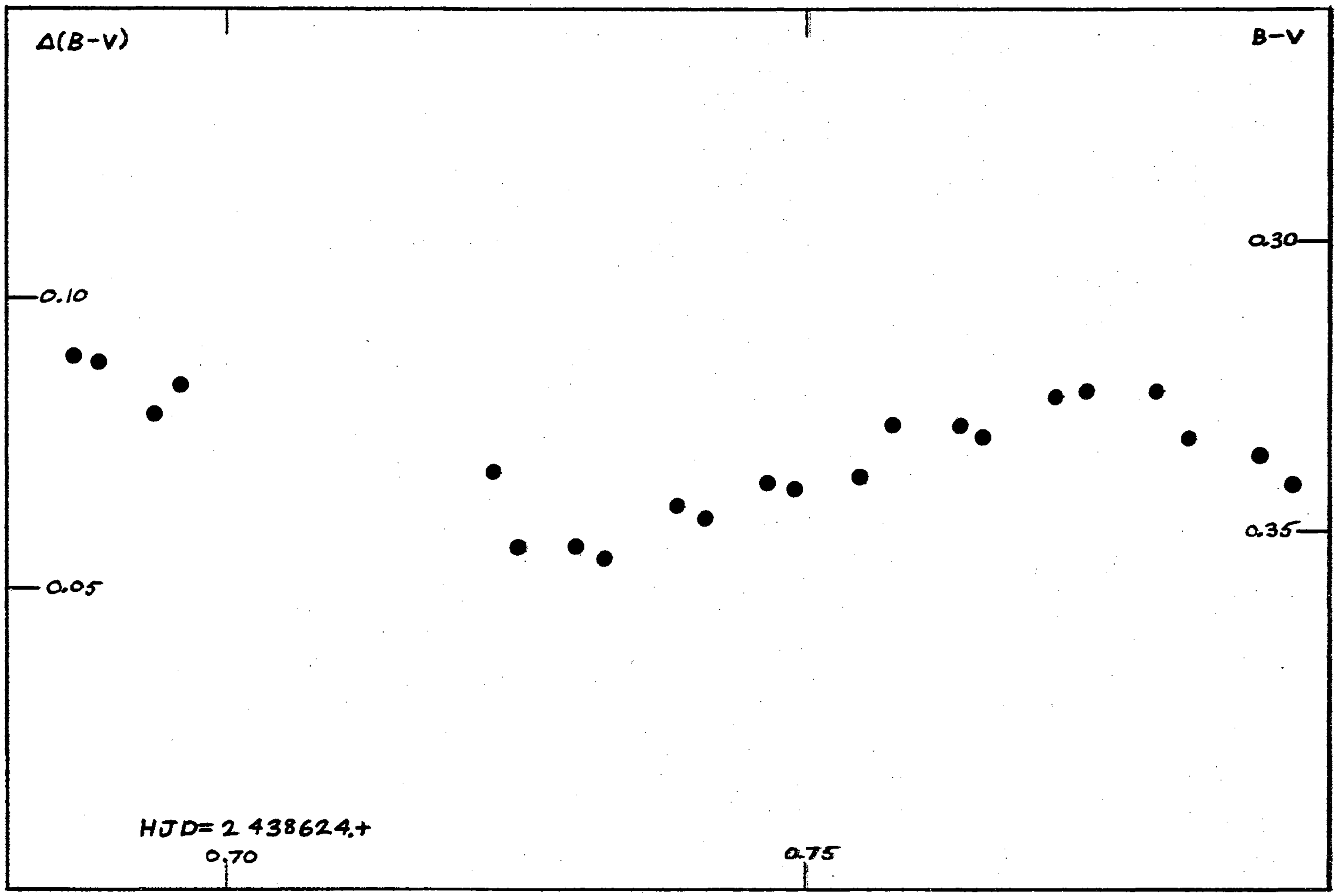

Figure 36. Light Curve in B-V of DQ Cephei for August 17, 1964 (Early).

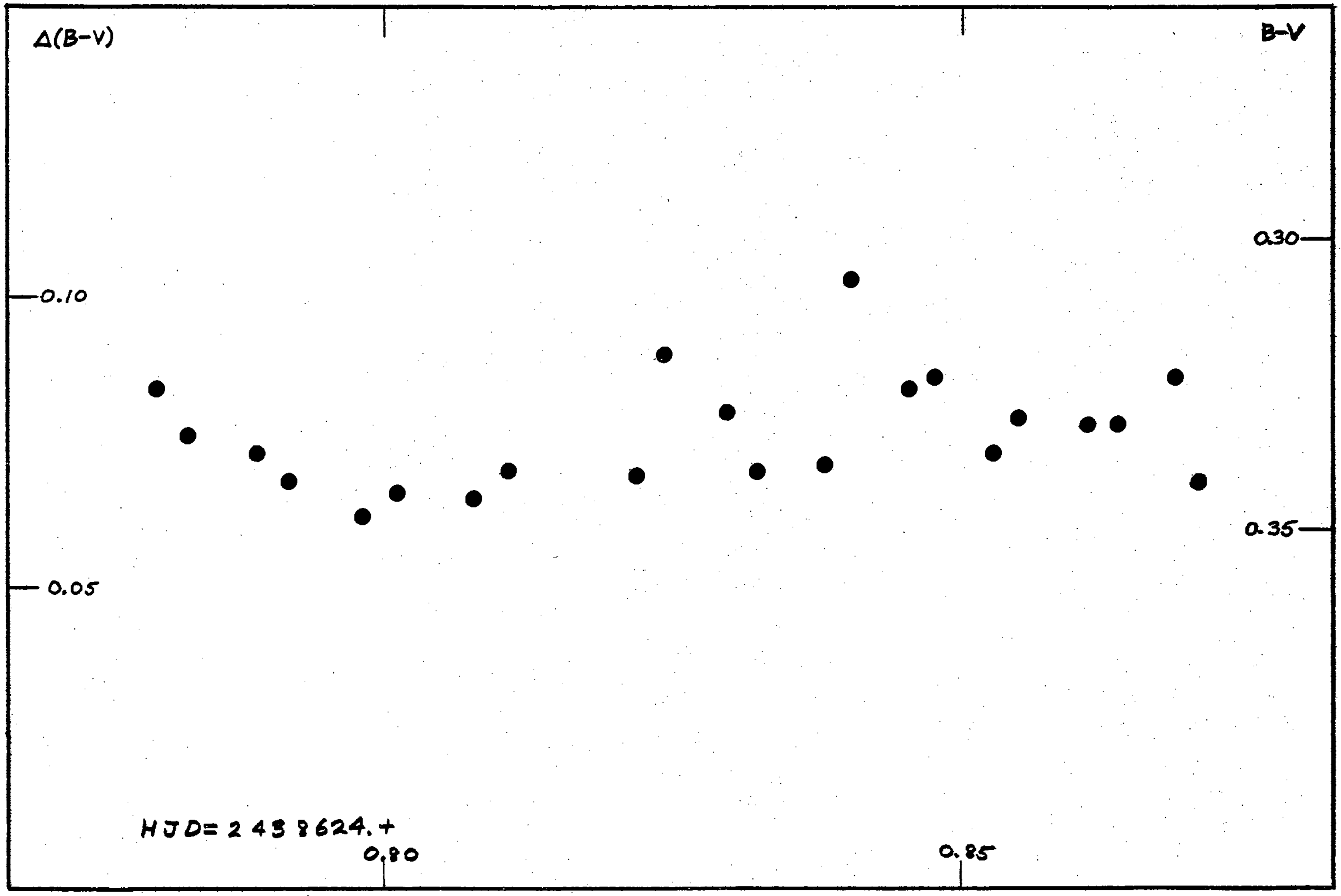

Figure 37. Light Curve in B-V of DQ Cephei for August 17, 1964 (Late).

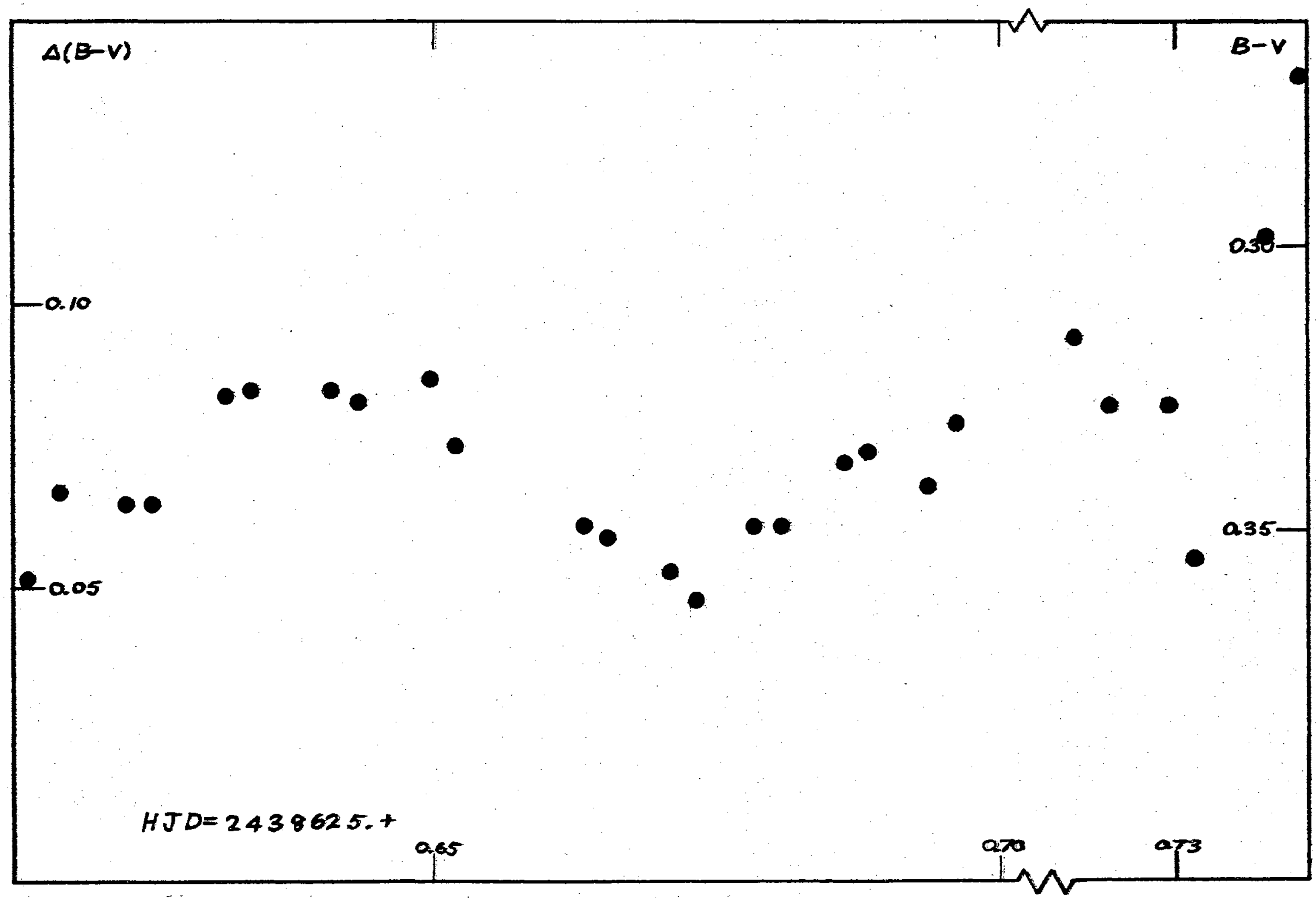

Figure 38. Light Curve in B-V of DQ Cephei for August 18, 1964.

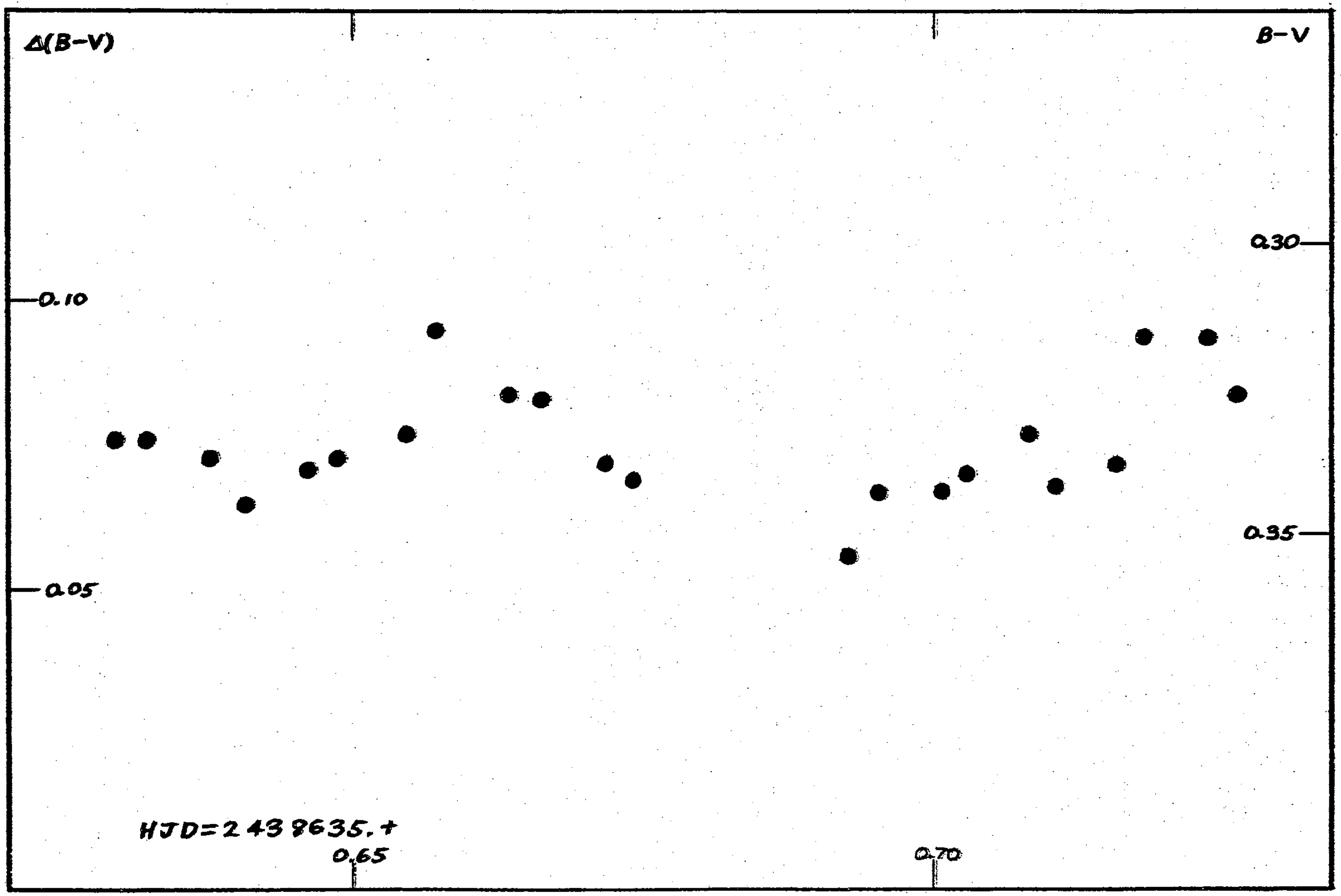

Figure 39. Light Curve in B-V of DQ Cephei for August 28, 1964.

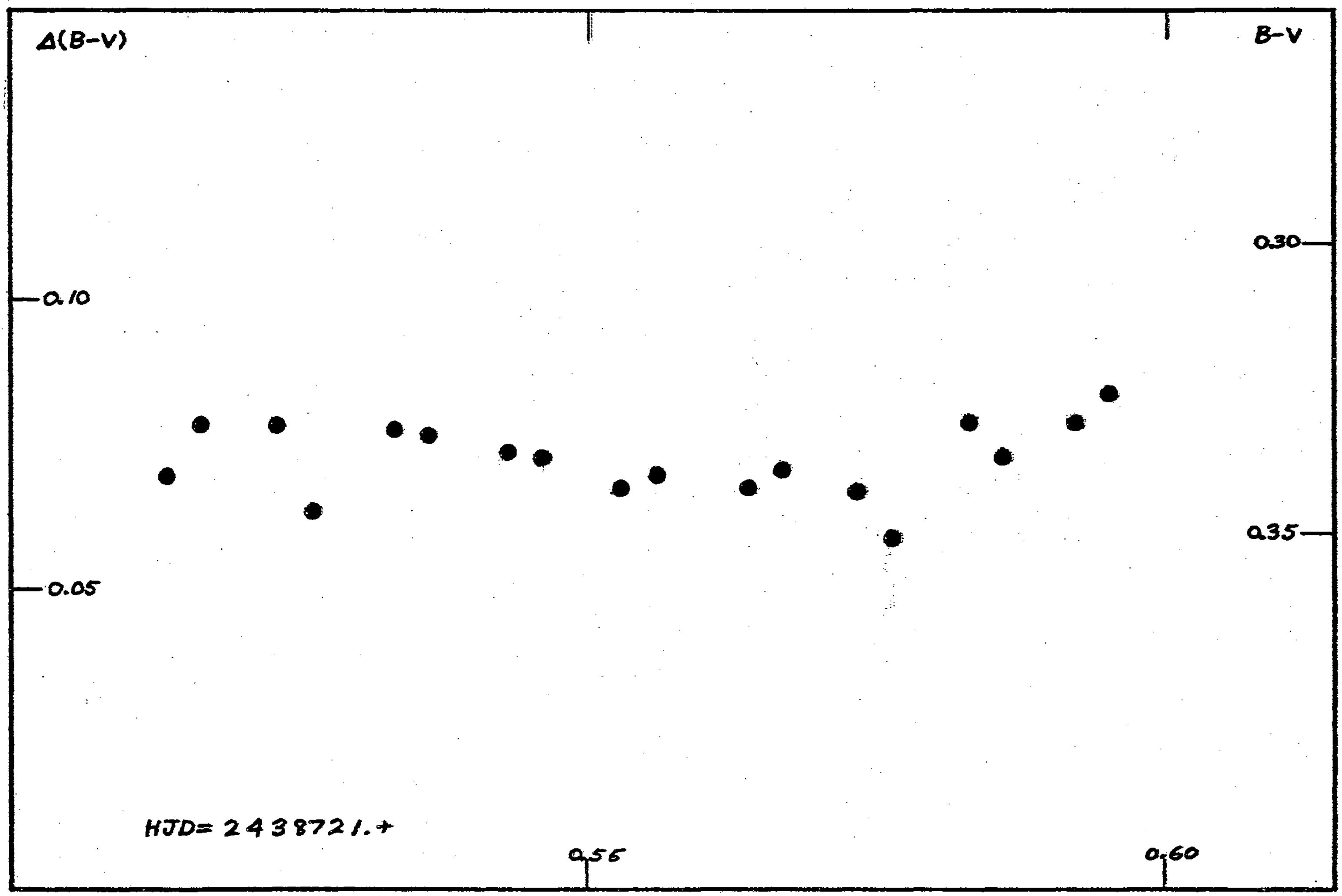

Figure 40. Light Curve in B-V of DQ Cephei for November 22, 1964.

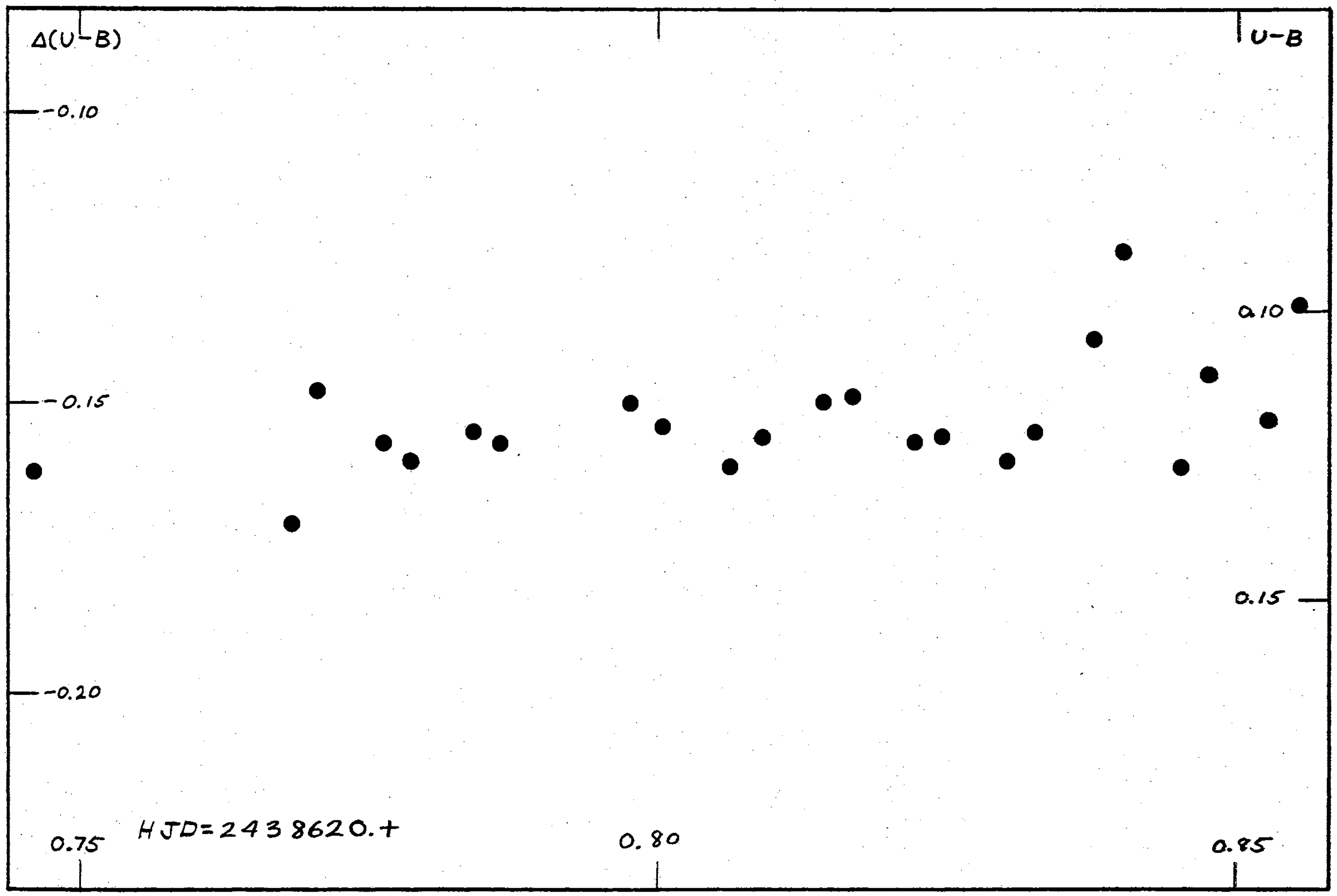

Figure 41. Light Curve in U-B of DQ Cephei for August 13, 1964.

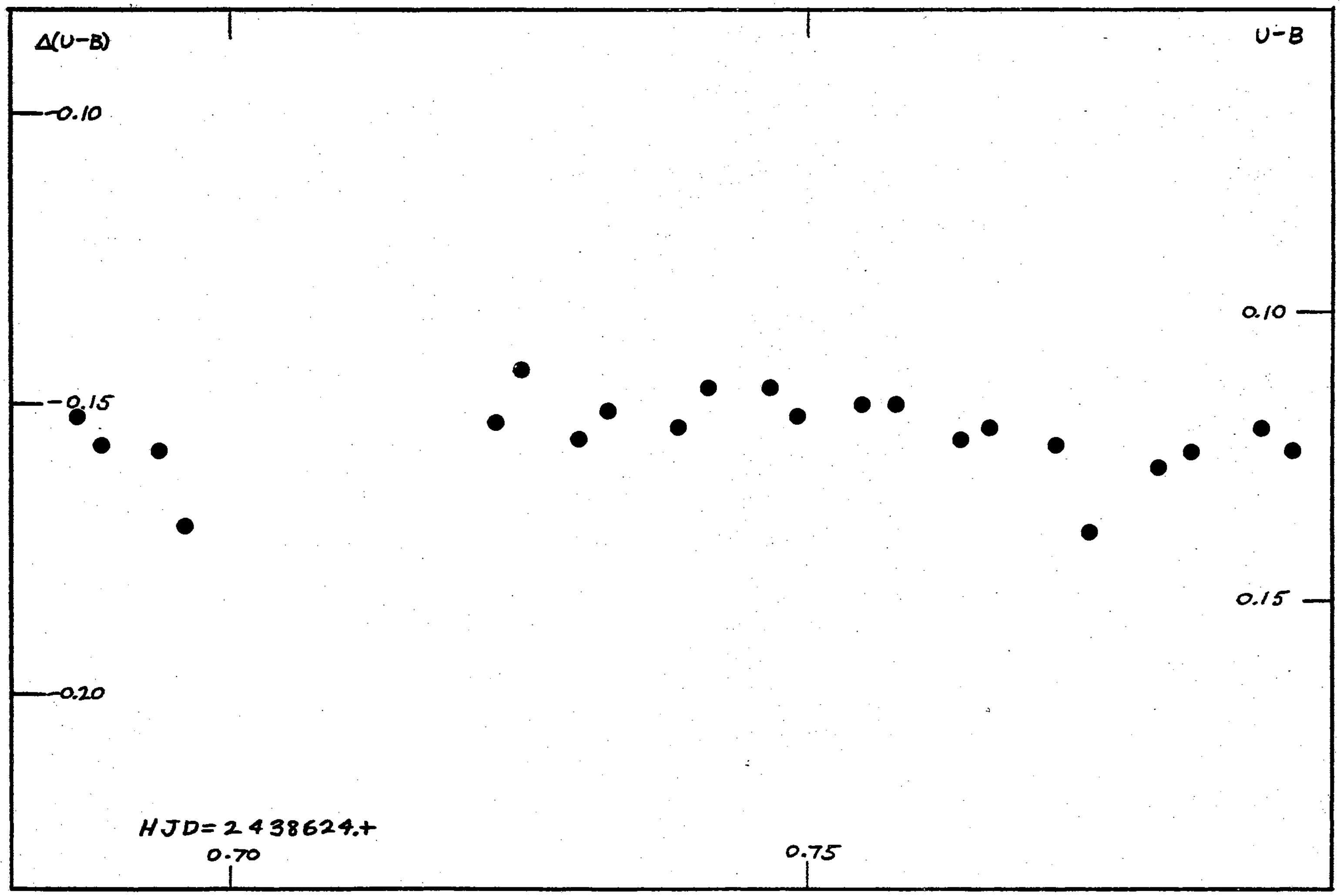

Figure 42. Light Curve in U-B of DQ Cephei for August 17, 1964 (Early).

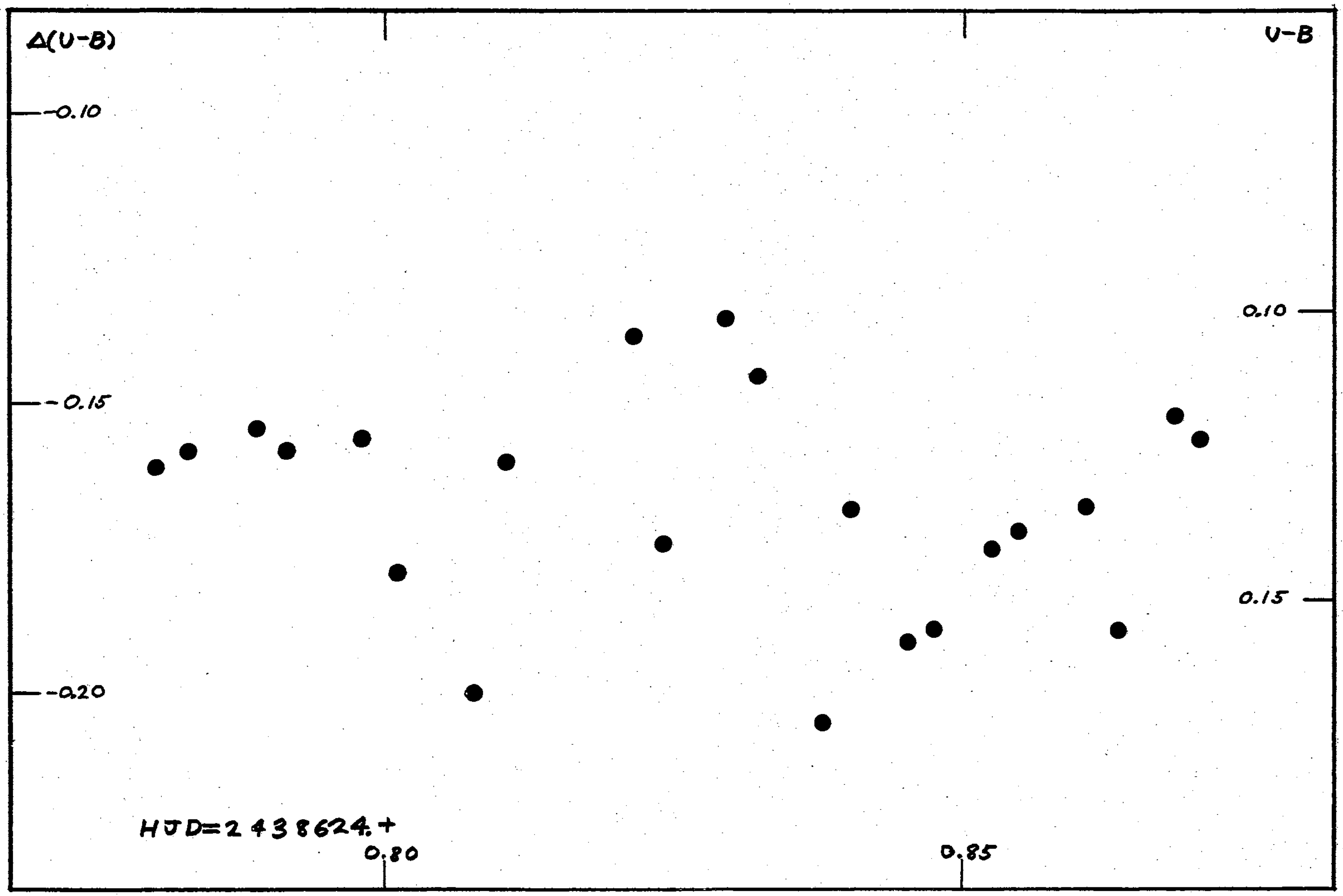

Figure 43. Light Curve in U-B of DQ Cephei for August 17, 1964 (Late).

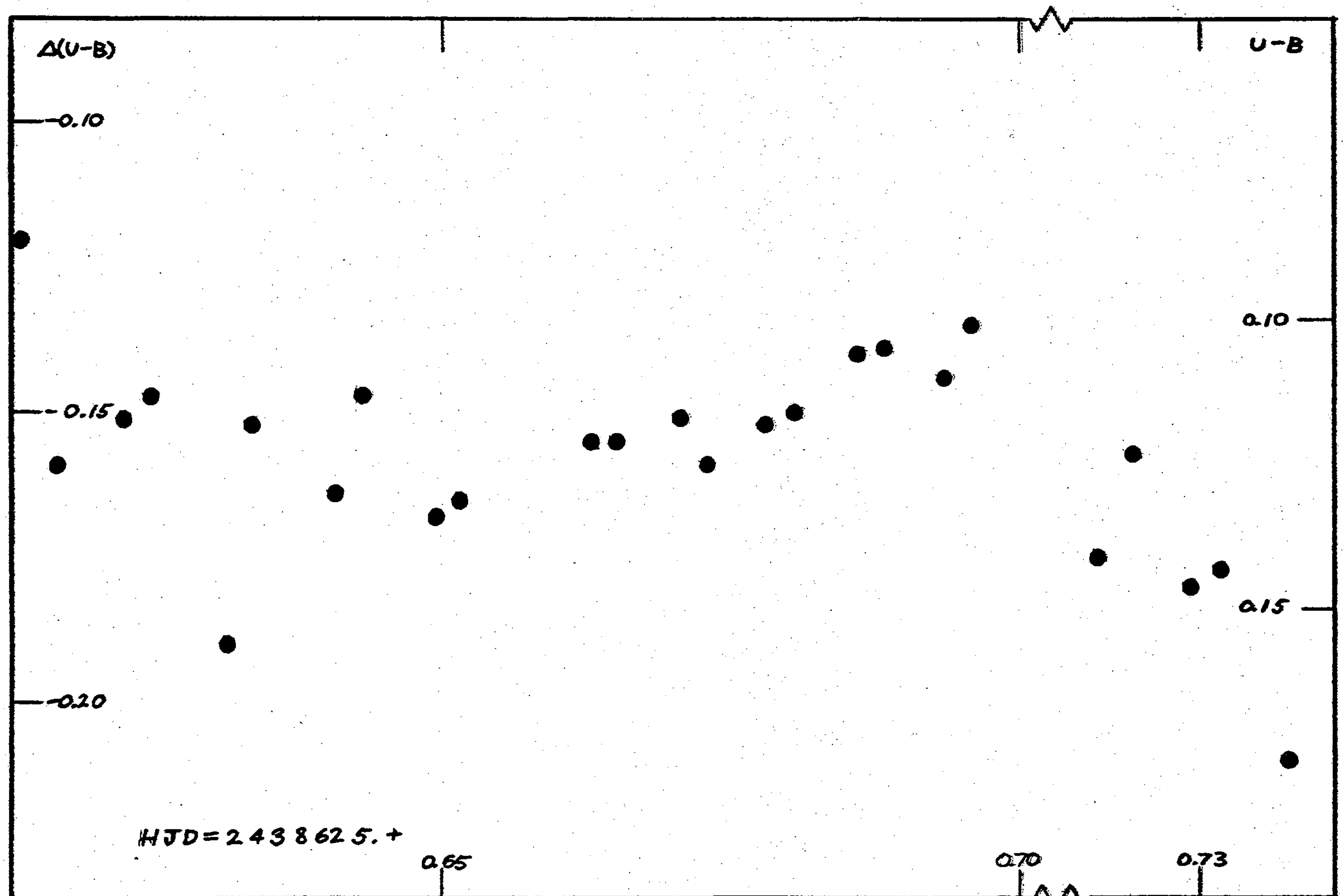

Figure 44. Light Curve in U-B of DQ Cephei for August 18, 1964.

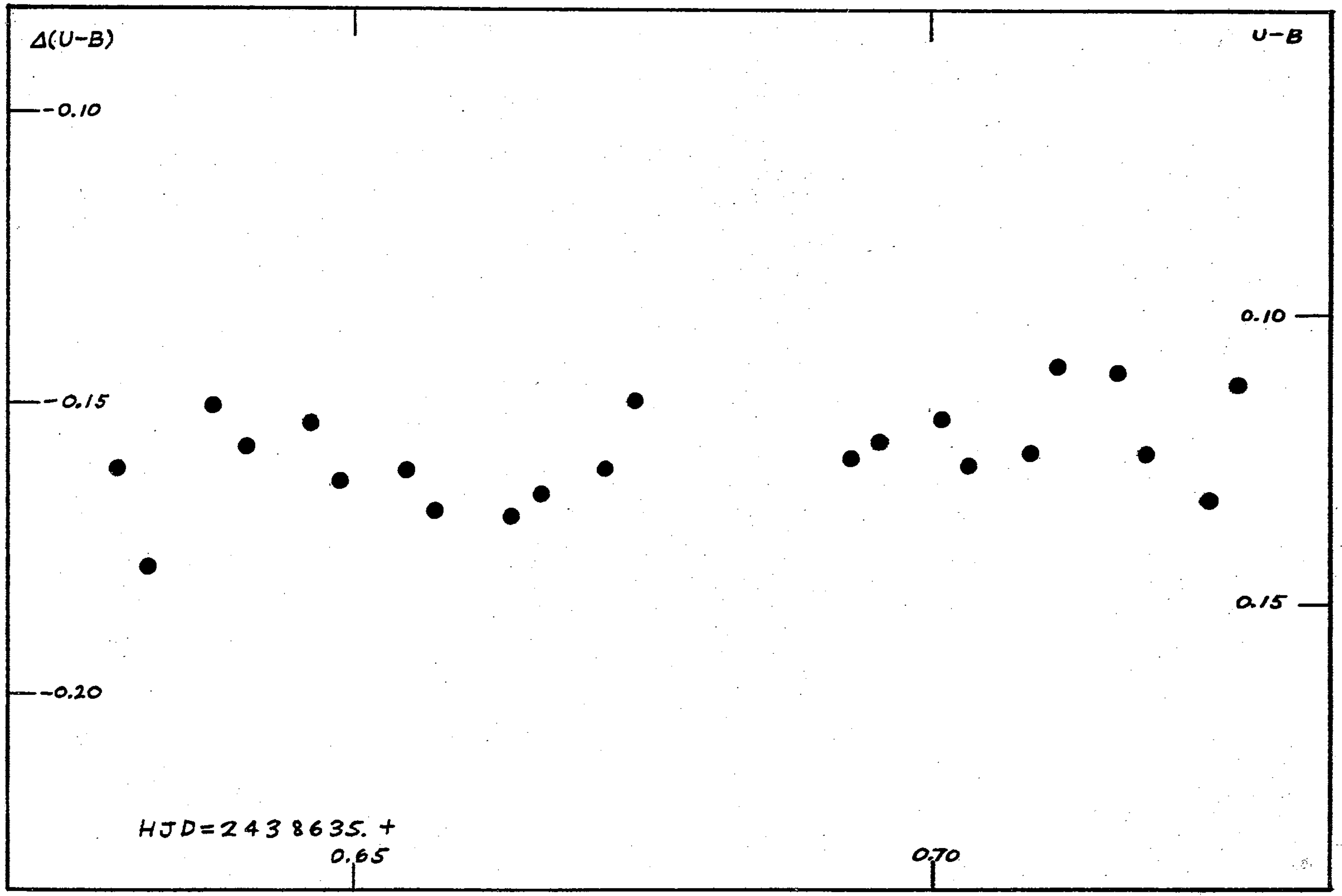

Figure 45. Light Curve in U-B of DQ Cephei for August 28, 1964.

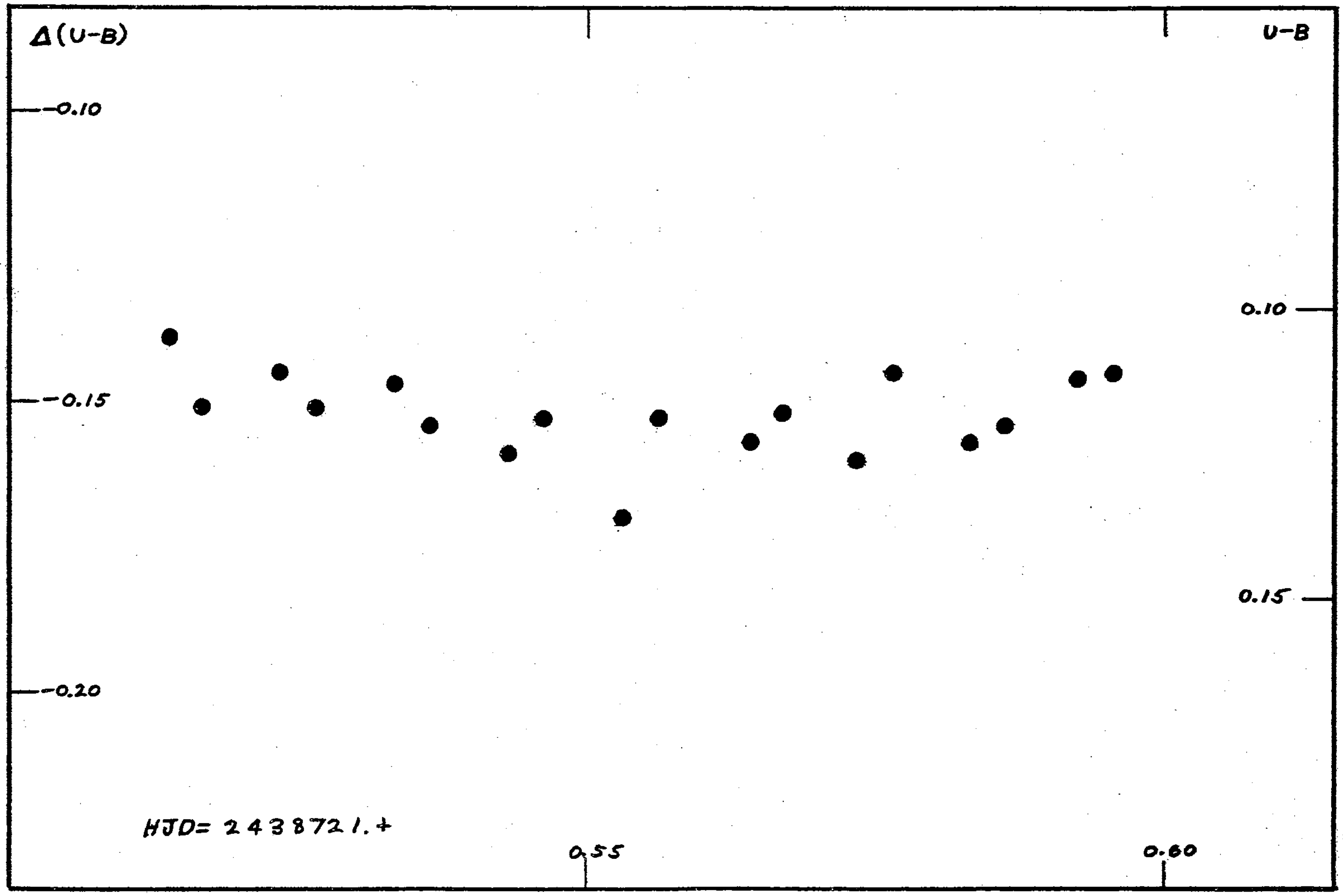

Figure 46. Light Curve in U-B of DQ Cephei for November 22, 1964.

CHAPTER IV

PERIOD DETERMINATION

The periods of variable stars are often given as numbers of seven or eight significant digits. Such amazingly precise values are of course not directly observed. The moment at which the peak of a light curve occurs can be observed with a precision of at most a thousandth of a cycle. By combining observations of such moments separated by a long time interval which contains thousands of cycles a very accurate value of the period can be derived.

Extraction of All Possible Periods

Suppose that a series of light curve maxima of a star, not necessarily consecutive, have been observed with a maximum error of ϵ, and let us suppose that we have an initial estimate of the period with a maximum tolerance. Let the intervals between adjacent observed maxima (which are not necessarily consecutive) be called primary intervals and the intervals between observed maxima which are separated by one or more other observed maxima, secondary intervals. Thus, every secondary interval is the sum of two or more primary intervals. If the number of cycles in each of the primary intervals contained in a secondary interval is known, the secondary interval has been spanned, since, obviously, the number of cycles occurring in it is the sum of the number in the primary intervals.

Let the initial estimates of the extremes of the period be written as P_{1max}, P_{1min}, and the gap between the ith and jth maxima be Δt_{ijmax}, Δt_{ijmin}. These maximum and minimum values are derived from the spread in the observations of the light curve maxima. In beginning the search for possible periods, the smallest interval is selected. This is of course a primary interval. The largest number of cycles which could have occurred in this interval is found by assuming the interval to be as long as possible and the period as short as possible. That is

$$N_{i,i+1,1max} = \frac{\Delta t_{i,i+1max}}{P_{1min}} , \qquad (4.1)$$

where the subscript, 1, on the N associates it with period P_1. Later if new possible periods develop, each will need separate cycle numbers. Since the cycle number is known to be a whole number the fractional part can be truncated. From similar considerations we have

$$N_{i,i+1,1min} = \frac{\Delta t_{i,i+1min}}{P_{1max}} . \qquad (4.2)$$

In this case the cycle number should be truncated up to the next higher integer. It may happen that we find $N_{i,i+1,1max} < N_{i,i+1,1min}$ because of these truncations. In this case we can only conclude that the proposed period gives rise to inconsistent results and must be discarded.

After obtaining all possible cycle numbers for the interval it is necessary to determine the period that corresponds to each of them. If we are fortunate, there will be only one cycle number and, hence, one period to determine, but it will frequently happen that the interval is too long to prevent ambiguity from occurring. For each of the possible cycle numbers, the maximum possible period is obtained by assuming the interval to be as long as possible.

$$P_{k\max} = \frac{\Delta t_{i,i+1\max}}{N_{i,i+1,k}} , \qquad (4.3)$$

where $N_{i,i+1,k}$ is the kth possible cycle number. Similarly,

$$P_{k\min} = \frac{\Delta t_{i,i+1\min}}{N_{i,i+1,k}} . \qquad (4.4)$$

Now, $P_{k\max}$ is compared with the original estimate $P_{1\max}$, and the smaller of these values is retained. $P_{k\min}$ is compared with $P_{1\min}$ and the larger retained.

Using the P_k's as new estimates for the periods, the next larger primary interval is selected and for each possible period the maximum and minimum cycle numbers determined by

$$N_{i,i+1,k\max} = \frac{\Delta t_{i,i+1\max}}{P_{k\min}} ,$$

$$N_{i,i+1,k\min} = \frac{\Delta t_{i,i+1\min}}{P_{k\max}} , \qquad (4.5)$$

where the subscript i has been retained even though the interval under consideration is new. Again, if $N_{k\max} < N_{k\min}$ after truncation, the kth period can be eliminated, and if $N_{j\max} > N_{j\min}$ each intervening integer must be considered as giving rise to a new possible period. For each cycle number new periods are found using Equations (4.3) and (4.4).

It may be that we obtain $P_{kmin} > P_{kmax}$ from this process. Then, the kth period must be eliminated.

Eventually, a secondary interval must be spanned. In this case, we know the cycle number N_{ijk} to be the sum of the cycle numbers of the primary intervals, so

$$N_{ijk} = \sum_{h=i}^{j-1} N_{h,h+1,k} , \qquad (4.6)$$

and we can go immediately to Equations (4.5) to find new estimates of the periods. We continue in this way until all intervals have been exhausted or all possible periods eliminated.

Optimization of Periods

After the analysis of the last section has been performed, a set of possible periods and the corresponding cycle numbers are available. If we have been fortunate, the period has been uniquely determined and only one period and one set of cycle numbers will remain. This period is reported in terms of its extreme tolerance limits and it remains for us to find an optimum value in some sense.

Since the maxima (or minima) of the light curve are supposedly separated by equal intervals of time, the epochs of maximum will be given by an equation of the form

$$MAX = T + P \cdot E , \qquad (4.7)$$

where T is the epoch of maximum at a cycle taken as the zeroeth cycle. Then, as E assumes the values 1, 2, 3, . . ., the equation will generate the times of the first, second, third, . . . maxima.

If we have done our analysis correctly we know the cycle numbers and, hence, E for each observed maximum. In fact

$$E_i = N_{1i} \ . \qquad (4.8)$$

Now, E_i is a whole number known without error, and there is no reason to suppose that the estimation of the observed maxima will depend on the cycle number. Therefore the situation fits the classical least squares model where the independent variable is known without error and the variance of the dependent variable is constant. The theory of fitting straight line data by least squares techniques is well known. See, for example, Acton (1959). The normal equations corresponding to formula (4.7) are

$$\begin{aligned} TN + P\Sigma E_i &= \Sigma Max_i, \\ T\Sigma E_i + P\Sigma E_i^2 &= E_i Max_i, \end{aligned} \qquad (4.9)$$

which can easily be solved for T and P.

It might happen that several features of the pulsating star might be measured (such as variations in brightness and in radial velocity), possibly in separate series of cycles, and precision in the estimate of the period will be gained if all the observations can be used. If k separate series of observations are available each series will give rise to a predictive formula

$$FEATURE_{ij} = F_{ij} = T_j + PE_{ij} \quad ; \quad j = 1, 2, \ldots, k. \qquad (4.10)$$

The k + 1 unknown parameters in Equation (4.10) can be found by solving the normal equations

$$N_j \, T_j + P\sum_i E_{ij} = \sum_i F_{ij} \; ; \quad j = 1, 2, \ldots, k,$$

$$\sum_j T_j \Big(\sum_i E_{ij}\Big) + P\sum_{i,j} E_{ij}^2 = \sum_{i,j} E_{ij} F_{ij}, \tag{4.11}$$

while the standard errors of the parameters are given by

$$S_{T_j}^2 = \frac{S_j^2}{N_j} \, , \text{ where } S_j^2 = \frac{\sum_i \delta_{ij}^2}{N_j - 2} \, ,$$

$$S_p^2 = \frac{S_T^2}{\sum_{ij} E_{ij}^2 - N_T \bar{E}^2} \, , \text{ where } S_T^2 = \frac{\sum_{ij} \delta_{ij}^{\,2}}{\sum_j N_j - (k+1)} \; . \tag{4.12}$$

See Brownlee (1960). δ_{ij} is the residual between the i, jth observed and predicted value.

CHAPTER V

DETAILED COMPUTATION OF THE PERIOD

Location of Extrema

To locate the times of maximum and minimum light of DQ Cephei, the light curves in U, B, V were smoothed by averaging each pair of observations and their times. These averaged points were then plotted in each color for each night and a freehand curve fitted to each plot. The maxima and minima were then located on the curves. Figures 47 through 64 show these plots. Table XVI lists the times thus obtained. The maximum error in these times was taken to be ±0.004 day.

TABLE XVI

OBSERVED MAXIMA AND MINIMA OF DQ CEPHEI
HJD = 2438600.+

MAX_V	MAX_B	MAX_U	MIN_V	MIN_B	MIN_U
--	--	--	20.783	20.788	20.785
20.825	20.825	20.823	--	--	--
--	--	--	24.727	24.731	24.731
24.766	24.769	24.767	24.807	24.806	--
24.842	24.843	--	--	--	--
25.632	25.634	25.636	25.673	25.673	25.673
35.644	35.648	35.646	35.686	35.689	35.688
121.537	121.537	121.534	121.568	121.570	121.570

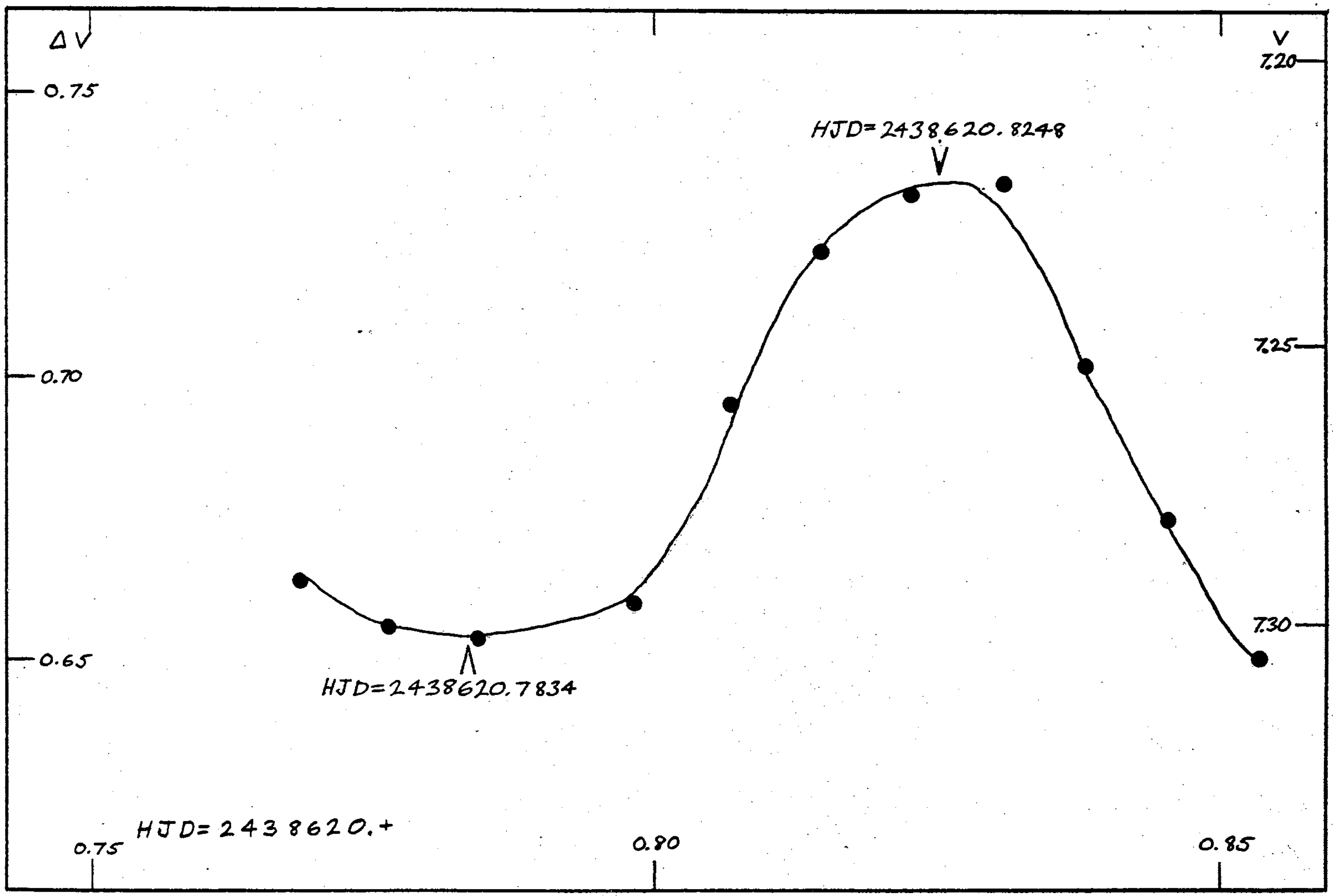

Figure 47. Extrema in V of DQ Cephei for August 13, 1964.

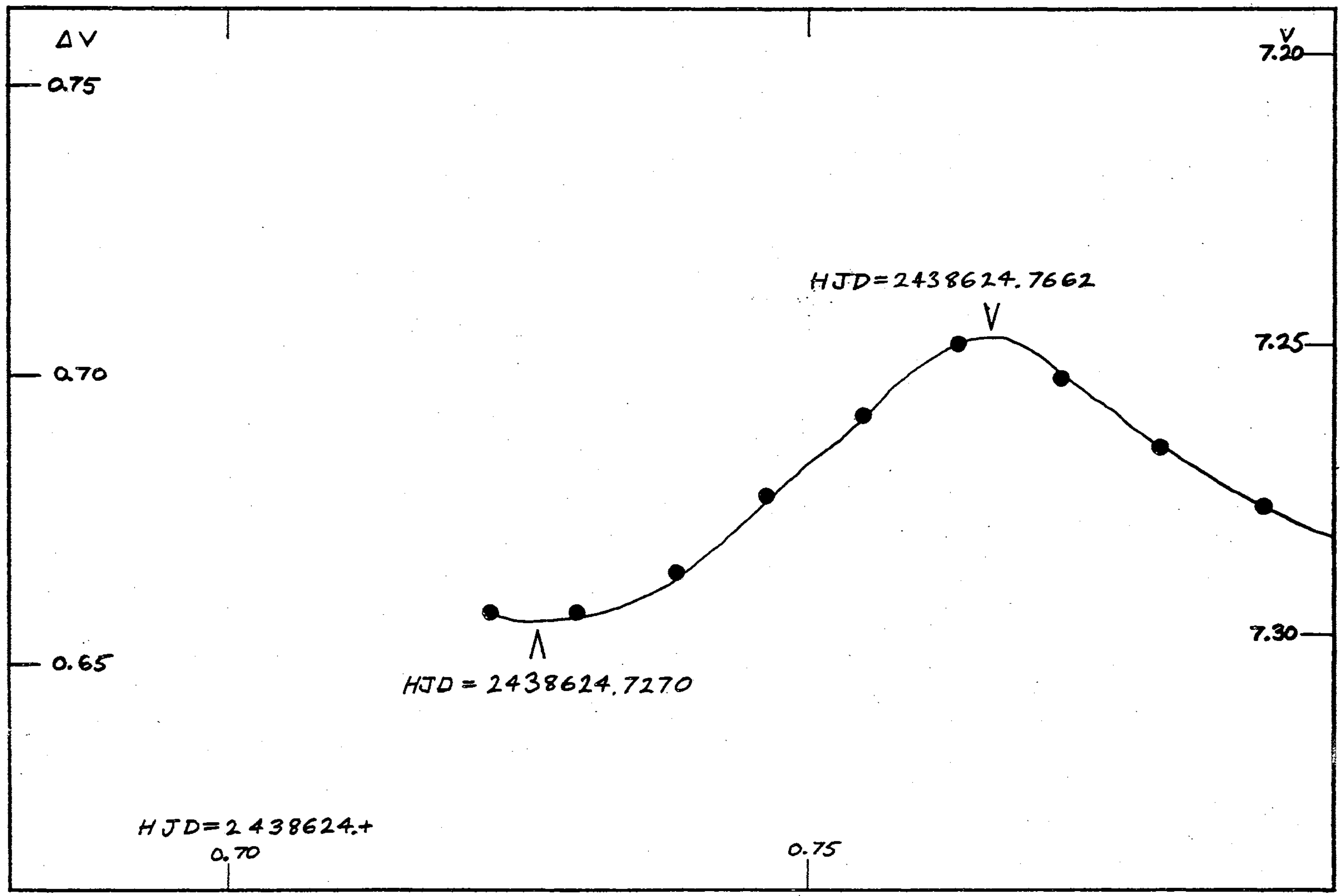

Figure 48. Extrema in V of DQ Cephei for August 18, 1964 (Early).

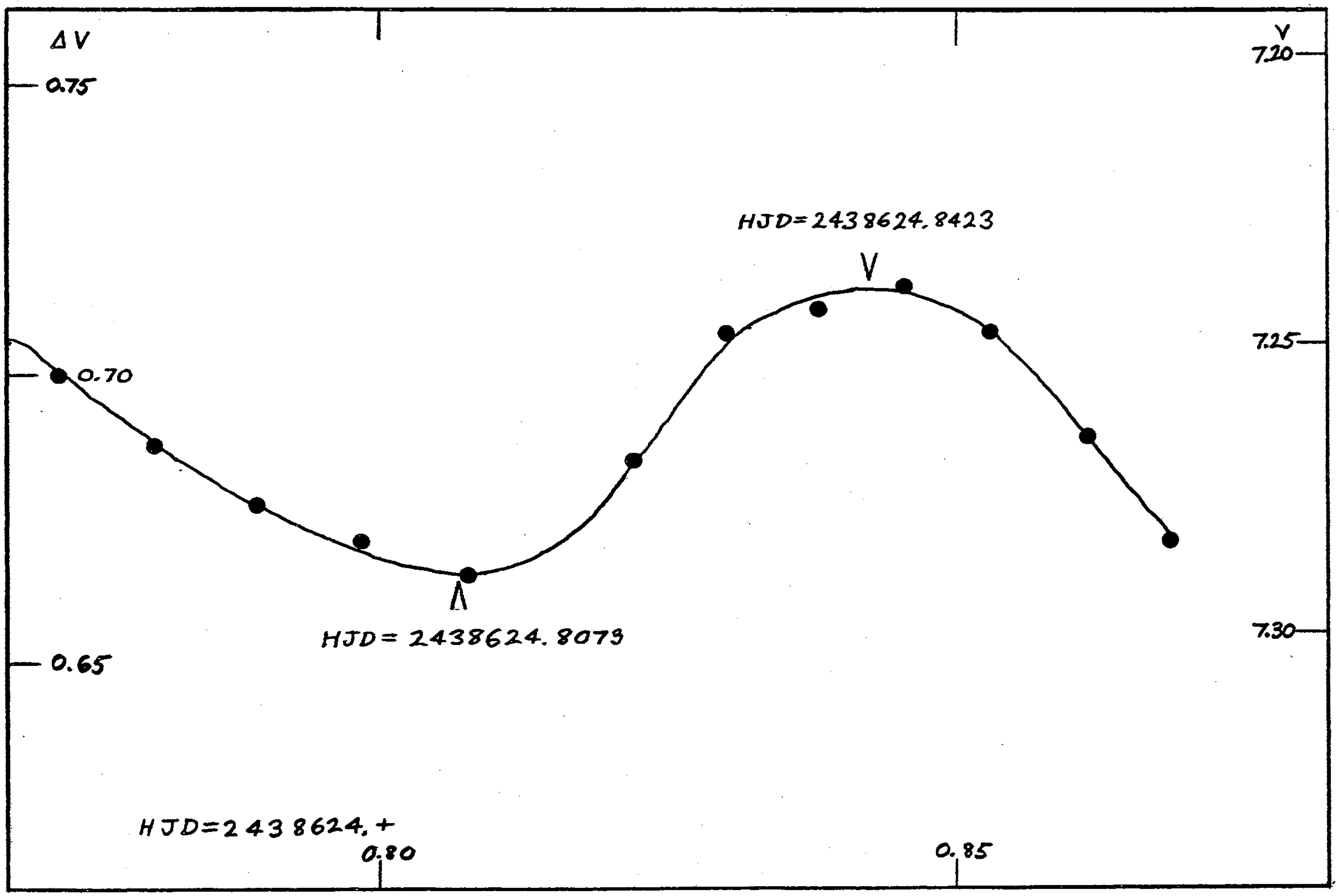

Figure 49. Extrema in V of DQ Cephei for August 17, 1964 (Late).

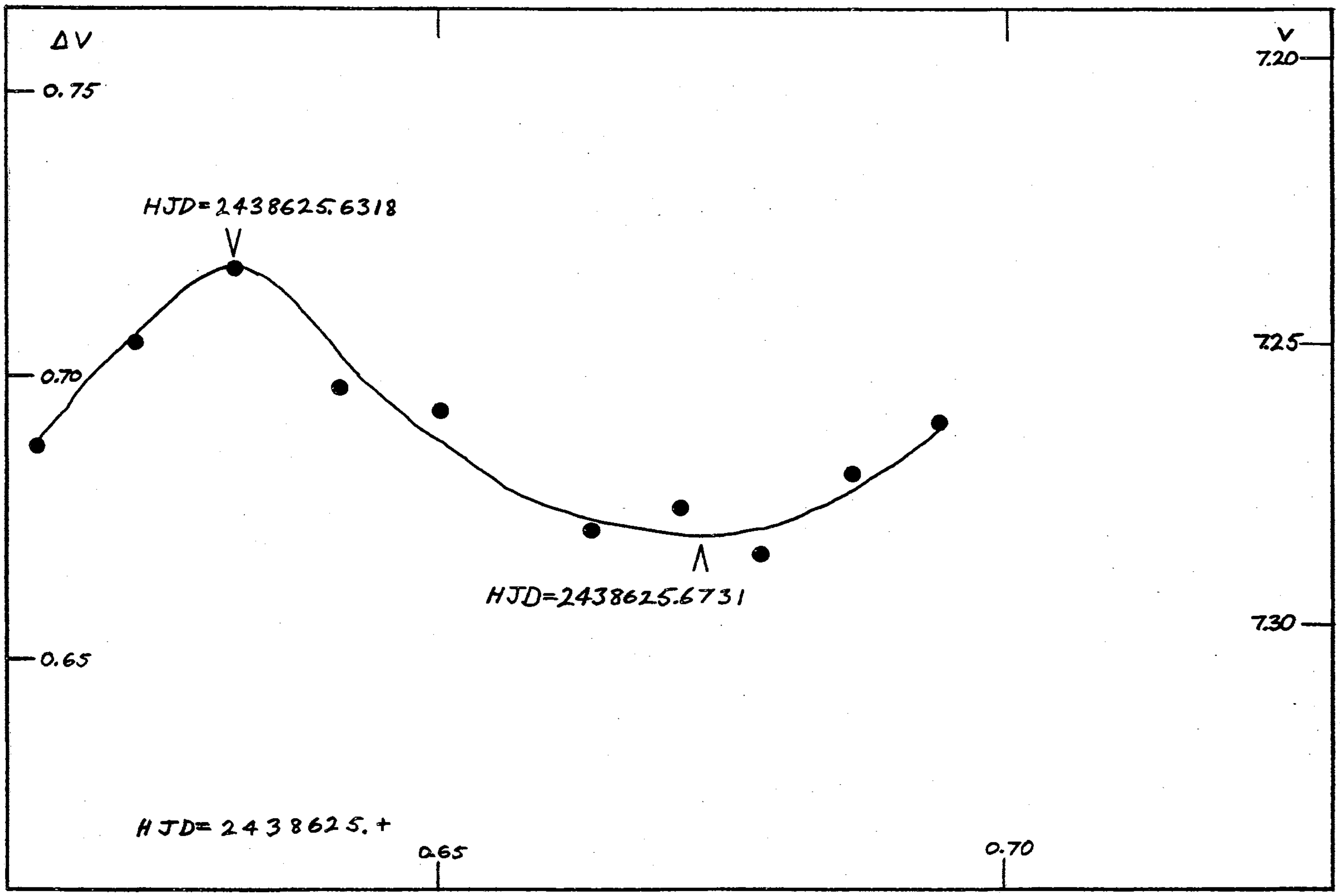

Figure 50. Extrema in V of DQ Cephei for August 18, 1964.

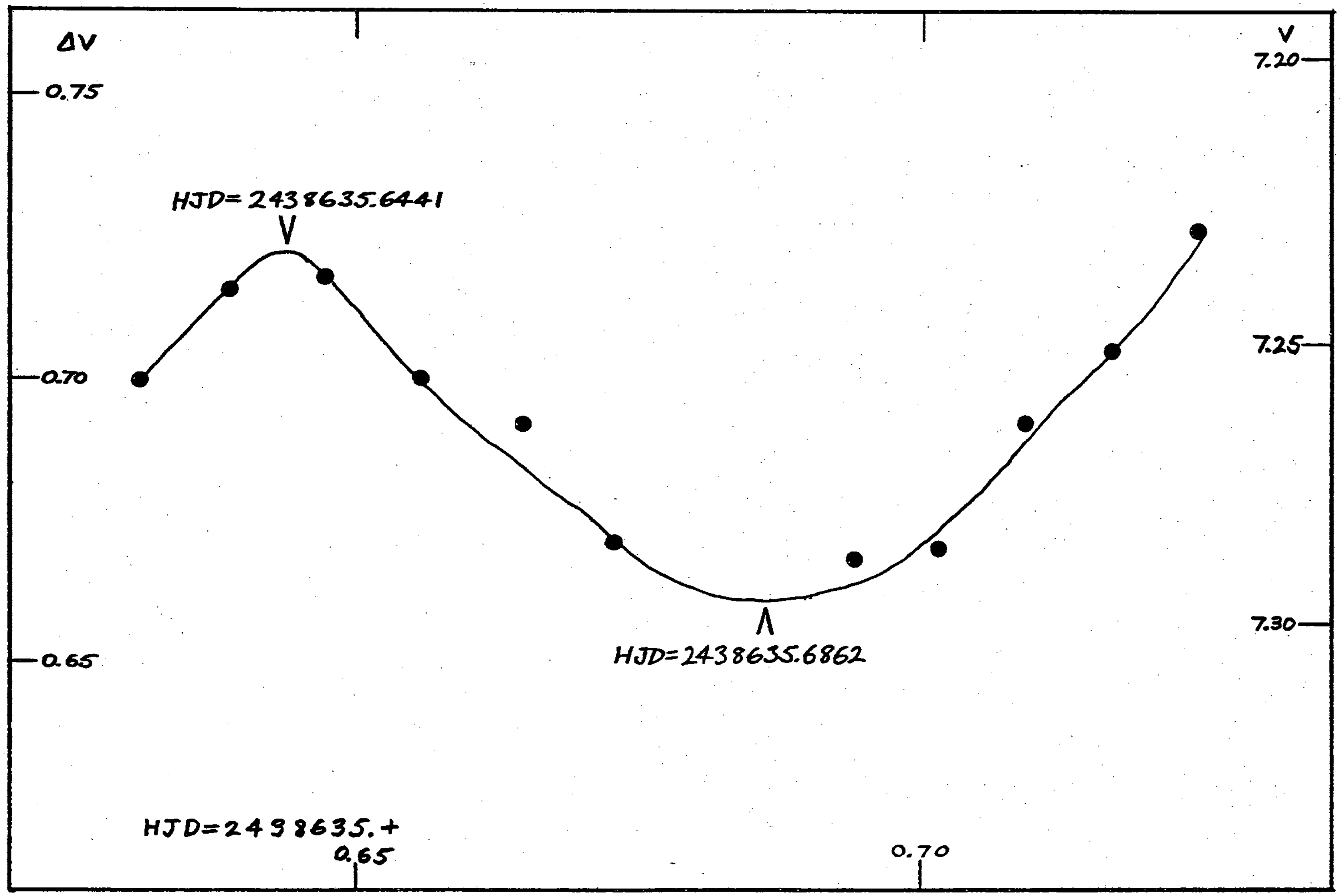

Figure 51. Extrema in V of DQ Cephei for August 28, 1964.

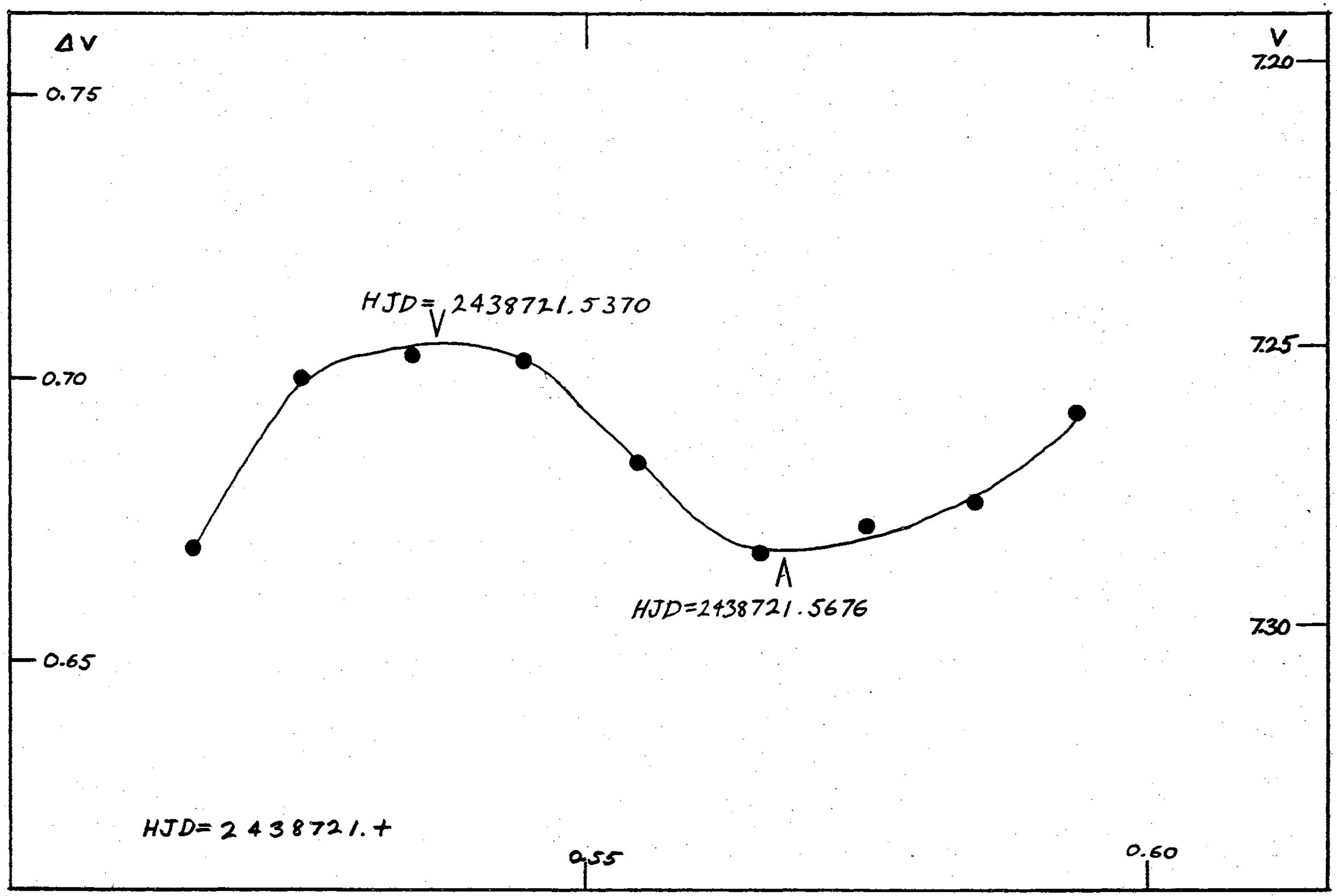

Figure 52. Extrema in V of DQ Cephei for November 22, 1964.

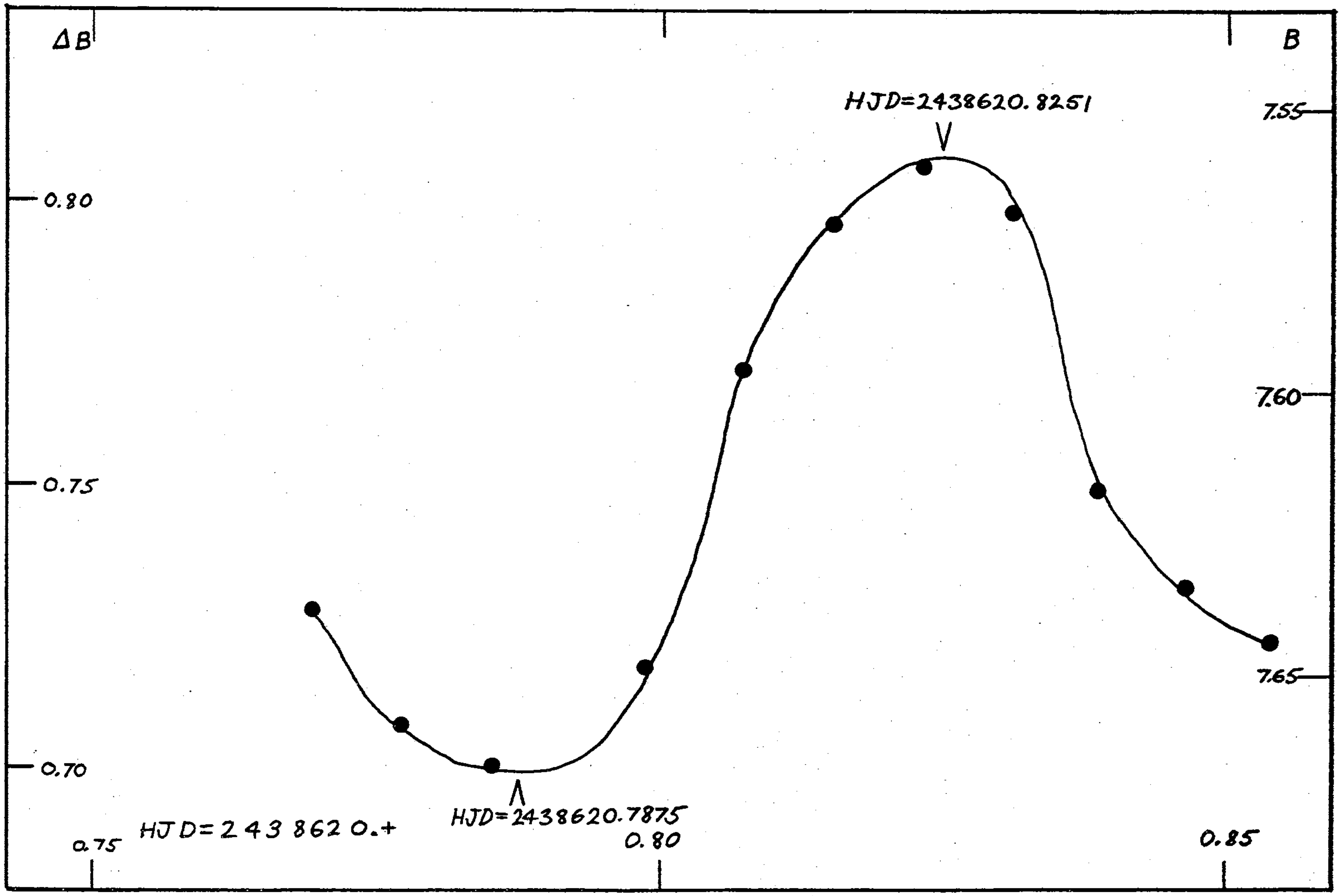

Figure 53. Extrema in B of DQ Cephei for August 13, 1964.

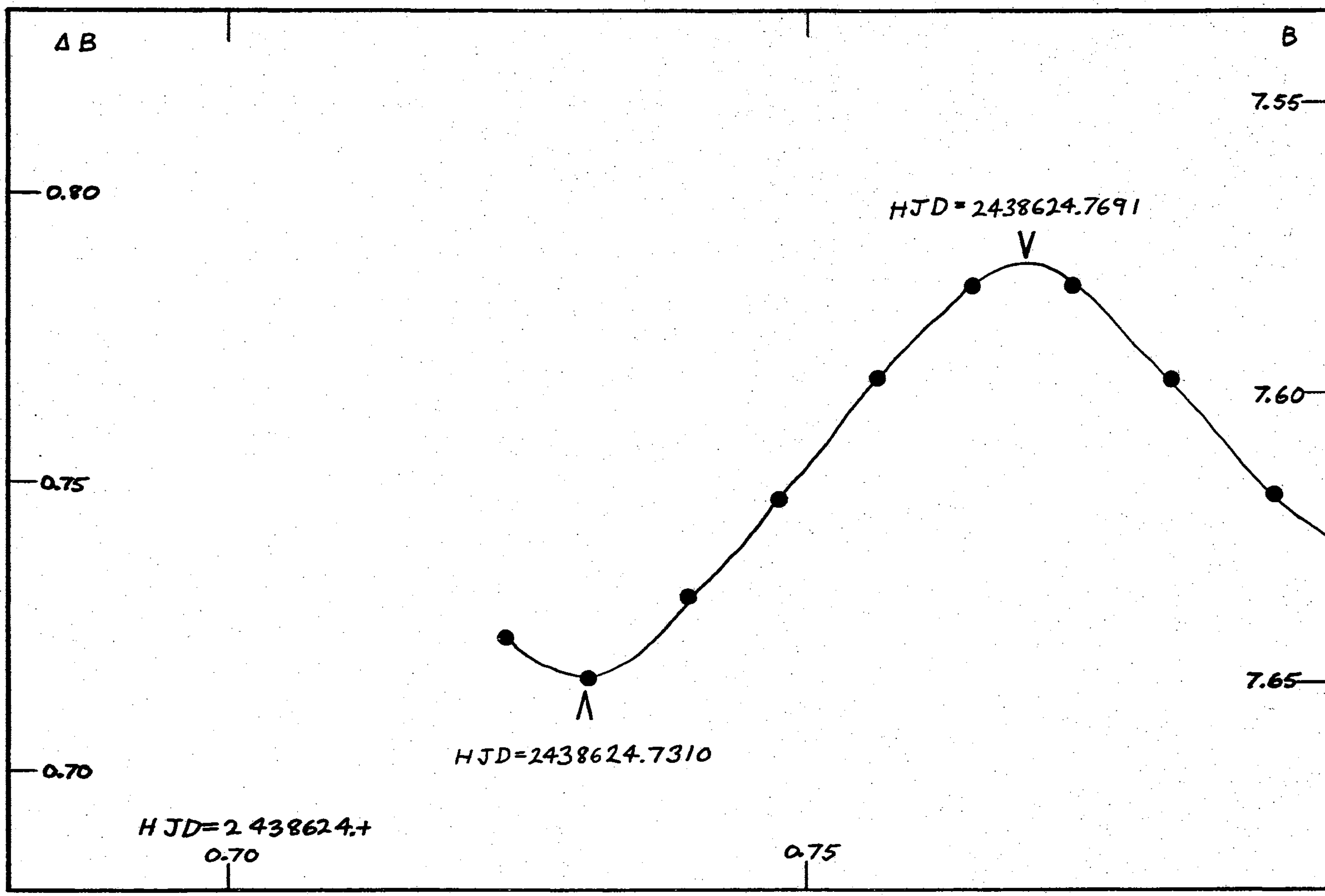

Figure 54. Extrema in B of DQ Cephei for August 18, 1964 (Early).

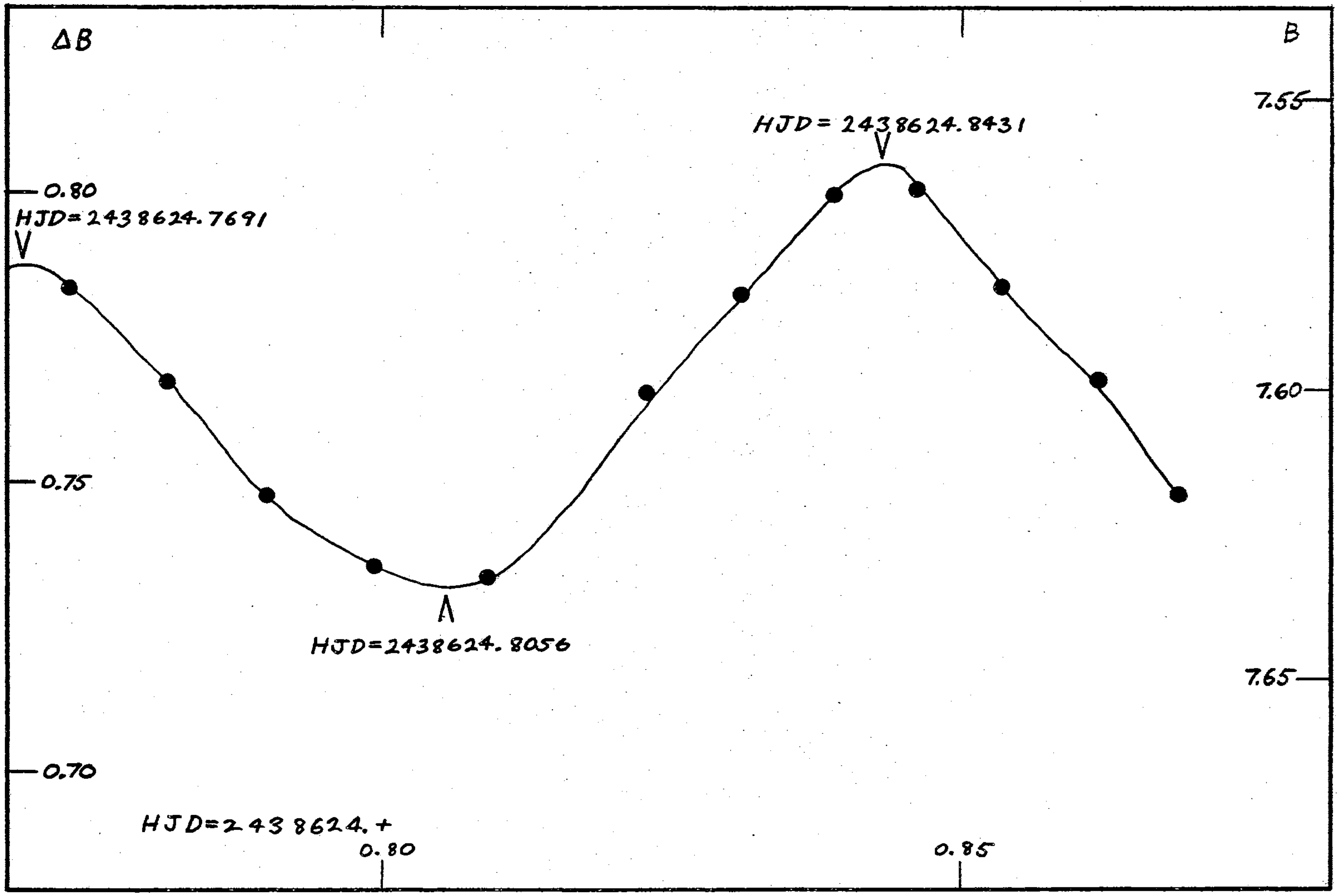

Figure 55. Extrema in B of DQ Cephei for August 17, 1964 (Late).

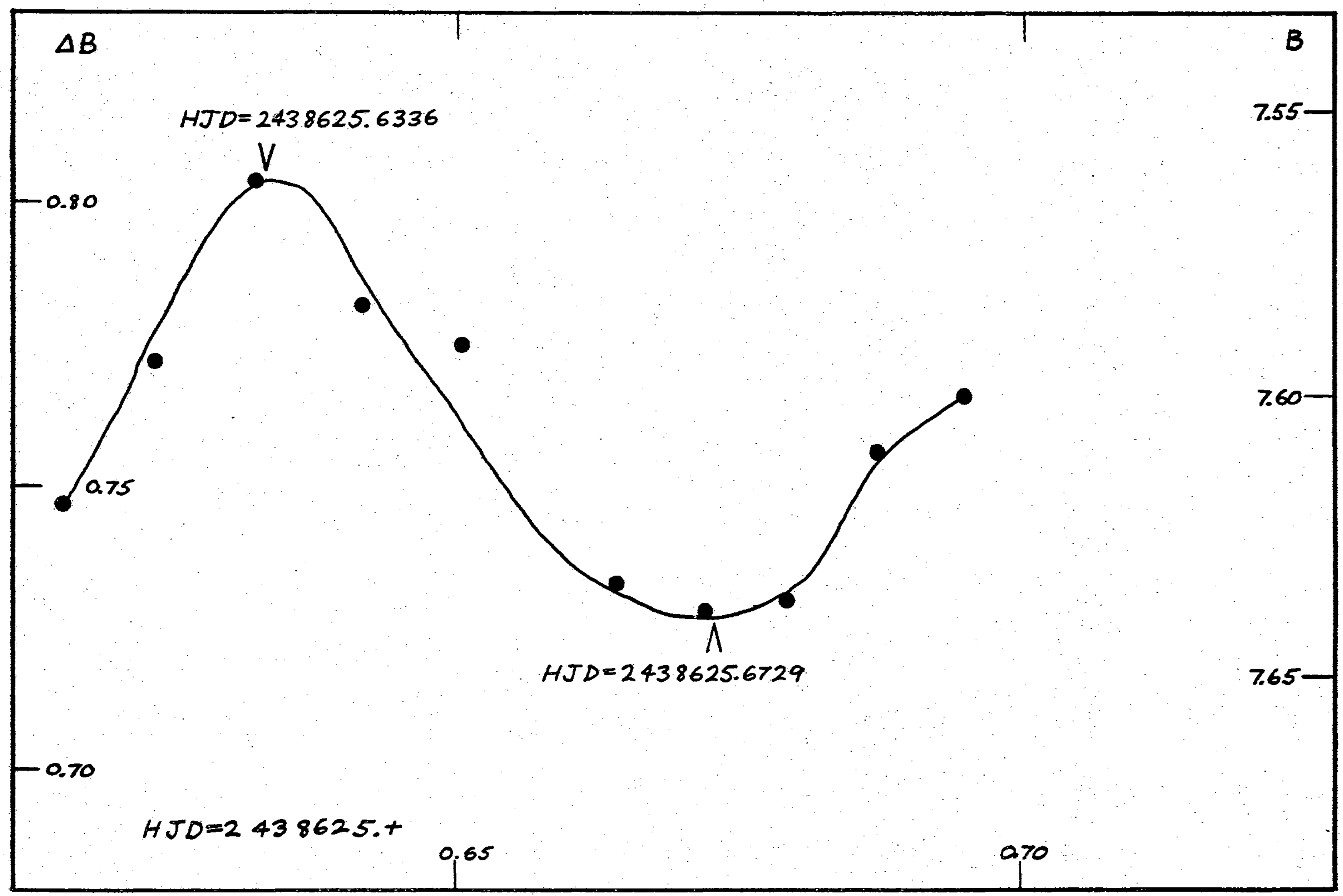

Figure 56. Extrema in B of DQ Cephei for August 18, 1964.

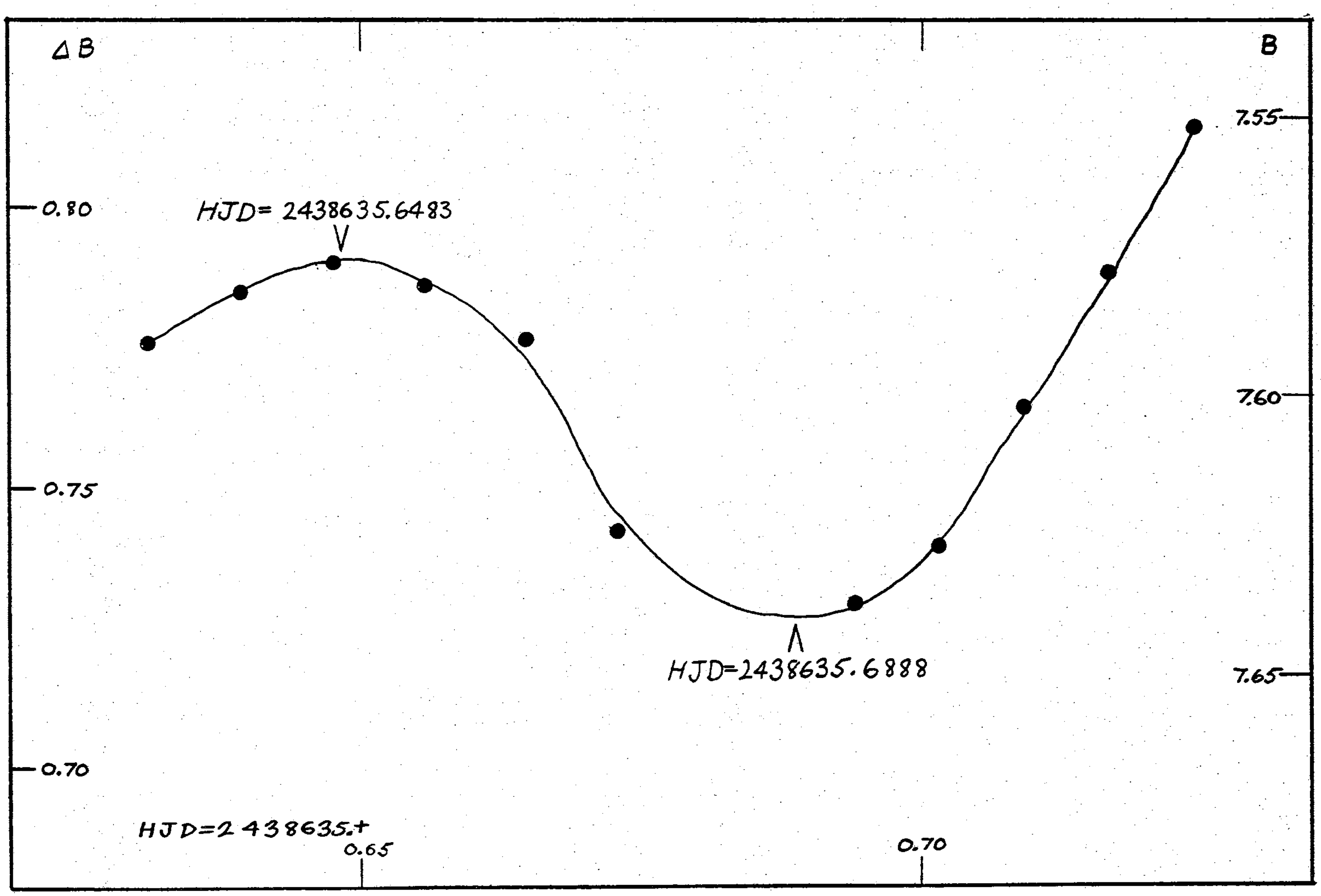

Figure 57. Extrema in B of DQ Cephei for August 28, 1964.

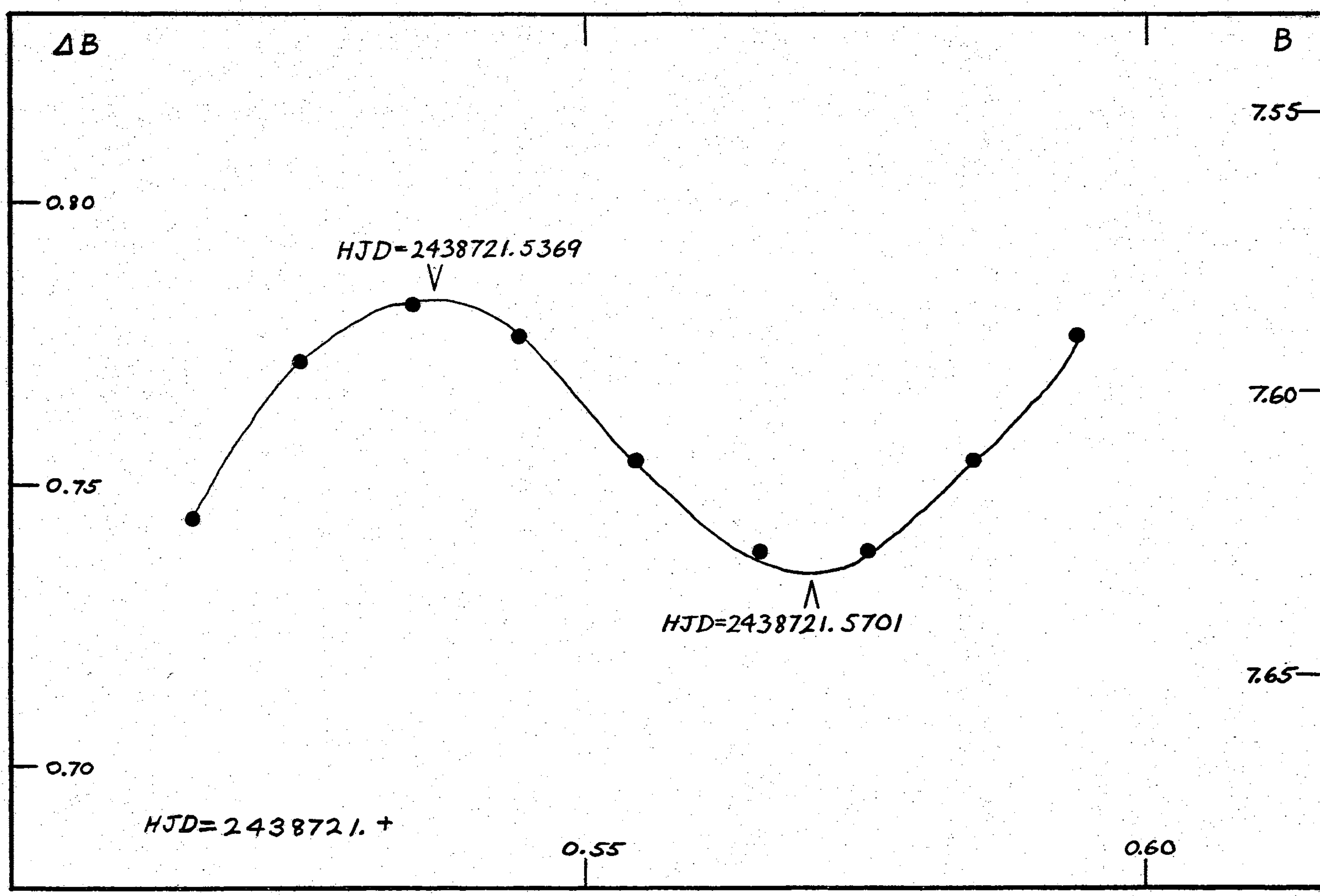

Figure 58. Extrema in B of DQ Cephei for November 22, 1964.

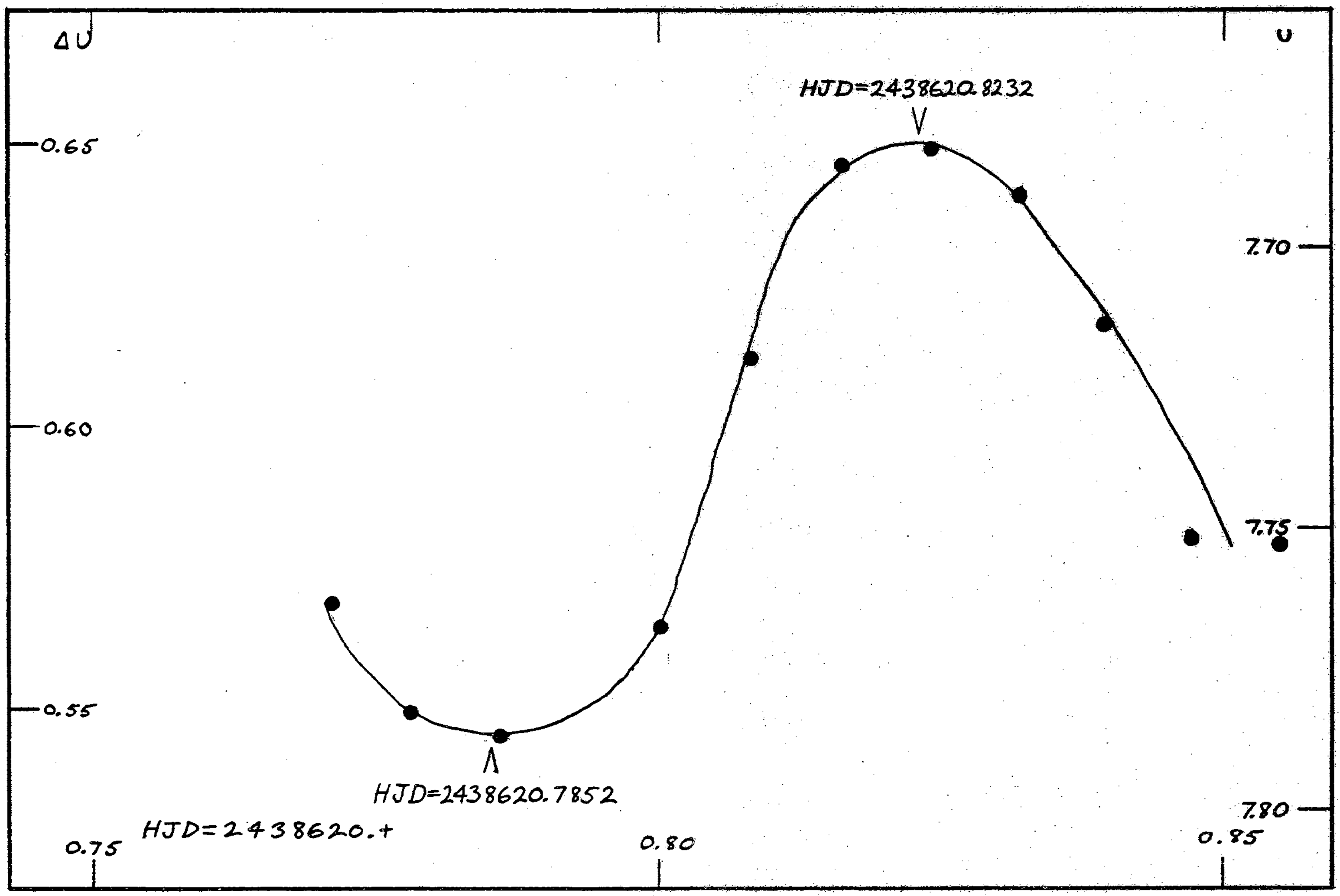

Figure 59. Extrema in U of DQ Cephei for August 13, 1964.

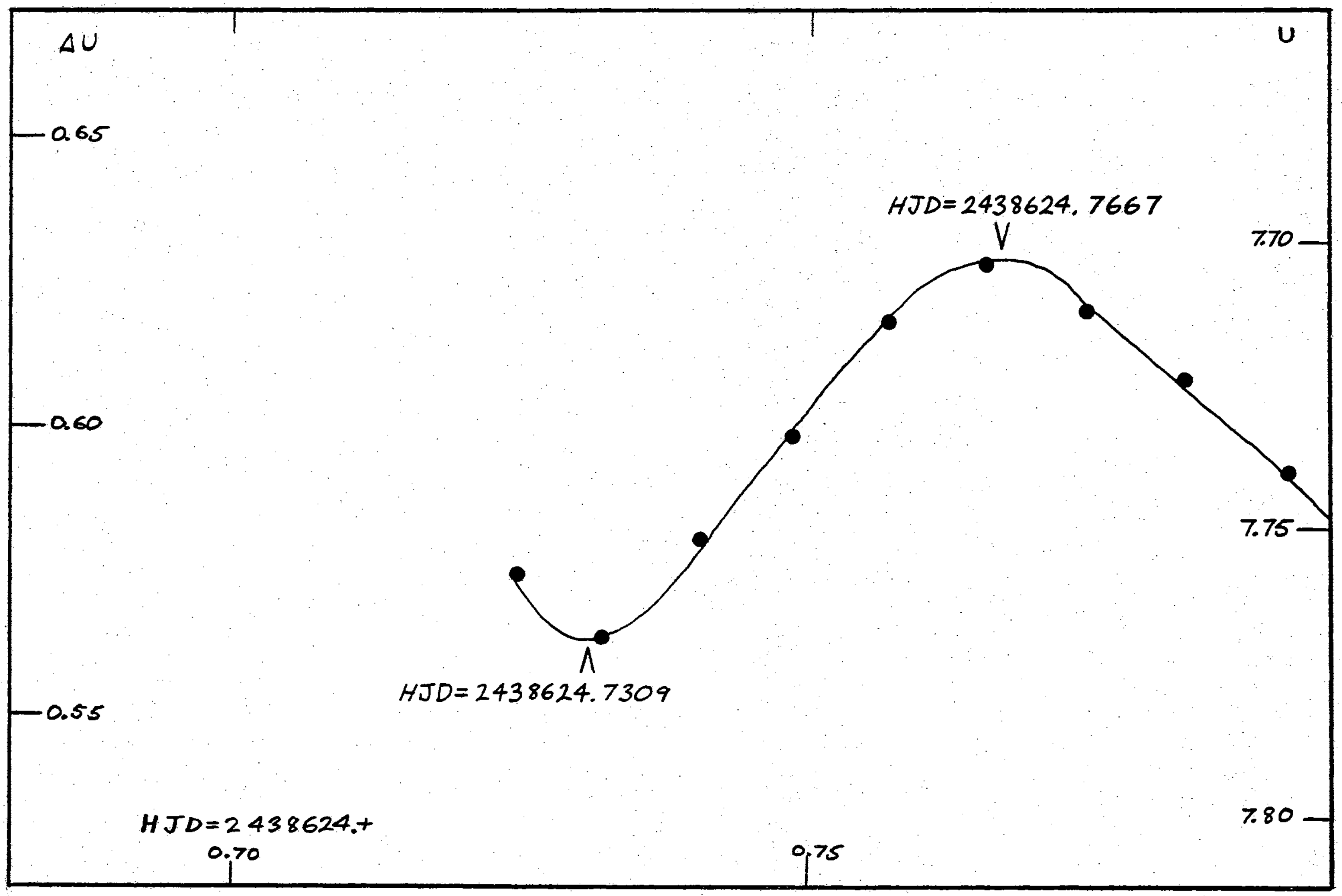

Figure 60. Extrema in U of DQ Cephei for August 18, 1964 (Early).

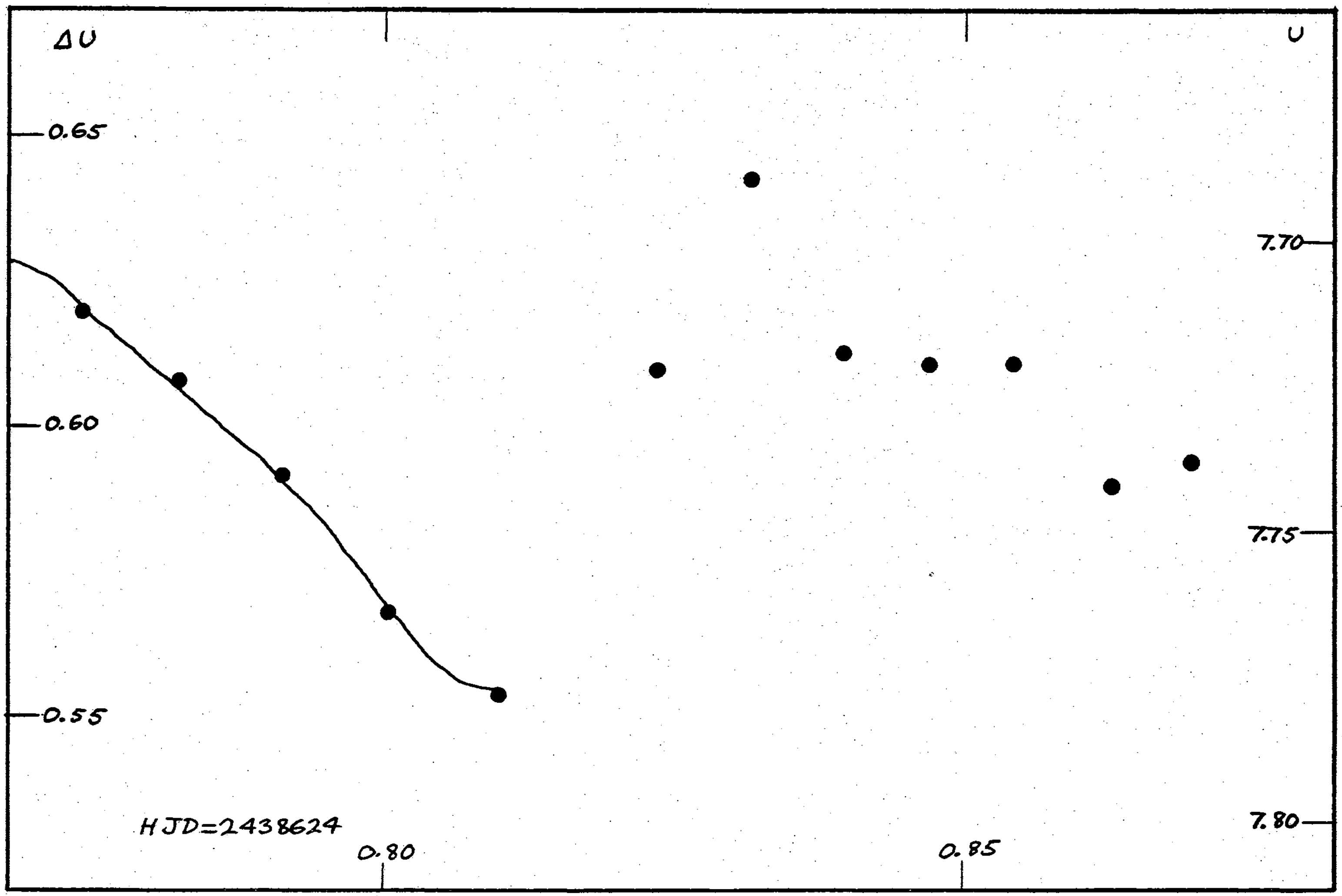

Figure 61. Extrema in U of DQ Cephei for August 17, 1964 (Late).

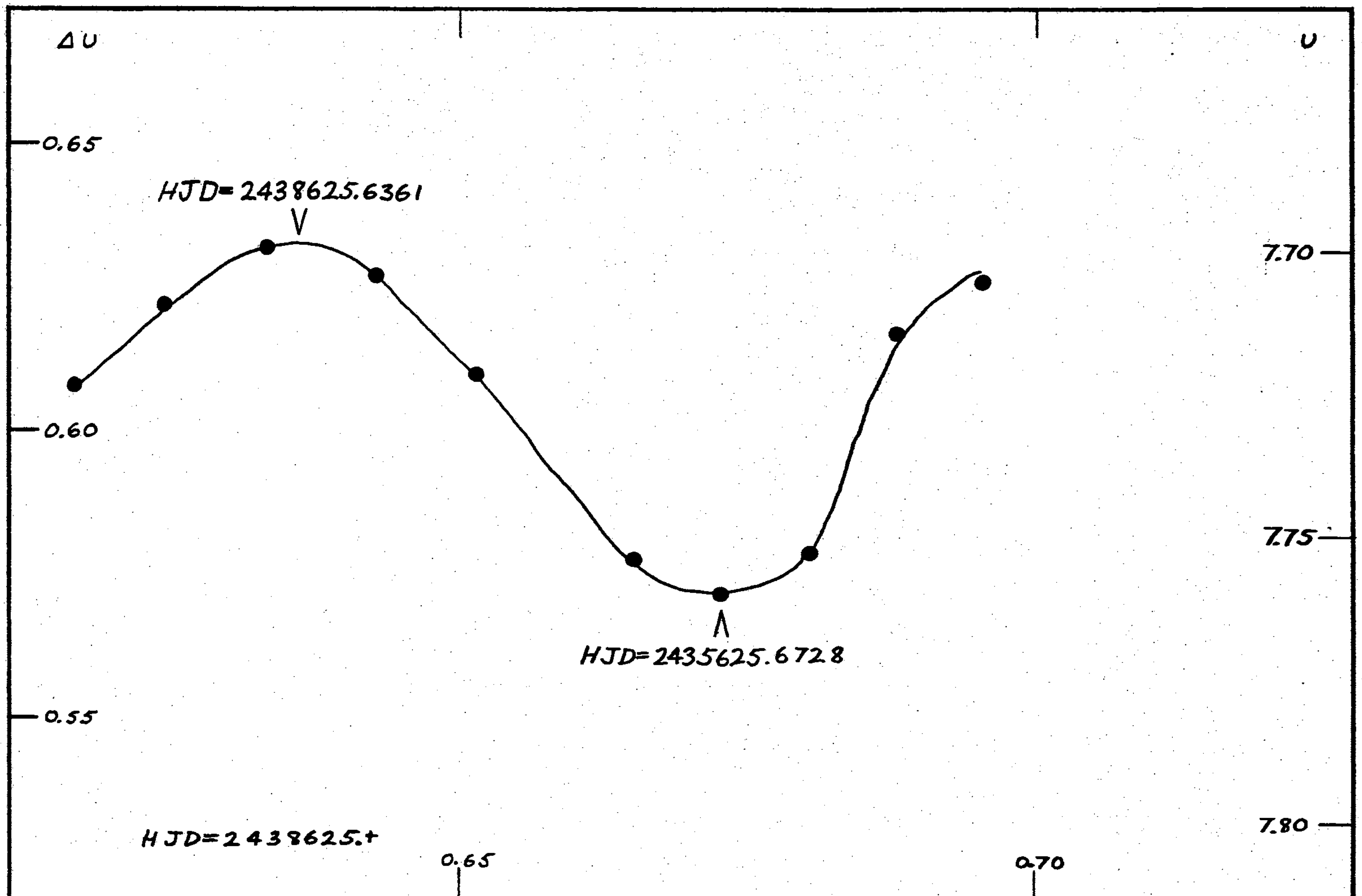

Figure 62. Extrema in U of DQ Cephei for August 18, 1964.

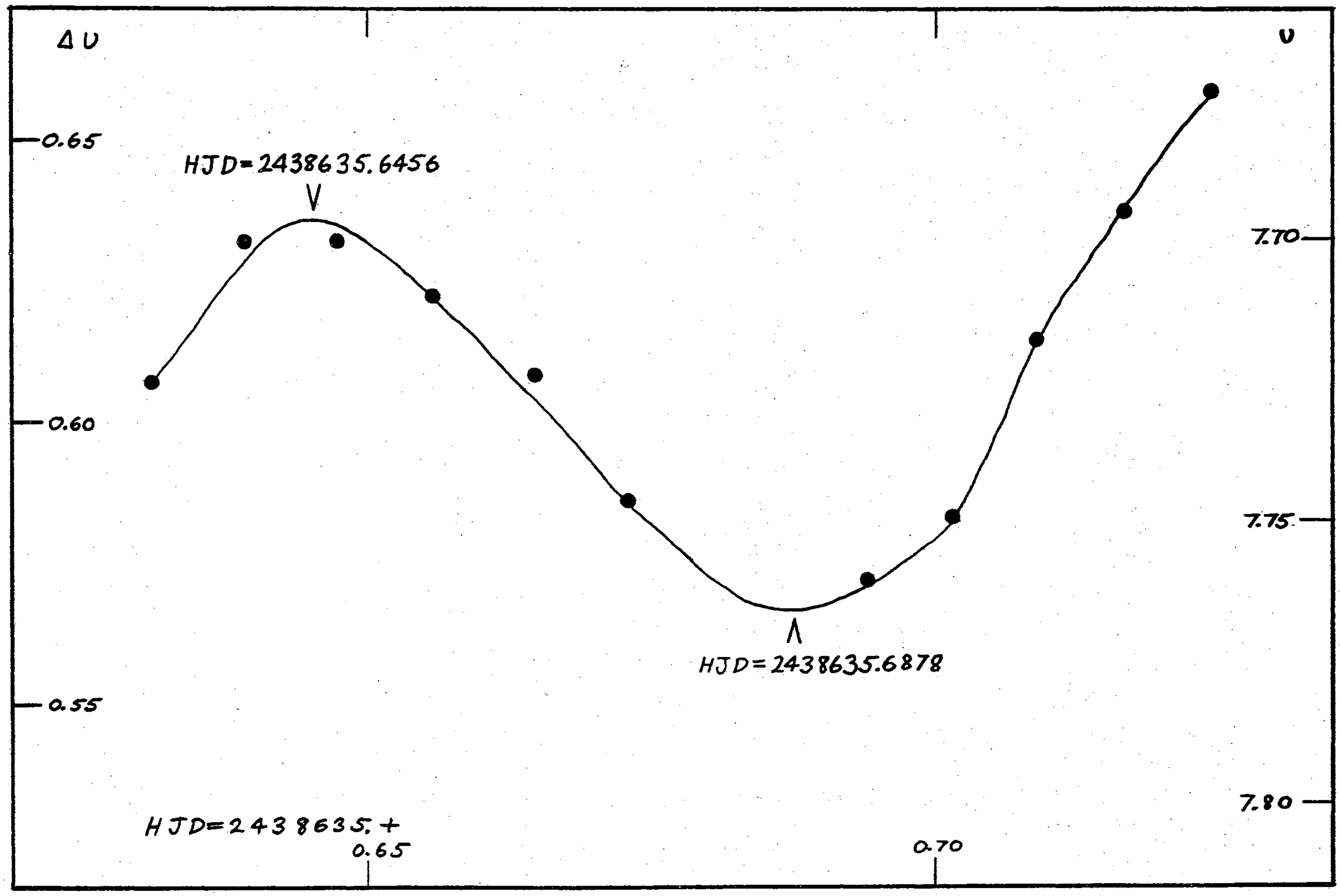

Figure 63. Extrema in U of DQ Cephei for August 28, 1964.

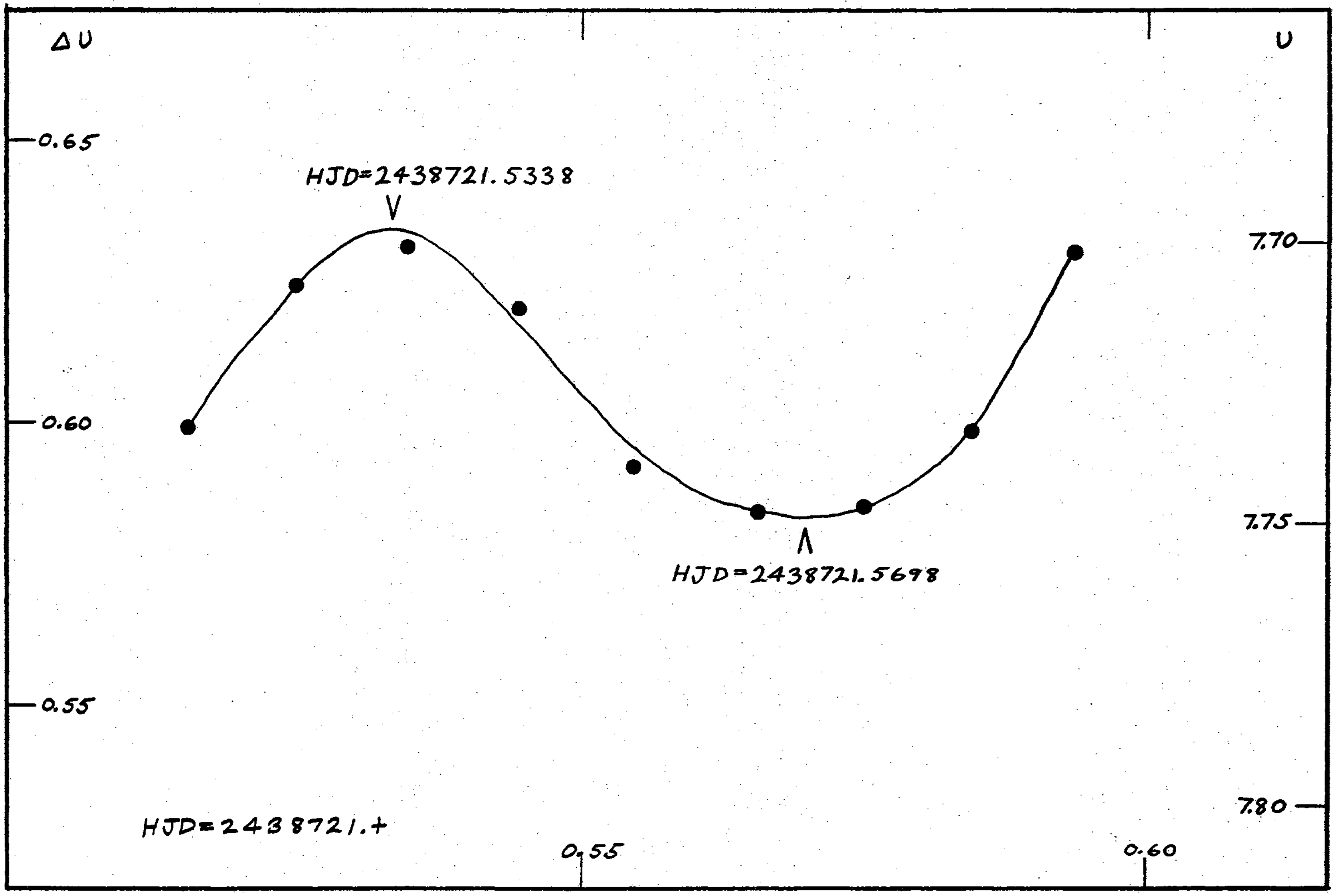

Figure 64. Extrema in U of DQ Cephei for November 22, 1964.

Extraction of Possible Periods

Using the maxima in V, all possible periods were extracted by the method described in the previous chapter. Two possible periods resulted from the analysis. In order to remove the ambiguity, the minima in V were examined and a unique period was found which agreed with one of those obtained in the study of the maxima. The periods and number of cycles between observations are given in Table XVII. Comparison of the intervals between maxima and minima shows that a phase change occurs on the fourth cycle. Examination of Table XVI, or of the light curves, confirms this.

TABLE XVII

RESULTS OF PERIOD EXTRACTION

	From V Maxima		From V Minima
	P_1	P_2(Eliminated)	P
Period	.078866d$\pm$0.000006	.078804d$\pm$0.000006	.078862d$\pm$0.000006
N_{12}	50	50	50
N_{13}	51	51	51
N_{14}	61	61	61
N_{15}	188	188	189
N_{16}	1277	1278	1278

Optimization of the Period

Using Equations (4.8) and (4.9) we can obtain an improved value for the period. Using the maxima in V we find

$$P = 0.078868^d,$$

$$T = 2438620.8212,$$

$$e = 0.002,$$

where e is the rms residual of the observed minus computed epochs.

Three Color Analysis of the Maxima

Table XVIII lists the differences in days between times of maximum and minimum light for the three colors. These figures would suggest that

TABLE XVIII

PHASE SHIFT BETWEEN COLORS IN DAYS AT MAXIMUM AND MINIMUM

Date	$Max_B - Max_V$	$Max_U - Max_V$	$Max_B - Max_U$	$Min_B - Min_V$	$Min_U - Min_V$	$Min_B - Min_U$
Aug. 13	.000	-.002	+.002	+.005	+.002	+.003
Aug. 17 early	+.003	+.001	+.002	+.004	+.004	.000
Aug. 17 late	+.001	--	--	-.001	--	--
Aug. 18	+.002	+.004	-.002	.000	.000	.000
Aug. 28	+.004	+.002	+.002	+.003	+.002	+.001
Nov. 27	.000	-.003	+.003	+.002	+.002	.000

the maxima and minima in B and possibly U are occurring somewhat later than those in V. However, it must be kept in mind that these times have been measured to no better than ± 0.008 day which is greater than any of the observed differences.

If the maxima in all three colors are fitted by means of Equations (4.11), constraining the period to be the same for each color, we obtain

$$P = 0.078867^d,$$
$$T_V = 2438620.8217,$$
$$T_B = 2438620.8234,$$
$$T_U = 2438620.8223,$$
$$e = 0.002,$$

and the differences between the epochs are seen to be about 0.001 day, which is much smaller than our error of observation. When the maxima are fitted separately with no restraint on the period, the results are

$$P_V = 0.078869^d,$$
$$P_B = 0.078867^d,$$
$$P_U = 0.078865^d,$$
$$T_V = 2438620.8212,$$
$$T_B = 2438620.8232,$$
$$T_U = 2438620.8228,$$
$$e = 0.002,$$

with about the same differences in the epochs. The differences in the period for the three colors give some estimate as to the accuracy of the figure. We find, approximately,

$$P = 0.078867^d \pm 0.000002.$$

Walker's Data

Walker's (1952) early data were analyzed for ambiguous periods and the results agreed completely with those that he obtained. The periods found were

$$P_1 = 0.07886^d \pm 0.00002,$$
$$P_2 = 0.07546^d \pm 0.00002.$$

Later, Walker (1953) made additional observations and eliminated the second of these periods. However, the refined value of P_1 remained ambiguous. He reported the possible periods

$$P_1 = 0.0788850^d,$$
$$P_2 = 0.0788653^d,$$
$$P_3 = 0.0788456^d.$$

On the basis of our own value for the period, the second of these values was selected and the resulting cycle numbers used for a least-squares fit. Our result was

$$P = 0.0788651^d,$$

in excellent agreement with Walker's value.

Sahade's Data

Sahade <u>et al</u> (1956) investigated the radial velocity of DQ Cephei and found that it varied with the same period as the light curve. They reported a best fitting period of

$$P = 0.0788650^d,$$

which agrees with Walker's value very well. However, when their reported epochs were fitted by least squares, periods based on the maxima, minima, and both were found to be

$$P_{RV(MAXIMA)} = 0.0788647^d,$$
$$P_{RV(MINIMA)} = 0.0788637^d,$$
$$P_{RV} = 0.0788642^d.$$

Sahade did not specify his criterion of a "best" fit.

Spanning the Gaps

The periods arrived at so far are

$$P = 0.078867^d \text{ (Present Data)},$$
$$= 0.0788653^d \text{ (Walker's Figure)},$$
$$= 0.0788650^d \text{ (Sahade's Figure)},$$
$$= 0.0788642^d \text{ (New fit of Sahade's Data)}.$$

A new estimate of the period can be made from these results. We obtain an average figure of

$$P = 0.078865^d \pm 0.000001$$

The last reported maximum observed by Walker occurred at HJD 2434263.724 and the first one observed in this study occurred at HJD 2438620.825. Thus, a gap of 4357.101 days exists between the two maxima. Since the phase difference between the radial velocity and light curve is only roughly known, Sahade's epochs cannot be used to reduce the gap. Assuming the gap to be known to $\pm 0.008^d$ and the maximum and minimum periods to be our latest estimates, the number of cycles separating the maxima is ambiguous. It is either 55247 or 55248 cycles.

Fitch's Data

W. S. Fitch (1959) mentioned in a note on the δ Scuti variables that photoelectric measures of the yellow light of DQ Cephei were gotten at the Steward Observatory on six nights in 1958. Observations made in 1958 would almost exactly bisect those made by Walker and those of this study. Fitch (1965) kindly supplied a listing of his observed maxima and minima as well as Walker's unpublished minima. He reported a period and epoch of

$$T = 2433924.8404 \pm 0.0008,$$

$$P = 0.07886455^d \pm 0.00000004,$$

where the errors are mean errors. His figures have since been published in a study by himself and Wehlau (1965).

The gaps between Walker's and Fitch's data and between Fitch's and the present data are unambiguously spanned. The gaps are 2130.053^d and 2105.133^d respectively, and with a period as uncertain as $P = 0.078865^d \pm 0.000002$ give the cycle numbers N = 27009 and N = 22693 respectively.

Optimization of the Period Using All Data

Since Sahade (1956) noted that maximum brightness occurs about halfway on the descending branch of the velocity curve, it is possible now to assign an unambiguous cycle number to each maximum and minimum which has been observed from Walker's original data through the present data. As a first step, all maxima and all minima in V were fitted by least square. The periods and epochs obtained were

$$P_{V(MAXIMA)} = 0.07886443^d,$$
$$P_{V(MINIMA)} = 0.07886446^d,$$
$$T_{V(MAXIMA)} = 2433924.8405,$$
$$T_{V(MINIMA)} = 2433924.8821.$$

Finally, a least squares fit was made to all maxima and minima, holding the period to be the same, and the standard errors of the parameters were computed using Equation (4.12). The results obtained were:

$$P = 0.07886444^d \pm 0.00000002,$$
$$T_{V(MAXIMA)} = 2433924.8404 \pm 0.0008,$$
$$T_{V(MINIMA)} = .8823 \pm 0.0008,$$
$$T_{B(MAXIMA)} = .8411 \pm 0.0008,$$
$$T_{B(MINIMA)} = .8806 \pm 0.0011,$$
$$T_{U(MAXIMA)} = .8401 \pm 0.0010,$$
$$T_{U(MINIMA)} = .8801 \pm 0.0014,$$
$$T_{RV(MAXIMA)} = .8150 \pm 0.0013,$$
$$T_{RV(MINIMA)} = .8526 \pm 0.0014.$$

Observed and Predicted Epochs are listed in Table XIX. In this table, W stands for Walker, S for Sahade et al., F for Fitch, and J for Jenks, et al. O and C represent observed and computed values, respectively.

TABLE XIX

OBSERVED AND PREDICTED EPOCHS

Observer	E		MAX$_V$ O	MAX$_V$ C	O-Cx10^3		MIN$_V$ O	MIN$_V$ C	O-Cx10^3
W	0	24339	24.836	24.840	- 4	24339	24.879	24.882	- 3
W	1		24.919	24.919	0		24.954	24.961	- 7
W	23		26.655	26.654	+ 1		26.695	26.696	- 1
W	24		26.731	26.733	- 2				
W	88		31.781	31.780	+ 1		31.820	31.822	- 2
W	89		31.861	31.859	+ 2				
W	201		40.686	40.692	- 6		40.721	40.734	- 13
W	3892	24342	31.781	31.781	0	24342	31.825	31.823	+ 2
W	3942		35.722	35.724	- 2		35.765	35.766	- 1
W	3954						36.707	36.712	- 5
W	3955		36.745	36.749	- 4				
W	3967		37.708	37.696	+ 12		37.740	37.738	+ 2
W	3968		37.776	37.774	+ 2				
W	3980		38.726	38.721	+ 5		38.762	38.763	- 1
W	3992						39.705	39.709	- 4
W	3993		39.742	39.746	- 4				
W	4005						40.738	40.734	+ 4
W	4006		40.768	40.771	- 3				
W	4018		41.711	41.718	- 7		41.761	41.760	+ 1
W	4030						42.705	42.706	- 1
W	4031		42.750	42.743	+ 7		42.784	42.785	- 1
W	4296						63.689	63.684	+ 5
W	4297		63.724	63.721	+ 3				

TABLE XIX (Continued)

Ob-ser-ver	E		MAX$_{RV}$ O	MAX$_{RV}$ C	O-Cx10^3		MIN$_{RV}$ O	MIN$_{RV}$ C	O-Cx10^3
S	13667					24350	02.700	02.693	+ 7
S	13669	24350	02.812	02.813	- 1		02.844	02.851	- 7
S	13680		03.680	03.680	0		03.731	03.718	+ 13
S	13681		03.765	03.759	+ 6				
S	13692						04.671	04.664	+ 7
S	13693		04.705	04.706	- 1		04.741	04.743	- 2
S	13705		05.650	05.652	- 2		05.692	05.690	+ 2
S	13706		05.732	05.731	+ 1				
S	16586					24352	32.885	32.898	- 13
S	16587	24352	32.960	32.939	+ 21		32.983	32.977	+ 6
S	16637		36.893	36.882	+ 11		36.910	36.920	- 10
S	16638		36.962	36.961	+ 1				
S	17005		65.894	65.905	- 11		65.943	65.942	+ 1
S	17017		66.847	66.851	- 4		66.903	66.889	+ 14
S	17018		66.922	66.930	- 8		66.957	66.968	- 11
S	17019		66.983	67.009	- 26				
S	17030						67.913	67.914	+ 1
S	17031		67.951	67.955	- 4				
S	17042		68.822	68.823	- 1		68.852	68.860	- 8
S	17043		68.899	68.902	- 3		68.937	68.939	- 2
S	17044		68.972	68.980	- 8				
S	17447	24353	00.770	00.763	+ 7	24353	00.808	00.800	+ 8
S	17448						00.888	00.879	+ 9
S	17449		00.908	00.920	- 12		00.951	00.958	- 7
S	17450		00.988	00.999	- 11				

TABLE XIX (Continued)

Observer	E		MAX_RV O	MAX_RV C	MAX_RV O-Cx10^3		MIN_RV O	MIN_RV C	MIN_RV O-Cx10^3
S	17460		01.790	01.788	+ 2		01.812	01.826	- 14
S	17461		01.875	01.867	+ 8		01.910	01.904	+ 6
S	17462		01.945	01.946	- 1				
S	18120		53.845	53.839	+ 6		53.880	53.876	+ 4
S	18121		53.917	53.917	0		53.948	53.955	- 7
S	18130						54.670	54.665	+ 5
S	18131	29353	54.713	54.706	+ 7	29353	54.747	54.744	+ 3
S	18143		55.655	55.652	+ 3		55.695	55.690	+ 5
S	18144		55.737	55.731	+ 6		55.768	55.769	- 1
S	18145		55.820	55.810	+ 10		55.845	55.848	- 3
S	18146		55.891	55.889	+ 2		55.937	55.927	+ 10
S	18156		56.663	56.678	- 15		56.712	56.715	- 3
S	18157						56.794	56.794	0
S	18158		56.843	56.835	+ 8		56.861	56.873	- 12
S	18159		56.926	56.914	+ 12				

Observer	E		MAX_V O	MAX_V C	MAX_V O-Cx10^3		MIN_V O	MIN_V C	MIN_V O-Cx10^3
F	31306	24363	93.777	93.770	+ 7	24363	93.820	93.812	+ 8
F	31307		93.846	93.849	- 3				
F	31318						94.760	94.759	+ 1
F	31319		94.793	94.796	- 3		94.846	94.838	+ 8
F	31320		94.877	94.874	+ 3		94.920	94.916	+ 4

TABLE XIX (Continued)

Observer	E		MAX$_V$ O	MAX$_V$ C	O-C$\times10^3$		MIN$_V$ O	MIN$_V$ C	O-C$\times10^3$
F	31321		94.954	94.953	+ 1				
F	31331						95.792	95.784	+ 8
F	31332		95.819	95.821	- 2		95.863	95.863	0
F	31333		95.902	95.900	+ 2		95.947	95.942	+ 5
F	32470					24364	85.613	85.610	+ 3
F	32471	24364	85.647	85.648	- 1		85.690	85.689	+ 1
F	32472		85.731	85.726	+ 5		85.772	85.768	+ 4
F	32496		87.619	87.619	0				
F	32850					24365	15.580	15.579	+ 1
F	32851	24365	15.617	15.616	+ 1		15.663	15.658	+ 5
F	32852		15.692	15.695	- 3				
J	59544					24386	20.783	20.786	- 3
J	59545	24386	20.825	20.823	+ 2				
J	59594						24.727	24.729	- 2
J	59595		24.766	24.766	0		24.807	24.808	- 1
J	59596		24.842	24.845	- 3				
J	59606		25.632	25.634	- 2		25.673	25.676	- 3
J	59733		35.644	35.650	- 6		35.686	35.692	- 6
J	60822	24387	21.537	21.533	+ 4	24387	21.568	21.575	- 7

TABLE XIX (Continued)

Observer	E		MAX_B O	MAX_B C	O-Cx10^3		MIN_B O	MIN_B C	O-Cx10^3
J	59544					24386	20.788	20.785	+ 3
J	59545	24386	20.825	20.824	+ 1				
J	59594						24.731	24.728	+ 3
J	59595		24.769	24.767	+ 2		24.806	24.807	- 1
J	59596		24.843	24.846	- 3				
J	59606		25.634	25.635	- 1		25.673	25.674	- 1
J	59733		35.648	35.650	- 2		35.689	35.690	- 1
J	60822	24387	21.537	21.534	+ 3	24387	21.570	21.573	- 3

Observer	E		MAX_U O	MAX_U C	O-Cx10^3		MIN_U O	MIN_U C	O-Cx10^3
J	59544					24386	20.785	20.784	+ 1
J	59545	24386	20.823	20.823	0				
J	59594						24.731	24.727	+ 4
J	59595		24.767	24.766	+ 1				
J	59596								
J	59606		25.636	25.634	+ 2		25.673	25.674	- 1
J	59733		35.646	35.649	- 3		35.688	35.689	- 1
J	60822	24387	21.534	21.533	+ 1	24387	21.570	21.573	- 3

Secular Variations in the Period

Strictly speaking, by the above method only the mean period is determined and the question of how precise and stable the real period is remains open. Changes in the period can be discovered only when, after a sufficient number of cycles, the difference between the observed phase and the phase predicted with the original period becomes noticeable. Thus, small periodic changes in the length of the period may escape attention, but secular changes in period must become observable in due time.

If a star has a constant period, its maxima will be predicted by an equation of the form

$$\text{Max} = T + PE,$$

or, by changing the form slightly, the phase, θ, can be predicted by

$$\theta = \theta_o + P_\theta E. \tag{5.1}$$

In differential form Equation (5.1) becomes

$$d\theta = P_\theta dE. \tag{5.2}$$

Now suppose, instead of being constant the period is given by

$$P_\theta = P_{o\theta}(1 + \beta E), \tag{5.3}$$

where β is a measure of the secular change of the period. Then we have

$$\theta = \theta_o + P_{o\theta}\int_o^E (1+\beta E)dE = \theta_o + P_{o\theta}(E+\tfrac{1}{2}\beta E^2), \tag{5.4}$$

or, changing back to the discontinuous form,

$$\text{Max} = T + P_o E + \tfrac{1}{2}P_o \beta E^2. \tag{5.5}$$

By fitting this equation to a large number of maxima the coefficients can be determined by the normal equations

$$\begin{aligned} TN + P_o\Sigma E_i + \tfrac{1}{2}P_o \beta \Sigma E_i^2 &= \Sigma\, \text{Max}_i, \\ T\Sigma E_i + P_o\Sigma E_i^2 + \tfrac{1}{2}P_o \beta \Sigma E_i^3 &= \Sigma E_i \text{Max}_i, \\ T\Sigma E_i^2 + P_o\Sigma E_i^3 + \tfrac{1}{2}P_o \beta \Sigma E_i^4 &= \Sigma E_i^2 \text{Max}_i, \end{aligned} \tag{5.6}$$

which yield for β and P_o,

$$\beta = -2\,\frac{AB - CD}{AE - CF},$$

$$P_o = \frac{AE - CF}{DE - BF},$$

$$\begin{aligned} \text{where}\quad A &= \Sigma E_i \Sigma \text{Max}_i - N\Sigma E_i \text{Max}_i, \\ B &= (\Sigma E_i^2)^2 - \Sigma E_i \Sigma E_i^3, \\ C &= \Sigma E_i^2\, \Sigma E_i \text{Max}_i - \Sigma E_i\, \Sigma E_i^2 \text{Max}_i, \\ D &= (\Sigma E_i)^2 - N\Sigma E_i^2, \\ E &= \Sigma E_i^2\, \Sigma E_i^3 - \Sigma E_i\, \Sigma E_i^4, \\ F &= \Sigma E_i\, \Sigma E_i^2 - N\Sigma E_i^3. \end{aligned} \tag{5.7}$$

Using the maxima in V we arrive at the quantities

$$\beta = -4 \times 10^{-11},$$

$$P_o = 0.07886452^d,$$

so

$$P = 0.07886452^d(1 - 4 \times 10^{-11}\, E).$$

The period at the beginning and end of the base line (1951-1964) then would be

$$P(0) = 0.07886452,$$

$$P(60822) = 0.07886433.$$

A discussion of the secular term β is given by Ledout (1958) where he indicates that values smaller than 10^{-9} probably do not represent real secular changes in the period.

It is of interest to note that the period P_o has undergone a Doppler shift due to the radial velocity of the star. If the star is receding from the observer with velocity v, then after a period of time, P_1, has elapsed, the star has receded a distance vP farther from the observer. The light leaving the star at this point then requires an additional time of $\frac{v}{c}$ P to reach the observer. The observed period P_o is then

$$P_o = P + \frac{v}{c} P = (1 + \frac{v}{c})P. \qquad (5.8)$$

Sahade (1956) found the mean radial velocity of DQ Cephei to be -21.9 km/sec. Taking c to be 299,791 km/sec according to Allen (1955), we have

$$P_o = 0.99992695P,$$

or,

$$P = 1.00007305P_o.$$

Taking

$$P_o = 0.07886444^d$$

we obtain

$$P = 0.07887020^{d}$$

as the intrinsic period of the star. The relativistic form of the Doppler shift equation leads to the same result.

CHAPTER VI

WAVEFORM ANALYSIS AND REDDENING

Walker (1952) and Sahade (1956) both noticed, during their studies of DQ Cephei, that the amplitude of the light curve varied from cycle to cycle. This effect has been noticed in several short-period variables and the interpretation has been advanced that the observed curve results from the interference between first and second modes of radial pulsation. The beat phenomenon has been described by Ledout (1958) as resembling the modulation of a carrier wave by a wave of lower frequency, such as occurs in telecommunication.

Variations in the Light Curves

In order to compare the amplitudes of the light curves obtained on the different cycles, the curves are plotted versus phase in Figures 65 through 69. As can be seen, the amplitudes vary in V from about 0.04 magnitude on November 22, 1964 (crosses) to 0.10 magnitude on August 13, 1964 (circles). The general variation in B-V indicates the variable is bluest when brightest and there appear to be differences in amplitude from cycle to cycle. Variations in (U-B) are less clearly defined. The scatter in the U-B curve is such that no definitive shape is apparent while the B-V curve appears to be a reduced image of the V light curve. When the observations in each 10° interval are averaged and a formula fitted by harmonic analysis to the curves in V, B-V and U-B,

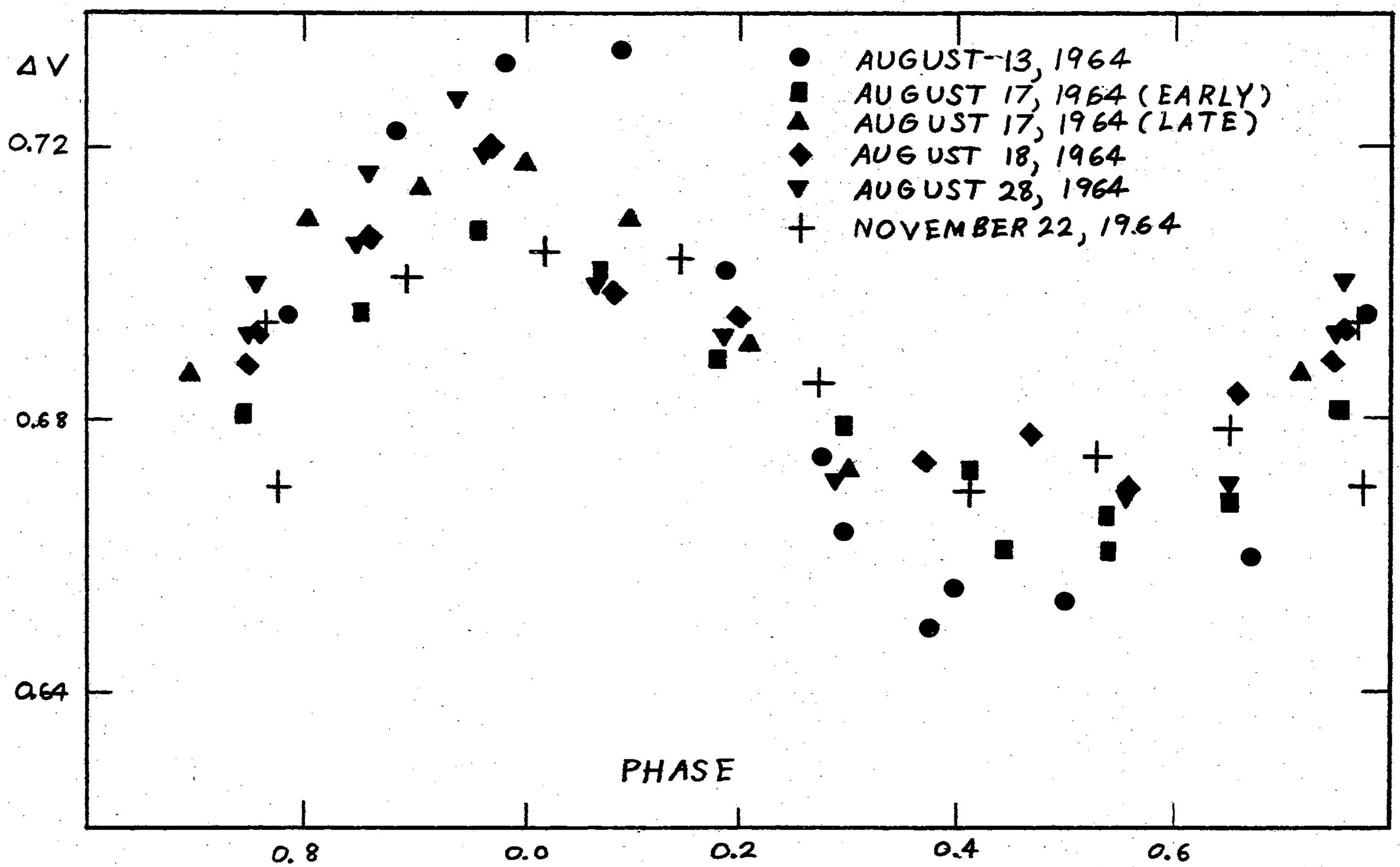

Figure 65. Light Curve in V *Versus* Phase of DQ Cephei.

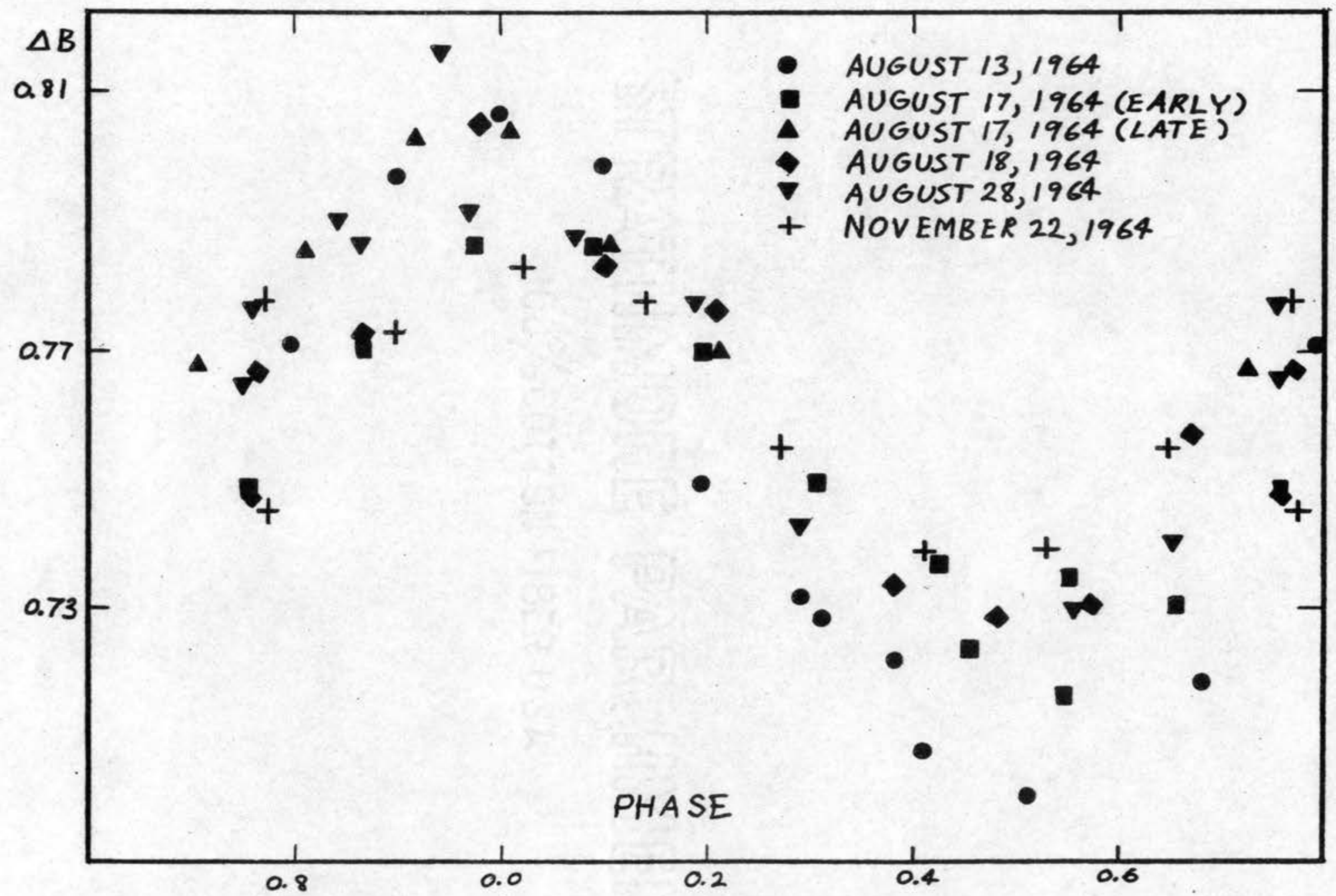

Figure 66. Light Curve in B *Versus* Phase of DQ Cephei.

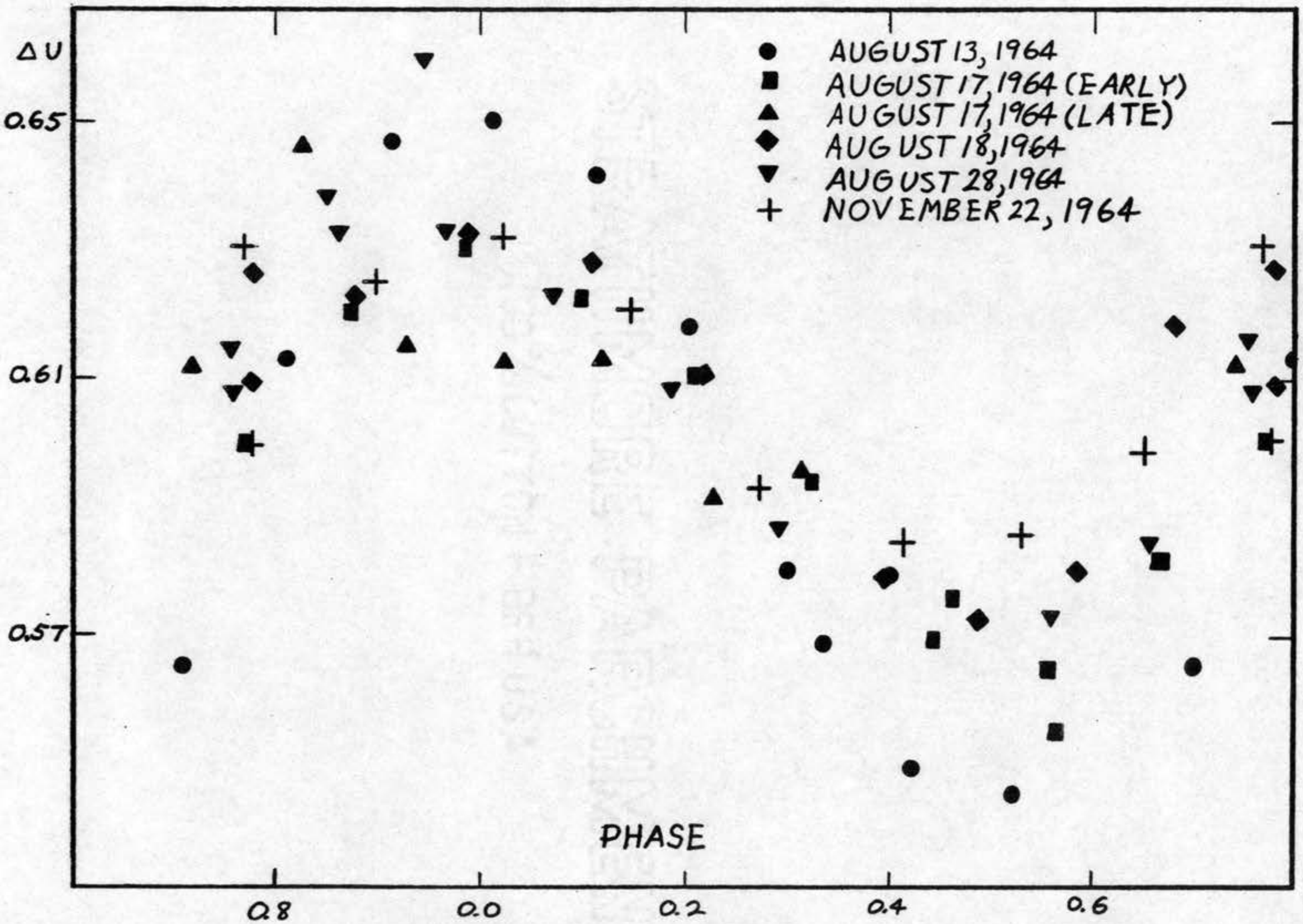

Figure 67. Light Curve in U Versus Phase of DQ Cephei.

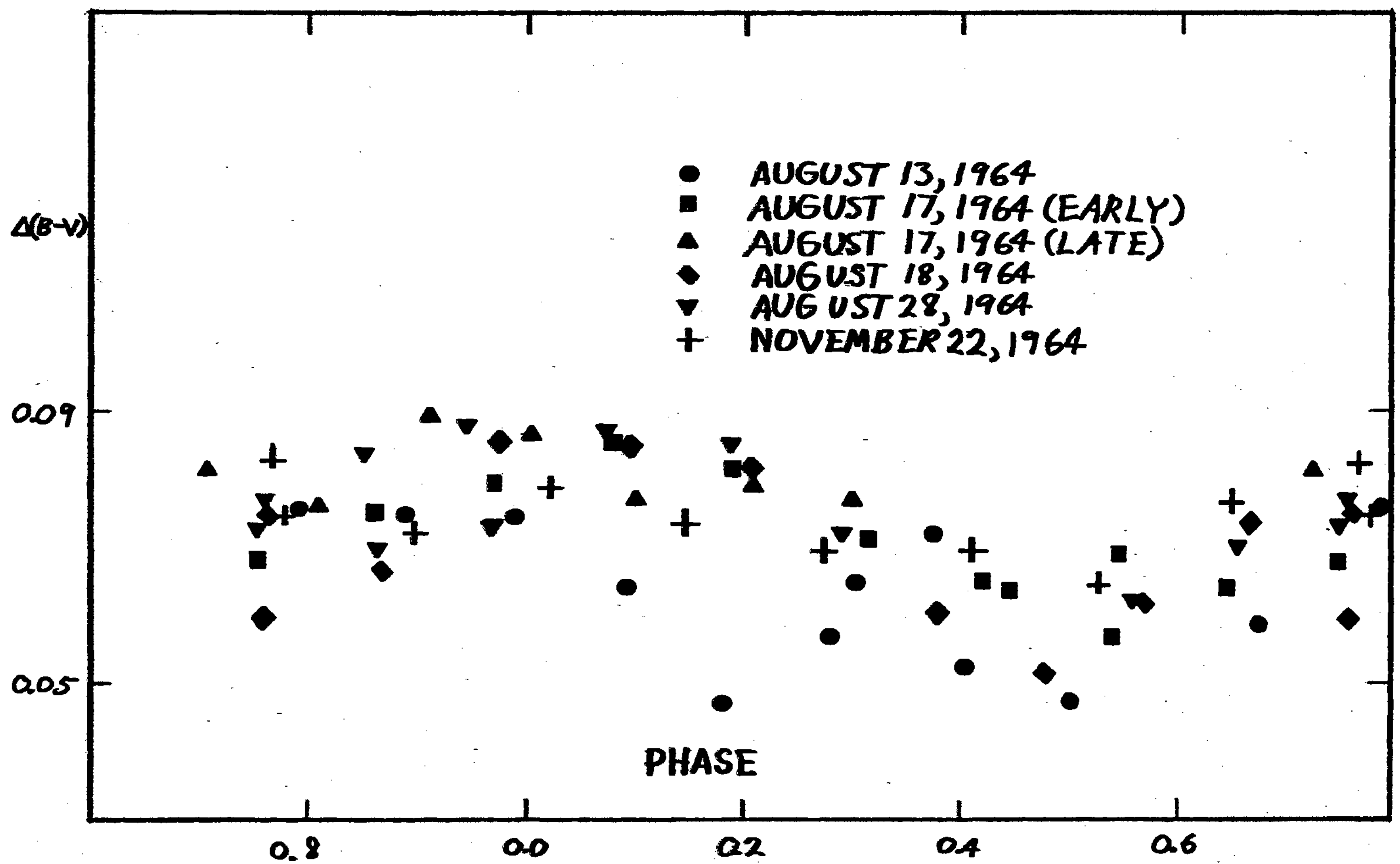

Figure 68. Light Curve in B-V *Versus* Phase of DQ Cephei.

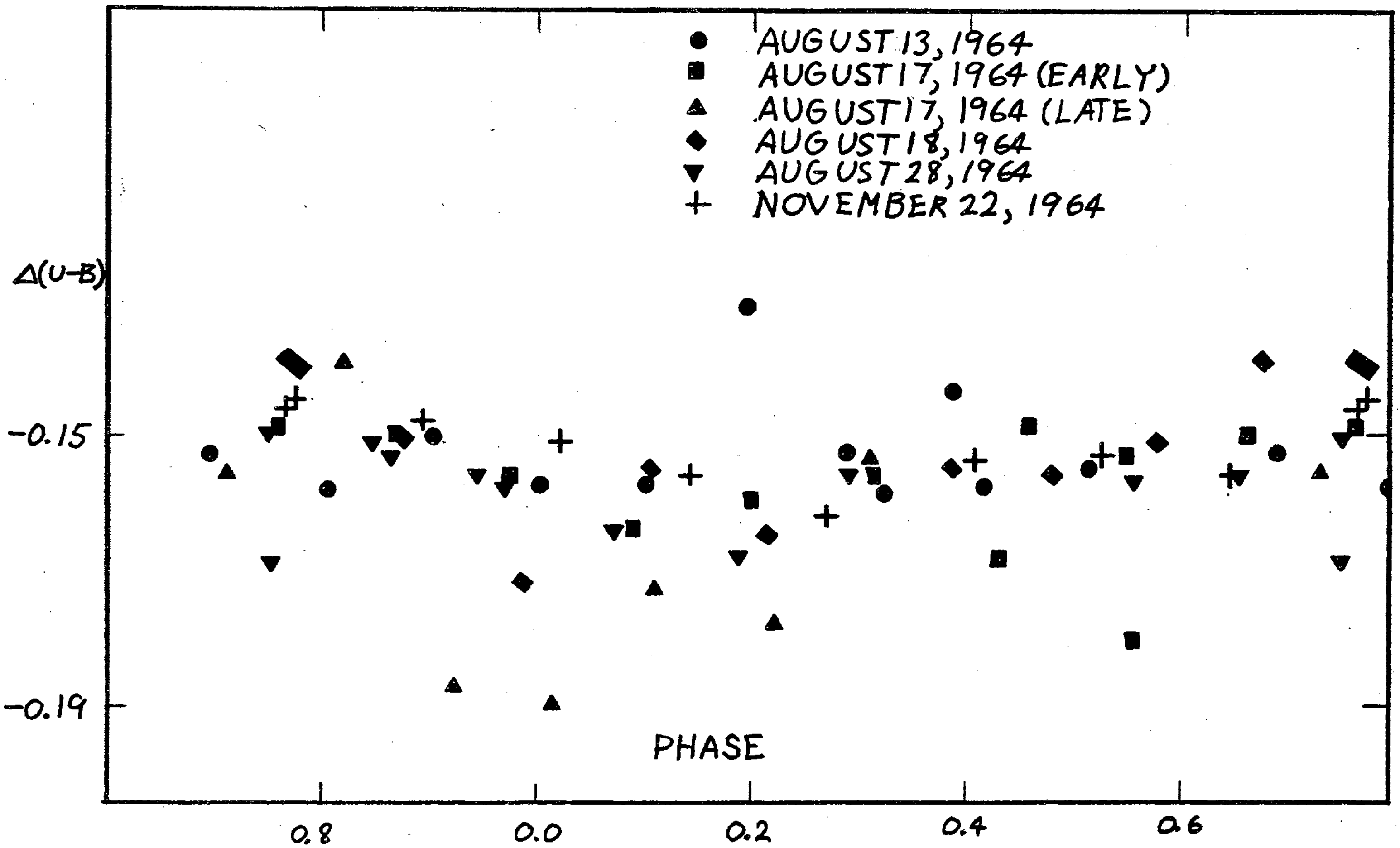

Figure 69. Light Curve in U-B *Versus* Phase for DQ Cephei.

the results are:
$$V_\theta = 7^m\!.268 - 0^m\!.028\cos\theta, \tag{6.1}$$

$$(B\text{-}V)_\theta = 0^m\!.340 - 0^m\!.010\cos\theta, \tag{6.2}$$

$$(U\text{-}B)_\theta = 0^m\!.123 + 0^m\!.005\cos(\theta-53^\circ) + 0^m\!.003\cos(2\theta-45^\circ), \tag{6.3}$$

where

$$\theta = 360^\circ\,\frac{t-2433924^d\!.8404}{0^d\!.07886444}\,. \tag{6.4}$$

The Color-Color Curve

If the values of $(B\text{-}V)_\theta$ and $(U\text{-}B)_\theta$, found by Equations 6.2 and 6.3, are plotted parametrically in θ the color-color curve of Figure 70 is obtained. The loop is described in a counter-clockwise sense. The line upon which unreddened main-sequence stars should fall has been taken from the figures given by Johnson and Morgan (1954). The reddening line, as indicated by the short arrow, has a slope of 0.72 as determined by Blanco (1955) and by Hiltner and Johnson (1956). The basic, unreddened colors of DQ Cephei should lie in the direction of the arrow, provided that the reddening law is not unusual in this region of space. From the position of the B-V, U-B loop in relation to the main sequence line, it seems that the star has been somewhat reddened. However, when dealing with a star whose physical properties are imperfectly understood, the unreddened U-B, B-V curve for that type of star may deviate significantly from the main sequence line.

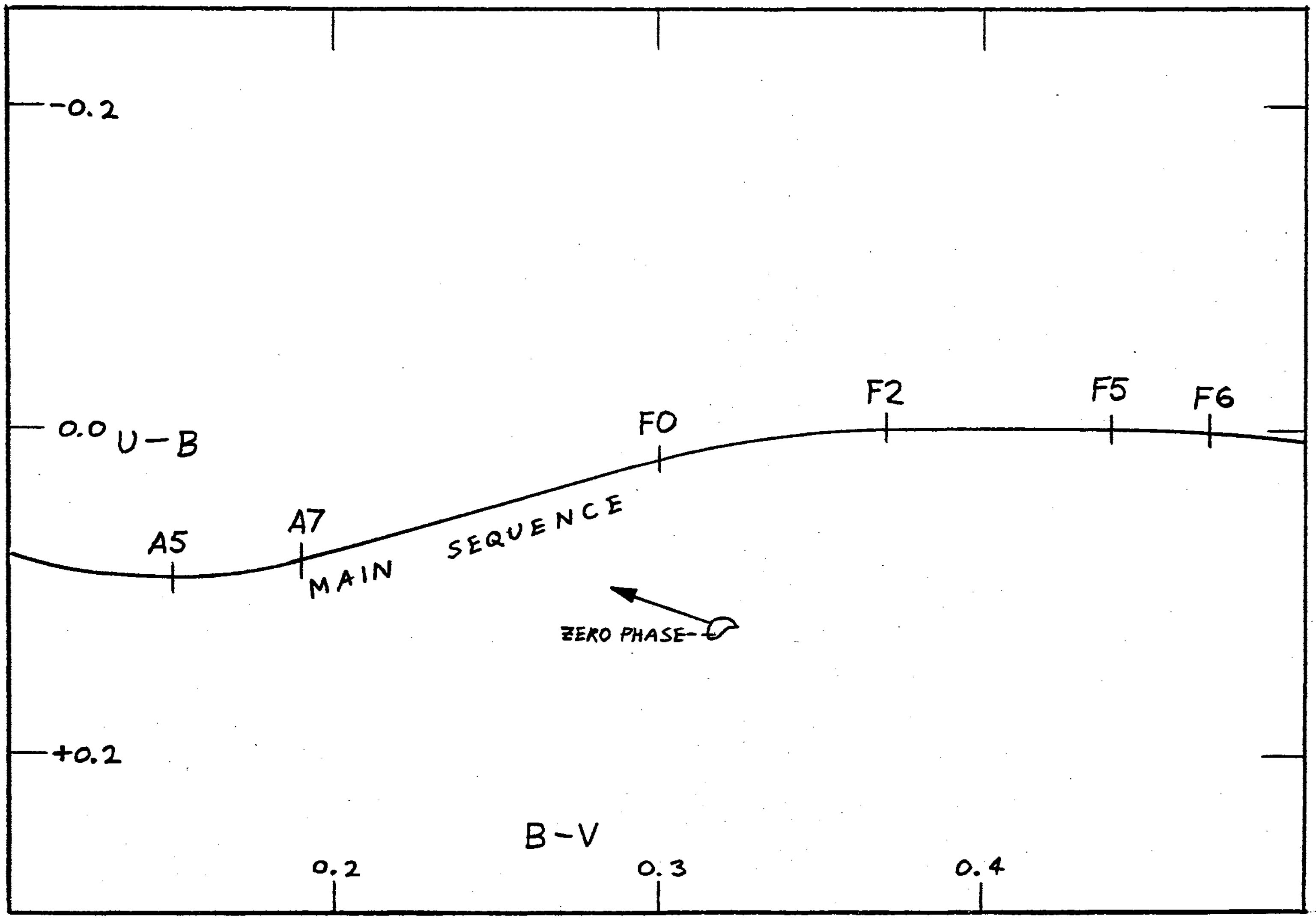

Figure 70. Color-Color Curve of DQ Cephei.

Extraction of the Modulation Envelope

If a waveform is made up of two interfering waves of differing phase and frequency, it can be represented as

$$Y = a\cos w(t+\Delta t) + b\cos(w+\Delta w)t, \qquad (6.5)$$

where

$$t = T - T_o.$$

Equation (6.5) can be cast into the form

$$Y = \sqrt{a^2+b^2+2ab\cos(\Delta wt - w\Delta t)} \cdot \cos w\left[t+\frac{1}{w}\tan^{-1}\left(\frac{b\sin\Delta wt + a\sin w\Delta t}{b\cos\Delta wt + a\cos w\Delta t}\right)\right]. \qquad (6.5)$$

Equation (6.5) is in the form of a harmonic wave modulated by a function of the form

$$m(t) = \sqrt{1 + \gamma\cos t} \quad ; \quad \gamma \leq 1. \qquad (6.6)$$

In order to simplify the form of Equation (6.6) we can expand it into a Fourier series. Accordingly, let us set

$$m(t) = \tfrac{1}{2}a_o + \sum_{n=1}^{\infty} a_n \cos nx, \qquad (6.7)$$

where

$$a_n = \frac{1}{\pi}\int_{-\pi}^{+\pi} m(t)\cos nt\,dt = \frac{2}{\pi}\int_{0}^{\pi} m(t)\cos nt\,dt. \qquad (6.8)$$

Expanding m(t) by the binomial theorem:

$$m(t) = (1+\gamma\cos t)^{\frac{1}{2}} = 1-\sum_{k=1}^{\infty}(-1)^k\gamma^k \frac{(2K-2)!}{2^{2k-1}k!(k-1)!}\cos^k t, \tag{6.7}$$

and we obtain

$$\begin{aligned} a_n &= \frac{2}{\pi}\int_0^{\pi}\cos nt\,dt - \frac{2}{\pi}\int_0^{\pi}\sum_{k=1}^{\infty}(-1)^k\gamma^k \frac{(2K-2)!}{2^{2k-1}k!(k-1)!}\cos^k t\cos nt\,dt, \\ &= 2\delta_{o,n} - \frac{2}{\pi}\sum_{k=1}^{\infty}(-1)^k\gamma^k \frac{(2k-2)!}{2^{2k-1}k!(k-1)!}\int_0^{\pi}\cos^k t\cos nt\,dt, \end{aligned} \tag{6.8}$$

where the integration and summation can be interchanged for the series is uniformly convergent. Now, $\cos^k t\cos nt$ is symmetric or antisymmetric about $\pi/2$ according as $k+n$ is even or odd, so

$$\int_0^{\pi}\cos^k t\cos nt = \begin{cases} 2\int_0^{\pi/2}\cos^k t\cos nt\,dt; & k_{odd}^{even},\ n_{odd}^{even}, \\ 0; & k_{odd}^{even},\ n_{even}^{odd}. \end{cases}$$

The value of the last integral is known. It is

$$\int_0^{\pi/2}\cos^k t\cos nt\,dt = \begin{cases} \frac{\pi}{2^{k+1}}\frac{k!}{\left(\frac{k+n}{2}\right)!\left(\frac{k-n}{2}\right)!}; & k \geq n, \\ 0; & k < n. \end{cases}$$

From the requirement that k and n both be even or odd, and that $k \geq n$, we write $k = n + 2i$ and obtain

$$a_n = 2\delta_{0,n} - \frac{4}{\pi}(-1)^n\gamma^n \sum_{i=0}^{\infty} \gamma^{2i} \frac{(2n+4i-2)!}{2^{2n+4i-1}(n+2i)!(n+2i-1)!} \int_0^{\pi/2} \cos^{n+2i}t \cdot \cos nt\,dt,$$

$$= 2\delta_{0,n} - 4(-1)^n\gamma^n \sum_{i=0}^{\infty} \gamma^{2i} \frac{[2(n+2i-1)]!}{2^{3(n+2i)}(n+2i-1)!(n+1)!i!} . \tag{6.9}$$

Comparing the kth and k+1st terms of this series, we find their ratio to approach $\gamma^2 < 1$, so the series is convergent. In order to approximately evaluate the a_i, recall that the maximum amplitude of the light curve is about $0^m.10$ and the minimum $0^m.04$. Therefore, we can write

$$\frac{\sqrt{1+\gamma}}{\sqrt{1-\gamma}} = \frac{0.1}{0.04} ,$$

or

$$\gamma = 0.72 .$$

Inserting this value of γ into Equation (6.9), we find

$$\tfrac{1}{2}a_0 = 0.96,$$
$$a_1 = 0.38,$$
$$a_2 = -0.04,$$
$$a_3 = 0.01,$$
$$a_4 = 0.00.$$

And so, to a good approximation,

$$\sqrt{1+\gamma\cos t} = 1 + m\cos t, \tag{6.10}$$

and the equation of the light curve can be written

$$V = V_0 - (A + m(t))\cos\theta, \tag{6.11}$$

where m(t) should be approximately harmonic. Equation (6.1) is of the form $V_\theta = V_o - A\cos\theta$, so Equation (6.11) can be written

$$V = V_\theta - m(t)\cos\theta,$$

or

$$m(t) = -\frac{V - V_\theta}{\cos\theta} . \qquad (6.12)$$

Since the values of V are measured with error, the error in m(t) will be amplified by sec θ. Therefore, a weight of zero has been attached to those values of m(t) which occur within $\pm 30^\circ$ of 90° or 270°. The values of m(t) and the weights are listed in Table XX. To reduce the variability of m(t), Formula (6.12) was used to compute $\langle m(t) \rangle$ at the average values of V used in Chapter V to locate the extrema of the light curve. These values of $\langle m(t) \rangle$ and the weights are listed in Table XXI and the points are plotted in Figures 71-75.

The plot for August 17 shows a fairly well defined half-cycle of the modulation. A curve was drawn through the points and this curve fitted to the plots of the other nights. In doing this, two assumptions were made: that the other half cycle was the same in both length and shape. As can be seen from the figures, the curve was ill defined on some nights and a fairly wide margin of error was possible.

Extraction and Optimization of the Beat Period

The passages of the curve through zero are better defined and more numerous than extrema and so these are used to define the epochs. The observed epochs are listed in Table XXII.

TABLE XX

VALUES OF m(t)

HJD 2438600+	m(t)	Weight	HJD 2438600+	m(t)	Weight
20.7461	+0.030*	1	24.7548	-0.019	1
20.7687	+0.029	0	24.7577	-0.017	1
20.7708	+0.029	0	24.7634	-0.007	1
20.7765	+0.018	1	24.7659	-0.011	1
20.7788	-0.001	1	24.7718	-0.015	1
20.7843	+0.012	1	24.7745	-0.012	1
20.7866	+0.002	1	24.7805	-0.026	0
20.7979	+0.057	0	24.7832	-0.031	0
20.8006	+0.037	0	24.7892	+0.009	0
20.8065	-0.038	0	24.7919	0.000	0
20.8092	+0.009	0	24.7983	-0.011	1
20.8145	+0.017	1	24.8013	-0.008	1
20.8169	+0.014	1	24.8079	-0.008	1
20.8225	+0.021	1	24.8108	-0.003	1
20.8248	+0.011	1	24.8218	-0.016	0
20.8306	-0.004	1	24.8243	-0.024	0
20.8330	+0.037	1	24.8298	+0.026	0
20.8381	+0.010	0	24.8325	+0.018	1
20.8405	+0.038	0	24.8381	+0.007	1
20.8455	+0.006	0	24.8404	-0.006	1
20.8478	+0.034	0	24.8453	+0.003	1
20.8529	+0.012	1	24.8476	-0.003	1
20.8554	+0.019	1	24.8527	+0.004	1
24.6870	+0.004	1	24.8550	0.000	1
24.6890	+0.009	1	24.8609	-0.018	0
24.6941	+0.012	1	24.8635	-0.029	0
24.6962	+0.010	1	24.8683	+0.054	0
24.7232	+0.003	1	24.8703	+0.005	0
24.7253	-0.001	1	25.6141	+0.171	0
24.7304	0.000	1	25.6170	0.000	0
24.7328	+0.003	1	25.6229	+0.016	1
24.7389	+0.010	1	25.6252	-0.005	1
24.7415	+0.016	0	25.6317	+0.003	1
24.7468	+0.882	0	25.6340	+0.004	1
24.7492	-0.040	0	25.6411	-0.015	1

TABLE XX (Continued)

HJD 2438600+	m(t)	Weight	HJD 2438600+	m(t)	Weight
25.6435	-0.015	1	35.6743	+0.034	0
25.6498	0.000	0	35.6929	-0.008	1
25.6520	-0.006	0	35.6954	-0.003	1
25.6633	-0.007	1	35.7009	+0.010	1
25.6655	-0.008	1	35.7032	-0.002	0
25.6710	-0.011	1	35.7085	-0.058	0
25.6732	-0.022	1	35.7108	+0.003	0
25.6783	-0.006	1	35.7160	+0.006	1
25.6808	-0.006	1	35.7183	-0.003	1
25.6863	-0.011	1	35.7238	+0.011	1
25.6885	-0.024	0	35.7262	+0.012	1
25.6939	-0.057	0	121.5140	-0.628	0
25.6962	+0.013	0	121.5169	-0.089	0
25.7212	-0.012	1	121.5236	-0.016	1
25.7242	-0.003	1	121.5266	-0.009	1
25.7294	-0.040	0	121.5336	-0.016	1
25.7317	+0.080	0	121.5366	-0.007	1
25.7377	+0.075*	0	121.5434	-0.007	1
25.7406	+0.199*	1	121.5464	+0.002	1
35.6296	-0.173	0	121.5532	∞	0
35.6323	+0.083	0	121.5564	+0.004	0
35.6379	+0.012	1	121.5643	0.000	1
35.6408	+0.016	1	121.5672	-0.010	1
35.6463	-0.007	1	121.5736	-0.013	1
35.6489	+0.001	1	121.5766	-0.016	1
35.6546	-0.010	1	121.5833	-0.012	1
35.6572	-0.020	1	121.5862	-0.010	0
35.6637	-0.011	0	121.5926	∞	0
35.6663	-0.029	0	121.5955	+0.027	0
35.6719	+0.040	0			

*Doubtful Data

TABLE XXI

VALUES OF $\langle m(t) \rangle$

HJD 2438600+	$\langle m(t) \rangle$	Weight	HJD 2438600+	$\langle m(t) \rangle$	Weight
20.7689	+0.029	0	25.6321	+0.004	1
20.7768	+0.009	1	25.6414	-0.015	1
20.7846	+0.007	1	25.6502	-0.003	0
20.7981	+0.047	0	25.6636	-0.008	1
20.8068	+0.024	0	25.6713	-0.016	1
20.8148	+0.014	1	25.6787	-0.006	1
20.8228	+0.016	1	25.6867	-0.018	0
20.8310	+0.017	1	25.6943	-0.022	0
20.8383	+0.024	0	25.7218	-0.012	0
20.8458	+0.020	0	25.7297	-0.060	0
20.8533	+0.016	1	35.6310	-0.045	0
24.6872	+0.006	1	35.6394	+0.014	1
24.6944	+0.011	1	35.6476	-0.003	1
24.7234	+0.001	1	35.6559	-0.015	1
24.7307	+0.001	1	35.6650	-0.020	0
24.7393	+0.013	0	35.6731	-0.037	0
24.7471	∞	0	35.6942	-0.006	1
24.7553	-0.018	1	35.7020	+0.004	0
24.7637	-0.009	1	35.7096	-0.028	0
24.7723	-0.014	1			0
24.7808	-0.028	0	35.7172	+0.001	0
24.7896	+0.004	0	35.7250	+0.012	1
24.7987	-0.010	1	121.5155	-0.358	0
24.8083	-0.006	1	121.5251	-0.012	1
24.8222	-0.020	0	121.5351	-0.011	1
24.8302	+0.021	0	121.5449	-0.002	0
24.8383	0.000	1	121.5548	+0.004	0
24.8456	0.000	1	121.5658	-0.005	1
24.8530	+0.002	1	121.5751	-0.014	1
24.8615	-0.023	0	121.5848	-0.011	0
24.8685	+0.030	0	121.5940	+0.027	0
25.6146	+0.085	0			
25.6233	+0.016	1			

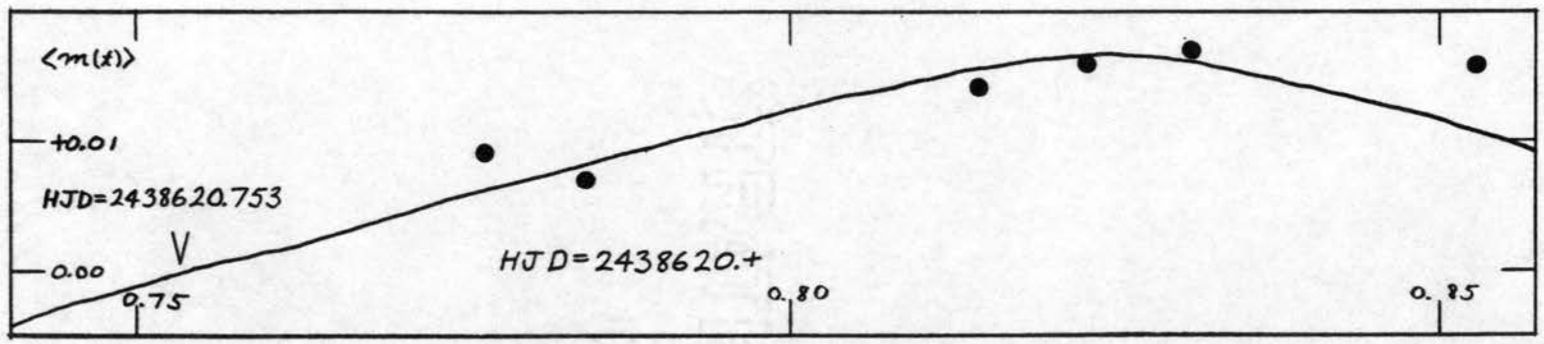

Figure 71. Modulation Envelope of DQ Cephei for August 13, 1964.

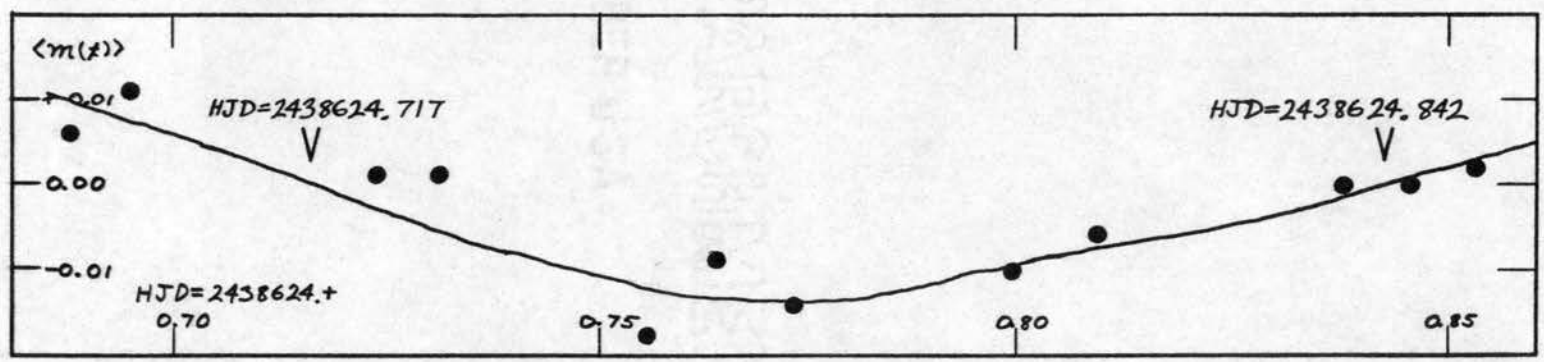

Figure 72. Modulation Envelope of DQ Cephei for August 17, 1964.

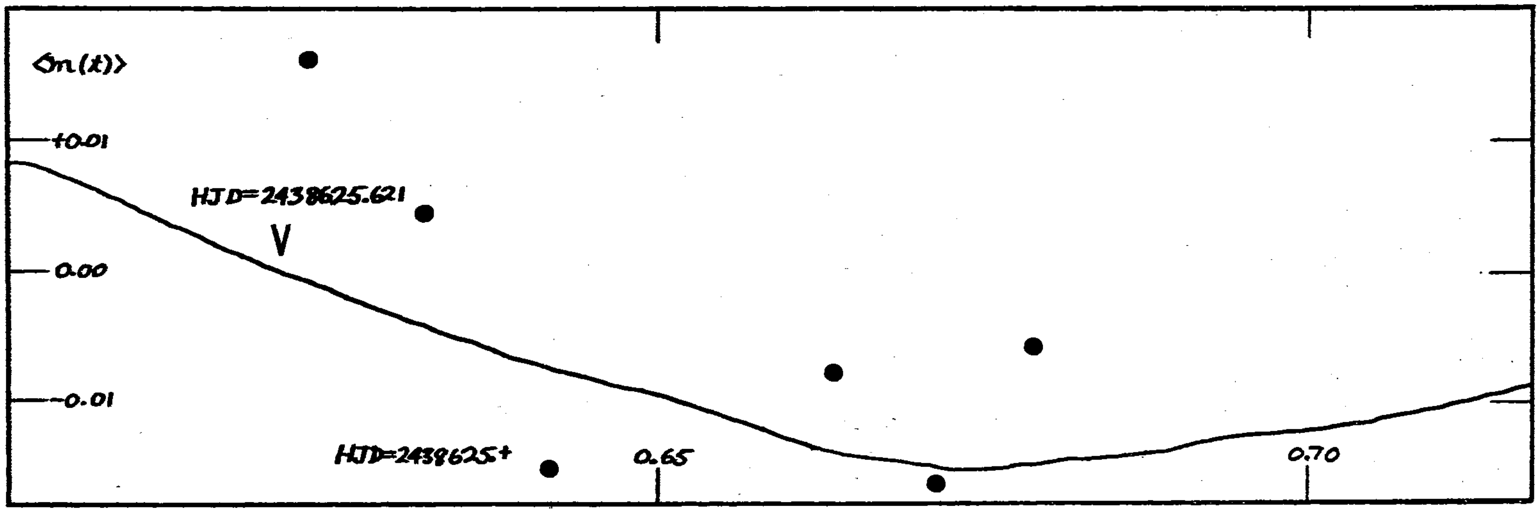

Figure 73. Modulation Envelope of DQ Cephei for August 18, 1964.

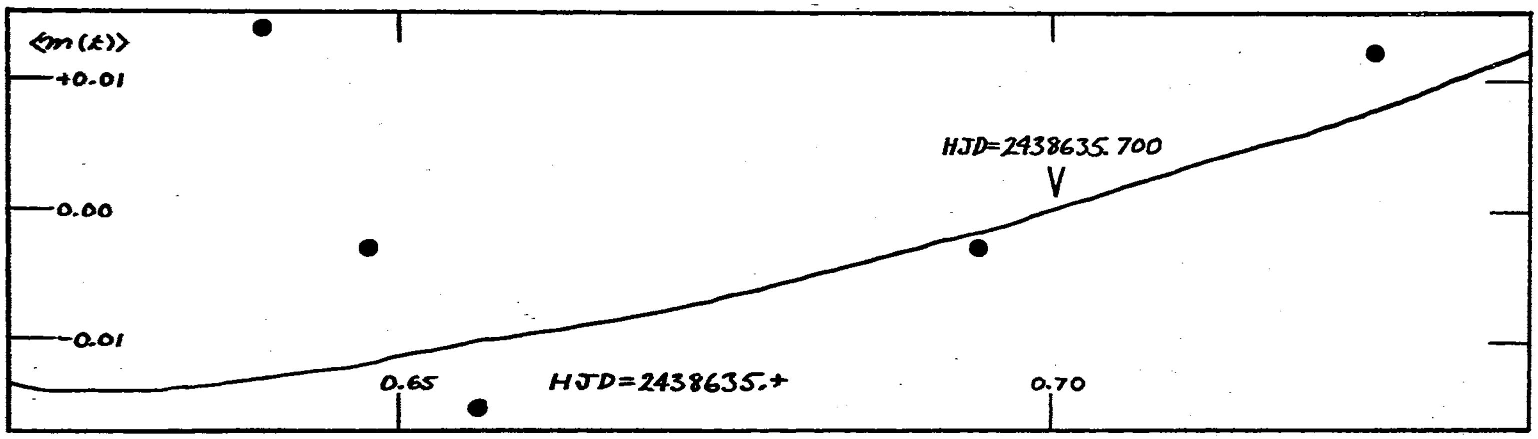

Figure 74. Modulation Envelope of DQ Cephei for August 28, 1964.

TABLE XXII

OBSERVED EPOCHS OF $\langle m(t) \rangle$

Date	Ascending Zero (HJD)	Descending Zero (HJD)
Aug. 13, 1964	2438620.753	
Aug. 17, 1964	2438624.842	2438624.717
Aug. 18, 1964		2438625.621
Aug. 28, 1964	2438635.700	
Nov. 22, 1964	24386121.608	

Using the methods of Chapter IV, a period of $0^d.22610 \pm 0.00002$ was found from these epochs assuming an uncertainty of ± 0.02 day. Data used are listed in Table XXIII. The estimate of ± 0.02 day was made from modulation envelope curves, noting the uncertainty with which they have been determined.

TABLE XXIII

RESULTS OF BEAT PERIOD EXTRACTION

Interval	Number of Cycles
n_{12}	17.5
n_{13}	18
n_{14}	21.5
n_{15}	66
n_{16}	446

By least squares fit we obtain:

$$P_b = 0^d.22611 \pm 0.00003,$$

$$T_{Beat(Ascending\ Zero)} = 2438624.837 \pm 0.006.$$

This beat period corresponds to an interfering period of either $P_1 = 0^d.058471$ or $P_1 = 0^d.12110$.

Evaluation of the Modulation Term

When m(t) is plotted versus phase, its similarity to a sine curve is striking but it is necessary to keep in mind that, to at least some extent, the plot has been forced into this shape by our choice of epochs. If the values of m(t) are averaged in each 30° interval and a formula fitted by harmonic analysis the result is

$$m_{\Psi} = +0^m.014 \sin \Psi, \tag{6.13}$$

where

$$\Psi = 360^{\circ} \frac{t-2438624^d.837}{0^d.22611}. \tag{6.14}$$

The equation of the light curve can be written in the form of Equation (6.11):

$$V = 7^m.268-(0^m.028 + 0^m.014 \sin\Psi)\cos\theta, \tag{6.15}$$

$$\theta = 360^{\circ} \frac{t-2433924^d.8404}{0^d.07886444}, \tag{6.16}$$

$$\Psi = 360^{\circ} \frac{t-2438624^d.837}{0^d.22611}. \tag{6.17}$$

The residuals remaining after the predicted values of V were subtracted from the observations are shown in Figures 76 - 80. Systematic variability is no longer evident in the plots except for a small hump in the curve on the first part for August 28th.

Periodogram Analysis

The method used in the last few sections for extraction of the modulation term is subject to a large margin of error because of the errors possible in measuring the epochs of the modulation envelope. It is desirable to reanalyze the light curve by an unrelated method in order to determine whether the secondary period we have found is real or spurious. The method selected is that of periodogram analysis. Suppose we wish to test whether a time series contains a harmonic term with period T. Consider the series

$$A = \frac{2}{n}\sum_{j=1}^{n} u_j \cos\frac{2\pi j}{T}, \tag{6.18}$$

$$B = \frac{2}{n}\sum_{j=1}^{n} u_j \sin\frac{2\pi j}{T}. \tag{6.19}$$

Suppose the time series is in fact given by

$$u_j = a \sin\frac{2\pi j}{P} + b_j \tag{6.20}$$

where b_j is a component which we assume to contain no cyclical element, so that its correlation with the other component is zero for long series. Then we have

$$A = \frac{2a}{n}\sum_{j=1}^{n} \sin\frac{2\pi j}{P}\cos\frac{2\pi j}{T} + \frac{2}{n}\sum_{j=1}^{n} b_j \cos\frac{2\pi j}{T}, \tag{6.21}$$

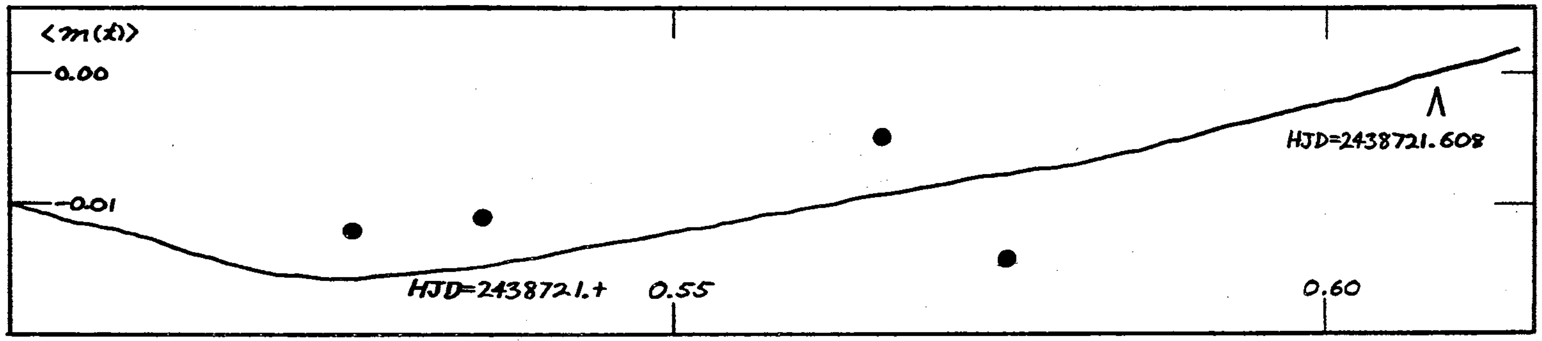

Figure 75. Modulation Envelope of DQ Cephei for November 22, 1964.

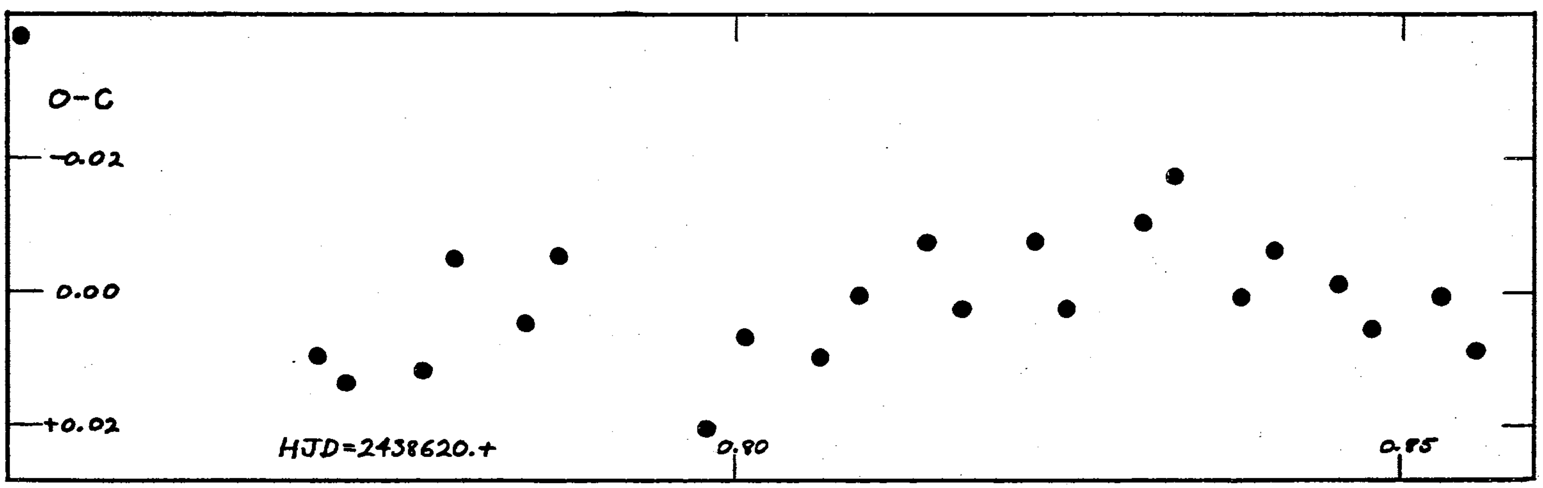

Figure 76. Residuals in V for August 13, 1964.

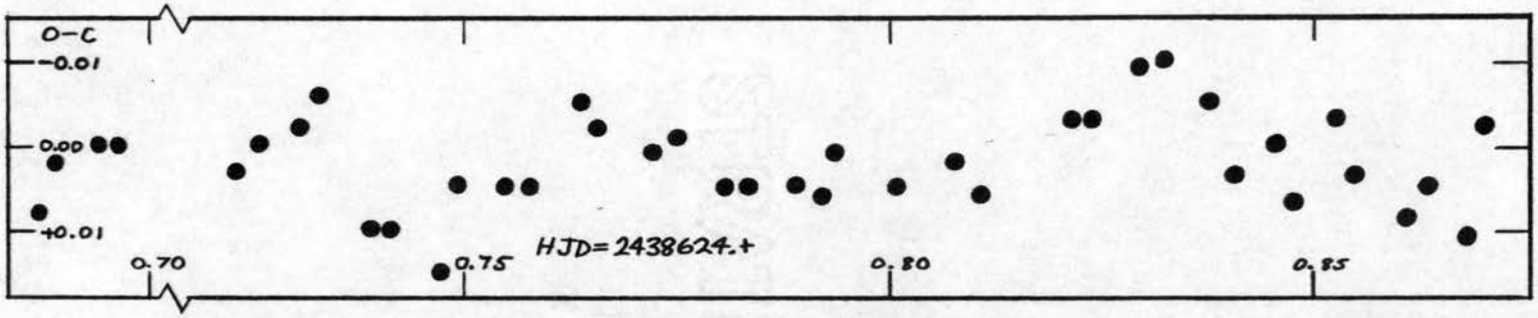

Figure 77. Residuals in V for August 17, 1964.

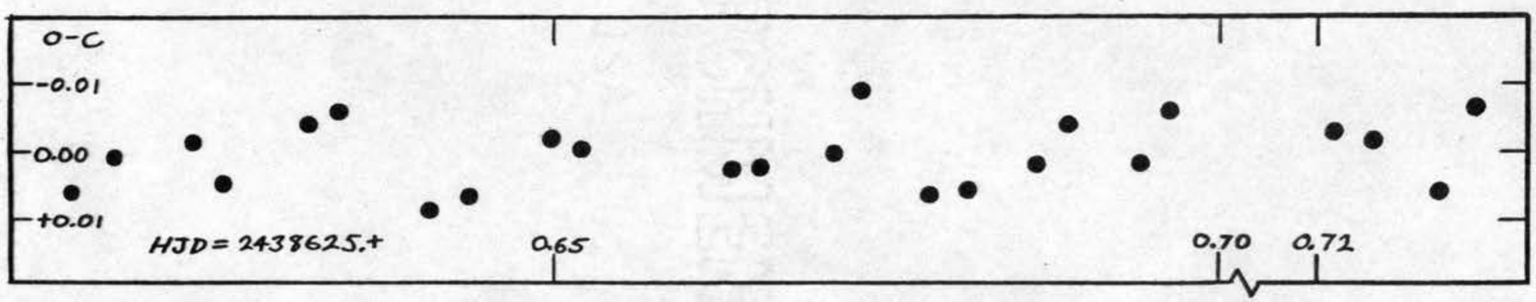

Figure 78. Residuals in V for August 18, 1964.

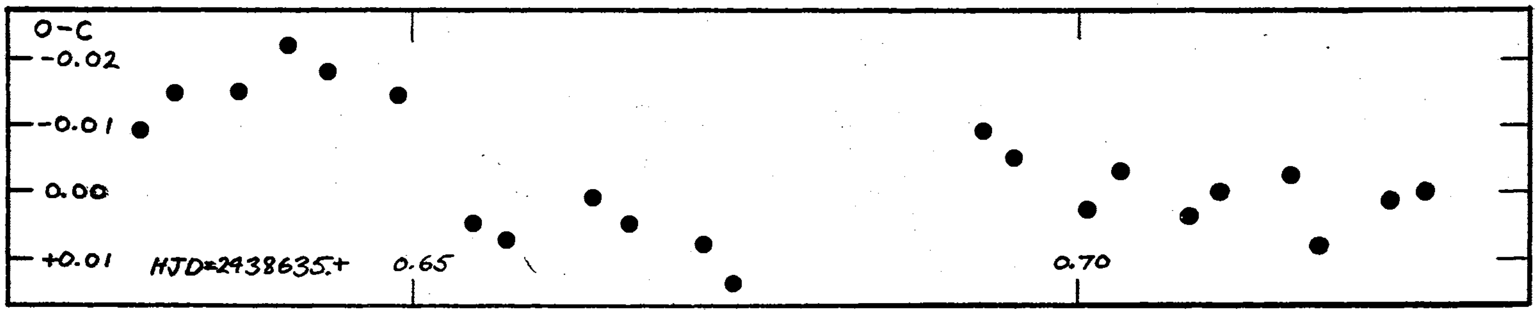

Figure 79. Residuals in V for August 28, 1964.

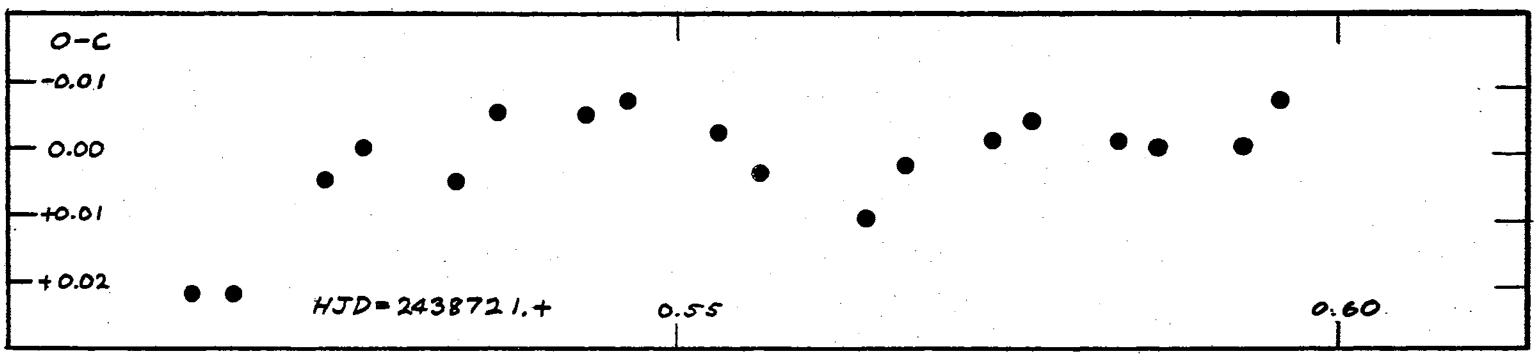

Figure 80. Residuals in V for November 22, 1964.

and the second term may be neglected. We then have

$$A = \frac{2a}{n} \sum_{j=1}^{n} \sin \frac{2\pi j}{P} \cos \frac{2\pi j}{T} ,$$

$$= \frac{2a}{n} \sum_{j=1}^{n} \left[\sin 2\pi(\frac{1}{P} - \frac{1}{T}) j + \sin 2\pi(\frac{1}{P} + \frac{1}{T}) j \right] ,$$

$$= \frac{a}{n} \left\{ \frac{\sin \pi(\frac{1}{P} - \frac{1}{T}) n \sin \pi(\frac{1}{P} - \frac{1}{T})(n+1)}{\sin \pi(\frac{1}{P} - \frac{1}{T})} + \frac{\sin \pi(\frac{1}{P} + \frac{1}{T}) n \sin \pi(\frac{1}{P} + \frac{1}{T})(n+1)}{\sin \pi(\frac{1}{P} + \frac{1}{T})} \right\} . \tag{6.22}$$

For large n this remains small unless T approaches P, and in that case we have

$$A \rightarrow a \sin \pi(\frac{1}{P} - \frac{1}{T})(n+1) . \tag{6.23}$$

Similarly,

$$B \rightarrow a \cos \pi(\frac{1}{P} - \frac{1}{T})(n+1) . \tag{6.24}$$

Now, let us set

$$R^2 = A^2 + B^2 = a^2 . \tag{6.25}$$

Thus R remains small unless the "trial" period approaches the real period P and in that case equals the amplitude a. Similarly, we may expect that if the series consists of a sum of harmonics with periods P_o, P_1, . ., P_m, R will be small unless T is close to one of these periods in which case R will be close to the amplitude of the term concerned.

This result forms the basis of periodogram analysis. We select several trial periods for different values of T and calculate R for each of them. R is then plotted <u>versus</u> T. The diagram obtained by joining the points is the periodogram. If this figure has peaks at certain values T_0, T_1,.., T_m and we are prepared to assume that these are not sampling accidents, the values are the appropriate periods of the harmonic terms.

In practice, Equations (6.18) and (6.19) are modified to allow for the existence of gaps in the data. If the trial period T is equal to n times the basic sampling interval, then we write

$$A = \frac{2}{n}\sum_{j=1}^{n} \langle u_j \rangle \cos 2\pi \frac{j}{n} , \tag{6.26}$$

$$B = \frac{2}{n}\sum_{j=1}^{n} \langle u_j \rangle \sin 2\pi \frac{j}{n} , \tag{6.27}$$

$$\langle u_j \rangle = \frac{1}{k}\sum_{\ell=1}^{k} u_{j+i_\ell n} , \tag{6.28}$$

where the i_ℓ are chosen to include the available u_j in the summation.

Since the mathematics of periodogram analysis depends on equally spaced data, at least in each group of data, it is necessary to find the values of V at equally spaced intervals by some interpolation method. It was decided to read the values of V from Figures 47 through 64 used in determining the times of maximum and minimum in the three colors. The time interval was chosen to be 0.005 day which is about the spacing of the original data. Table XXIV lists the equally spaced values of V. The periodogram resulting from these values appears in Figure 81. $P_1(S)$ refers to the secondary periods implied by Sahade's observed beat period, $P_1(F)$ refers to the secondary period presumed by Fitch to fit his interpolation formula, $P_1(W)$ indicates the secondary period observed by Wehlau

TABLE XXIV

EQUALLY SPACED VALUES OF V

JD 2438600+	V=7.+	JD 2438600+	V=7.+	JD 2438600+	V=7.+
20.770	.293	24.815	.285	35.655	.254
20.775	.299	24.820	.275	35.660	.264
20.780	.301	24.825	.262	35.665	.271
20.785	.302	24.830	.249	35.670	.279
20.790	.300	24.835	.243	35.675	.288
20.795	.298	24.840	.241	35.680	.292
20.800	.290	24.845	.241	35.685	.295
20.805	.273	24.850	.244	35.690	.294
20.810	.248	24.855	.252	35.695	.291
20.815	.233	24.860	.263	35.700	.285
20.820	.225	24.865	.275	35.705	.276
20.825	.222	24.870	.286	35.710	.266
20.830	.225	25.615	.266	35.715	.256
20.835	.240	25.620	.254	35.720	.245
20.840	.261	25.625	.246	35.725	.232
20.845	.280	25.630	.238	121.515	.287
24.725	.297	25.635	.239	121.520	.271
24.730	.296	25.640	.249	121.525	.256
24.735	.294	25.645	.260	121.530	.252
24.740	.288	25.650	.267	121.535	.250
24.745	.280	25.655	.274	121.540	.250
24.750	.271	25.660	.279	121.545	.252
24.755	.263	25.665	.281	121.550	.262
24.760	.253	25.670	.284	121.555	.272
24.765	.249	25.675	.284	121.560	.281
24.770	.251	25.680	.282	121.565	.286
24.775	.259	25.685	.278	121.570	.286
24.780	.267	25.690	.271	121.575	.284
24.785	.273	25.695	.263	121.580	.281
24.790	.279	35.630	.258	121.585	.277
24.795	.283	35.635	.248	121.590	.270
24.800	.287	35.640	.238	121.595	.260
24.805	.289	35.645	.234		
24.810	.289	35.650	.243		

and Fitch, and $P_1(J)$ refers to the secondary periods implied by the beat period observed in the present study. A prominent peak is apparent close to the primary period, P_o, and another prominent peak appears at the longer secondary period implied by Sahade's observed beat period. Neither Fitch's, Fitch and Wehlau's, nor the present study's period is represented by a prominent peak.

Caution must be exercised in ascribing reality to the peak which occurs at 0.100 day, however. The presence of a harmonic term is known to produce secondary "wings" in the periodogram, as examination of Equation (6.22) shows. Also, the presence of windows (gaps in the observed data) introduces peaks in the diagram where no real frequencies exist. If the gap between two cycles of the curve is nP in length, where P is the true period, then a trial period T such that $kT = nP$ will result in the trial and observed curves being in phase and produce a peak in the periodogram. The smallest gap in the present data occurs between August 17 and August 18 for which $n = 10$. If the peaks due to this gap are obtained by setting k equal to integral values, and the minima by setting k equal to half-integers, the fractional distance from each computed point on the periodogram to a maximum can be determined by dividing the distance from the point on the periodogram to the maximum by the distance from the nearest minimum to the maximum. These fractional distances are listed in Table XXV. The periods corresponding to the smaller distances have been underlined. The peaks on the periodogram can be seen to correspond quite well with these periods. We must then assume that the peaks other than the one occuring at $T = 0.080$ day may well be spurious and caused by the gaps in the data.

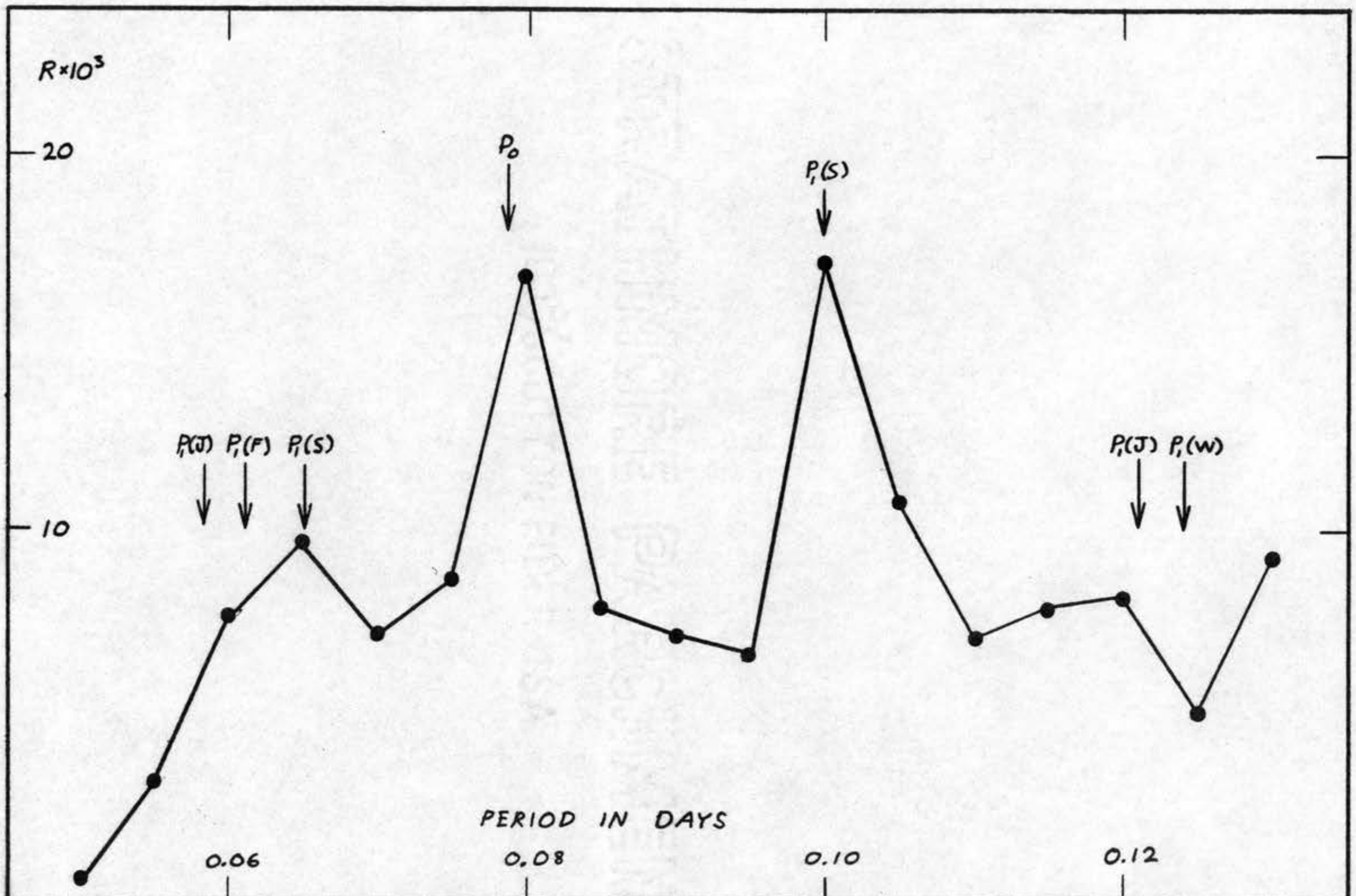

Figure 81. Periodogram of DQ Cephei.

TABLE XXV

FRACTIONAL DISTANCES OF PERIODOGRAM POINTS FROM PEAKS DUE TO GAP n = 10

T^d	Distance	T^d	Distance	T^d	Distance
0.050	0.44	0.080	0.27	0.110	0.36
0.055	0.68	0.085	0.57	0.115	0.27
0.060	0.30	0.090	0.46	0.120	0.85
0.065	0.27	0.095	0.62	0.125	0.63
0.070	0.55	0.100	0.22	0.130	0.16
0.075	0.97	0.105	0.98		

To better detect any secondary period occuring in the light curve, the effects of the primary period can be suppressed by "prewhitening" the data by subtracting the primary component from the data before another spectrum is computed. The term given by Equation (6.1), the primary component, is subtracted from the equally spaced values of V given in Table XXIV. The resulting prewhitened values are listed in Table XXVI. The periodogram resulting from these prewhitened values is given in Figure 82. The amplitude of the peaks has been much reduced because much of the variability of the data has been removed by the subtraction.

In order to make the peaks in the two periodograms comparable in significance we can divide the values of each periodogram by the variance of its original data. In Figure 83 we plot $K = \frac{NR^2}{4\sigma^2}$, the measure of significance commonly found in the literature, for both the original and the prewhitened data. N is the number of data used and σ^2 is the

TABLE XXVI

PREWHITENED VALUES OF V

JD 2438600+	$Vx10^3$	JD 2438600+	$Vx10^3$	JD 2438600+	$Vx10^3$
20.770	+11	24.815	- 4	35.655	+11
20.775	+ 9	24.820	- 5	35.660	+16
20.780	+ 6	24.825	- 6	35.665	+12
20.785	+ 6	24.830	- 9	35.670	+ 9
20.790	+ 7	24.835	- 5	35.675	+ 7
20.795	+12	24.840	- 1	35.680	+ 2
20.800	+15	24.845	+ 1	35.685	0
20.805	+ 9	24.850	+ 2	35.690	- 2
20.810	- 6	24.855	+ 4	35.695	- 2
20.815	-12	24.860	+ 5	35.700	- 1
20.820	-16	24.865	+ 6	35.705	0
20.825	-18	24.870	+ 6	35.710	+ 1
20.830	-19	25.615	0	35.715	+ 2
20.835	-12	25.620	- 1	35.720	- 1
20.840	- 1	25.625	0	35.725	- 9
20.845	+ 7	25.630	- 3	121.515	+23
24.725	+ 1	25.635	- 1	121.520	+18
24.730	+ 1	25.640	+ 5	121.525	+11
24.735	+ 4	25.645	+ 9	121.530	+12
24.740	+ 6	25.650	+ 6	121.535	+ 8
24.745	+ 9	25.655	+ 2	121.540	+ 6
24.750	+11	25.660	- 3	121.545	0
24.755	+13	25.665	- 9	121.550	0
24.760	+10	25.670	-11	121.555	- 1
24.765	+ 9	25.675	-12	121.560	- 3
24.770	+ 9	25.680	-10	121.565	- 6
24.775	+13	25.685	- 7	121.570	- 9
24.780	+12	25.690	- 3	121.575	-11
24.785	+ 7	25.695	0	121.580	-10
24.790	+ 2	35.630	-10	121.585	- 6
24.795	- 4	35.635	- 9	121.590	- 2
24.800	- 7	35.640	-13	121.595	- 2
24.805	- 7	35.645	- 8		
24.810	- 5	35.650	+ 3		

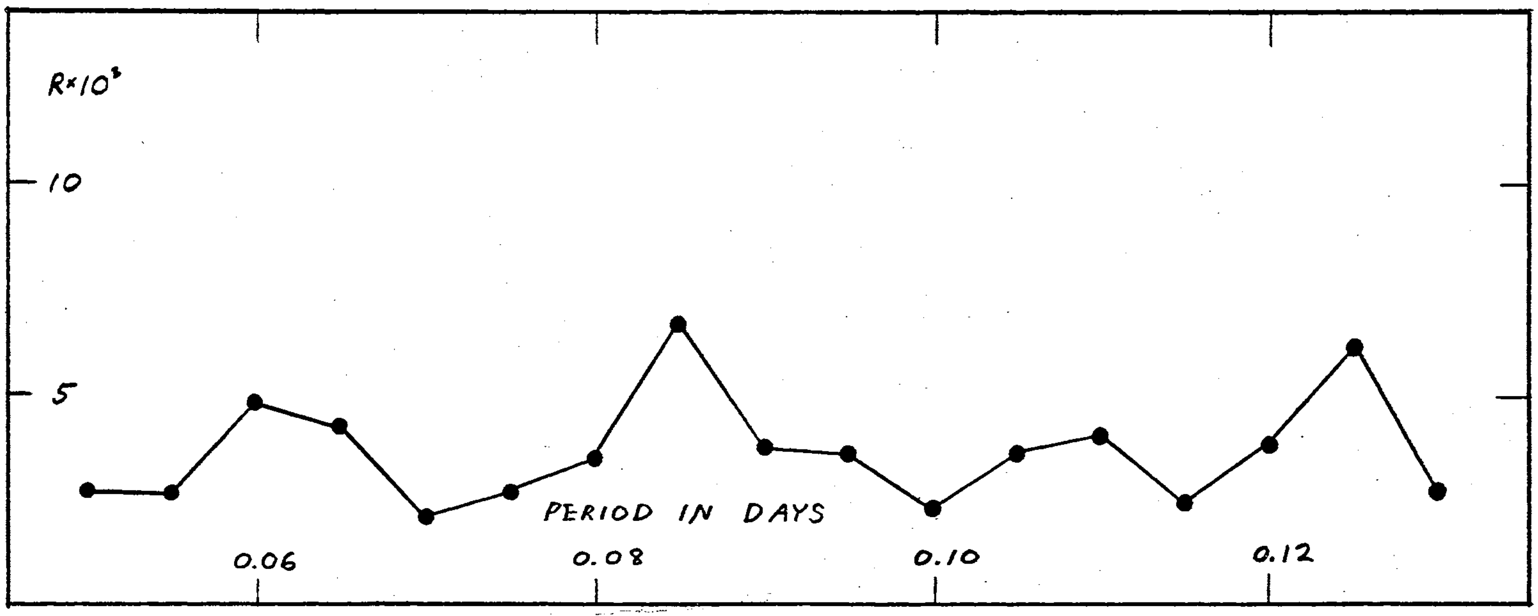

Figure 82. Periodogram of DQ Cephei (Prewhitened Data).

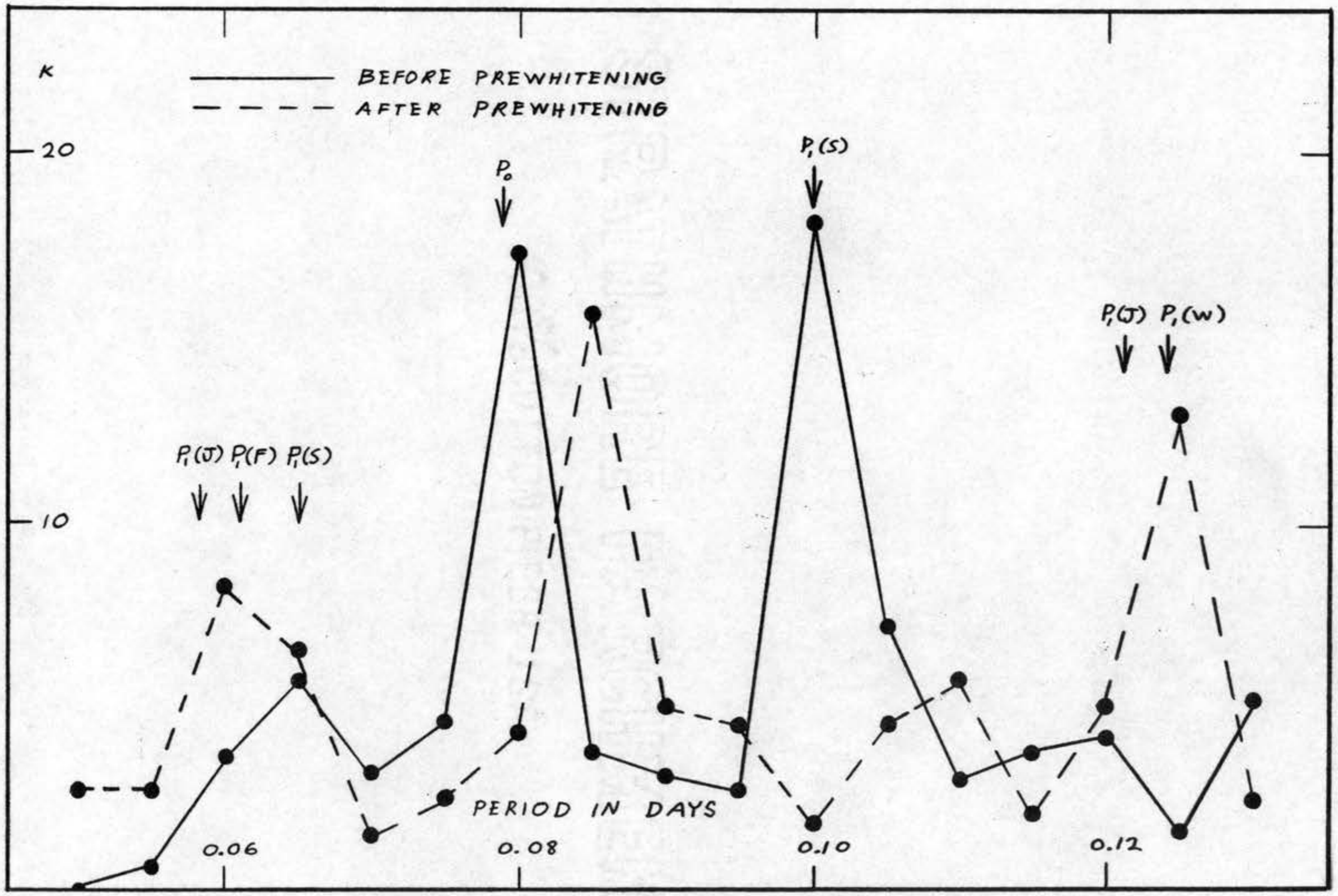

Figure 83. Normalized Periodogram of DQ Cephei.

variance of the data. For a discussion of tests of significance see, for example, Davis (1941).

Examination of Figure 83 shows that the prominent peak corresponding to Sahade's beat period has completely disappeared after prewhitening, and that two main peaks have appeared: one at 0.085 day and one at 0.125 day.

The peak at 0.085 day corresponds to no period yet detected. From the peak's position it is possible that the primary component has been imperfectly removed by subtracting Equation (6.1) from the data. On the other hand, such imperfect removal should not result in a shift of the period. A component with period 0.085 day interfering with the primary period would result in a beat period of 1.1 day. A beat period of this length cannot account for the observed changes in amplitude from cycle to cycle which imply a much shorter period. The peak at 0.085 day is therefore probably due to a residual of the primary period remaining in the prewhitened data.

The peak at 0.125 day corresponds well with the period of 0.1242 day reported by Fitch and Wehlau (1965) and is in the neighborhood of the period of 0.1211 corresponding to the beat period found earlier in this study. The small amplitude of the component would make its reality questionable were it not for the independent detection of this period in Walker's and Fitch's data, which were analyzed by Fitch and Wehlau by Fourier Transform, and in the present data by the examination of the modulation envelope. The period, therefore, is probably real.

CHAPTER VII

MACHINE PROGRAM DESIGN

During the course of this study it has been noted that many of the computations involved in the reduction require excessive amounts of time when done on a desk calculator. Therefore, in order to facilitate subsequent types of studies, some of the more laborious and frequent computations have been selected to be performed by automatic machines. The design of the programs is described in this chapter. Program specifications are given in Appendix C.

Extinction and Reduction

The program which performs several of the extinction and reduction computations uses the method of Hardie (1962) which was described in Chapter II. The various operations involved in computing the extinction and reduction depend on solving Equations (2.17) in different ways. In solving these equations, the program accepts the parameters k''_{bv}, k''_{ub}, ϵ, μ, and ψ as known values. The declination and hour angle of each star and latitude of the observatory are used to compute the air mass by means of Formula (2.8).

If the equations are to be used in order to determine the extinction and zero points, then the program is placed into EXT mode of operation. In this mode, for each standard star, the local magnitudes v, b, u, and the values V, B-V, U-B, and read by the program. The output for each star includes the values $v + \varepsilon(B-V)-V, \mu J_x(b-v)-(B-V), \psi G_x(u-b)-(U-B)$, and X. When the first three terms are plotted versus the air mass, the slopes of the best fitting straight lines yield k_v, $\mu k'_{bv}$, and $\psi k'_{ub}$ and the intercepts will give the zero-point terms ζ_v, ζ_{bv}, and ζ_{ub}. In order to be able to determine the quality of the night's seeing, it is advantageous if the above output information is available for inspection rather than just having the resulting values of the principle extinction coefficients and zero-point terms.

If the equations are to be used in order to prepare a table of zero-point terms used in differential reduction, the program is placed into ZERO mode of its operation. A detailed discussion of the equivalence of using interpolated zero-point values obtained from assuming the constancy of the comparison star's magnitude and the differential reduction terms given by Hardie (1952) is given in Appendix B. In this mode, for each comparison star observation, the local magnitudes v, b, u, the standard colors V, B-V, U-B, the time in JD, and the extinction coefficients k_v, $\mu k'_{bv}$, $\psi k'_{ub}$ are read by the program. The output for each observation is the time, JD, and the zero-point values ζ_v, ζ_{bv}, ζ_{ub}, needed to keep the magnitude of the comparison star constant. If these values are plotted versus time it is quite simple to read the zero-point values at the time of program star observations. If the quantities described are the delta magnitudes, that is program star minus comparison star, these may be obtained by computing the zero-point values with the comparison star colors V, B-V, U-B set equal to zero.

If the equations are to be used to reduce local magnitudes v, b, u to standard magnitudes V, B-V, U-B, then the program is placed into RDUC mode of operation. In this mode, for each program star, the local magnitudes v, b, u, the zero-points ζ_v, ζ_{bv}, ζ_{ub}, the time in JD, and the extinction coefficients k_v, $\mu k'_{bv}$, and $\psi k'_{ub}$ are read. The output for each observation includes V, B-V, U-B, or ΔV, Δ(B-V), Δ(U-B) and JD, depending on the zero-point terms used. A flow chart of the program is given in Figure 84.

Heliocentric Julian Day Correction

The Heliocentric Julian Day correction program is based on the formulas derived in Chapter II. Since Δt, the correction, equals $\frac{d}{c}$, Equation (2.21) can be written

$$\Delta t = -\frac{r}{c}\left[\cos\delta\cos\alpha\cos\Theta + (\sin\epsilon\sin\delta + \cos\epsilon\cos\delta\sin\alpha)\sin\Theta\right] . \quad (7.1)$$

From the geometry of an elliptical orbit,

$$r = a\,\frac{1 - e^2}{1 + e\cos\Theta} , \quad (7.2)$$

where a is the astronomical unit and e is the eccentricity of the orbit. Equation (7.1) then becomes

$$\Delta t = -\frac{a}{c}\ \frac{1 - e^2}{1 + e\cos\Theta}\left[\cos\delta\cos\alpha\cos\Theta + (\sin\epsilon\sin\delta + \cos\epsilon\cos\delta\sin\alpha)\sin\Theta\right] . \quad (7.3)$$

In this last equation all quantities are known except the sun's longitude Θ. To determine the accuracy to which the longitude must be calculated, change the form of Equation (7.3) to resemble Equation (2.19). Then,

$$\Delta t = -\frac{a}{c}\,\frac{1 - e^2}{1 + e\cos\Theta}\ \cos\beta\cos(\lambda - \Theta). \quad (7.4)$$

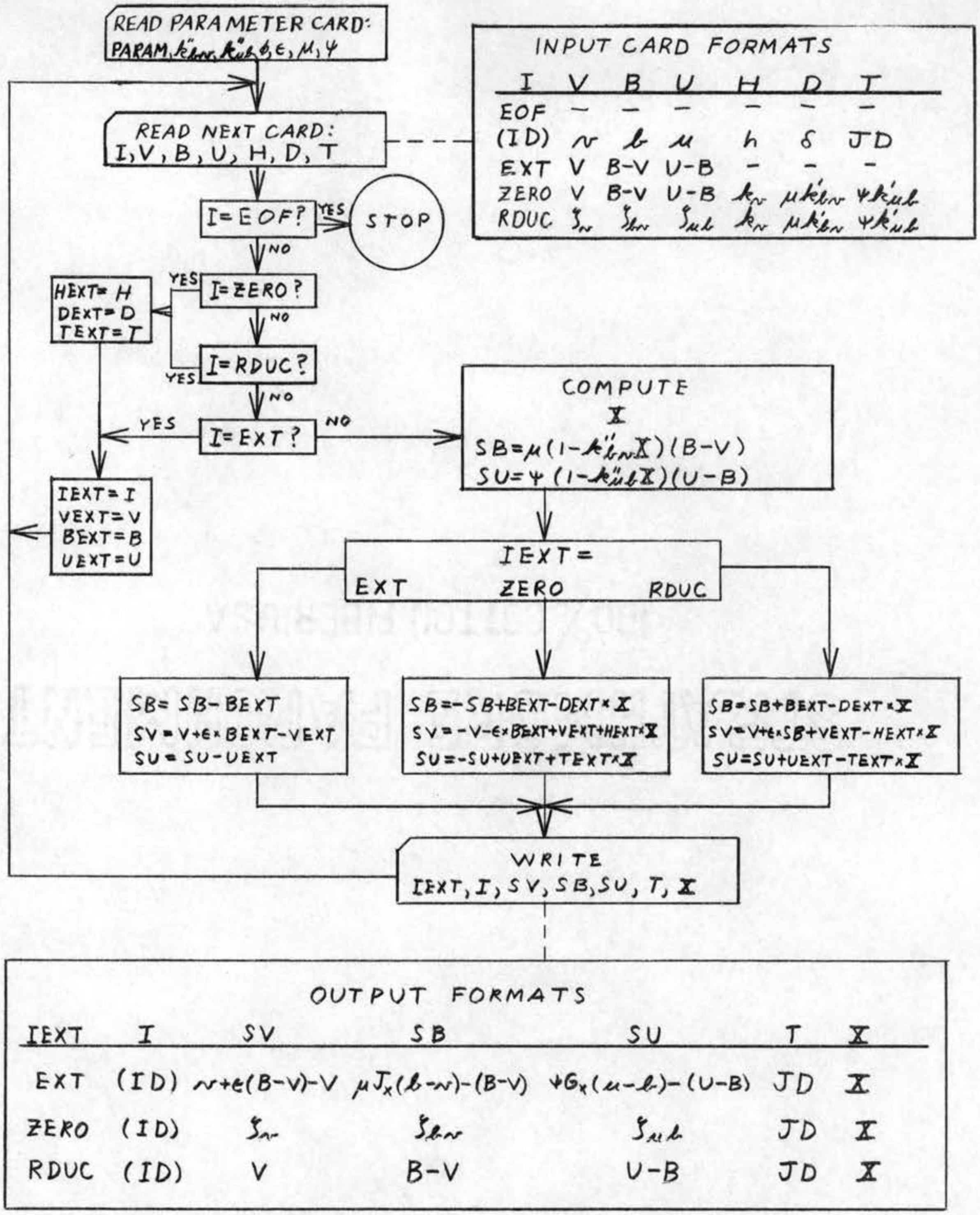

Figure 84. Flow Chart of Reduction Program.

Taking differentials,

$$d(\Delta t) = \frac{a}{c} \frac{1 - e^2}{(1 + e\cos\odot)^2} \cos\beta(\sin(\odot - \lambda) - e\sin\lambda)\,d\odot, \tag{7.5}$$

and, since e is small, the maximum error in Δt is approximately

$$d(\Delta t)_{MAX} = \frac{a}{c}\,d\odot, \tag{7.6}$$

and so the largest error we can permit in $\odot$ is

$$d\odot_{MAX} = \frac{c}{a}\,d(\Delta t)_{MAX} . \tag{7.7}$$

Evaluating this numerically, we wish to compute the time to 0.0001 day, so we must limit the error to at most 0.00005 day. From Allen (1955) we note:

$$a = 1.496 \times 10^{13} \text{ cm},$$

$$c = 2.99791 \times 10^{10} \text{ cm/sec},$$

$$\frac{c}{a} = 173.14 \text{ day}^{-1},$$

and

$$d\odot_{MAX} = 173.14 \times 0.00005 = 0.009 \text{ radian} = 0^{\circ}\!.5. \tag{7.8}$$

From Figure 1 we see that

$$\odot = f + \Gamma, \tag{7.9}$$

where f is the true anomaly and Γ is the longitude of perigee. The true anomaly is related to the mean anomaly by the equation of the center given, for example, by Watson (1900):

$$f = M + (2e - \frac{1}{4}e^3 + \frac{5}{96}e^5 - \frac{107}{4608}e^7 + \ldots)\sin M$$

$$+ (\frac{5}{4}e^2 - \frac{11}{24}e^4 + \frac{17}{192}e^6 - \ldots)\sin 2M$$

$$+ (\frac{13}{12}e^3 - \frac{43}{64}e^5 + \frac{95}{512}e^7 - \ldots)\sin 3M$$

$$+ (\frac{103}{96}e^4 - \frac{451}{480}e^6 + \ldots)\sin 4M$$

$$+ (\frac{1097}{960}e^5 - \frac{5957}{4608}e^7 + \ldots)\sin 5M$$

$$+ (\frac{1223}{960}e^6 - \ldots)\sin 6M$$

$$+ (\frac{47273}{32256}e^7 - \ldots)\sin 7M$$

$$+ \ldots \qquad (7.10)$$

From the Explanatory Supplement of the American Ephemeris and Nautical Almanac (1961), we have

$$e = 0.01675.$$

To obtain the required accuracy, only the terms linear in e must be retained. Thus

$$f = M + 2e\sin M. \qquad (7.11)$$

The mean anomaly and the longitude of perigee are given by the Explanatory Supplement as

$$M = 358^\circ\!.475845 + 0^\circ\!.9856002670d - 0^\circ\!.0000121D^2 - 0^\circ\!.00000007D^3, \qquad (7.12)$$

$$\Gamma = 281^\circ\!.22083\ 3 + 0^\circ\!.00004\ 70684d + 0^\circ\!.00003\ 39D^2 + 0.00000\ 007D^3, \quad (7.13)$$

where

$$d = 10000\ D, \quad (7.14)$$

and

$$d = JD - 2415020^d\!.0. \quad (7.15)$$

All the information needed to compute the Heliocentric Julian Day Correction is now available. A flow chart of the computation is given in Figure 85. The right ascension, α, the declination, δ, and Julian Day, JD, are read and the Heliocentric Julian Day Correction, Δt, is written as output.

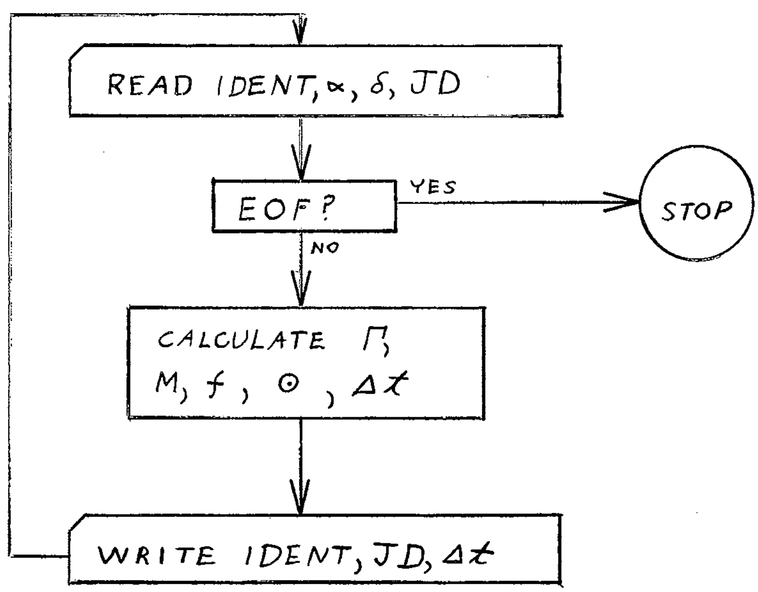

Figure 85. Flow Chart of Heliocentric Julian Day Correction Program.

Since Δt changes slowly with time, its calculation is needed only once for each day's observations.

CHAPTER VIII

CONCLUSIONS

The results obtained in the previous chapters are gathered together in this final chapter for review.

First, and parenthetically, it was found that the comparison and control stars used in this study, HR199938 and HR199067, do not vary periodically in magnitude by more than a few thousandths of a magnitude, if at all. Standard U, B, V magnitudes for these stars have been found and are given in Table XI.

Light curves for the variable star DQ Cephei have been obtained in standard U, B, V magnitudes. Epochs of maximum and minimum light were determined from the light curves and the primary period determined, both independently and by utilizing all available epochs since the star's variability was discovered. The period has been examined for the existence of any secular change and none was found.

The shapes of the light curves are quite symmetrical and resemble harmonic curves. The curves show that the star is brightest when bluest although the variation in color is quite small. No demonstratable phase shift has been observed between the colors although there is some evidence that the curves in B and possibly those in U may occur later than those in V.

From the position of the typical short-period variable star loop in the color-color diagram, it is suggested that this star is slightly reddened by interstellar absorption. However, it must be noted that the correct position of the intrinsic colors of stars of this type in the color-color diagram is imperfectly known.

The light curves clearly vary in amplitude from cycle to cycle, and this phenomenon can be interpreted as being caused by the presence of an interfering secondary component. To determine the period of this postulated secondary component, two methods of analysis were used. The modulation envelope of the light curve was extracted to determine a beat period and a periodogram analysis was made to find a secondary period. The modulation envelope and periodogram suggest a secondary period in fair agreement with one detected by Fitch and Wehlau but no evidence was found, after prewhitening, of a beat period reported by Sahade based on radial velocity measures. Because of the uncertainty of the epochs of the modulation envelope and because of the notorious propensity of the periodogram to "detect" non-existant periods, this last finding must be considered unfirm.

Future work on this star and other δ Scuti variables should include determination of their intrinsic colors, and more investigation of the stability and periods of their secondary pulsations. Such information would be useful in contructing theoretical models of these stars.

REFERENCES

Acton, Forman S. 1959, Analysis of Straight-Line Data. Wiley and Sons.

Allen, C. W. 1955, Astrophysical Quantities. Athlone Press.

American Ephemeris and Nautical Almanac. 1964, Nautical Almanac Office of the United States.

Blanco, V. M. 1955, Ap. J., 123, 64.

Brownlee, K. A. 1960, Statistical Theory and Methodology in Science and Engineering. Wiley.

Davis, Harold T. 1941, The Analysis of Economic Time Series. Principia Press.

Eggen, O. 1957, A. J., 62, 45.

Explanatory Supplement to the Ephemeris. 1961, Nautical Almanac Offices of the United Kingdom and United States.

Fitch, W. S. 1959, Ap. J., 130, 1022.

__________. 1965, private correspondence.

__________, and Wehlau, William. 1965. Ap. J., 142, 1616.

Hardie, Robert H. 1959, Ap. J., 130, 663.

__________. 1962, "Photoelectric Reductions", Chapter VIII, Astrophysical Techniques, Vol. II, Ed. Hiltner, University of Chicago Press.

Hiltner, W. A., and Johnson, H. L. 1956, Ap. J., 124, 367.

Hulst, H. C. van de. 1949, The Atmospheres of the Earth and Planets, Chapter 3, Ed. G. P. Kuiper, University of Chicago Press.

Johnson, H. L., and Morgan, W. W. 1953, Ap. J., 117, 313.

__________. 1954, Ap. J., 117, 343.

Ledoux, P., and Walraven, T. R. 1958, "Variable Stars", Handbuch der Physik, Vol. 51, Ed. S. Flügge, Berlin.

Sahade, J., Struve, O., Wilson O. C., and Zebergs, V. 1956, Ap. J., 123, 399.

Walker, Merle F., 1952, Pub. A.S.P. 64, 192.

__________. 1953, ibid, 65, 39.

Watson, James C. 1900, Theoretical Astronomy, J.B.L. Lippincott Co.

APPENDIX A

DERIVATION OF SOME AIR MASS FORMULAS

If we assume the atmosphere to be plane-parallel, with index of refraction 1.0, then

$$X = \frac{\tau_z}{\tau_0} \quad \frac{\int_0^\infty K\rho\, ds}{\int_0^\infty K\rho\, dh} \qquad \frac{\int_0^\infty K\rho \sec z\, dh}{\int_0^\infty K\rho\, dh} = \frac{\tau_0}{\tau_0} \sec z \ ,$$

or,

$$X = \sec z \ , \tag{A.1}$$

where z is the zenith angle.

If we permit refraction in this model, we must make allowance for bending of the light. Let us suppose that the index of refraction depends only upon the vertical distance above the surface of the earth. If the index at the surface is n, then from Snell's law:

$$n(h)\sin\Psi = n\sin z \tag{A.2}$$

where Ψ is the angle between a ray and the vertical at height h. The relative air mass is

$$X = \frac{\tau_z}{\tau_0} = \frac{1}{\tau_0} \int_0^\infty K\rho \sec\Psi\, dh. \tag{A.3}$$

Now, if we set $n'(h) = \frac{n(h)}{n}$, we have $\sin\Psi = \frac{\sin z}{n'}$, or, $\sec\Psi = \frac{n'}{\sqrt{n'^2-\sin^2 z}}$ and

$$X = \frac{1}{\tau_o} \int_0^\infty \frac{K\rho n'}{\sqrt{n'^2-\sin^2 z}}\, dh. \tag{A.4}$$

$n(h) \leq n$ for the earth's atmosphere, so $n' \leq 1$. Since $n = 1.0002926$ and $n(\infty) = 1.0$ we have $1 \geq n' \geq \frac{1}{1.0002926} = 0.99970748 = 1-0.0002925$. Now, if we let

$$n' = 1 - \eta, \tag{A.5}$$

we know that $\eta \leq 0.0002925$.

If we substitute Equation (A.5) into Equation (A.4) and ignore all powers of η higher than the first we obtain

$$\begin{aligned} X &= \frac{1}{\tau_o} \int_0^\infty K\rho \frac{1-\eta}{\sqrt{\cos^2 z - 2\eta}}\, dh = \frac{1}{\tau_o} \int_0^\infty K\rho \frac{1-\eta}{\cos z - \frac{\eta}{\cos z}}\, dh \\ &= \frac{1}{\tau_o} \int_0^\infty K\rho(\sec z + \eta \sec z \tan^2 z)\, dh. \end{aligned} \tag{A.6}$$

The first term in the integrand can be easily integrated:

$$X = \sec z + \frac{1}{\tau_o} \sec z \tan^2 z \int_0^\infty \eta K\rho\, dh. \tag{A.7}$$

By the mean value theorem we know that

$$\int_0^\infty \eta K\rho\, dh = \bar{\eta} \int_0^\infty K\rho\, dh = \bar{\eta}\tau_o, \tag{A.8}$$

$$0 < \bar{\eta} < 0.0002925,$$

so we have for the air mass:

$$X = \sec z(1 + \bar{\eta}\tan^2 z). \qquad (A.9)$$

Since the estimate X = secz is already too large, this estimate is even worse. In order to improve our estimate of X let us consider a spherically symmetric atmosphere in which n = 1.

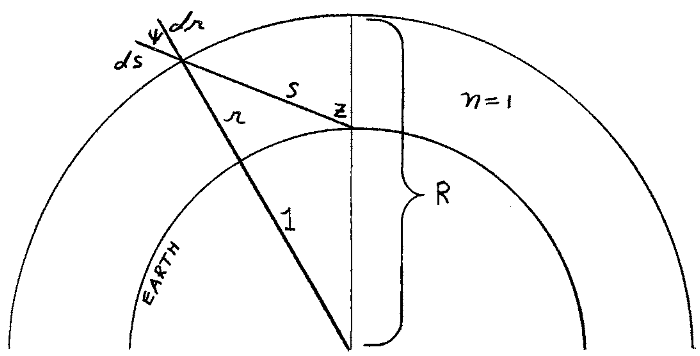

Figure 86. Spherically Symmetric Atmosphere Without Refraction.

From the figure we have $ds = \sec\Psi dr$ and $\sin\Psi = \frac{1}{R}\sin z$, so $\sec\Psi = \frac{R}{\sqrt{R^2 - \sin^2 z}}$.

Setting the earth's radius at 1, the air mass is

$$X = \frac{1}{\tau_0}\int_1^{\infty} K\rho \sec\Psi \, dR = \frac{1}{\tau_0}\int_1^{\infty} \frac{K\rho R}{\sqrt{R^2 - \sin^2 z}} \, dR. \qquad (A.10)$$

If the atmosphere becomes insensibly thin above a small fraction of the earth's radius, then we can set R = 1 + r and Equation (A.10) is cast in the same form as Equation (A.6) except for a sign

$$X = \frac{1}{\tau_0}\int_0^{\infty} K\rho(\sec z - r\sec z\tan^2 z)dr, \qquad (A.11)$$

or,

$$X = \sec z(1 - \bar{r}\tan^2 z). \qquad \text{(A.12)}$$

In order to allow for refraction, let us observe the behavior of a ray traveling through a shell of atmosphere of index n(R) when it meets a shell of index n(R').

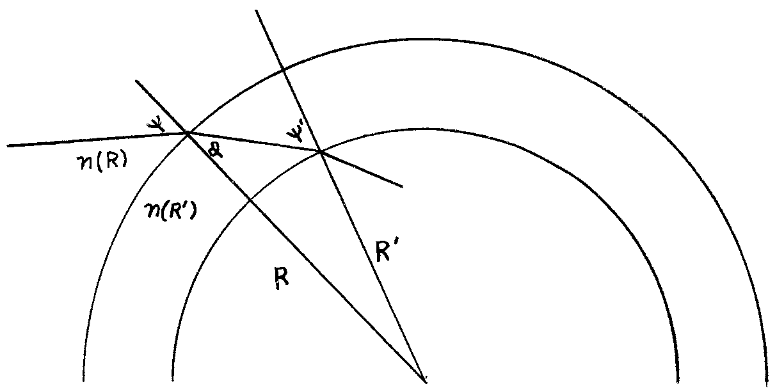

Figure 87. Spherically Symmetric Atmosphere With Refraction.

From the law of refraction we have

$$n(R)\ \sin\Psi = n(R')\sin\varphi, \qquad \text{(A.13)}$$

and, from the geometry of the figure we have

$$\frac{R}{\sin(\pi-\Psi')} = \frac{R}{\sin\Psi'} = \frac{R'}{\sin\varphi} \ . \qquad \text{(A.14)}$$

Combining Equations (A.13) and (A.14) yields

$$Rn(R)\sin\Psi = R'n(R')\sin\Psi' \ . \qquad \text{(A.15)}$$

This relation holds between each adjacent pair of shells, so,

$$R\, n(R)\sin\Psi = R'n(R')\sin\Psi' = R''n(R'')\sin\Psi'' = \ldots = R_o n \sin z. \quad (A.16)$$

Using the conventions $R_o = 1$, $n' = \frac{n(R)}{n}$, Equation (A.16) becomes

$$\sin\Psi = \frac{\sin z}{Rn'} \; ; \; \sec\Psi = \frac{Rn'}{\sqrt{(Rn')^2 - \sin^2 z}} \; . \quad (A.17)$$

The previous approximations were $n' = 1-\eta$, $R = 1+r$. Since η and r are small, approximately,

$$Rn' = 1 + (r-\eta),$$
$$(Rn')^2 = 1 + 2(r-\eta).$$

By the same process used to obtain Equations (A.9) and (A.12), we obtain

$$X = \sec z \left[1 - \overline{(r-\eta)}\tan^2 z \right] . \quad (A.18)$$

We can regard Equation (A.18) as an equation with an unknown parameter, $\overline{(r-\eta)}$. If we fit the equation to values of X, we determine the value of the parameter. By least squares, the parameter is given by

$$\overline{(r-\eta)} = \frac{\Sigma \sec z_i \tan^2 z_i (\sec z_i - X_i)}{\Sigma \sec^2 z_i \tan^4 z_i} . \quad (A.19)$$

The value of $\overline{(r-\eta)}$ obtained by using the air masses given in Hardie's (1962) tabulation is 0.00088, so Equation (A.18) becomes

$$X = \sec z \; (1-0.00088\tan^2 z). \quad (A.20)$$

Table XXVII lists differences between values of X obtained from Equation (A.20) and from Hardie's (1962) tabulation.

TABLE XXVII

ACCURACY OF AIR MASS FORMULA

z^{o}	secz	X	secz(1-0.00088 $\tan^2 z$)	Difference
0	1.000	1.000	1.000	0.000
30	1.155	1.154	1.155	+0.001
60	2.000	1.995	1.994	-0.001
61	2.063	2.057	2.057	0.000
62	2.130	2.123	2.124	+0.001
63	2.203	2.196	2.196	0.000
64	2.281	2.273	2.272	-0.001
65	2.366	2.356	2.357	+0.001
66	2.459	2.448	2.449	+0.001
67	2.559	2.546	2.546	0.000
68	2.670	2.655	2.657	+0.002
69	2.790	2.773	2.773	0.000
70	2.924	2.904	2.904	0.000
71	3.072	3.049	3.050	+0.001
72	3.236	3.209	3.210	+0.001
73	3.420	3.388	3.389	+0.001
74	3.628	3.588	3.588	0.000
75	3.864	3.816	3.818	+0.002
76	4.134	4.075	4.076	+0.001
77	4.445	4.372	4.369	-0.003
78	4.810	4.716	4.719	+0.003
79	5.241	5.120	5.120	0.000

Another form of the air mass equation can be found by noting that

$$\sec\psi = \frac{1}{\sqrt{1-\sin^2\psi}} = 1 + \sum_{k=1}^{\infty} \frac{(2k-1)!}{2^{2k-1}k!(k-1)!} \sin^{2k}\psi \qquad \text{(A.21)}$$

as long as $\sin^2\psi < 1$. In view of Equation (A.17), then we have

$$\sec\Psi = 1 + \sum_{k=1}^{\infty} \frac{(2k-1)!}{2^{2k-1}k!(k-1)!} \quad \frac{1}{(Rn')^{2k}} \sin^{2k}z,$$

$$\sec z = 1 + \sum_{k=1}^{\infty} \frac{(2k-1)!}{2^{2k-1}k!(k-1)!} \sin^{2k}z,$$

$$\sec\Psi - \sec z = -\sum_{k=1}^{\infty} \frac{(2k-1)!}{2^{2k-1}k!(k-1)!} \sin^{2k}z\left(1 - \frac{1}{(Rn')^{2k}}\right), \quad \text{(A.22)}$$

so,

$$X - \sec z = \frac{1}{\tau_o}\int_0^{\infty} K\rho(\sec\Psi - \sec z)dr$$

$$= -\frac{1}{\tau_o} \sum_{k=1}^{\infty} \frac{(2k-1)!}{2^{2k-1}k!(k-1)!} \sin^{2k}z \int_1^{\infty} K\rho\left(1 - \frac{1}{(Rn')^{2k}}\right)dR. \qquad \text{(A.23)}$$

Now, if we let

$$a_k = \frac{1}{\tau_o} \frac{(2k-1)!}{2^{2k-1}k!(k-1)!} \int_1^{\infty} K\rho\left(1 - \frac{1}{(Rn')^{2k}}\right)dR,$$

we have

$$X = \sec z - \sum_{k=1}^{\infty} a_k \sin^{2k}z, \qquad \text{(A.24)}$$

and, if we desire, we can determine the a_k empirically to obtain arbitrary accuracy.

APPENDIX B

EQUIVALENCE OF DIFFERENTIAL REDUCTION AND ZERO-POINT INTERPOLATION

Let the subscript p apply to a selected observation of the program star at time t_p, and the subscripts c- and c+, respectively, to the preceeding and subsequent observations of a comparison star at times t_{c-} and t_{c+}.

Hardie's (1962) differential magnitude reduction equations are:

$$\Delta V = \Delta v - k_v \Delta X + \epsilon \Delta(B-V),$$

$$\Delta(B-V) = \mu \Delta(b-v) - \mu k'_{bv} \Delta X - \mu k'' \Delta(b-v)\bar{X}, \qquad (B.1)$$

$$\Delta(U-B) = \psi \Delta(u-b) - \psi k'_{ub} \Delta X - \psi k''_{ub} \Delta(u-b)\bar{X},$$

where the symbol Δ stands for the difference in the associated quantity for the two stars taken in a consistent sense and $\bar{X}$ is the mean air mass for the two stars.

Since the observation of the program star is usually bracketed by observations of the comparison star, it is usual to interpolate the comparison star's magnitude and air mass to the time of the program star's observation. That is, we let

$$v_c = \frac{t_{c+} - t_p}{t_{c+} - t_{c-}} v_{c-} + \frac{t_p - t_{c-}}{t_{c+} - t_{c-}} v_{c+}, \qquad (B.2)$$

and we define b_c, u_c, and $\mathbf{X}_c$ similarly. The first of Equations (B.1) then becomes, taking $\Delta v = v_p - v_c$,

$$\Delta V = v_p - \frac{t_{c+} - t_p}{t_{c+} - t_{c-}} v_{c-} - \frac{t_p - t_{c-}}{t_{c+} - t_{c-}} v_{c-}$$

$$-k_v \mathbf{X}_p + \frac{t_{c+} - t_p}{t_{c+} - t_{c-}} k_v \mathbf{X}_{c-} + \frac{t_p - t_{c-}}{t_{c+} - t_{c-}} k_v \mathbf{X}_{c+}$$

$$+ \epsilon(B-V)_p - \epsilon(B-V)_c ,$$

which becomes, by rearranging terms,

$$\Delta V = v_p - k_v \mathbf{X}_p + \epsilon(B-V)_p$$

$$-[v_{c-} - k_v \mathbf{X}_{c-} + \epsilon(B-V)_c] \frac{t_{c+} - t_p}{t_{c+} - t_{c-}}$$

$$-[v_{c+} - k_v \mathbf{X}_{c+} + \epsilon(B-V)_c] \frac{t_p - t_{c-}}{t_{c+} - t_{c-}} . \qquad \text{(B.3)}$$

Now, if we recall, again from Hardie (1962),

$$V = v - k_v \mathbf{X} + \epsilon(B-V) + \zeta_v ,$$

$$B-V = \mu(b-v)J_x - \mu k'_{bv} \mathbf{X} + \zeta_{bv} ,$$

$$U-B = \psi(u-b)G_x - \psi k'_{ub} \mathbf{X} + \zeta_{ub} , \qquad \text{(B.4)}$$

Equation (B.3) can be written

$$\Delta V = V_p - \zeta_{v_p} - \left[V_{c-} - \zeta_{vc-}\right] \frac{t_{c+} - t_p}{t_{c+} - t_{c-}} - \left[V_{c+} - \zeta_{vc+}\right] \frac{t_p - t_{c-}}{t_{c+} - t_{c-}}$$

$$\Delta V = V_p - \left(\frac{t_{c+} - t_p}{t_{c+} - t_{c-}} V_{c-} + \frac{t_p - t_{c-}}{t_{c+} - t_{c-}} V_{c+}\right)$$

$$- \mathcal{J}_{vp} + \left(\frac{t_{c+} - t_p}{t_{c+} - t_{c-}} \mathcal{J}_{vc-} + \frac{t_p - t_{c-}}{t_{c+} - t_{c-}} \mathcal{J}_{vc+}\right)$$

$$= V_p - V_c - \mathcal{J}_{vp} + \mathcal{J}_{vc} .$$

So if we let $\mathcal{J}_{vp} = \mathcal{J}_{vc}$ we obtain

$$\Delta V = Vp - V_c \quad , \tag{B.5}$$

and the two methods of reduction are equivalent. Similarly, for the second of Equations (B.1), we have

$$\Delta(B-V) = \mu(b-v)_p - \mu k'_{bv} X_p - \mu k''_{bv}(b-v)_p \bar{X}$$

$$- \left[\mu(b-v)_{c-} - \mu k'_{bv} X_{c-} - \mu k''_{bv}(b-v)_{c-}\bar{X}\right] \frac{t_{c+} - t_p}{t_{c+} - t_{c-}}$$

$$- \left[\mu(b-v)_{c+} - \mu k'_{bv} X_{c+} - \mu k''_{bv}(b-v)_{c+}\bar{X}\right] \frac{t_p - t_{c-}}{t_{c+} - t_{c-}} \tag{B.6}$$

where $\bar{X} = \frac{1}{2}(X_p + X_c)$.

Since $J_x = 1 - \mu k''_{bv} X$ is a slowly varying function of X we can take $J_{\bar{X}} \approx J_{X_{c-}} \approx J_{x_p} \approx J_{X_{c+}}$ and Equation (B.6) becomes

$$\Delta(B-V) = (B-V)_p - \mathcal{J}_{bvp}$$

$$- \left[(B-V)_{c-} - \mathcal{J}_{bvc-}\right] \frac{t_{c+} - t_p}{t_{c+} - t_{c-}}$$

$$- \left[(B-V)_{c+} - \mathcal{J}_{bvc+}\right] \frac{t_p - t_{c-}}{t_{c+} - t_{c-}}$$

$$\Delta(B-V) = (B-V)_p - (B-V)_c - \zeta_{bvp} + \zeta_{bvc} \quad . \tag{B.7}$$

Again, by selecting $\zeta_{bvp} = \zeta_{bvc}$ we have

$$\Delta(B-V) = (B-V)_p - (B-V)_c \quad . \tag{B.8}$$

The argument for the third equation of (B.1) is similar.

APPENDIX C

PROGRAM SPECIFICATIONS

Two programs are described in this section: UBV Photometric Reduction Program and Heliocentric Julian Day Correction Program. The design of these programs was discussed in Chapter VII. This appendix describes the input-output formats and gives the program listings. The programs were written in FORTRAN IV and can be run on any machine which accepts source programs in this language.

The Photometric Reduction Program first reads a Parameter Card which has the following format: The first nine columns are punched with the card identification, for example PARAM. These nine columns are ignored by this program. The remaining fields on the card are each ten columns wide. The number punched into each field should have a decimal point and any unused columns may be left blank. Plus signs need not be punched. The fields contain the following data: columns 10-19, k''_{bv}; 20-29, k''_{ub}; 30-39, observatory latitude expressed in degrees with decimal fraction; 40-49, ϵ; 50-59, μ; 60-69, ψ. The remainder of the card may be left blank since it is not read by the program.

Each observation that is processed by the program requires an Extinction Card whose format varies according to the mode specified on it. If the mode desired is the extinction mode, this is obtained by punching the letters EXT into the first three columns of the card. The remainder of the card is punched with decimal numbers in the following format: columns 10-19, V; 20-29, B-V; 30-39, U-B. The remainder of the card may be left blank. If the mode desired is the zero-point mode, this is obtained by punching ZERO in the first four columns. The remainder of the card is punched as follows: columns 10-19, V; 20-29, B-V; 30-39, U-B; 40-49, k_v; 50-59, k'_{bv}; 60-69, k'_{ub}. If the mode desired is the reduction mode, this is obtained by punching RDUC in the first four columns. The remaining columns are punched: columns 10-19, ζ_v; 20-29, ζ_{bv}; 30-39, ζ_{ub}; 40-49, k_v; 50-59, k'_{bv}, 60-69, k'_{ub}.

After each Reduction Card there must be an Observation Card. In the first nine columns of this card are punched the star's identification, for example, DQ CEPHEI. The remaining columns are punched as follows: columns 10-19, v; 20-29, b; 30-39, u; 40-49, hour angle expressed in hours and minutes separated by a decimal point (whether the angle is east or west may be ignored; 50-59, declination in degrees with decimal fraction; 60-71, Julian day with decimal fraction.

The program processes each pair of Extinction and Observation cards separately and produces output depending on the mode of operation specified on the Extinction card. The headings for the data are: MODE, STAR, V, B-V, U-B, JD, X. In the extinction mode the data printed are: EXT, star identification, $v + \epsilon(B-V) - V$, $\mu J_x(b-v)-(B-V)$, $\psi G_x(u-b)-(U-B)$, Julian day, air mass. In the zero-point mode they are: ZERO, identification, ζ_v, ζ_{bv}, ζ_{ub}, Julian day, air mass. In the reduction mode they are: RDUC, identification, V, B-V, U-B, Julian day, air mass.

The program must be terminated after the last observation has been processed by means of the End of File card. This card simply has the letters EOF punched into the first three columns.

The FORTRAN IV program listing of the UBV Photometric Reduction Program is shown in Table XXVIII.

TABLE XXVIII

FORTRAN IV LISTING OF REDUCTION PROGRAM

```
C      UBVPHOTOMETRIC REDUCTION PROGRAM
       DATA IEOF,IEXT, IZERO, IRDUC/3HEOF,3HEXT,4HZERO,4HRDUC/
       DOUBLE PRECISION T
   1   FORMAT (5H MODE,4X,4HSTAR,11X,1HV, 9X,3HB-V,8X,3HU-B9X2HJD,11X,1HX)
   2   FORMAT(A6,A3,5F10.0,D12.0)
   3   FORMAT(1X,A4,A8,A3,1X,3F11.4,7PD17.4,0PF7.4)
       WRITE(6,1)
       READ(5,2)IDENTL,IDENTR,EX2BV,EX2UB,PHI,EPSLON,EMU,PSI
   4   READ(5,2)IDENTL,IDENTR,V,B,U,H,D,T
       IF(IDENTL-IEOF)6,5,6
   5   STOP
   6   IF(IDENTL-IZERO)7,9,7
   7   IF(IDENTL-IRDUC)8,9,8
   8   IF(IDENTL-IEXT)11,10,11
   9   HEXT=H
       DEXT=D
       TEXT=T
  10   IEXT=IDENTL
       VEXT=V
       BEXT=B
       UEXT=U
       GOTO4
  11   SNLAT=SIN(.174532925E-1*PHI)
       COSLAT=COS(.174532925E-1*PHI)
       SNDEC=SIN(.174532925E-1*D)
       COSDEC=COS(.174532925E-1*D)
       COSH=COS(.436332312*H-.174532925*AINT(H))
       SECZ=1./(SNLAT*SNDEC+COSLAT*COSDEC*COSH)
       X=SECZ-.0018167*(SECZ-1.)-.002875*(SECZ-1.)**2
      1-.0008083*(SECZ-1.)**3
       SB=EMU*(1.-EX2BV*X)*(B-V)
       SU=PSI*(1.-EX2UB*X)*(U-B)
       IF(IEXT-IZERO)12,13,12
  12   IF(IEXT-IRDUC)15,14,15
  13   SB=-SB+BEXT+DEXT*X
       SV=-V-EPSLON*BEXT+VEXT+HEXT*X
       SU=-SU+UEXT+TEXT*X
       GOTO16
  14   SB=SB+BEXT-DEXT*X
```

TABLE XXVIII (Continued)

```
      SV=V+EPSLON*SB+VEXT-HEXT*X
      SU=SU+UEXT-TEXT*X
      GOTO16
15    SB=SB-BEXT
      SV=V+EPSLON*BEXT-VEXT
      SU=SU-UEXT
16    WRITE (6,3)IEXT,IDENTL,IDENTR,SV,SB,SU,T,X
      GOTO4
      END
```

The Heliocentric Julian Day Correction Program accepts as input data cards of the following format: columns 1-9, star's identification; 10-19, right ascension expressed in hours and minutes separated by a decimal point; 20-29, declination in degrees with decimal fraction; 30-39, Julian day with decimal fraction. As output, for each input card, the program writes: identification, Δt, Julian day. The Heliocentric Julian Day for each observation may be obtained by noting HJD = JD + Δt. Since Δt varies slowly with the date, more than one determination per night is not required.

To terminate the program, an End of File Card is inserted after the data cards. Its format is the same as in the reduction program.

The FORTRAN IV program listing of the Heliocentric Julian Day Correction Program is shown in Table XXIX.

TABLE XXIX

FORTRAN IV LISTING OF JULIAN DAY CORRECTION PROGRAM

```
C     HELIOCENTRIC JULIAN DAY CORRECTION PROGRAM
      DATA IEOF/3HEOF/
    1 FORMAT(A6,A3,3F10.0)
    2 FORMAT(1X,A6,A3,10H  DELTA T=,F8.5,5H  JD=,F10.1)
    3 READ(5,1)IDENTL,IDENTR,ALPHA,DELTA,TIME
      IF(IDENTL-IEOF)5,4,5
    4 STOP
    5 EPOCH=TIME-2415020.
      GAMMA=4.9082294+.821499E-6*EPOCH
      ANAM=6.2565835+.1720197E-1*EPOCH
      E2=.03350208-.228884E-8*EPOCH
      TRUAN=ANAM+E2*SIN(ANAM)
      SLONG=TRUAN+GAMMA
      OBLIQ=.40931975-.3562628E-6*EPOCH
      SNOBLQ=SIN(OBLIQ)
      CSOBLQ=COS(OBLIQ)
      SINDEC=SIN(.174532925E-1*DELTA)
      COSDEC=COS(.174532925E-1*DELTA)
      SNLONG=SIN(SLONG)
      CSLONG=COS(SLONG)
      SNALPH=SIN(.436332312*ALPHA-.174532925*AINT(ALPHA))
      CSALPH=COS(.436332312*ALPHA-.174532925*AINT(ALPHA))
      ECC=.01675104-.114442E-8*EPOCH
      DELTAT=-.00577567*(1.-ECC**2)/(1.+ECC*CSLONG)*(COSDEC*CSALPH
     1*CSLONG+(SNOBLQ*SINDEC+CSOBLQ*COSDEC*SNALPH)*SNLONG)
      WRITE(6,2)IDENTL,IDENTR,DELTAT,TIME
      GO TO 3
      END
```

VITA

Robert L. Jenks

Candidate for the Degree of

Doctor of Philosophy

Thesis: UBV PHOTOMETRY OF DQ CEPHEI

Major Field: Physics

Biographical:

Personal Data: Born at Omaha, Nebraska on September 22, 1933, the son of E. Hart and Ruth N. Jenks.

Education: Attended grade school at Omaha, Nebraska; graduated from South High School in 1952; received the Bachelor of Arts degree from the University of Omaha, with majors in Physics and Mathematics, in January, 1959; attended Oklahoma State University during the Spring semester, 1959, and Santa Monica City College during 1961-62; received the Master of Science degree from Oklahoma State University, with a major in physics, in August, 1963.

Organizations: Member of American Astronomical Society, Sigma Pi Sigma Physics Honor Society, and Pi Mu Epsilon Honorary Mathematics Fraternity.

Professional Experience: Employed as space vehicle control systems designer from 1959-62. Primary job was the design of the Thor-Delta space vehicle attitude control system and test equipment.